Physiological and metabolic characteristics of polar diatoms: insights into cold adaptation and potential for biotechnology

Sam Christopher Coffin

Department of Plant Sciences

and

The British Antarctic Survey

Wolfson College

University of Cambridge

September 2021

This thesis is submitted for the degree of Doctor of Philosophy

Declaration

This thesis is the result of my own work and includes nothing which is the outcome of work done in collaboration except as declared in the Preface and specified in text.

It is not substantially the same as any work that I have submitted, or is being submitted for a degree, diploma or other qualification at the University of Cambridge or any other University or similar institution except as declared in the Preface and specified in text. I further state that no substantial part of my thesis has already been submitted at the University of Cambridge or any other university of similar institution except as declared in the Preface and specified in text.

The work contained in Chapter three has been submitted for peer review in *Diatom Research*. Work detailed in Chapter five section 5.2.1 is a result of a collaboration with four PhD students within the Plant Metabolism group at the University of Cambridge: Shelby Newsad, Dominic Absolon, Ellen Harrison and Nhan-An Tran.

This thesis does not exceed the prescribed word count set by the Biology Degree Committee.

Summary

Name: Sam Christopher Coffin

Title: Physiological and metabolic characteristics of polar diatoms: insights into cold adaptation and potential for biotechnology

The polar regions represent two of the most extreme environments on Earth, with sub-zero temperatures, sustained light in the summer and complete darkness in the winter. Marine diatoms are prevalent in the polar oceans, significantly contributing to primary productivity and ecosystem functioning. They are characterized by having optimal growth at low temperatures (<10°C) and have developed various genetic adaptations to cope with these extreme environments. The polar regions, however, are experiencing unprecedented environmental changes because of regional climate change. We currently lack detailed knowledge on polar diatom ecophysiology and metabolism, which means we do not know how these species may be impacted by future environmental changes. One barrier to our understanding of polar diatoms is the availability of living strains for experimental study. The number of polar diatom strains in public collections is low and of those that are available, many have been kept in culture for many decades. Hence, there is an urgent requirement to isolate new environmental strains that have not been exposed to artificial conditions for many decades and also to increase the number and diversity of species available. In this project I conducted fieldwork in Antarctica to isolate several new Antarctic strains and used these alongside Arctic and Antarctic strains from culture collections to study whether physiological and metabolic characteristics are conserved between diatoms from the two regions. My studies focused primarily on the response to temperature with the aim of predicting the effects of future climate change on polar diatom physiology and metabolism. The project also aimed to identify potential candidate strains for biotechnological exploitation.

Conducting fieldwork on the Western Antarctic Peninsula, I isolated 36 strains encompassing 12 different species of polar diatoms. These have been genetically and morphologically identified and representatives deposited in the Culture Collection for Algae and Protozoa. I investigated the ecophysiology of two diatom species found in both polar regions, *Fragilariopsis cylindrus* and *Porosira glacialis*. My results showed how the thermal tolerance

differed between Arctic and Antarctic strains with optimal growth temperatures of the Arctic *F. cylindrus* being 3°C higher than the Antarctic strain. On the contrary, *P. glacialis* from the Arctic had an optimal growth temperature 5.5°C lower than the Antarctic strain. In addition, the thermal tolerance of newly isolated strains of *F. cylindrus* was investigated and found to be similar to the laboratory strain except for one, which was able to grow at 12°C. The difference in temperature tolerance between the Arctic and Antarctic *F. cylindrus* strains led me to investigate the vitamin B_{12} requirements of these strains. Previously it had been suggested that there are links between B_{12} dependency and temperature tolerance, and the Antarctic *F. cylindrus* was previously found to be B_{12} independent. My results demonstrated that all three Arctic *F. cylindrus* strains had an obligate requirement for exogenous vitamin B_{12}, whereas all three Antarctic strains did not. Further investigation failed to isolate and identify the B_{12}-independent methionine synthase gene (*METE*) in Arctic strains, but this gene was identified in Antarctic strains. In contrast, the B_{12}-dependent methionine synthase gene (*METH*) was identified and partially sequenced in all strains. Several single nucleotide polymorphisms were identified in the Arctic strains which are hypothesised to be non-deleterious. These results provide a potential explanation for the B_{12} dependency in Arctic isolates, and reasons for how this might have arisen are considered. Lastly, polar diatoms are thought to offer a unique resource for biotechnology offering potentially novel metabolites or increased biomass production during winter months when temperatures decrease. Pilot experiments indicate that there is no advantage in growth over a temperate strain during the winter months in the UK, but further work focusing on optimisation is needed.

Acknowledgements

First and foremost, I give my utmost thanks to my supervisory team for their guidance, patience, and feedback. Specifically, I thank Melody for her hands on approach to her PhD teachings and expertise in polar science, I have learnt a great deal regarding molecular techniques and of the polar regions as a whole. I am grateful for you always being there to talk things over and provide feedback. I thank Alison for always making time for regular meetings and for your wealth of knowledge in algae, helping to bring further context to my work. Last but no means least, I thank Matt for his outstanding ethic for experimental methods and design as well as training, and for providing constructive feedback.

I would also like to thank NERC for funding this PhD and BAS for funding my Antarctic fieldwork through the CASS scheme. My thanks are given to the 2019 summer season members of the Bonner laboratory. In addition, I thank Dougie at Xanthella Ltd for the research and development of the Cryopharos bioreactors which were instrumental for experiments. I must also thank CCAP for their guidance and supplying/deposition of strains.

I have been incredibly lucky to spend the last four years in two incredibly welcoming and kind research groups. Firstly, it has been a pleasure to be part of the Biodiversity, Evolution and Adaptations research group at BAS. It has been wonderful to get to know so many senior scientists at the top of their field who always have the time to chat and discuss elements of my work including Lloyd Peck, Kevin Newsham, Alistair Crame, Simon Morley, and Chester Sands. I would like to thank Paul, Guy, and Becs, for their support in the laboratories. I would like to also thank the student cohort at BAS for being so supportive in regard to both work and social activities. Special thanks are given to the students in office 333C who have made the last four years so enjoyable: Kirstie, Arlie, Leo, Ryan S, and Ryan P. I also thank my diatom colleagues, Matt, and Dieter, despite us all studying incredibly different fields it was great sharing our passion for diatoms.

Secondly, I have enjoyed every minute of being part of the Plant Metabolism group in lab 220. The relationship and bond that this group forms are credible to the wonderful past and present members within it. To the current and past members of 220, I would like to thank

you all for making the lab so enjoyable and sharing such interesting work: Maria, Freddy, Ian, Aleix, Andy, Marcel, Stefan, Patrick, Dom, Ellen, Shelby, An, Carrie, Katie, Payam, Gonzalo, Katrin, Pawel, Lorraine, and Sue. Special thanks are given to Andre for being my cohort buddy and for genuinely being a wonderful scientist and friend. Lastly, I would like to thank a past member of the group and my girlfriend, Monika, for being my rock the last two years. Despite you moaning about the cold British weather every five minutes, you have been there when times were at their hardest. Your support over the last two years has been fundamental to getting me through the last stages of the PhD.

Lastly, I must send my thanks to my Maa and Paa for the immense support they have granted me during my studies. They have been by my side throughout and I would not be in this position without them. I must also thank my sister, Cherry, for your support and for being an inspiration of mine, especially regarding the adversities you have had to face.

Table of contents

Table of figures

Table of tables

List of abbreviations

AABW	Antarctic bottom water
ACC	Antarctic circumpolar current
AIC	Algal innovation centre
AIC	Akaike information criteria
AMAP	Arctic monitoring and assessment programme
APHA	Animal and plant health agency
ASW	Artificial sea water
ATR	Attenuated total reflection
B_1	Thiamine
B_{12}	Cobalamin
B_7	Biotin
BAS	British Antarctic survey
CBA1	Cobalamin acquisition protein 1
CCAP	Culture collection for algae and protozoa
CDS	Coding sequence
COI	Cytochrome c oxidase subunit I
CTD	Conductivity, temperature and depth
Dd	Diadinoxanthin
DEFRA	Department for environment, food and rural affairs
DES	De-epoxidation state
Df	Degrees of freedom
DHA	Docosahexaenoic acid
DMF	Dimethylformamide
DNA	Deoxyribonucleic acid
DOC	Dissolved organic carbon
Dt	Diatoxanthin

EPA	Eicosapentaenoic acid
FACS	Fluorescence-activated cell sorting
FAME	Fatty acid methyl esters
Fe	Iron
FFA	Free fatty acids
FT-IR	Fourier transform – infrared spectroscopy
GC	Gas chromatography
GC-FID	Gas chromatography – flame ionization detection
GC-MS	Gas chromatography – mass spectrometry
GLM	General linear model
HNLC	High nutrient low chlorophyll
HPLC	High performance liquid chromatography
IPCC	Intergovernmental panel for climate change
ITS1	Internal transcribed spacer region 1
ITS2	Internal transcribed spacer region 2
LED	Light emitting diode
LTER	Palmer long term ecological research
MCM	Methylmalonyl-CoA mutase
METE	B_{12}-independent methionine synthase
METH	B_{12}-dependent methionine synthase
MMETSP	Marine eukaryotic transcriptome sequencing project
MY	Million years
MYA	Million years ago
NCBI	National center for biotechnology information
NCMA	National center for marine algae and microbiota
OD	Optical density
OUT	Operational taxonomic unit
PCR	Polymerase chain reaction

PUFA	Polyunsaturated fatty acid
RaTs	Rothera oceanographical and biological time series
*rbc*L	Ribulose-1,5-biphosphate carboxylase/oxygenase (RuBiScO)
RCC	Roscoff culture collection
RNR	Ribonucleotide reductase class II
SD	Standard deviation
SEM	Scanning electron microscopy
SNP	Single nucleotide polymorphism
SST	Sea surface temperature
T_{opt}	Thermal optimum
TPC	Thermal performance curves
UTEX	University of Texas culture collection
UTR	Untranslated region
UV	Ultraviolet
WAP	Western Antarctic Peninsula

Chapter 1 - Introduction

1.1 The polar regions

The polar regions are comprised of the Arctic in the Northern hemisphere and Antarctica in the Southern hemisphere. Both are characterized by extremely cold temperatures and extreme seasonality. During the polar winters there is 24-hour darkness where the sun does not appear above the horizon lasting for 6 months at the poles. The opposite is true during the summer where the sun does not dip below the horizon. In the present day, the polar regions look like very similar environments with regard to environmental conditions, but their evolutionary history is significantly different, starting with the fact that one is an ocean and the other is a continent. To understand the formation of the polar regions and their evolutionary history, it is first necessary to understand the historic supercontinent of Pangea and the subsequent breakup of this continent into Gondwana and Laurasia. Pangea was a supercontinent thought to be created ~300 Mya and began breaking apart ~200 Mya during the Triassic into two separate supercontinents, Gondwana and Laurasia (Stampfli *et al.*, 2013). Laurasia contained the likes of present-day North America, Eurasia, and Siberia and Gondwana contained present-day South America, Africa, Antarctica, and Australia. The formations of the Arctic and Antarctica are described individually below.

1.1.1 Evolutionary history of the Arctic

The Arctic is an ocean situated over the North pole, much of it surrounded by land. Currently, modelling indicates that 120 Mya the Arctic was primarily a bay influenced by the North Pacific Ocean (Lawver *et al.*, 1990). Around 80 Mya the connection to the Pacific Ocean was cut off by present-day North America and Siberia colliding and an opening to the North Atlantic created between 54-27 Mya (Dunton, 1992 and references therein; Lindstrom, 2001 and references therein). The opening to the Atlantic was thought to be shallow with a deep water connection predicted to have developed only in the last 20 My (Lawver *et al.*, 1990). Connection to the Pacific Ocean, now known as the Bering Sea, was re-established somewhere between 7.4-4.8 Mya but the exact timing of this is still a strongly debated topic (Marincovich & Gladenkov, 2001). Cooling of the Arctic Ocean to below 10°C is thought to

have occurred firstly when the connection to the Atlantic Ocean was made and during a second cooling event ~12 Mya (Dunton, 1992 and references therein). The cooling periods mean that the Arctic Ocean was characterized by cold temperatures but the occurrence of sub-zero temperatures did not happen until glaciation and sea ice formation, which occurred around 0.7-2 Mya (Clark, 1990). Surrounded by North America, Greenland, and Eurasia, the Arctic spans ~14 million km^2 and is the world's smallest ocean. Due to the connections at the Pacific and Atlantic, ocean currents are important factors influencing Arctic climate and oceanography. The Pacific connection attributes to only 10-13% of total inflow, whereas the Atlantic connection is attributed to ≥80% of inflow and outflow (Wassmann *et al.*, 2010). Moreover, the Atlantic ocean is a source of warmer, saltier water into the Arctic basin (Beszczynska-Möller *et al.*, 2012).

1.1.2 Evolutionary history of Antarctica

Antarctica was part of the Gondwana supercontinent that, after separating from Pangea, began breaking up around 170 Mya (Blakey, 2008). By 120 Mya Antarctica coupled to Australia broke away and moved towards the South pole. From ~105 Mya Australia began breaking away from Antarctica and the two completely separated between 50-75 Mya (Blakey, 2008). What followed was a series of tectonic movements resulting in the opening of a water passage between East Antarctica and Australia ~32 Mya and the opening of the Drake Passage between 31-25 Mya (Lawver & Gahagan, 2003). The opening of these two sea passages resulted in the creation of the Antarctic Circumpolar Current (ACC) ~25 Mya, which isolates the Southern Ocean and Antarctica from the rest of the world (Lawver & Gahagan, 2003). The ACC means the Southern Ocean is minimally influenced by the Atlantic, Pacific and Indian Oceans and the boundary it creates is known as the polar front or Antarctic convergence. Antarctica first became glaciated ~35 Mya with sea ice present from ~15 Mya (Barrett, 1996), much longer ago than in the Arctic. The size of the Antarctic continent is similar to the Arctic Ocean at ~14 million km^2, but with the Southern Ocean around Antarctica being ~20 million km^2 the total area encompassed is more than twice that of the Arctic.

1.1.3 Bipolar species

The Arctic is often considered young in comparison to the Antarctic, and this is definitely true in terms of glaciation and sub-zero temperatures, but the cold ocean appears to be much older. Despite the two different evolutionary histories of the Arctic and Antarctica the occurrence of similar taxa present in both regions has previously been described. These similar taxa are described as having a bipolar distribution, whereby they only appear in the polar regions and nowhere in between. Species of marine molluscs (Crame, 1993), plants (Villaverde *et al.*, 2017), mosses (Biersma *et al.*, 2017), fungi (Cox *et al.*, 2016), and microorganisms including bacteria (Sul *et al.*, 2013), algae (Hasle, 1976; Montresor *et al.*, 2003), and ciliates (Di Giuseppe *et al.*, 2015) have all been described as having bipolar distributions. The mechanisms that led to this phenomenon however are not fully understood. Three of these mechanisms, vicariance, dispersal, and glacial colonizations were described by Crame (1993). The vicariance mechanism is based on a species having had a cosmopolitan distribution, which is then separated because of physical or climatic events resulting in two or more distinct or disjunct populations. The dispersal mechanism proposes that an organism present in one polar region moves into the other region via dispersal. Both mechanisms have been suggested as potential methods for the bipolarity in macroscopic organisms. Thirdly, glacial colonisations are thought to be a possibility during Quaternary glaciation events, where global cooling enabled species to disperse when temperatures were cooler.

It becomes increasingly difficult to understand the mechanisms involved in the bipolarity of microorganisms, however. In 1934, Lourens Baas Becking put forward a hypothesis relating to microorganism biogeography that "Everything is everywhere, but the environment selects" (Becking, 1934). Becking hypothesised that microorganisms can be homogeneously distributed around the world, but the ones we find in a particular environment are the result of environmental selection and their ecological niche (Becking, 1934; de Wit & Bouvier, 2006). This is because microorganisms are thought not to be constrained by dispersal ability as larger organisms are. Considering the environmental features of the Arctic and the Antarctic are so similar it might be expected to see a larger number of bipolar organisms if distribution followed Becking's hypothesis. However, testing of this hypothesis in marine bacteria found that the number of bipolar bacterial species is less than what would be

expected by Becking's hypothesis (Sul *et al.*, 2013). Instead, the common consensus among scientists studying bipolar species is dispersal by deep underwater currents. Hasle, (1976) suggested this to be a possible explanation for the bipolar diatom species *Thalassiosira antarctica*, *Porosira glacialis* and *Fragilariopsis cylindrus*. Both *T. antarctica* and *P. glacialis* produce resting spores (Pike *et al.*, 2009), whereas the production of spores is not known in *F. cylindrus*. These resting spores could potentially enable safe transit through warmer temperatures. Deep water bacterial communities have also been shown to have higher biodiversity compared to surface communities with ocean circulation presented as a potential mechanism for this (Ghiglione *et al.*, 2012). Furthermore, gene flow between Arctic and Antarctic populations of planktonic foraminiferal species has been identified, suggesting there is the potential for gene flow through the tropics (Darling *et al.*, 2000). Darling *et al.*, (2000) explains that cold water upwelling zones may act as refugia for bipolar species but admits that species will encounter the warm surface waters of the tropics. Pawlowski *et al.*, (2007) added to this by identifying genetically similar bipolar benthic foraminifera. The influence of the Antarctic bottom water (AABW) has been suggested as a possible route for dispersal and gene flow between the polar regions (Pawlowski *et al.*, 2007; Kuklinski & Barnes, 2010). There is, however, a lot still to be learned regarding the distribution of bipolar species as a whole and the mechanisms involved.

The occurrence of bipolar organisms, however this has arisen, does pose a certain quandary. If one examines, or experiments with, a specimen or population from the Arctic, then if they are truly the same species the results would be predicted to be the same for the Antarctic and *vice versa*. This hypothesis however is seldom tested, but with the recent advances in molecular tools there is the potential to investigate this more deeply. One example in the literature looks at the Pteropod species *Limacina helicina* and finds that Arctic and Antarctic specimens are genetically different from one another (Hunt *et al.*, 2010). Hunt *et al.*, (2010) found that specimens from the two regions differed by 33.56% in the cytochrome c oxidase subunit I (COI) gene and the authors stress that as a result they may show species specific physiological differences. A similar result has also been found in the marine mollusc *Clione limacina* (Sromek *et al.*, 2015). The opposite was true in the deep-sea amphipod *Eurythenes gryllus* which exhibits a cosmopolitan distribution. Havermans *et al.*, (2013) identified genetic divergence in many populations of *E. gryllus* but specimens from the polar regions were

genetically similar suggesting gene flow. Although there is now more research looking at bipolar organisms more deeply, especially genetically, there is a distinct lack of research focusing on associated physiological characteristics.

1.2 Algae

1.2.1 Evolution and classification

Algae are a large group of unicellular and multicellular eukaryotic organisms with representatives at both the macro scale e.g., seaweeds such as the giant kelp (*Macrocystis pyrifera*) and micro scales e.g., single celled microalgae such as *Chlamydomonas reinhardtii* and *Phaeodactylum tricornutum*. Algae are somewhat loosely defined taxonomically, but modern definitions have algae as a paraphyletic group of photosynthetic organisms which do not show the same level of complexity to that of plants. Lacking true stems, leaves and roots. Algae can be loosely divided into three groups: green, red and brown algae and these groups can be discriminated by their photosynthetic pigments. They all use chlorophyll *a* in their photosystems but differ in the accessory light-harvesting pigments. Green algae use chlorophyll *b*, red algae use phycobilins and brown algae primarily use chlorophyll *c* and fucoxanthin. The evolution of photosynthetic eukaryotes involved an early primary endosymbiosis event featuring the engulfment of a photosynthetic cyanobacterium by a non-photosynthetic eukaryote resulting in the primary plastid estimated at around 1.5-1.6 billion years ago (Yoon *et al.*, 2004). This endosymbiosis event gave rise to three algal lineages, Chlorophyta or green algae (from which land plants were derived), Rhodophyta or red algae and, Glaucophytes. These three groups are collectively termed the Archaeplastida or Plantae. These early algal lineages are thought to be a monophyletic group (Rodríguez-Ezpeleta *et al.*, 2005; Deschamps & Moreira, 2009), but the evolutionary history of algal lineages derived after this evolutionary divergence is more complex.

Secondary endosymbiosis events have occurred in both the Chlorophyta and the Rhodophyta, whereby a heterotrophic eukaryotic cell assimilates a cell from the primary endosymbiosis. Two individual endosymbiosis events have been reported involving the plastid from the Chlorophyta resulting in the Chlorarachinophyta and Euglenophyta (McFadden, 2001), although the plastid origin in the latter has been disputed (Takahashi *et*

al., 2007). Takahashi *et al.*, (2007) identified that secondary plastids of Euglenophyta did not fall within the Chlorophyta and may in fact be the result of an earlier endosymbiosis with an unknown green plant relative. Secondary endosymbiosis between another heterotrophic eukaryote and a Rhodophyte is predicted to have occurred first ~0.7-1.1 billion years ago (Douzery *et al.*, 2004), and multiple independent endosymbioses have led to the derivation of six algal groups: Cryptophyta, Dinophyta (or dinoflagellates), Haptophyta, Heterokontophyta (which include the diatoms), Perkinsidae and Apicomplexa, the latter two of which have since lost their photosynthetic capacity (Gould *et al.*, 2008). Dinoflagellates have also been derived through tertiary endosymbiosis (assimilation of a secondary endosymbiont) and through serial secondary endosymbiosis (assimilation of a primary endosymbiont by a secondary endosymbiont), (Archibald, 2009). The evolutionary history of these secondary endosymbiosis events has resulted in significant complexity, which is further confused by the large presence of green algal genes within Rhodophyte endosymbionts (Dorrell & Smith, 2011). The complex evolutionary history of algae has resulted in significant morphological and genetic diversity and an ability to occupy almost all environments on Earth.

1.2.2 Diatoms

The diatoms were derived through a secondary endosymbiosis and are thought to have evolved somewhere between the Triassic and Jurassic 200-190 Mya (Nakov *et al.*, 2018). Diatoms are morphologically diverse around two key morphological forms: centric which exhibit radial symmetry and pennate which exhibit bilateral symmetry (Fig. 1.1). Nakov *et al.*, (2018) describes how classification can be taken further by discriminating methods of sexual reproduction and motility, the latter of which is suggested as a precursor to the diatom diversity boom. Centric taxa display oogamy and are non-motile and the pennate taxa are split into two with the araphid taxa, displaying anisogamy and are non-motile, and the raphid taxa, which display anisogamy but are motile (Nakov *et al.*, 2018 and references therein). Diatoms are unique in their ability to incorporate silica into their cell walls, taking up the element and depositing it into two halves (valves) that together form a frustule. The unique trait of silica utilization has identified possible historical events which may be responsible for diatom proliferation such as weathering. Diatom diversity and abundance has

been linked to weathering of silicate rocks during the Cenozoic, specifically during the early Oligocene and late Miocene leading to increased silica in the surface waters (Cermeño *et al.*, 2015). A recent study however, argues that increases in diversity during the Cenozoic period may be due to a changing ability for diatom frustules to be preserved as a result of changing climatic conditions giving the impression of higher abundance (Westacott *et al.*, 2021). The silica frustules are intricately detailed with pores and appendages, which makes them an important characteristic used for identification since the form is genetically determined. In addition, the presence or absence of a raphe (which enables movement) allows for the discrimination between araphid and raphid taxa. The current number of described species is estimated at 12,000 with an estimated 8,000 left to be described (Guiry, 2012). Besides their morphology and life history, diatom genetics is a mosaic of evolutionary history. Our understanding of diatoms has improved with the sequencing of their genomes and a total of nine diatom genomes have been sequenced, each revealing molecular insights into diatom biology and evolution. Diatom genomes have been described as being a chimera of genes, with the presence of green algal, red algal and even bacterial genes (Moustafa *et al.*, 2009; Bowler *et al.*, 2010; Dorrell *et al.*, 2017; Vancaester *et al.*, 2020). This genetic diversity has likely been a prominent factor influencing the success of this algal group.

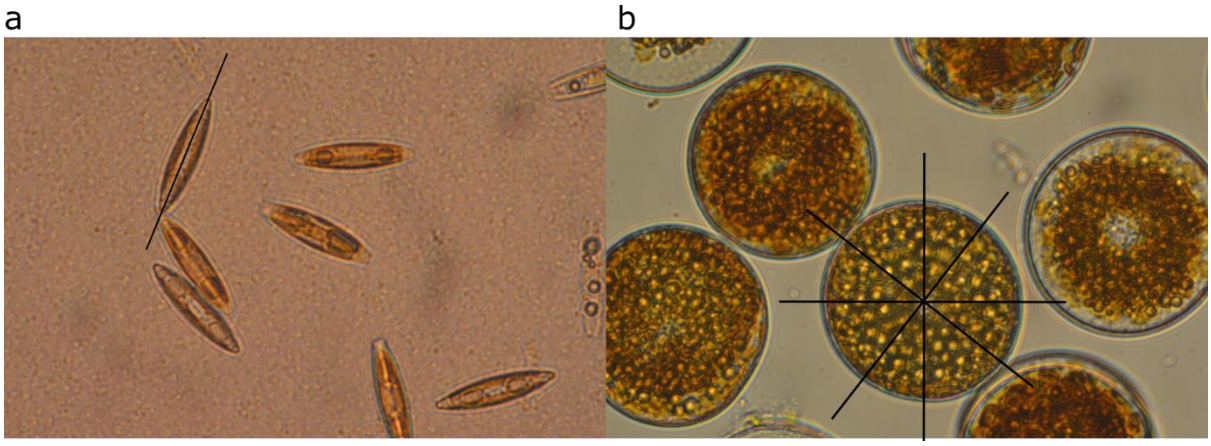

Figure 1.1 Diatom morphology and symmetry. Light microscopy images of a) pennate diatom displaying bilateral symmetry and b) centric diatom displaying radial symmetry.

1.2.3 Diatom distribution

Diatoms are regarded as one of the most successful algal groups with representatives in terrestrial, freshwater, and marine environments. Their global presence has led to many

researchers questioning the drivers behind diatom distribution. Following Becking's (1934) hypothesis "Everything is everywhere, but, the environment selects", the global distribution of diatoms could be considered to agree with this hypothesis. However, if this hypothesis were true, we would predict a low number of diatom species as allopatric speciation would be very low due to unlimited gene flow. In contrast, the number of species and the occurrence of endemic species suggests that the distribution of diatoms argues against this hypothesis. In 2009, Cermeno & Falkowski analysed the diatom fossil record over the past 1.5 My and found that ocean basins did not differ significantly in their taxa, suggesting that diatoms were not limited by dispersal and showed a cosmopolitan distribution. Relying on morphological features however was a limitation and the authors acknowledged this and stressed the potential for cryptic species as an important consideration. Indeed, when the distribution of a cosmopolitan diatom *Pseudo-nitzschia pungens* was analysed genetically, divergence was observed between isolates from different regions, signifying limitations to dispersal (Casteleyn *et al.*, 2010). Casteleyn *et al.*, (2010) went on to suggest that these genetic differences may well be the beginning of allopatric speciation in some of these isolates. Conversely the opposite was found for *Thalassiosira rotula* where gene flow does not seem to be limited but genetic divergence is possible through environmental selection (Whittaker & Rynearson, 2017). As a result, there is still no solid consensus on what drives the distribution of diatoms in the oceans, and it remains a contentious field of study, although diatom distribution does appear to be species-specific and recent work analysing the Tara Oceans dataset adds to this view. Malviya *et al.*, (2016) identified certain taxa which seem to exhibit cosmopolitan distributions e.g., *Thalassiosira* and *Pseudo-nitzschia* and other taxa that were more geographically constrained e.g., *Leptocylindrus* and *Attheya*.

1.2.4 Ecological significance

The global distribution and abundance of diatoms has led to a variety of ecological functions. The first and arguably biggest function is the contribution to global primary production, to which diatoms are estimated to contribute 40% in the marine environment alone, which equates to 20% globally (Nelson *et al.*, 1995; Field *et al.*, 1998; Falkowski, 1998). The contribution of diatoms to primary production is highest in the higher latitudes (>40°) where sea water is typically cooler and contains more nutrients (Rousseaux & Gregg, 2014).

As one of the biggest utilizers of silica, diatoms are fundamentally important in the cycling of this nutrient (Yool & Tyrrell, 2003). Furthermore, many diatom species exhibit a bloom characteristic, whereby rapid growth occurs upon favourable conditions, which includes nutrient concentrations. Two other important macronutrients driving the abundance of diatoms are phosphate and nitrate and diatoms are also key players in the cycling of both of these nutrients (Armbrust, 2009). In addition, increased light irradiance in the spring enables diatoms to rapidly utilize nutrients after winter months. The "boom and bust" life cycle of many pelagic diatom species contributes to the cycling of carbon through the high levels of dissolved organic carbon (DOC) released upon cell death (Tréguer *et al.*, 2018) and the contribution of diatoms to the exportation of carbon in the oceans is estimated at 43% (Jin *et al.*, 2006). The ability to rapidly uptake carbon during blooms and the relatively rapid sinking of cells due to their silica frustules is likely to be a key reason for their ability to export large amounts of both elements to the deep sea.

In addition, since diatoms are an important food source for marine organisms such as zooplankton, they export carbon into higher trophic levels. In Georges Bank and the Gulf of Maine (USA), diatoms were estimated to contribute ~40% and 0-25% of carbon to zooplankton diet (Fry & Wainright, 1991). The size fraction of diatoms also helps to shorten trophic food webs as they are directly grazed upon by copepods, this results in positive increases at the highest trophic levels, as smaller organisms enter the trophic levels through the microbial food web instead of herbivores (Sommer *et al.*, 2002). It should be mentioned that whilst diatoms have a major role in marine food webs, there are some species which have adapted mechanisms to negate herbivory. The interaction between diatoms and copepods has long been studied because diatoms are a suitable food source but some induce negative effects in copepods. Ban *et al.*, (1997) tested the co-culture of diatoms and copepods and found that 17 out of the 18 diatom species induced decreased fecundity and/or hatching success in 16 copepod species. Therefore, whether it be through positive or negative impacts, diatoms are an ecologically important group of algae in the marine environment.

1.2.5 Diatoms in the polar regions

Despite the inhospitable environments, the polar regions have a wealth of marine biodiversity. Diatoms are the dominant phytoplankton in the sea ice and open oceans of both polar regions. They form extensive blooms between early and late summer, taking advantage of turbulent water bringing nutrients to the surface and increased light (Medlin & Priddle, 1990). The abundance of diatoms can often be linked to three factors 1) nutrient availability 2) light irradiance and 3) temperature. Temperature is thought not to be as limiting as the other two factors considering that diatoms in these regions are adapted to growing in the cold. In the Arctic, diatoms are limited by nitrate (Tremblay *et al.*, 2002; Walsh *et al.*, 2004; Mills *et al.*, 2018; Krisch *et al.*, 2020). Conversely the Southern Ocean around Antarctica is described as a High Nutrient Low Chlorophyll (HNLC) region where limitation is usually caused by low iron and possibly vitamin B_{12} (Martin, 1990; Sedwick *et al.*, 2000; Bertrand *et al.*, 2007). During the polar winter, diatoms in both regions are limited by light availability.

Despite the limitations they experience at both poles, diatoms play a significant ecological role in terms of primary production and trophic assimilation of energy. In the central Arctic ocean, ice algae contribute 57% of total primary production and diatoms have been found to be the dominant phytoplankton in ice algae, making up 93% of the carbon biomass (Gosselin *et al.*, 1997). Arctic diatoms have been identified as a key nutrition source for a variety of organisms including zooplankton (Budge *et al.*, 2008), filter feeding mussels, and the polar cod (Kohlbach *et al.*, 2017; Thyrring *et al.*, 2017). In the Antarctic, the estimated contributions of diatoms to total primary production vary between 48% (Person *et al.*, 2018), 50% (Alvain *et al.*, 2008) and 89% (Rousseaux & Gregg, 2014). Variation in primary productivity estimates arise from differing model utilization and methods to determine phytoplankton groups. Diatoms are also key nutritional sources for zooplankton, especially Antarctic krill (Moline *et al.*, 2004) and dominate carbon export in the Southern Ocean (Tréguer *et al.*, 2018). The nutritional significance of this algal group stems from the production of fatty acids and, in particular, omega-3 fatty acids such as eicosapentaenoic acid (EPA). Polyunsaturated fatty acids (PUFAs) are fundamental components to all food webs and polar organisms tend to have high concentrations of PUFAs as these lipids help to maintain membrane fluidity, which would otherwise be reduced in the freezing temperatures

(Nichols *et al.*, 1993; Russell & Nichols, 1999; Chintalapati *et al.*, 2004). The increased PUFA concentrations does not come without consequences however, as PUFAs are more susceptible to lipid peroxidation (Girotti, 1990; Crockett, 2008).

As was previously mentioned in Section 1.1.3, there are species of diatoms that show a bipolar distribution. The occurrence of bipolarity immediately leads to questions regarding comparisons between Arctic and Antarctic specimens. Despite this, the only work published on bipolar diatom species is limited to three (*T. antarctica*, *P. glacialis*, and *F. cylindrus*) and the studies are primarily regarding their morphology. Arctic and Antarctic strains of *T. antarctica* were found to have large morphological differences in resting spore morphology, suggesting some aspect of genetic divergence (Fryxell *et al.*, 1981). As a result, the Arctic strains were referred to as *T. antarctica* var *borealis* and Antarctic strains as *T. antarctica* var *antarctica*. In contrast, *T. antarctica* and *P. glacialis* were analysed for their morphological characteristics in their vegetative state and Arctic and Antarctic strains were shown to be morphologically the same both under light and electron microscopy (Villareal & Fryxell, 1983). The only work published in Arctic and Antarctic strains of *F. cylindrus* found no features (morphological or genetic) to discriminate between the two regions (Lundholm & Hasle, 2008). Both *P. glacialis* and *F. cylindrus* are common species in the open ocean and sea ice of both polar regions (Garrison, 1991; Abelmann, 1992). There is, therefore, a variety of work yet to be carried out on these bipolar species regarding physiology, metabolism, genetics, and responses to climate change.

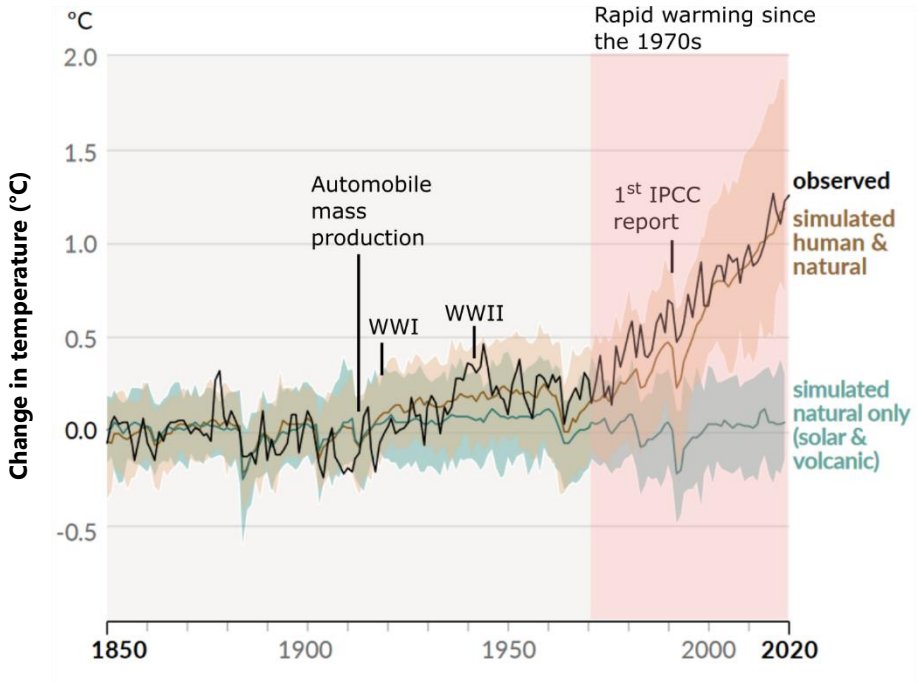

Figure 1.2 Global air temperature change since the 1st industrial revolution. Temperature change since 1850-present displaying key historic events and highlighting the rapid warming since the 1970s. Figure adapted from IPCC, (2021).

1.3 Climate change and responses

Since the dawn of the industrial revolution, the effects of human society on the Earth have been monumental. The use of fossil fuels has resulted in a steady accumulation of greenhouse gases, Carbon dioxide (CO_2), methane (CH_4), as well as Nitrogen oxides (NOx) and Sulphur oxides (SOx), which trap heat in the atmosphere resulting in the "greenhouse effect". Climate change events are not new in the Earth's history with various warm and cold phases occurring through geological time, but the rate at which changes are occurring in the present are alarming and unprecedented (Fig. 1.2). The Intergovernmental Panel for Climate Change (IPCC) was created to collate and synthesize the science on climate change to advise governments on climate driven policy. The IPCC has released as of 2021, six reports on climate change. The most recent of these documents on the first page alone states: increased global surface temperatures, increased greenhouse gases, retreating of glaciers, increased precipitation, increased sea surface temperatures (SST), sea level rise, and poleward shifts in biomes (IPCC, 2021). The polar regions have seen some of the biggest environmental changes as a result of climate change (IPCC, 2021) and especially in the

marine environments (Hoegh-Guldberg & Bruno, 2010). The response of the two polar regions however is fundamentally different.

The Arctic undoubtedly has seen some of the biggest changes in the world. Air temperatures have increased by 3.1°C over the last 49 years (AMAP, 2021). Large reductions in sea ice, which is a vital ecosystem for polar diatoms, have been reported (Comiso *et al.*, 2008; Overland & Wang, 2013; , 2021) and the number of days the Arctic Ocean is ice free has increased in some regions e.g., Barents sea has seen ice free water increase from 80 days to 289 days a year between 1979-2015 (Kahru *et al.*, 2016). This reduction in sea ice interestingly, has led to increased primary production as melting ice allows for increased light penetration into the open water (Pabi *et al.*, 2008; Arrigo & van Dijken, 2015; Kahru *et al.*, 2016). However, not only does this reduction in sea ice reduce the area of habitat for ice diatoms it has also led to a northward expansion of phytoplankton blooms in some regions due to increased light penetration as ice melts e.g., Barents sea, but a southern expansion in the Greenland sea (Renaut *et al.*, 2018). Renaut *et al.*, (2018) explained how the southward expansion of blooms in the Greenland sea coincides with a trend showing increased sea ice export out of the Fram Strait which could limit light penetration (Smedsrud *et al.*, 2017). The melting of both Arctic sea ice and land-based ice from places like Greenland (Trusel *et al.*, 2018) results in increased volumes of cold, fresh water into the ocean. Cold, fresher water is less dense than seawater and thus results in the stratification of the water column, leading to a reduction in vertical mixing and transfer of nutrients to the surface. Although average SST remains low in the Pan-Arctic at ~1°C, there is a warming trend of 0.032°C/year (Carvalho & Wang, 2020).

In the Antarctic, the Western Antarctic Peninsula (WAP) has been the object of major climate driven changes. Over the whole continent, air temperatures have been variable with much of the warming trends only being shown on the WAP, with some cooling trends in East Antarctica (Turner *et al.*, 2016). In 2005, Turner *et al* (2009) reported significant warming trends on the WAP over the last 50 years and increases in air temperatures of 7°C, although in recent years there appears to be a reduction in this trend (Turner *et al.*, 2016). In contrast to the Arctic, Antarctica has seen some increases in sea ice extent but much like air temperatures there is regional variability. Increases in sea ice extent have been seen in the Ross Sea, Weddel Sea, Indian Ocean, and Western Pacific Ocean, whereas decreases have

been seen in Bellingshausen Sea and the Amundsen sea on the western side of Antarctica (Turner *et al.*, 2015). One might expect primary productivity and algal blooms to increase with this reduction in sea ice much like the Arctic, but the opposite has been observed. Montes-Hugo *et al.*, (2009) reported a decrease in primary production (using chlorophyll *a* as a proxy) in the northern tip of the WAP, however, primary production was increased in the southern WAP despite also seeing reductions in sea ice. Montes-Hugo *et al.*, (2009) explains that this is likely due to the ice melt occurring in areas where sea ice was previously maintained all year round and therefore follows the characteristics of the Arctic ice loss with deglaciation increasing light irradiance. The increase in productivity in the southern region of the WAP has also been documented by Peck *et al.*, (2010), who reports an increase in phytoplankton blooms in areas that were previously glaciated. The WAP has seen a 1°C increase in SST since the 1950s (Meredith & King, 2005) but remains in the range of -1.5°C – 1°C (Cook *et al.*, 2016). Although the Southern Ocean, as a whole, has largely shown a cooling trend (Fan *et al.*, 2014), there is now evidence that it is now warming (Meehl *et al.*, 2019). An increase in water temperature of deeper water has been suggested as a possible factor as well as air temperatures contributing to the continued retreat of glaciers on the WAP (Cook *et al.*, 2016). Aside from decadal trends the threat of extreme weather events is also being realised in Antarctica, specifically on the WAP, where in 2020 a heatwave resulted in a maximum air temperature of 20.75°C at the Argentinian Marambio Base (Robinson *et al.*, 2020).

In the Arctic, phytoplankton blooms are occurring earlier than they did before (Kahru *et al.*, 2011; Ardyna *et al.*, 2014; Renaut *et al.*, 2018) but there is a lack of detail in the composition of these blooms. In the Antarctic however, a reduction in diatoms has been a common finding in phytoplankton blooms as a result of seawater freshening (Moline *et al.*, 2004) and decreased water stratification (Rozema *et al.*, 2017). More recently, an analysis of the WAP over the past five years has seen a reduction in diatoms in years that had higher SST and less sea ice (Lin *et al.*, 2021). In most cases in the Antarctic, cryptophytes benefit in the warmer, fresher, and less stratified conditions, whereas diatoms lose out (Moline *et al.*, 2004; Rozema *et al.*, 2017; Lin *et al.*, 2021). This is somewhat opposite to the historical view on diatom growth characteristics. Diatoms were said to thrive in areas of cold, turbulent, and nutrient rich waters, but the evidence from the Antarctic suggests that diatoms benefit from the

stratification and reduced mixing. Indeed, a recent review finds that many diatoms have adapted to thrive in more stratified waters and that our historical view is somewhat outdated (Kemp & Villareal, 2018). The stratification of the water column makes it important to understand the water temperature over depth profiles as they may not show the same characteristics as SST.

1.3.1 Diatom species-specific responses to temperature

Increasing temperatures are a common theme in both polar regions, yet very few papers describe the physiological or metabolic responses of polar diatoms to temperature. Eppley, (1972) famously carried out a review of temperature on phytoplankton because at the time temperature was not seen as a factor influencing the abundance of phytoplankton, producing a model which could be used to determine the temperature at which the maximum growth rate of ectotherms would be shown. Today these models are referred to as thermal performance curves (TPC). Temperature, although not a large factor governing the life strategies of diatoms i.e., blooming, does have a direct impact on growth rate and metabolism. The optimal growth temperature of phytoplankton follows a latitudinal pattern, that is optimal temperatures are highest at the equator and decrease on moving towards the higher latitudes (Thomas *et al.*, 2012). Polar diatoms are adapted to grow at cold temperatures and therefore it is vital we understand their response to increasing temperatures. Both Arctic and Antarctic diatom strains have shown optimal growth temperatures largely below 10°C (Fiala & Oriol, 1990; Suzuki & Takahashi, 1995; Longhi *et al.*, 2003). However, our knowledge of growth responses to temperature have come from only a handful of scientific articles. For example, Fiala & Oriol, (1990) is a commonly cited paper on the thermal traits of Antarctic diatoms. More recently, Coello-Camba & Agustí, (2017) have collated the thermal responses of polar phytoplankton documenting the responses of 22 diatoms strains across 15 species. The main similarity between polar diatoms identified by Coello-Camba & Agustí, (2017) was low optimal growth temperatures (<10°C) and they showed that these optimal growth temperatures were slightly higher in Arctic strains. Obviously, climate change and the studies mentioned in Section 1.3 describing changes in assemblage composition are important to understand the ecological effects of climate

change. However, it is still important to study species-specific responses on key ecological species, as it is not possible to study all species and assemblages within an ecosystem.

Aside from the growth responses to temperature it is also important to understand the effects on metabolism. As mentioned in Sections 1.2.3 diatoms are a key nutritional source for a variety of organisms. Changes in lipid metabolism and composition have been seen in polar diatoms in response to increased temperatures (Schaub *et al.*, 2017; Svenning *et al.*, 2019). Svenning *et al.*, (2019) identified a reduction in PUFAs in response to increasing temperature in Arctic *P. glacialis*, although the amount of PUFAs was still high. Individual metabolic changes could impact the nutritional content of diatoms affecting higher trophic levels. Overall, the impact of temperature of polar diatoms is scarcely studied and there is large scope to increase this area of research.

1.4 Algal biotechnology

Understanding diatom physiology and metabolism not only increases our knowledge in respect to their persistence and interactions in the natural environment but can also give insights into alternative uses. The threat of climate change and the extensive use of fossil fuels has changed the attitude of human society over recent years. There is a growing need to make society more environmentally friendly and reduce our carbon footprint on Earth. One promising avenue to do this is the use of microalgae for a variety of industries including biodiesel production, waste remediation, and animal feed. Diatoms, in particular, have been put under the magnifying glass because they are autotrophic, show rapid growth and produce useful metabolic products (Lebeau & Robert, 2003; Bozarth *et al.*, 2009). Diatoms produce of variety of lipids which have uses for fuel production (Hildebrand *et al.*, 2012; d'Ippolito *et al.*, 2015; Yi *et al.*, 2017), aquaculture feed (Patil *et al.*, 2005; Hemaiswarya *et al.*, 2011) and human health (Boelen *et al.*, 2013; Hamilton *et al.*, 2015). Diatoms also produce of variety of pigments e.g., fucoxanthin which have a variety of industrial uses (Kuczynska *et al.*, 2015). Metabolites such as lipids and light harvesting pigments are considered primary metabolites as they are essential for biological function, but diatoms are also known to produce secondary metabolites which are not essential. Secondary metabolites produced by diatoms include the polyunsaturated fatty aldehydes e.g., 2,4-decadeienal and 2,4-octadienal used in herbivore defence (Pohnert, 2005) and the polyphenol, rosmarinic acid which has

recently been shown to encourage attachment of bacterial cells to the diatom *Asterionellopsis glacialis* (Shibl *et al.*, 2020). Although diatoms are an interesting source of metabolic products, the optimisation of large-scale production is problematic with various issues of growth inhibition and biological contamination. Many strains used in biotechnology often have optimal growth temperatures >20°C. The high growth temperatures immediately impose limits on suitable locations at which these strains can be grown at scale even in closed photobioreactors, and in any case the cost for heat and illumination is much higher for photobioreactors than open ponds (Gupta *et al.*, 2015). In addition, for algal biotechnology to be economical, production needs to be maintained as long as possible, preferably all year round, and not limited by seasonal temperature changes at the location.

Polar organisms have been earmarked as potential biotechnological candidates especially in cold climates due to their adaptations to the polar environments including growth at cold temperatures and low light intensities (Margesin & Schinner, 1994; Kvíderová *et al.*, 2017). A review on the potential of biotechnology in Nordic countries identifies a need for locally adapted strains, i.e. strains which are adapted to the low temperatures and low light conditions of the high latitudes (Cheregi *et al.*, 2019). Both *P. glacialis* and *P. tricornutum* have shown promising lipid production at scale under natural or artificially simulated conditions in the high northern latitudes (Steinrücken *et al.*, 2018b; Svenning *et al.*, 2019). Extracts of *P. glacialis* and diatom communities have shown promising bioactivity (meaning to have some beneficial biological interaction) in a variety of assays including anti-cancer, anti-diabetic and antibacterial (Ingebrigtsen *et al.*, 2016, 2017). Although Antarctic strains are not necessarily adapted to the conditions of the northern hemisphere, the characteristics of low temperature and high light during the summer are synonymous between the two. In addition, adaptations to the isolated Antarctic region may result in interesting metabolic products. If culture conditions are not optimal there is also the potential for stress induced metabolic products (Fu *et al.*, 2015; Sun *et al.*, 2018) but this has not been explored in polar species. Two Antarctic ice diatoms *F. cylindrus* and *Chaetoceros neogracile* have been shown to produce antifreeze proteins linked to an adaptation to their life in sea ice (Bayer-Giraldi *et al.*, 2010; Gwak *et al.*, 2010). Antifreeze proteins have a variety of uses including cryopreservation, crop protection, and food processing (Xiang *et al.*, 2020). There is then, a

large potential to investigate the use of Antarctic and in general, polar diatom strains, in algal biotechnology.

1.5 Thesis aims

The overarching objective of this thesis is to further the understanding of polar diatom physiology and metabolism including vitamin dependency primarily in respect to bipolar species and to scope polar diatom potential for biotechnology. In this thesis I had three main objectives:

Firstly, the isolation of new, environmental strains of Antarctic marine diatoms. Isolated strains of algae are fundamentally important to algal research, enabling the growth of species in laboratory settings resulting in controlled observations and measurements of biological characteristics. Although the diversity and number of strains from temperate environments are large, there is an underrepresentation from polar environments. Coupled to this is the length of time some strains have been maintained in laboratory conditions under temperatures outside of their normal environmental ranges, which means there is a need to provide access to freshly isolated strains. Moreover, increasing the diversity of isolated species will help further our understanding of diatoms as a whole.

Secondly, to investigate how polar diatoms respond to temperature both physiologically and metabolically and to investigate whether characteristics are shared between the Arctic and the Antarctic. The interesting biological phenomenon of bipolarity has largely gone unstudied within diatoms, therefore investigating bipolar strains will help our understanding of this relatively rare phenomenon. Climate change is becoming an ever-increasing problem in the World's oceans, particularly in the polar regions. As diatoms are a key group within both polar regions it is vital that we understand how changes in temperature will affect their growth and metabolism. In addition, vitamins are important in algal metabolism and dependency is thought to arise through environmental selection. The vitamin dependency was therefore investigated in the bipolar *F. cylindrus* as the vitamin requirements of the Antarctic strain are already known and the bipolar distribution provides a unique opportunity to investigate this trait.

Lastly, I wanted to scope the potential of polar diatom species for biotechnology. Autotrophic algae are seen as a green, clean source of energy and biological products, but production is either limited to warmer climates or ceased during winter months. Furthermore, the adaptations to the polar environments may have led to novel metabolites that could be utilized within biotechnology.

In summary, this thesis comprises seven chapters:

Chapter one is an introduction to the subject area. Chapter two describes the methods utilized throughout this thesis. In chapter three I describe the isolation of new environmental strains of marine diatoms from Ryder Bay and Marguerite Bay, Antarctica. In chapter four I investigate the thermal tolerance of two bipolar diatom species and investigate basic metabolic characteristics. In chapter five I describe a unique phenotype in Arctic *F. cylindrus* strains exhibiting an obligate requirement for vitamin B_{12}. Chapter six, I present a preliminary experiment utilizing polar strains in the British winter. Finally in chapter seven I bring the results of these previous chapters into context and detail further work.

Chapter 2 - Materials and Methods

The following outlines the general methods used throughout the thesis. More specific methods not related to the whole thesis are detailed in "Additional methods" within the chapter it relates to.

2.1 Culturing and general techniques

2.1.1 Diatom strains

Diatom strains used throughout the thesis are detailed in Table 2.1, strains were obtained through the Culture Collection for Algae and Protozoa (CCAP, (Gachon *et al.*, 2007)) located at the Scottish Association for Maine Science (SAMS, Oban UK), Roscoff Culture Collection (RCC, Roscoff, France, (Vaulot *et al.*, 2004)) or isolated during the fieldwork aspect of this thesis in Antarctica (Chapter 3). Strains were grown in artificial seawater (ASW) with *f*/2 nutrients (Guillard & Ryther, 1962) and the full media recipe is detailed in Appendix 1. Strains acquired through culture collections were maintained in 30ml culture flasks (Sarstedt, Nümbrecht, Germany) in a 4°C incubator (Sanyo, Osaka, Japan). Light was provided by cool white LEDs (Sylvania, Budapest, Hungary) at an intensity of 30 µmol m^{-2} s^{-1} under a photoperiod of 16:8 hours (light:dark).

2.1.3 Sterilisation techniques

Solutions stable at high temperatures were autoclaved at 121°C for 15 minutes. Solutions not stable at high temperatures were filter sterilised (0.2 µm) via vacuum filtration in a class II cabinet. All consumables and apparatus were either pre-sterilised or autoclaved under the conditions stated above.

Table 2.1 Diatom strains used in this thesis. Strains acquired through CCAP (Gachon *et al.*, 2007), RCC (Vaulot *et al.*, 2004), and UTEX (University of Texas Culture Collection). Isolation location and growth parameters are also displayed.

Species name	Strain ID	Isolation location	Culture temperature	Lighting	Growth media
Fragilariopsis cylindrus	RCC4289	Arctic	4°C	30µmol m^{-2} s^{-1}	*f*/2 + Si
Fragilariopsis cylindrus	RCC 5232	Arctic			
Fragilariopsis cylindrus	RCC 5822	Arctic			
Fragilariopsis sp.	CCAP 1023/3	Arctic			
Phaeodactylum tricornutum	CCAP 1055/9	Arctic			
Porosira glacialis	RCC 1995	Arctic			
Thalassiosira antarctica	CCAP 1085/33	Arctic			
Thalassiosira gravida	CCAP 1085/24	Arctic			
Fragilariopsis cylindrus	CCAP 1023/1	Antarctica			
Fragilariopsis cylindrus	CCAP 1023/10	Antarctica			
Fragilariopsis cylindrus	RCC 6866	Antarctica			
Fragilariopsis sp.	CCAP 1023/6	Antarctica			
Porosira glacialis	CCAP 1060/10	Antarctica			
Thalassiosira antarctica	CCAP 1085/25	Antarctica			
Phaeodactylum tricornutum	CCAP 1055/1	Plymouth, UK	15°C		
Phaeodactylum tricornutum	UTEX 646	Finland			

2.1.4 DNA extraction for Polymerase Chain Reaction (PCR)

In most cases the Phire plant direct PCR kit (Thermo Scientific, Massachusetts, USA) was used for PCR amplification. Cell culture (2 µl) was added to 18 µl dilution buffer and 5µl was used directly into the PCR reaction mixture.

For recalcitrant templates where the Phire plant direct PCR kit failed to achieve amplification, DNA was extracted using the MyTaq extract PCR kit (Bioline, London, UK). 1-2 ml of diatom culture was pelleted in a microcentrifuge tube using a benchtop centrifuge at 10,000 rpm and the supernatant removed. Buffer A (20 µl) was added as well as 10 µl buffer B and 70 µl

nuclease free water. The tube was placed into a heat block at 75°C for 5 minutes and vortexed twice during this time. The reaction was then quenched by incubating the tube at 95°C for 10 minutes after which the mixture was centrifuged for 1 minute at 10,000 rpm to pellet cell debris and the supernatant carefully removed and dispensed into a sterile microcentrifuge tube. DNA extract (0.5-1 µl) was used in PCR reactions.

2.1.5 Polymerase chain reaction (PCR)

All PCRs used the Phire plant direct PCR kit using either the dilution buffer for DNA templates or the extracted DNA as stated above. Water or dilution buffer was used as negative controls in all PCRs and *F. cylindrus* was used as a positive control for all genes including 18S, *rbcL,* B_{12}-dependent methionine synthase and B_{12}-independent methionine synthase. PCR conditions followed the manufactures guidelines and details can be found in Appendix 2, but in brief: 98°C for 5 minutes, 30-40 cycles of 98°C for 5 seconds, "annealing temperature" for 5 seconds, 72°C for 1 minute followed by a final extension of 72°C for 1 minute.

2.1.6 Gel electrophoresis

Agarose (Bioline) was added to Sodium Borate buffer ((Brody & Kern, 2004), Appendix 3) to reach a concentration of 0.8-1%. 1 ml GelRed 1X (Biotium, California, USA) was added to molten agarose before setting the gel. Gels were run at 90 V for 45-60 minutes and visualised under UV light.

2.1.7 Sequencing and sequence editing

PCR products were cleaned to remove PCR reagents and sequenced via Sanger sequencing through SourceBioscience (Cambridge, UK). Forward and reverse reads were trimmed and aligned using Geneious Prime software (https://www.geneious.com/) and consensus sequences produced.

2.1.8 Measuring growth and specific growth rate calculations

Growth was monitored either through direct cell counts using a haemocytometer and light microscope or through optical density readings (750 nm) using a Tecan Sunrise absorbance plate reader. Specific growth rates were calculated using Equation 1, where μ = specific growth rate, D1 and D2 correspond to density 1 and 2 and T1 and T2 correspond to time point 1 and 2.

Equation 1

$$\mu = \frac{Ln(D2) - Ln(D1)}{(T2 - T1)}$$

2.2 Fieldwork

2.2.1 Isolation of Antarctic diatom strains

Water samples for diatom isolations were collected during the Austral Summer season (January-February 2019) at the UK Rothera Research Station, Antarctica. Water samples were first passed through a 50 μm nylon mesh filter and the filter washed back into a separate container resulting into two size fractions, >50 μm and <50 μm. In some cases, a subsample of each size class was concentrated via centrifugation (800 *g* at 2°C) to aid isolation. Single diatom cells were isolated using glass micropipettes using an inverted microscope (Zeiss, Germany). The single cells were dispensed into sterile, filtered seawater to wash the cell, and the cleaning step repeated in triplicate. The cleaned cell was then dispensed into a 96-well microtiter plate containing 100 μl *f*/10 growth media (1:5 dilution of Guillard's *f*/2 nutrients, Guillard & Ryther 1962) and placed into a culture cabinet (Sanyo, Osaka, Japan) at 1 to 2°C under a constant light intensity of 50 μmol m^{-2} s^{-1}. The isolation procedures were carried out on ice at all times where possible. To increase the diversity of diatom species, a second isolation method was utilized to promote the growth of benthic species. Diluted samples were plated onto *f*/10 agar plates (1% agar, 100% seawater) and placed into a culture cabinet under the same conditions as above. As cultures grew, they were steadily upscaled into larger volumes and the nutrient concentrations progressively increased up to standard *f*/2. Cultures were shipped to the UK at 0 to 2°C in *f*/2 media under low constant light <15 μmol m^{-2} s^{-1} either in 48-well microtitre plates and/or agar slopes. Upon arrival at Cambridge, UK, samples were held under APHA/DEFRA license number 50971/198977/5 and were checked

to ensure they remained unialgal. They were upscaled to 30 ml for identification analysis, using molecular barcoding and morphological methods as described below. Strains have been deposited into CCAP.

2.2.2 Genetic identification of strains

Specific primers for the nucleus-encoded 18S ribosomal small-subunit V4 region (Zimmermann *et al.*, 2011) and the chloroplast-encoded large subunit of RuBiScO (*rbc*L) (Hamsher *et al.*, 2011) were amplified and sequenced (Appendix 4). Consensus sequences were sequence similarity searched using blast against the NCBI Blastn (nr/nt) database https://blast.ncbi.nlm.nih.gov/Blast.cgi (Altschul *et al.*, 1990) and the best match acquired to form putative identifications.

2.2.3 Morphological identification of strains

Morphology was used to validate genetic identification. To produce cleaned diatom frustule slides for morphological identification and imaging, the protocol of Trobajo & Mann, (2019) was followed. In short, ~1 ml of cell culture was fixed by adding ethanol to a concentration of 30% in a microcentrifuge tube and left overnight. The supernatant was gently removed, and the cells washed with distilled water and pipetted onto 18 mm diameter glass cover slips and left to dry in a fume hood overnight. Once dry, the cover slip was moved onto a ceramic hotplate at ~95°C and 30% hydrogen peroxide pipetted on top to oxidise biological material, repeating a total of three times when evaporated. Coverslips were then mounted onto glass microscope slides using Nortland Optical Adhesives No. 61 (Cranberry, USA). Slides were observed using an Olympus BX-51 microscope (Tokyo, Japan) using phase contrast optics and brightfield optics for live images, to identify morphological features, based on the descriptions of Hasle & Syvertsen, (1996) and Scott *et al.*, (2005).

2.3 Estimating thermal tolerance

2.3.1 Temperature growth assay

Experimental stock cultures (30 ml) were grown as already described under constant illumination at 30 µmol m^{-2} s^{-1} in 30 ml Nunc flasks in standard *f*/2 + Si media for two weeks. Cultures were diluted to exponential growth phase with sterile *f*/2+Si media before aliquots were transferred into universal tubes and placed into standing incubators (Sanyo, Camlab (Cambridgeshire, UK), LMS (Kent, UK), Labcold (Hampshire, UK), Vindon Scientific Ltd (Manchester, UK) and Snijder labs (Tilburg, Netherlands) at the experimental temperatures (-1.5°C, 1°C, 4°C, 7°C, 10°C, 12°C, 15°C and 18°C) at a light intensity of 30 µmol m^{-2} s^{-1}. Cultures were acclimated for one week, after which the cell density was estimated via cell counts in a haemocytometer using a light microscope. The cell density of experimental cultures were matched by diluting cultures to the culture with the lowest cell density. Cultures were inoculated into 96-well plates at cell densities of; $2.5x10^3$/ml for *T. antarctica* and *P. glacialis* strains, $10.5x10^3$/ml for *F. cylindrus* strains and $3.5x10^5$/ml for *P. tricornutum*, in a final volume of 200 µl sterile *f*/2+Si media. Plates were sealed with micropore tape and placed into standing incubators in the conditions stated above.

Growth was monitored by measuring the optical density at 750 nm at regular intervals. Representative cell counts using a haemocytometer were taken at a few time points during the experiment to produce standard curves of the relationship between OD and cell numbers.

2.3.2 Xanthella Ltd bioreactor growth assays

A second assay using a subset of the initial temperatures (-1, 4, 8 and 12°C) was carried out on both *F. cylindrus* and *P. glacialis* strains under more controlled conditions using the Zanthella Ltd CryoPharos bioreactors under a light intensity of 40 µmol m^{-2} s^{-1} with a 16:8h light dark cycle. 10 ml experimental cultures were acclimated for 1 week then inoculated into sterilised 30 ml glass tubes to reach starting densities of $3.9x10^3$ and $1x10^3$ for *F. cylindrus* and *P. glacialis,* respectively. Cultures were shaken once a day and cell counts used to estimate growth.

This same experiment was used to characterise the metabolomic characteristics of both *F. cylindrus* and *P. glacialis* strains, changing only the culture temperatures which were -1, 0, 2 and 4°C).

2.3.3 Modelling thermal tolerance

Specific growth rates were calculated and used to model the thermal performance curve of each strain using the "rTPC" package following the package guidelines (Padfield *et al.*, 2021). Models were first assessed by eye for goodness of fit, after which the package's in-built AICc (Akaike Information Criteria corrected for small sample size) score function was used to identify the best model. The three models with the lowest AICc score were assessed again and the model with the best fit used.

2.4 Metabolomic techniques

2.4.1 Pigment extraction and spectrophotometric quantification

To investigate the basic pigment composition, 1-2 ml of culture was pelleted in a microcentrifuge tube in a benchtop centrifuge at 3000 *g* at experimental temperature, the supernatant removed and the pellet flash frozen and stored at -80°C. To extract, samples were thawed and 1 ml dimethylformamide (DMF, ThermoFisher Scientific) added. Samples were vortexed for 15 minutes then centrifuged at 10,000 rpm in a benchtop centrifuge to pellet cell debris and the supernatant removed and pipetted into plastic cuvettes (resistant to DMF). A basic pigment composition analysis was measured in a spectrophotometer at the following absorbances; 480 (carotenoids), 630 (chlorophyll *c*1 + *c*2) and 664nm (chlorophyll a). To calculate the quantities of chlorophyll *a*, chlorophyll *c*1 + *c*2 and total chlorophyll the equations from Jeffrey & Humphrey, (1975) were used and to calculate total carotenoids the equation from Wellburn, (1994) was used (Equations 2-5 respectively). The equations used in Jeffrey & Humphrey, (1975) are based on 90% acetone, but there was found to be a negligible effect of applying these equations to DMF extracts (Speziale *et al.*, 1984). Samples were pipetted into 300 µl glass GC vials and stored at -80°C until further analysis.

Equation 2

$$Chl\ a = 11.47A_{664} - 0.40A_{630}$$

Equation 3

$$Chl\ c_1 + c_2 = 24.36A_{630} - 3.73A_{664}$$

Equation 4

$$Total\ Chl = 23.96A_{630} + 7.74A_{664}$$

Equation 5

$$C\ x + c = \frac{1000A_{480} - 0.89\ Chl\ a}{245}$$

2.4.2 High performance liquid chromatography (HPLC) analysis of pigments

To identify individual pigments, the extracted pigments in DMF were analysed via HPLC (Surveyor HPLC system, Thermo Scientific) using the tri-gradient method of Wright *et al.*, (1991). 25 µl of samples was injected using a 50 µl loop and pigments were separated on a C18 column (150 mm x 2.5 mm, Phenomenex, Macclesfield, UK). Pigments were detected using a photodiode-array detector at 430 and 664nm for carotenoids and chlorophylls respectively. Reference standards (diatoxanthin, diadinoxanthin, mixed pigments (DHI lab products, Hørsholm, Denmark) and Chl *a* and fucoxanthin (Sigma Aldrich, Missouri, USA) were used for identification based on coelution and standard curves created to enable quantification.

2.4.3 Metabolic fingerprinting using Fourier transform-infrared spectroscopy (FT-IR)

FT-IR was used to produce a basic metabolic fingerprint of algal samples. 4-5 ml of cell culture was pelleted at 2000 *g* at experimental temperature and flash frozen in a -80°C freezer and stored until analysis. Samples were thawed and washed with 0.5 M ammonium formate (Thermo Fisher) via centrifugation at 2000 *g*, the supernatant discarded and the cleaning step repeated. Sample pellets were resuspended in 100 µl 0.5 M ammonium formate and 20 µl pipetted onto the shiny side of a segment of tinfoil in triplicate. Tinfoil has previously been shown to be a good substrate for FT-IR analysis avoiding any confounding of biological properties (Cui *et al.*, 2016). Samples were placed into an oven at 40°C for 10

minutes to dry after which they were stored in a desiccator until analysis. Samples were analysed using a Perkin Elmer Spectrum Two FT-IR (Waltham, Massachusetts, USA) using attenuated total reflection (ATR) at an absorbance spectra range of 400-4000 cm^{-1}.

2.4.4 Lipid extraction and gas chromatography analysis

To further investigate the metabolomic composition of algae strains, lipids were extracted and analysed via gas chromatography. 10-15 ml of culture of culture was pelleted at 2000 *g* at experimental temperature, the supernatant removed and flash frozen at -80°C. Lipids were extracted from wet biomass using a modification of the Bligh & Dyer, (1959) described in Davey *et al.*, (2014). Pellets were first extracted in 5ml chloroform:methanol (2:1) with the addition of 200 µl pentadecanoic acid (C:15) internal spike (1 mg/ml) and transferred into 50 ml Schott bottles (Duran, Wolverhampton, UK), then sonicated in an ice cooled sonication water bath for 30 minutes. Samples were transferred into 30 ml Kimble tubes (DWK life Sciences, Mainz, Germany) and an additional 10 ml chloroform:methanol (2:1) added. Deionised water (5 ml) was added and tubes vortexed for 2 minutes and centrifuged at 972 *g* for 4 minutes at 4°C. The bottom chloroform phase containing lipids was removed and transferred into 30 ml tubes (Schott Duran) and the methanol phase transferred into 15 ml falcon tubes and stored at -80°C until further metabolite analysis. The chloroform phase was evaporated using a GeneVac EZ-2 centrifugal evaporator (GeneVac, Ipswich, UK) under a stream of nitrogen, samples were resuspended in 200 µl n-Heptane (Thermo Fisher) and analysed using Thermo-Fisher gas chromatography with flame ionization detection (GC-FID) using the method detailed in Horst *et al.*, (2012).

Lipid extracts were then derivatised to create fatty acid methyl esters (FAMEs) and analysed via gas chromatography – mass spectrometry (GC-MS). 75 µl of lipid extract was transferred to a 3 ml Kimble tube and 3 ml methanol:sulphuric acid (2.5%v/v) added, tubes were vortexed gently and the screw cap lids sealed with parafilm, before placing into a pre-heated water bath at 60°C and incubated for 4 hours. Samples were cooled to room temperature and 3 ml deionised water added to quench the reaction after which, FAMEs were extracted by adding 3 ml hexane (Thermo Fisher), vortexed and centrifuged at 2000 *g* at 20°C. The top hexane layer containing FAMEs was transferred into a 30 ml tube and the bottom phase re-extracted with another 3 ml hexane and the process repeated. The two hexane extracts were

combined and then evaporated (GeneVac) under a stream of nitrogen followed by resuspension in 120 µl n-heptane and transfer into a GC vial containing a 300 µl insert. Samples were analysed using a Thermo-Fisher gas chromatography with mass spectrometry (GC-MS) following the methods of Davey *et al.*, (2014).

2.5 Vitamin growth characteristics

2.5.1 Testing vitamin requirements of diatom strains

To investigate the vitamin requirements of diatom strains, a growth assay utilising the three vitamins present in *f*/2 media (cobalamin (B_{12}), thiamine (B_1) and biotin (B_7)) was developed. Experimental cultures (30 ml) were grown as detailed in section 2.1.1 for two weeks, after which 6 ml was centrifuged at 1000 *g* at 4°C for 5 minutes and the supernatant removed. The cell pellet was washed to remove traces of growth media by resuspension in sterile sea water followed by centrifugation and the wash step repeated. The cell density of cultures was estimated and adjusted so that 20 µl inoculated into 180 µl treatment media in a 96-well microtitre plate (Sarstedt, Germany) would provide a cell density of $17.6x10^3$/ml. Fig. 2.1 shows the layout of the microtitre plate and the various media treatments. Standard *f*/2 vitamin concentrations were 500 ng/L B_{12} and B_7 and 100 µg/L B_1. Plates were sealed with micropore tape (3M, Minnesota, USA) and grown at 4°C. Optical density at 750 nm was used as a proxy to monitor growth using a Tecan Sunrise absorbance plate reader (Männedorf, Switzerland). After the initial growth assay termed "1^{st} subculture", where B_{12} is not present in the media but likely to be present within the cells, cells were subcultured (1/10 dilution) into fresh media and the assay ran a second time termed the "2^{nd} subculture".

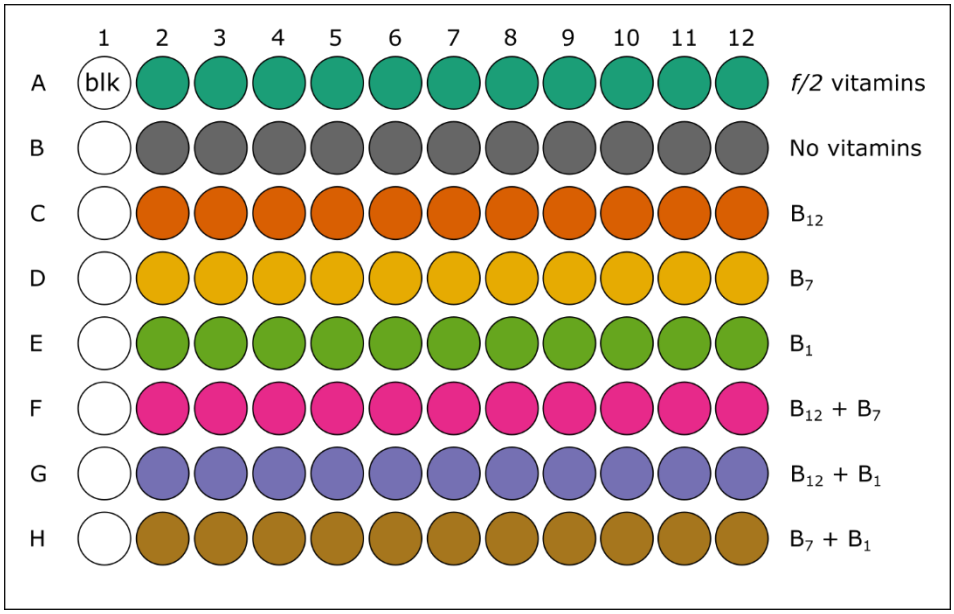

Figure 2.1 Microtitre plate configuration for determining B vitamin requirements. Treatment media (200 µl) contained various combinations of B vitamins: cobalamin (B_{12}, 500 ng/L), thiamine (B_1, 100 µg/L), and biotin (B_7, 500 ng/L) or no vitamins used to determine the requirements of strains.

2.5.2 B_{12} confirmation assay

To confirm B_{12} was a limiting factor in Arctic *F. cylindrus*, B_{12} was added back to "2nd subculture" cultures to see whether growth could be restored. Experimental cultures were grown and cleaned as described in Section 2.5.1. The cleaned cultures were resuspended in sterile seawater and inoculated into 40 ml *f*/2 media in sterile 100 ml Erlenmeyer flasks with or without the addition of vitamin B_{12} (500 ng/L or no B_{12} respectively) and grown for seven days to acclimate cells (1st subculture). Cultures were grown at 4°C under a light:dark cycle of 16hours:8hours at an intensity of 40 µmol m^{-2} s^{-1} and flasks were shaken once daily to resuspended cells. After seven days the cell density of the 1st subculture cultures was calculated and inoculated into fresh 40 ml *f*/2 media with or without the addition of B_{12} in triplicate at a cell density of 5x10^4 cells/ml (2nd subculture). Growth was monitored through cell counts using a haemocytometer. At mid-exponential phase B_{12} was added to all the cultures, resulting in B_{12} concentrations of 1000 ng/L and 500 ng/L in treatments with and without an initial B_{12} treatment, respectively.

2.5.3 Growth of diatom strains over B_{12} concentrations

Cells were grown and cleaned as described in Section 2.5.1. Cell culture (20 µl) was inoculated into 180 µl *f*/2 media in a 96-well microtitre plate. Eleven concentrations of B_{12} were used starting from 2000 ng/L serially diluted 1:2 to a final concentration of 1.9 ng/L and a no B_{12} control. Growth was monitored regularly by measuring OD at 750 nm.

2.5.4 Detection of *METE* and *METH* in *F. cylindrus*

Andre Holzer identified *METE* and *METH* gene sequences within the *F. cylindrus* genome (Mock *et al.*, 2017) by sequence similarity searching complementary sequences from *C. reinhardtii* (Appendix 5) using IGV (https://software.broadinstitute.org/software/igv/). Allelic variations of both genes were identified and extracted using Samtools (http://www.htslib.org/) and aligned to form a consensus sequence using Geneious Prime software.

Multiple primer sets were designed using Geneious Prime and SnapGene (https://www.snapgene.com/). Primer pairs of various lengths were used to identify the presence of *METE,* and an extended PCR product (c6000 bp) was designed by rooting primers within the two adjacent genes encompassing the entire *METE* gene. Further primer pairs were designed within the 3′ and 5′ UTR regions and within the CDS regions of the gene. The available genome sequence data for *METH* were poor and primers could only be designed within a ~900 bp region of CDS at the 3′ end. Primer details are described in Appendix 4). Three primer pairs were taken forward for future analysis and sequencing, SCME_5 and SCME_95 (2575bp), SCME_9 and SCME_91 (3277bp) for *METE* and SCMH_1 and SCMH_99 (828bp) for *METH* (Fig. 2.2).

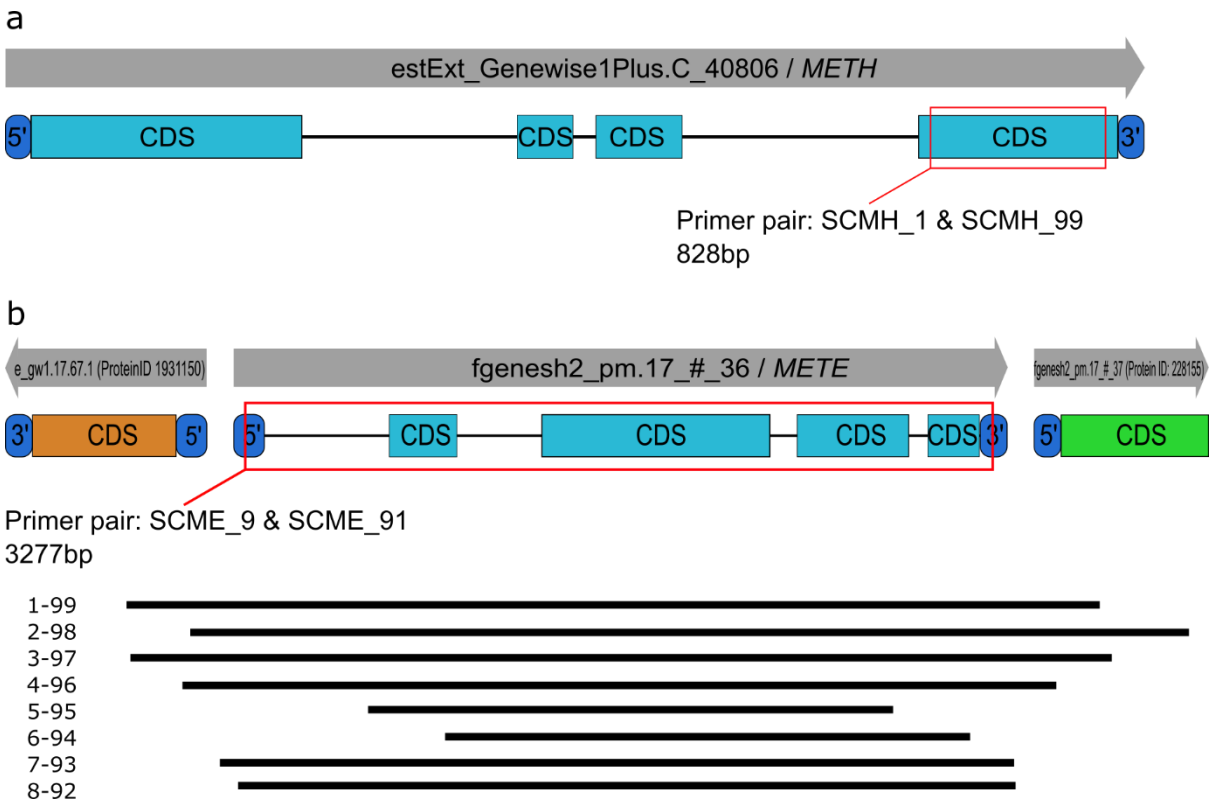

Figure 2.2 Methionine synthase gene model schematic. Primer locations used to amplify a) *METH* and b) *METE* are indicated by the red boxes. Additional primer pairs designed for *METE* are numbered forward primers 1-8 with the corresponding reverse primer 99-92. Primer information is displayed in Appendix 4 and are displayed as e.g., 1-99 = SCME1 and SCME99.

2.6 Statistical analysis

Statistical analyses were conducted in R (R Core Team, 2021) using R Studio (R Studio Team, 2021) or Excel unless otherwise specified. Graphs were produced using ggplot2 (Wickham, 2016). Specific statistical tests are specified within the results.

Chapter 3 - New environmental strains of Antarctic marine diatoms: increasing representation for experimental study

3.1 Introduction

With the polar regions experiencing various environmental changes as a result of anthropogenic activity, there is a need to study the organisms within these environments to understand future biodiversity. Although much can be learned through long term ecological monitoring programs e.g., Rothera Oceanographical and Biological Time Series (RaTS, (Clarke *et al.*, 2008)) and Palmer Long Term Ecological Research (LTER, (Smith *et al.*, 1995)), focusing on *in situ* responses, it is still important to study species in the laboratory. Laboratory study enables the controlled experimentation of specific factors and species-specific responses, helping to disentangle the complexity of natural environments. To study the biology of polar diatoms, it is vital to have living material available for experimentation. The isolation and deposition of strains into public culture collections has been instrumental to algal research and aids with scientific reproducibility. The number of polar diatom strains available however, is confounded by the difficulty in acquiring living material (expensive fieldwork and logistics) and the resources needed to keep these strains in culture (cold temperature incubators). These confounding factors mean there are a lower number of polar strains available compared to other strains from temperate or tropical environments. In three major culture collections (National Center for Marie Algae and Microbiota (NCMA), Culture Collection for Algae and Protozoa (CCAP) and Roscoff Culture Collection (RCC)) the number of polar diatom strains available are 78, 10 and 90, respectively, whereas the number of temperate strains available are 289, 92 and 337, respectively (as of June 2021).

The issue regarding the number of strains is exacerbated by the age of some strains available, with some isolates having been maintained in artificial conditions for more than 40 years. As an example, the polar diatom *F. cylindrus* (strain - CCMP1102, CCAP 1023/1), used extensively as a model diatom was isolated in 1979 (42 years in culture). Long term culturing at unrepresentative conditions might result in strains which are no longer representative of their environmental counterparts. Previously *Thalassiosira pseudonana* has shown changes in thermal tolerance when cultured at increased temperatures (O'Donnell *et al.*, 2018; Schaum

et al., 2018). Schaum *et al.*, (2018) identified that after ~300 generations or 1 year based on average doubling times, *T. pseudonana* showed a shift in thermal tolerance to high temperatures and genetic divergence through single nucleotide polymorphisms (SNP). Similarly, O'Donnell *et al.*, (2018) identified thermal tolerance shifts in *T. pseudonana* after 350 generations.

A lot of work in microalgal research focusses on one particular strain of a single species. Although the single strain results are important and aid our knowledge, the issue of intraspecific variation cannot be ignored. Diatoms have been shown to have a high degree of intraspecific variation in response to temperature. For instance, the cosmopolitan diatom *Clyndrotheca closterium* exhibited differences in the thermal tolerance over latitude, with Antarctic strains showing the lowest tolerance of higher temperatures (Stock *et al.*, 2019). In addition, Samuels *et al.*, (2021) isolated three strains of *Actinocyclus actinochilus* from the Ross Sea, Antarctica and reported differences in thermal tolerance between strains and the response of strains to simulated heatwaves. This highlights the importance of having multiple strains for experimental study in order to factor in any intraspecific variation.

The goals of this chapter are to:

- Isolate fresh strains of three target species *Thalassiosira antarctica*, *Porosira glacialis* and *Fragilariopsis cylindrus*.
- Isolate and culture a range of Antarctic diatom species.
- Deposit isolated strains into a public culture collection (CCAP).

3.2 Results

Rothera research station on the WAP was selected as a study site due to the logistical access offered through British Antarctic Survey (BAS) and the range of habitats in close proximity. Two months fieldwork was conducted at Rothera in January-February 2019. In order to maximise the diversity of diatom species, various sample sites were chosen based on their environmental features including glacial, neritic and open water (Fig. 3.1). A total of eight sampling events were successfully carried out through the duration of fieldwork with samples acquired via shore sampling, Niskin bottles via small boats and through the assistance of RV Laurence M Gould (National Science Foundation, Fig. 3.1). Site metadata

including temperature, salinity and water depth were recorded using CTD casts (conductivity, temperature, and depth).

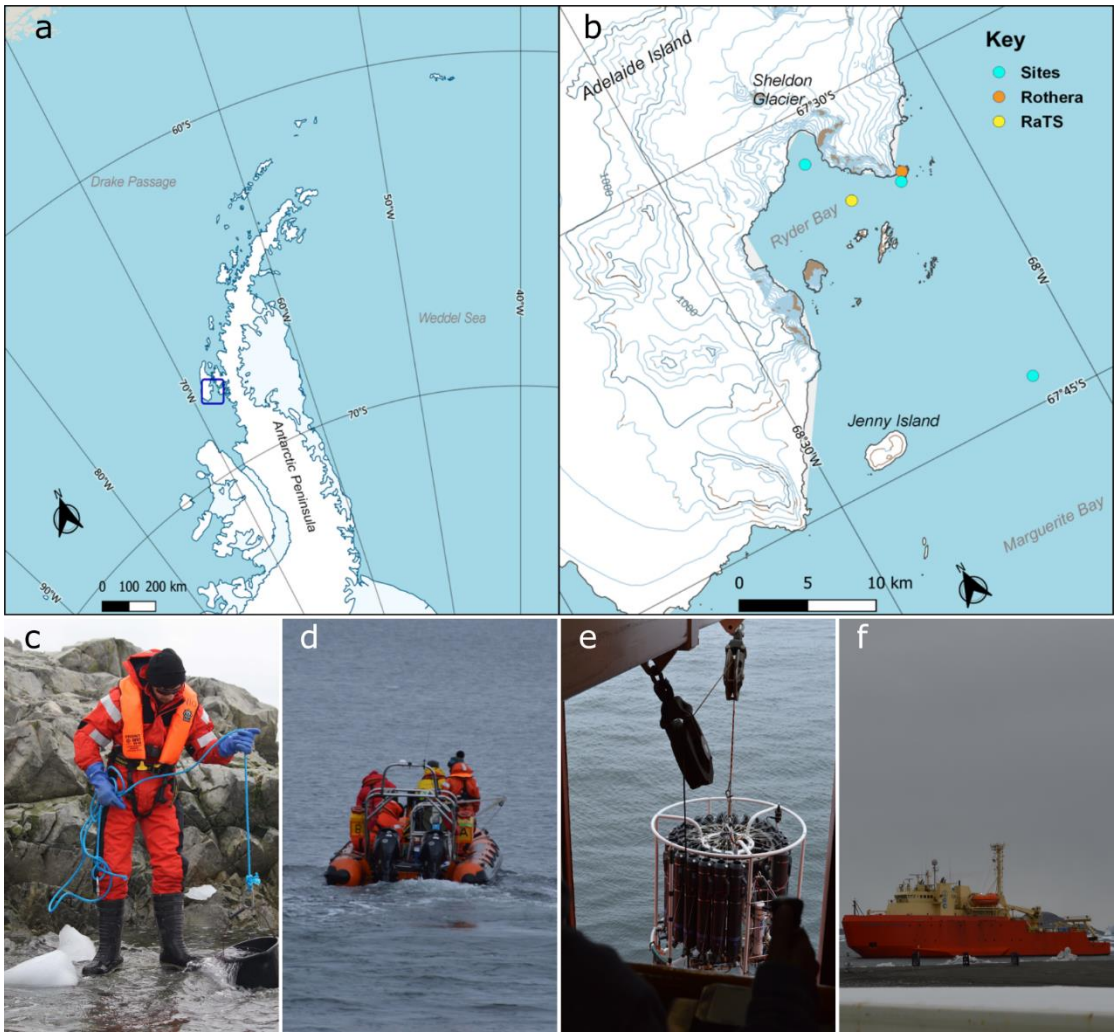

Figure 3.1 Field sample sites and sampling methods. a) Sample location of Adelaide Island on the Western Antarctic Peninsula. b) location of sample sites within Ryder and Marguerite Bay, adjoining Adelaide Island. Maps were produced in Qgis version 3.10.4 Coruña using the base maps derived through the scientific committee on Antarctic research (SCAR) Antarctic digital database collated through the Quantarctica package, Norwegian Polar Institute (https://www.npolar.no/quantarctica/). c) shore sampling d) Small boat sampling e) CTD rosette f) RV Laurence M Gould.

Table 3.1 Metadata of sample sites used for diatom isolations. Eight sample sites used for diatom isolations in Ryder Bay and Marguerite Bay Antarctica with corresponding water temperature and salinity at the specified depth. PSU = partial salinity unit.

Sample ID	Location	Date	Depth (m)	Water Temperature (°C)	Salinity (PSU)
S1	Rothera, South Cove (-67.572°S, -68.133°W)	14/01/2019	0.5	1	33
S2	Sheldon Glacier (-67.534°S, -68.265°W)	16/01/2019	0	1	33
S4	Jenny site (-67.731°S, -68.098°W)	19/01/2019	20	0	33
S6	RATs (-67.570°S, -68.225°W)	08/02/2019	15	0	32
S7	RATs (-67.570°S, -68.225°W)	18/02/2019	15	0	33
S8	RATs, site 3 (-67.574°S, -68.134°W)	16/02/2019	15	0	33

Metadata was collected at each sample site and is shown in Table 3.1 and CTD casts are shown in Appendix 6. Metadata is often lacking from strain isolations but is very important in understanding the responses of strains to environmental factors. Temperatures at the sample sites ranged between 0°C and 1°C in accordance with the range reported in the area (-1.8°C – 1°C, (Clarke *et al.*, 2008), these temperatures show how the 4°C maintenance temperature used in many culture collections may be unrepresentative of many polar species natural environments. Considering the sample site temperatures, efforts were made to keep isolated strains as close to these temperatures as possible during fieldwork, transport of strains to the UK and culture at BAS, Cambridge

Around 400 single cell isolations were conducted, of which a total of 36 cultures were successfully established in the laboratory, a success rate of 9.5%.

3.2.1 Genetic identification

In order to form putative species identifications, 18S V4 (Zimmermann *et al.*, 2011) and 3P-*rbc*L (Hamsher *et al.*, 2011) diatom specific barcodes were used. Genetic barcodes were successfully amplified and sequenced in all strains identifying 12 species. The 18S barcode failed to amplify in *C.* cf. *flexuosus* and the 3P-*rbc*L failed to amplify in *P. truncata* and in both cases the alternative barcode was amplified and sequenced to give putative identities. Genetic sequences were searched for sequence similarity in the NCBI BLASTn database (Altschul *et al.*, 1990) and maximum likelihood phylogenetic trees produced for 18S and *rbc*L genes (Fig. 3.2 and 3.3 respectively) using Mega X software (Kumar *et al.*, 2018) after performing multiple sequence alignments using MUSCLE (Edgar, 2004).

Both barcodes resulted in similar phylogenies, forming three clades comprising of two clades with centric diatoms and one pennate clade Fig. 3.2 and Fig. 3.3. Amongst the strains there was surprisingly high diversity with species of centric, raphid and araphid taxa represented. Centric taxa had the largest representation but the number of raphid and araphid taxa shows the sample sites and methods used was able to select for a wide range of taxa. Congruency was strong between the two trees with only one difference between the two phylogenies which was the grouping of *Synedropsis* spp. via the 3P-*rbc*L barcode into one of the centric clades instead of the pennate clade. Nodes were supported by high bootstrap values helping to confirm strong relationships between the isolated strains and the strongest similarity hit in the NCBI database. There was no intraspecific variation of either of the two barcodes in species for which multiple strains had been isolated i.e., *F. cylindrus*, *T. tumida*, *S. microtrias* and *P. pseudodenticulata*. However, intraspecific variation cannot be ruled out with these limited genetic analyses alone. Strain information including Genbank accession numbers are presented in Table 3.2.

3.2.2 Morphological identification

Though genetic barcoding is a good initial method to form putative identifications, for many species there is still a requirement to use morphological features to validate the identification. For example, species of the genera *Thalassiosira* are closely related and also have similar morphological features which need to be validated in order to be confident of identification. To do this, the silica frustules were cleaned and observed under phase contrast microscopy and detailed species identifications described below. Phase contrast was chosen because it was not possible to achieve the resolution needed to make out morphological features using brightfield. Despite this, acquiring images of intact cells at the correct orientation was often difficult, especially for cells with external appendages. There were no morphological differences other than size variation shown in strains within the same species.

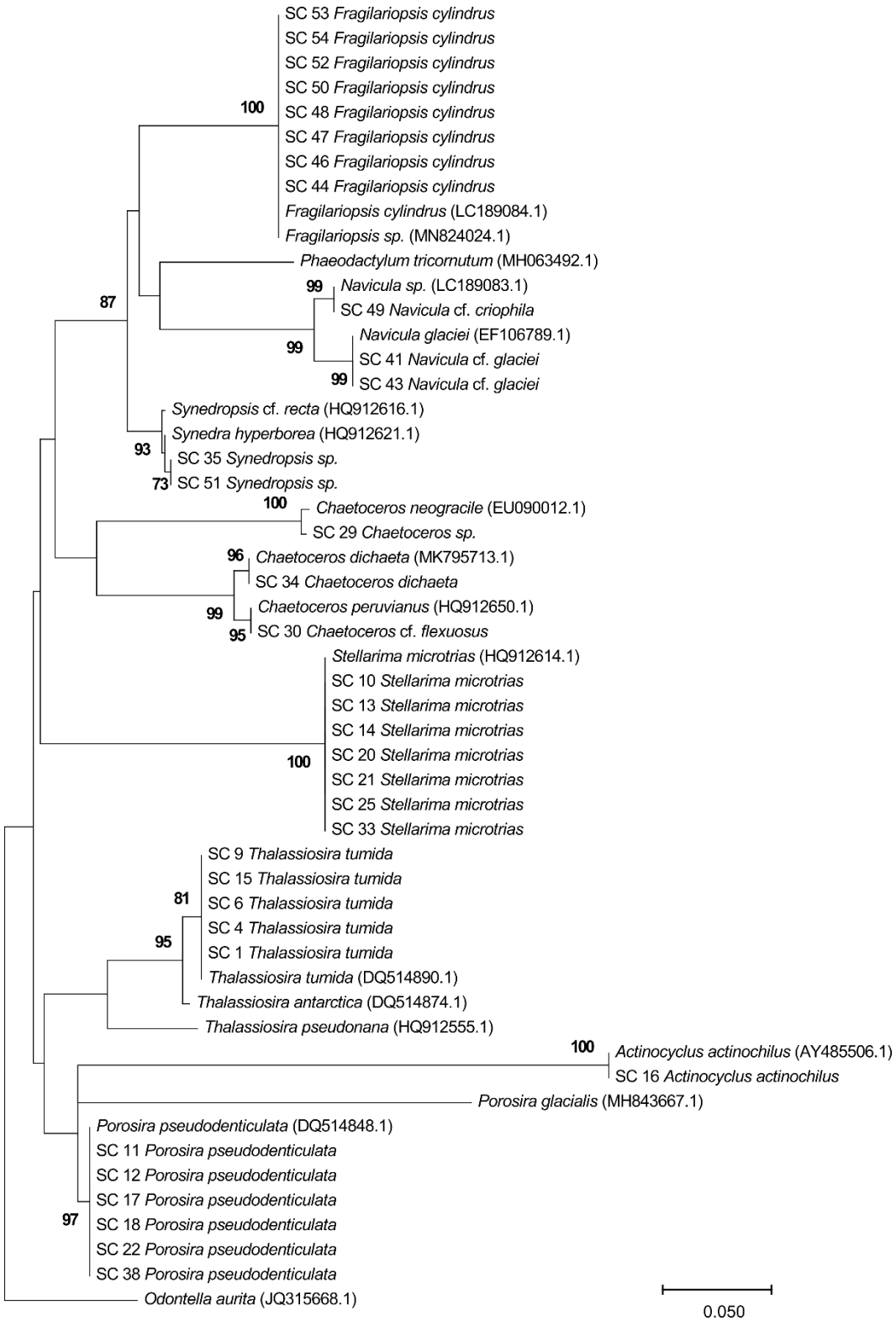

Figure 3.2 Phylogeny of the 18S V4 barcode across isolates. Inferred from a Maximum likelihood tree using the Tamura 3-parametre model + discrete Gamma distribution substitution model. The tree is drawn to scale, with branch lengths representing number of substitutions per site. Bootstrap values >70% are presented and are a result of 1000 replications. Closest NCBI sequence similarity hits are also included with the accession numbers. Produced using Mega X (Kumar *et al.*, 2018).

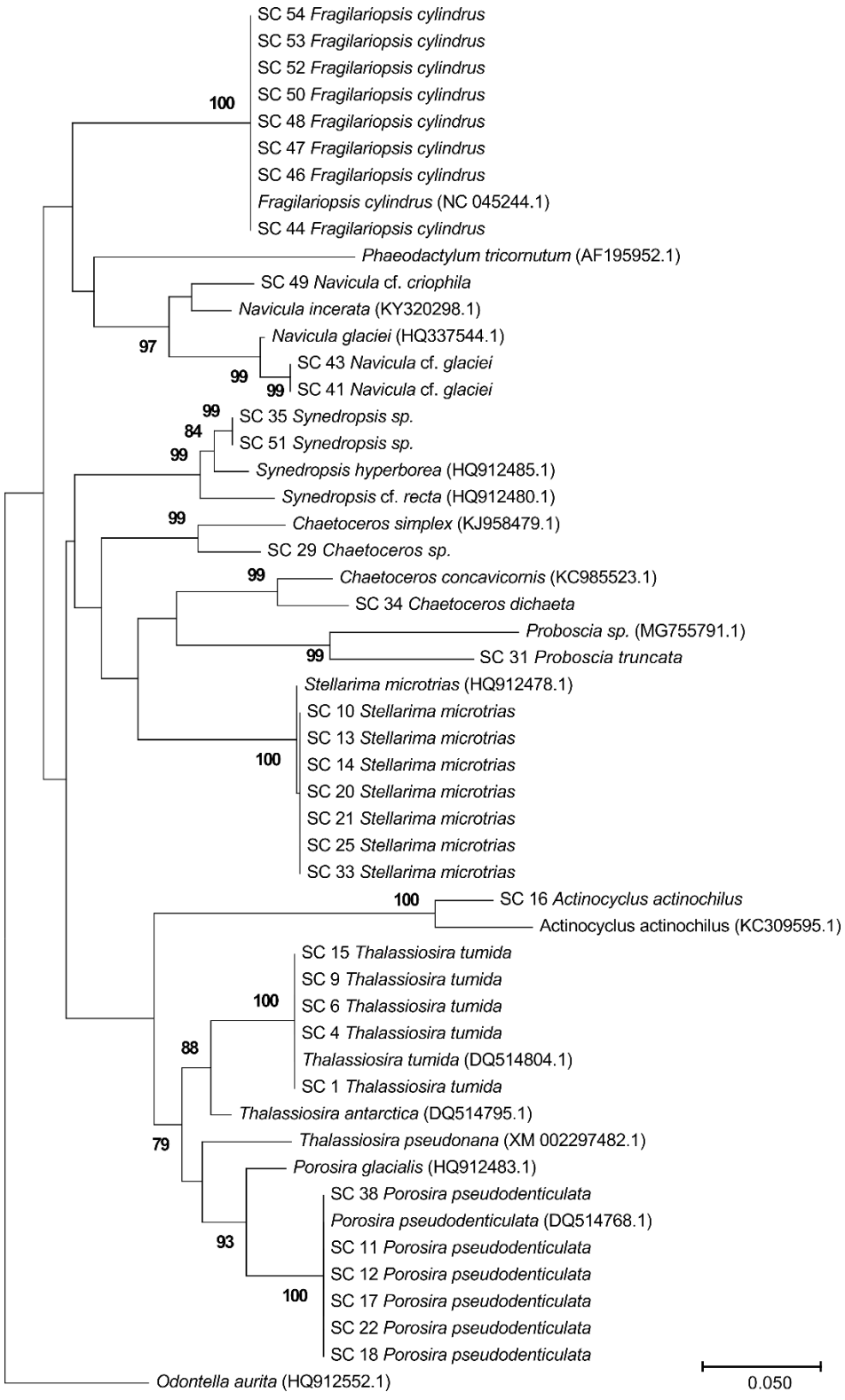

Figure 3.3 Phylogeny of the *rbc*L-3P barcode across isolates. Inferred from a Maximum likelihood tree using a General Time Reversible + discrete Gamma distribution (GTR+G) substitution model. The tree is drawn to scale, with branch lengths representing number of substitutions per site. Bootstrap values >70% are presented and are a result of 1000 replications. Closest NCBI sequence similarity hits are also included with the accession numbers. Produced using MEGA X (Kumar *et al.*, 2018).

Table 3.2 List of newly isolated Antarctic strains. Isolated strain information including strain IDs, CCAP strain identifier, collection site and GenBank accession numbers for molecular barcodes.

Strain ID	CCAP ID	Species	Site	Genbank Accession Number	
				18S-V4	***rbc*L-3P**
SC 1			1	MZ161866	MZ189324
SC 4	1085/37		4	MZ161867	MZ189325
SC 6		*Thalassiosira tumida*	4	MZ161868	MZ189326
SC 9			4	MZ161869	MZ189327
SC 15	1085/40		6	MZ161875	MZ189333
SC 11	1060/11		7	MZ161871	MZ189329
SC 12			7	MZ161872	MZ189330
SC 17		*Porosira*	6	MZ161877	MZ189335
SC 18		*pseudodenticulata*	6	MZ161878	MZ189336
SC 22			6	MZ161881	MZ189339
SC 38			8	MZ161888	MZ189346
SC 16	1000/2	*Actinocyclus actinochilus*	6	MZ161876	MZ189334
SC 10	1075/2		7	MZ161870	MZ189328
SC 13	1073/3		7	MZ161873	MZ189331
SC 14			7	MZ161874	MZ189332
SC 20		*Stellarima microtrias*	6	MZ161879	MZ189337
SC 21			6	MZ161880	MZ189338
SC 25			7	MZ161882	MZ189340
SC 33			8	MZ161885	MZ189343
SC 31	1064/3	*Proboscia truncata*	4	n/a	MZ189342
SC 29	1010/54	*Chaetoceros* sp.	4	MZ161883	MZ189341
SC 30	1010/55	*Chaetoceros* cf. *flexuosus*	4	MZ161884	n/a
SC 34	1010/56	*Chaetoceros dichaeta*	8	MZ161886	MZ189344
SC 41	1050/16	*Navicula* cf. *glaciei*	1	MZ161889	MZ189347
SC 43			1	MZ161890	MZ189348
SC 44	1023/7		2	MZ161891	MZ189349
SC 46			2	MZ161892	MZ189350
SC 47			2	MZ161893	MZ189351
SC 48	1023/10	*Fragilariopsis cylindrus*	2	MZ161894	MZ189352
SC 50			4	MZ161896	MZ189354
SC 52	1023/11		4	MZ161898	MZ189356
SC 53			7	MZ161899	MZ189357
SC 54			1	MZ161900	MZ189358
SC 49	1050/18	*Navicula* cf. criophila	4	MZ161895	MZ189353
SC 35	1063/1	*Synedropsis* sp.	8	MZ161887	MZ189345
SC 51	1063/2		4	MZ161897	MZ189355

3.2.2.1 Strain identifications:

Actinocyclus actinochilus (Ehrenberg) Simonsen 1844

(Fig.3.4 a-c)

Culture characteristics: Vegetative cells solitary with densely packed chloroplasts in both valves.

Frustule characteristics: Frustules show a central annulus with radial rows of areolae. A thin marginal ring of fascicles with distinct ring of large labiate processes and a pseudonodulus within the marginal ring can be seen in some cells. 25-30 µm diameter.

Stellarima microtrias (Ehrenberg) Hasle and Sims 1986

(Fig. 3.4 e-f)

Culture characteristics: Vegetative cells solitary or cells attached irregularly, attaching to the centre of valve face or the edge of the valve face in short or long chains (Fig. 3.6a). Densely packed chloroplasts of random size clearly distributed into each valve face when in girdle view.

Frustule characteristics: Frustules convex with three to five central labiate processes, with small fasciculate areolae. 35-70 µm diameter.

Thalassiosira tumida (Janisch) Hasle 1971

(Fig. 3.4 g-i)

Culture characteristics: Vegetative cells often in small chains connected by multiple threads from the centre of the valve (Fig. 3.6b), cells sometimes solitary. Strutted processes can sometimes be seen projecting from the valve face in girdle view with LM.

Frustule characteristics: Frustules show a centre ring of strutted processes and strutted processes distributed on the valve face. Areolae fasciculate, one marginal ring of strutted processes with numerous (3-7) labiate processes. 30-60 µm diameter.

Porosira pseudodenticulata (Hustedt) Jousé 1962

(Fig. 3.4 j-l)

Culture characteristics: Vegetative cells often solitary or joined tightly in small chains (Fig. 3.6c). Chloroplasts densely packed and multiple strutted processes can be seen with LM. Dense cultures are characteristically viscous.

Frustule characteristics: Frustules show radial areolae with numerous strutted processes distributed on the valve face. A large labiate process can be clearly seen in LM along the marginal ring. 40-60 µm diameter.

Proboscia truncata (Karsten) Nöthig & Ligowski – Identified using Jordan et al. (1991)

(Fig. 3.5 a-b)

Culture characteristics: Cells largely chain-forming, often with >7 cells, connected via the proboscis (Fig. 3.6d). Chloroplasts elongated and multiple.

Frustule characteristics: Bands are rhomboid and distributed in multiple columns. Heavily silicified proboscis, claspers present and located ventrally. Apical axis 80-125 µm.

Chaetoceros dichaeta Ehrenberg 1844

(Fig. 3.5 c-e)

Culture characteristics: Cells sometimes solitary but often in straight or sometimes curved chains, aperture is large and rectangular. Setae are long and crossed when in chains (Fig. 3.6e).

Frustule characteristics: Valve faces flat and central spine present. Setae long and highly silicified, protruding out from valve face within the cell margins and bending outwards about 45° and crossing over in a crisscross formation in chain form, forming a rectangle aperture. Apical axis 20-35 µm.

Chaetoceros cf. *flexuosus* Mangin 1915

(Fig. 3.5 f-h)

Culture characteristics: Cells often solitary, forming small chains occasionally with setae twisted around sibling setae, a characteristic of *C. flexuosus* (Fig. 3.6f and g). Slit like aperture between cells. Rectangular in girdle view with long setae sometimes filled with chloroplasts.

Frustule characteristics: Setae heavily silicified and finely spined which is uncharacteristic for *C. flexuosus*. There are no reports of *C flexuosus* having spinose setae and a similar species *C. criophilum* has coarsely spined setae. Top valve rounded with setae protruding from near the centre but as part of the valve face. Bottom valve flat, setae protruding from the cell margins. Apical axis 15-30 µm.

Navicula cf. *criophila* (Castracane) Van Heurck 1909

(Fig. 3.7a-b)

Culture characteristics: Cells solitary, occasionally clumping. Two large vacuoles clearly visible. Cells often on walls of culture vessel and motile.

Frustule characteristics: Frustules are lanceolate, raphe terminating in terminal nodules and a large central nodule. Interstriae radiate. Very similar to *Navicula directa* (W. Smith) Brébisson 1854 but the smaller size is outside of the reported range for *N. directa*. Apical axis of 40-50 µm, transapical axis 7-10 µm.

Chaetoceros sp. Ehrenberg 1844

(Fig. 3.7c-d)

Culture characteristics: Cells often solitary but occasionally in small chains. One or two large chloroplasts. Long, thin setae can be seen protruding from the cell corners.

Frustule characteristics: Setae lightly silicified and appearing from the cell corner. Girdle lightly silicified and could not be distinguished through LM. Cells joined with a slit like, circular aperture. Apical axis 10-20 µm.

Synedropsis sp. Hasle, Medlin & Syvertsen 1994 – Identified using Hasle et al. (1994)

(Fig. 3.7e-f)

Culture characteristics: Cells solitary or in ribbon colonies, rarely in stellate colonies. Cells are fusiform with two large chloroplasts. Forms very dense cultures.

Frustule characteristics: Frustules elliptical to lanceolate and weakly silicified, morphological features could not be fully distinguished using LM. Apical axis 20-30 µm, transapical axis 3-6 µm.

Navicula cf. *glaciei* Van Heurk 1909

(Fig. 3.7g-i)

Culture characteristics: Cells usually solitary and settled on the culture vessel walls and motile. Small clumps can also be seen. Chloroplasts are large and distributed either side of the raphe in valve view.

Frustule characteristics: Frustules are naviculoid and elliptical. Raphe is straight in most specimens and forms a central nodule which extends to the valve margin forming a stauros like feature. Interstriae are radiate. Cell size is smaller than the reported range for *N. glaciei*. Apical axis 7.5-12.5 µm, transapical axis 2.5-5 µm.

Fragilariopsis cylindrus (Grunow) Helmcke & Krieger 1954

(Fig. 3.7j-k)

Culture characteristics: Cells often solitary, rarely in ribbons, occasionally clumped.

Frustule characteristics: Cells cylindrical to rectangle with parallel sides. Apical ends are rounded. Interstriae are parallel with fibulae seen on one side of the frustule. Apical axis 3.5 12.5µm, transapical axis 1-5 µm.

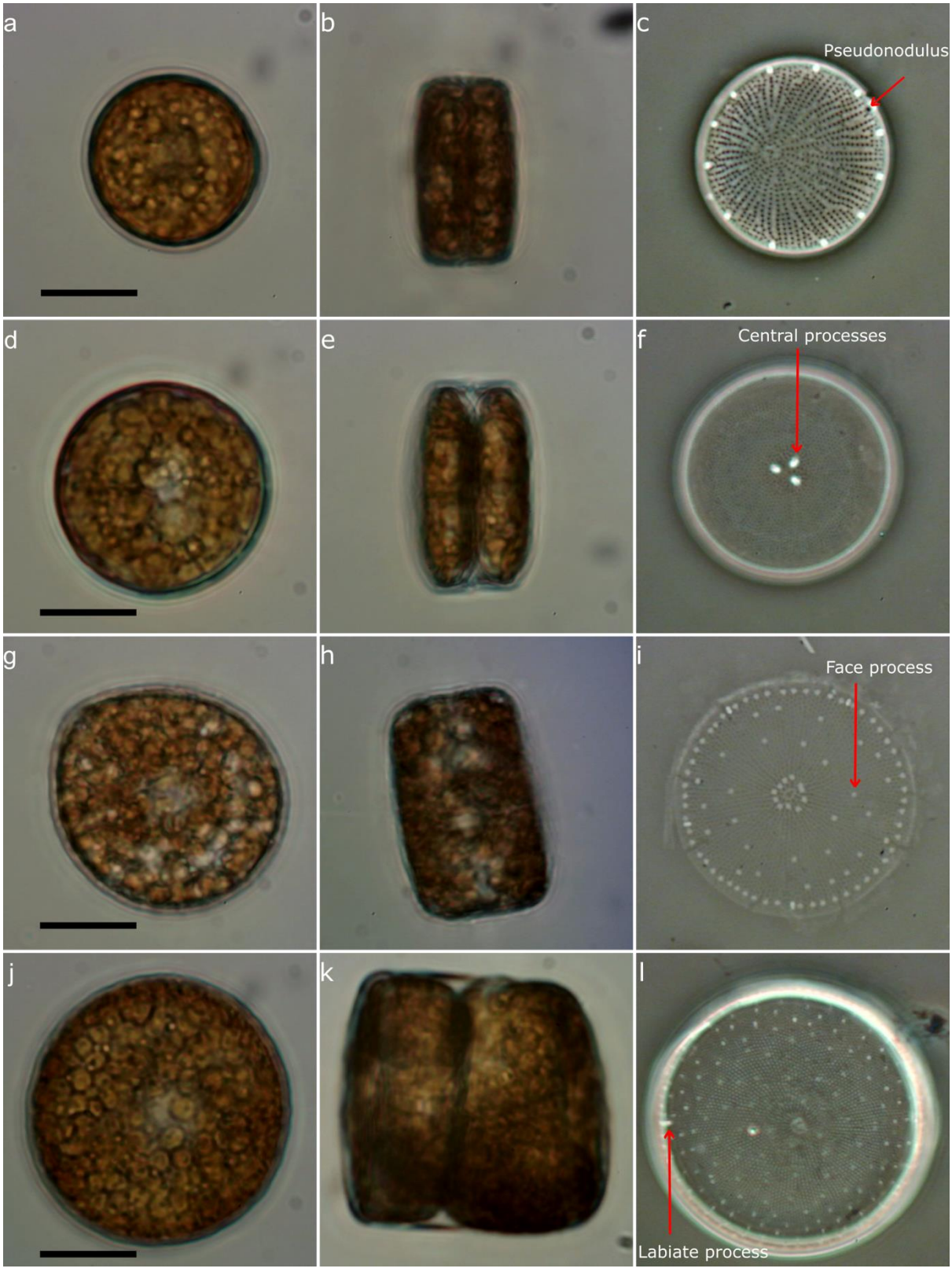

Figure 3.4 Plate 1: Light micrographs of live cells and cleaned frustules. Side by side comparisons of live cells and cleaned frustules of diatom strains. a-c) *Actinocyclus actinochilus*. d-f) *Stellarima microtrias*. g-i) *Thalassiosira tumida*. j-l) *Porosira pseudodenticulata*. Images taken at 600 x, scale bar = 20 µm.

Figure 3.5 Plate 2: Light micrographs of live cells and cleaned frustules. Side by side comparisons of live cells and cleaned frustules of diatom strains. a-b) *Proboscia truncata*. c-e) *Chaetoceros dichaeta*. f-h) *Chaetoceros* cf. *flexuosus*. Figs a-e taken at 400 x, scale bar = 40 µm and Figs f-h taken at 600 x, scale bar = 20 µm.

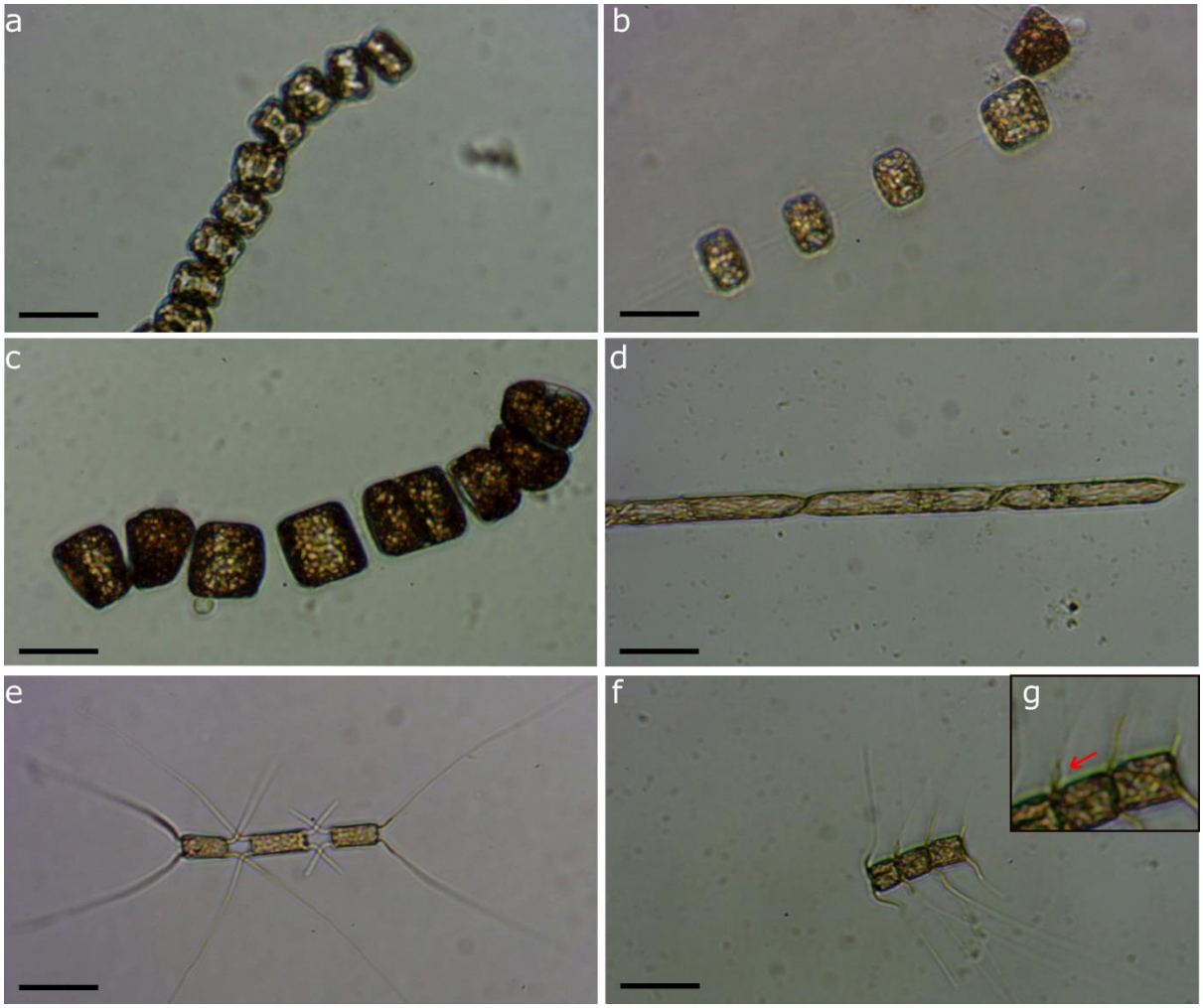

Figure 3.6 Plate 3: Light micrographs of live cells in chain formation. Live images showing the morphology of chain formation in Antarctic isolates. a) *S. microtrias*. b) *T. tumida*. c) *P. pseudodenticulata*. d) *P. truncata*. e) *C. dichaeta*, f) *C.* cf. *flexuosus* and g) superimposed view of the twisted setae in *C.* cf. *flexuosus*. 200 x, scale bar = 50 µm.

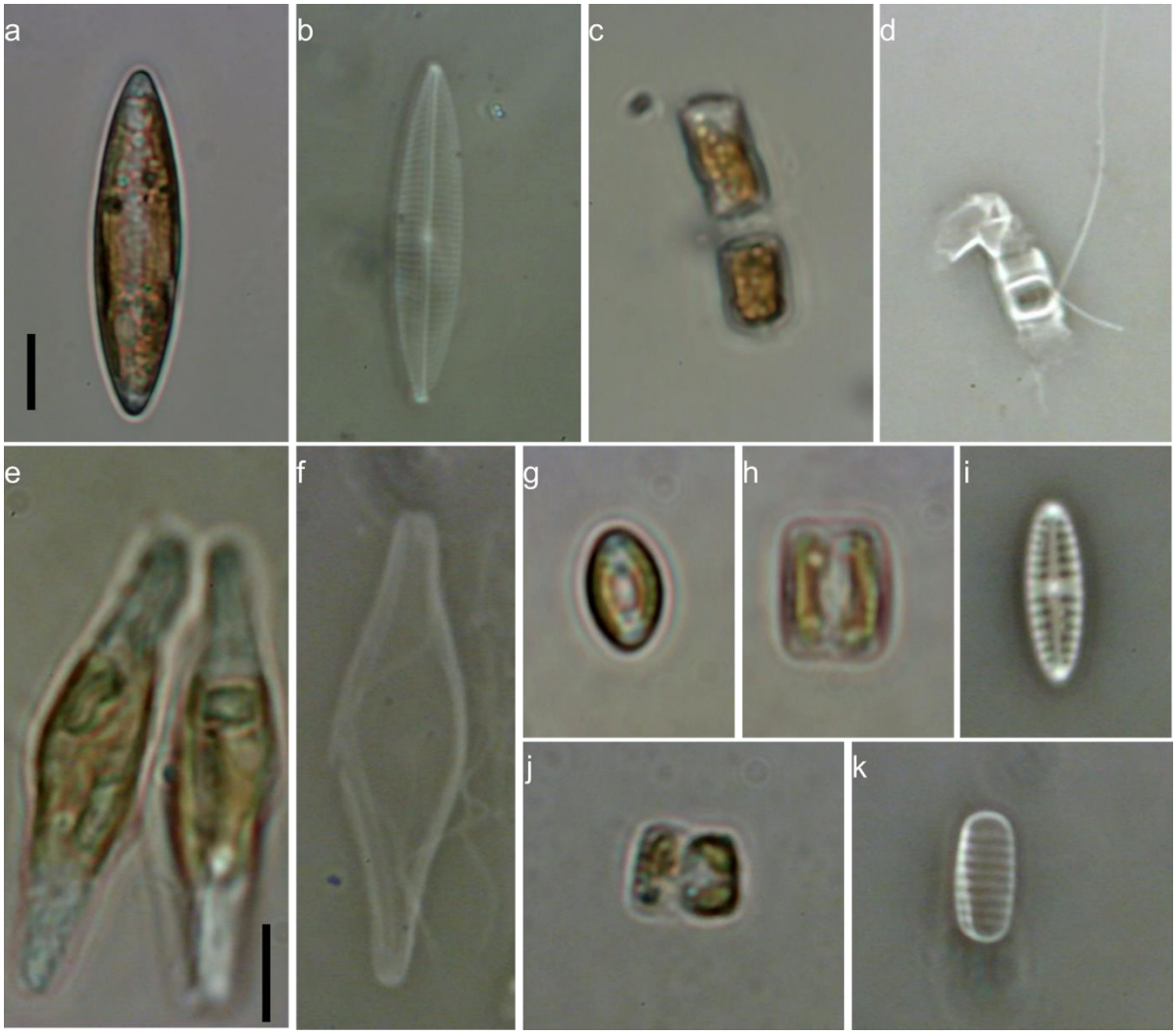

Figure 3.7 Plate 4: Light micrographs of live cells and cleaned frustules. Side by side comparisons of live cells and cleaned frustules of diatom strains. a-b) *Navicula* cf. *criophila*. c-d) *Chaetoceros* sp.. e-f) *Synedropsis* sp.. g-i) *Navicula* cf. *glaciei*. j-k) *Fragilariopsis cylindrus*. Figures a-d taken at 600 x, scale bar = 10 µm. Figures e-j taken at 1200 x, scale bar = 5 µm.

3.3 Discussion

Thirty-six strains across 12 species of Antarctic marine diatoms were successfully isolated from Ryder Bay and Marguerite Bay, Antarctica and representatives have been deposited into CCAP (Table 3.2). The isolated strains included a range of centric and pennate taxa of which seven species *A. actinochilus*, *C.* cf. *flexuosus*, *C. dichaeta*, *N.* cf. *glaciei*, *N.* cf. *criophila*, *P. truncata* and *Synedropsis* sp. are new additions to the CCAP collection. For *T. tumida*, *P. pseudodenticulata*, *S. microtrias* and *F. cylindrus* (which were already represented in CCAP), multiple strains across various sample sites were acquired. In the case of *F. cylindrus*, seven strains were isolated from different environments including near sea ice and open water (Fig.

3.1, Table 3.2). This species has been shown to have a highly plastic response to cope with these different environments (Sackett *et al.*, 2013), therefore these additional strains will be a useful resource to investigate adaptations. Moreover, diatoms are known to have a high degree of intraspecific variation (Godhe & Rynearson, 2017), therefore, acquiring multiple strains of the same species is important for experimental study as a way to validate results obtained with a single strain, by factoring in phenotypic diversity and potential founder effects. Phylogenetic analysis of the *rbc*L-3P and 18S barcodes did not identify any difference among these strains (Fig. 3.2 and 3.3 respectively), but it cannot be ruled out that these strains show aspects of intraspecific variation and phenotypic plasticity in other traits. Sequencing of the internal transcribed spacer regions (ITS1 and ITS2) has been used to discern genetic variation in closely related diatom species (von Dassow *et al.*, 2008; D'Alelio *et al.*, 2009; Stock *et al.*, 2019). More recently, *Leptocylindrus danicus* strains were shown to have high genetic variation within the internal transcribed spacer regions, as well as variation among functional traits e.g. Growth rate, biovolume, and silicification (Ajani *et al.*, 2021). Additionally, three genotypes of *A. actinochilus* showed varied responses to simulated heat waves, although genotypes were inferred through the method of single cell isolation rather than genetic sequencing (Samuels *et al.*, 2021). These results demonstrate that further genetic and physiological analyses of multiple strains of the same species will be important and may identify differences within species. Identifying and understanding intraspecific variation in functional traits as shown in Ajani *et al.*, (2021) in polar species will help to increase our understanding of how species will respond to future environmental changes.

The success of an isolate forming an established culture was 9.5% using both micropipette and plating methods. Failure to establish cultures could be due to damage incurred through physical isolation or selection bias when using a single growth medium. Gérikas Ribeiro *et al.*, (2020) used a variety of isolation methods for the isolation of Arctic phytoplankton including micropipette, dilution, and cell sorting, which resulted in >1000 strains, demonstrating the advantage of utilising multiple methods. They reported low numbers of strains derived from micropipetting (12%) but reported that some taxa could be isolated through this method alone e.g., Coscinodiscophyceae. Many marine protists remain unculturable (Massana *et al.*, 2014) and cell sorting technology e.g. flow cytometry and/or a combination of growth media and isolation methods might increase success in the future.

Many of the isolated genera have been identified as important prey for Antarctic krill (*E. superba*) including *Actinocyclus*, *Porosira*, *Thalassiosira* and *Chaetoceros* (Cleary *et al.*, 2018). Having these ecologically important species in culture offers the opportunity to study the direct effects of global change and potential impacts this may have on filter feeding organisms e.g., nutritional content of prey. Moreover, these new strains will be cultured at temperatures more representative of their natural environment (0 to 2°C), thus facilitating studies to understand mechanisms for cold adaptation, minimising impacts arising from long term culturing at elevated temperatures (O'Donnell *et al.*, 2018; Schaum *et al.*, 2018). A few of the species (*N.* cf. *glaciei*, *F. cylindrus* and *Synedropsis* sp.) are ice diatoms, which together form an important ecosystem for both primary productivity (Lizotte, 2001) and Antarctic food webs (Garrison, 1991).

One strain isolated in the current work, *C.* cf. *flexuosus* (strain CCAP 1010/55), was found to have spinose setae which is uncharacteristic of this species (Fig. 3.5h). The descriptions of Hasle & Syvertsen, (1996) described the setae of *C. flexuosus* as being "extremely delicate" and Priddle *et al.*, (1985) described the setae as being "unusually fine for a phaeocerid". *Chaetoceros* are split into two taxonomic groups, the Phaeoceros Gran 1897 and the Hyalochaete Gran 1897. The two groups are discriminated by a variety of features and one of these are setae characteristics. Phaeoceros tend to have long, thick, and spined setae which sometimes bear chloroplasts whereas, Hyalochaete have delicate, fine, sometimes spined setae which do not bear chloroplasts (Hasle & Syvertsen, 1996). *C. flexuosus* is in the Phaeoceros group but is described as having setae which show more similarity to Hyalochaete. The setae of 1010/55 are more characteristic of usual Phaeoceros setae however, the true structure of these setae should be examined more closely, preferably using scanning electron microscopy (SEM) to understand their characteristics. Both Hasle & Syvertsen, (1996) and Priddle *et al.*, (1985) describe *C. flexuosus* as having setae which twist around each other when in chain formation and that this is a characteristic of the species. Fig. 3.6g shows how strain 1010/55 exhibited this twisting of the setae when in chain formation and this feature was therefore used to form the putative identification. The similar species *C. criophilum* which shares some morphological features does not show this twisting formation in the setae so was ruled out.

Many attempts were made to resolve the morphological features of both *Synedropsis* sp. isolates 1063/1 and 1063/2, but these could not be resolved further than the frustule outline (Fig. 3.7f). *N.* cf. *criophila* showed similarities to both *N. criophila* and *N. directa* but was under the reported size range of the latter and this was also the case for *N.* cf. *glaciei* strains. These three species should be analysed using SEM analyses in order to confirm species identifications.

The use of omics analyses such as transcriptomics, proteomics and metabolomics, on polar algae has been a key resource to identify key adaptations to surviving the polar environments as well as understanding biochemical characteristics (Lyon & Mock, 2014). Carrying out omics research on novel Antarctic strains will increase our understanding of their biology and can be linked to global sequencing projects such as Tara Oceans (Karsenti *et al.*, 2011). There is currently growing interest in the study of polar diatoms for biotechnology, with species showing high levels of commercially interesting compounds e.g. polyunsaturated fatty acids such as EPA (Boelen *et al.*, 2013; Svenning *et al.*, 2019) and bioactive compounds e.g. anticancer (Ingebrigtsen *et al.*, 2016). With the limited number of representatives in culture collections, increasing the number and diversity of polar species will provide further scope for bioprospecting compounds of societal importance. Ice diatoms are known to produce compounds such as ice binding proteins (Janech *et al.*, 2006) and neutral lipids (Priscu *et al.*, 1990). It is hoped that these strains will further our understanding of polar diatoms and provide a useful resource for researchers. Strains isolated in this work have been used in the subsequent chapters of this thesis. *F. cylindrus* strains 1023/10 and 1023/11 were used in Chapter 4 to investigate thermal tolerance, and 1023/10 was again used in Chapter 5 looking at B_{12} dependency. *Chaetoceros sp* (CCAP 1010/54), *C.* cf. *flexuosus* (CCAP 1055/10), *C. dichaeta* (CCAP 1010/56), *P. truncata* (CCAP 1064/3) and *Synedropsis* sp. (CCAP 1063/1 and 1063/2) based on growth in the laboratory should be followed up for their biotechnological potential.

Chapter 4 - Thermal tolerance of bipolar species *Fragilariopsis cylindrus* and *Porosira glacialis*

4.1 Introduction:

In the polar regions, temperature is thought to be one of the largest abiotic factors influencing the biology and ecology of organisms. Both the Arctic and the Antarctic present similar environments (DeVries & Steffensen, 2005), especially in terms of SST. In the Arctic the average SST is ~1°C and 80% of the Arctic basin has temperatures between 0-1°C (Carvalho & Wang, 2020). In the Antarctic, water temperatures have been reported at an average of -1.8°C in McMurdo Sound varying by only 0.5°C (Littlepage, 1965) and between -1.8 - 1°C in Ryder Bay (Clarke *et al.*, 2008). Furthermore, the polar regions are very stable environments with the Antarctic having largely remained the same for the last 10-15 million years (Clarke & Crame, 1992) and the Arctic for 2 million years (Dunton, 1992 and references therein). The history of the polar regions means the biota have adapted to the freezing cold conditions over millions of years, but to a much greater extent in the Antarctic. Organisms which rely on the external environment for body temperature regulation (ectotherms) are described as being stenothermal in the polar regions which means they have a limited thermal tolerance range. Previously, Antarctic stenothermal marine invertebrates have shown a poor ability to adapt to warming temperatures (Peck *et al.*, 2010b, 2014) whereas, Arctic invertebrates have shown a greater ability (Richard *et al.*, 2012). Arctic ectotherms do not show the same level of adaption to the cold compared to Antarctic ectotherms, which is suggested to be a result of the differing evolutionary histories of the regions.

The ability to adapt to changing temperatures is likely to be more resilient in species which have faster generation times, as genetic divergence can arise much quicker reducing the reliance on plasticity (Somero, 2010; Peck, 2011). Generation times are also a trait which correlates with body size, with large organisms having the longest times and smaller organisms having the shortest (Peck, 2011). Microorganisms can have rapid generation times with diatoms having generation times ranging from hours to days (Baars, 1981). Despite diatoms having rapid generation times, the rate of adaptation in polar diatoms is not known and therefore, the evolutionary histories of the Arctic and Antarctica may have resulted in differing physiological and metabolic characteristics. Polar diatoms are described as

psychrophiles, which means their optimal growth occurs at temperatures below 15°C (Morita, 1975). These low optimal temperatures suggest that metabolism is also adapted to the cold. Metabolism is directly influenced by temperature and under higher temperatures it is predicted that there would be higher species diversity as there is more variability in metabolic niche, this is termed the "metabolic niche hypothesis" (Clarke & Gaston, 2006). Therefore, in the cold climates of the poles, metabolism is likely to be constrained and species may show similar metabolic needs.

The polar regions, however, are experiencing unprecedented changes as a result of anthropogenic climate change. The sixth IPCC report on climate change predicts that under 1.5°C of global warming above pre-industrial levels, Antarctica could see an increase in SST of nearly 1.2°C by the turn of the century, whilst the Arctic is predicted to increase by over 3°C (IPCC, 2021; Iturbide *et al.*, 2021). This signifies that these two regions are undergoing warming, and the rate at which it is occurring in the Arctic is the highest on the planet and is exacerbated by a reduction in sea ice extent and the albedo effect (Comiso & Hall, 2014). Furthermore, the real world effects of this Arctic warming are already being seen by the increasing utilization of shipping routes through the Arctic including the opening of the North-West Passage (Smith & Stephenson, 2013; Pizzolato *et al.*, 2016). There is already evidence that compositional changes in the phytoplankton, including a reduction in diatoms, is occurring due to the indirect effects of temperature e.g., changes in salinity and water column stratification (Moline *et al.*, 2004; Rozema *et al.*, 2017).

Modelling is often used to predict the effects of climate change on phytoplankton (Bopp *et al.*, 2005; Marinov *et al.*, 2010; Coello-Camba *et al.*, 2015). Although these models provide an important knowledge-base, it has been argued that their power is undermined by a lack of biological input and interpretation (Boyd *et al.*, 2013). Boyd *et al.,* (2013) suggests that there needs to be better harmonization between model outputs and physiological data of phytoplankton biology, specifically the effect of temperature. A recent study by Coello-Camba & Agustí, (2017) looked at doing this by evaluating the physiological growth data of Arctic and Antarctic phytoplankton in addition to relating the growth data of Arctic species to Arctic SST. Although Coello-Camba & Agustí, (2017) did not look at SST in the Antarctic, they showed that regions within the Arctic have already surpassed the average thermal optimum (T_{opt}) of Arctic phytoplankton. A common method to investigate the thermal

tolerance of organisms is through thermal performance curves (Schulte *et al.*, 2011). Surprisingly, despite the threat of climate change there is still very little physiological work carried out on polar diatoms to determine their thermal tolerance. Fiala & Oriol, (1990) reported the thermal tolerance of six Antarctic diatoms showing that optimal temperatures ranged between 3-5°C. In addition, the lethal temperatures ranged between 6-9°C with only one species showing growth above 10°C (Fiala & Oriol, 1990). Similar figures were reported in two benthic Antarctic diatoms, showing optimal growth at 0°C and thermal maxima of 7-9°C (Longhi *et al.*, 2003). Arctic diatoms have tended to show higher temperature tolerances with two benthic diatoms having optimal growth between 12-15°C (Karsten *et al.*, 2006) and *P. glacialis* showing higher growth rates at 12°C compared to lower temperatures (Svenning *et al.*, 2019). Furthermore, Arctic *F. cylindrus* strains have been shown to have higher growth rates at 8°C compared to 5°C and 1°C (Pančić *et al.*, 2015). These results suggest that Arctic diatom species may be able to better respond to increases in temperature due to a higher thermal tolerance and that Antarctic diatoms tend to have a narrower thermal niche.

In this chapter I aimed to investigate whether the thermal tolerance of Arctic and Antarctic strains of *F. cylindrus* and *P. glacialis* are conserved between the two regions. In addition, I wanted to determine some of the metabolic characteristics of these strains under cold, ecologically relevant temperatures to understand potential metabolic changes in response to climate change. The potentially deleterious impacts of long-term culturing mentioned in Chapter 3 were also investigated by additionally investigating two of the newly isolated Antarctic *F. cylindrus* strains from the field work carried out in the WAP and comparing the data from these with the CCAP strain.

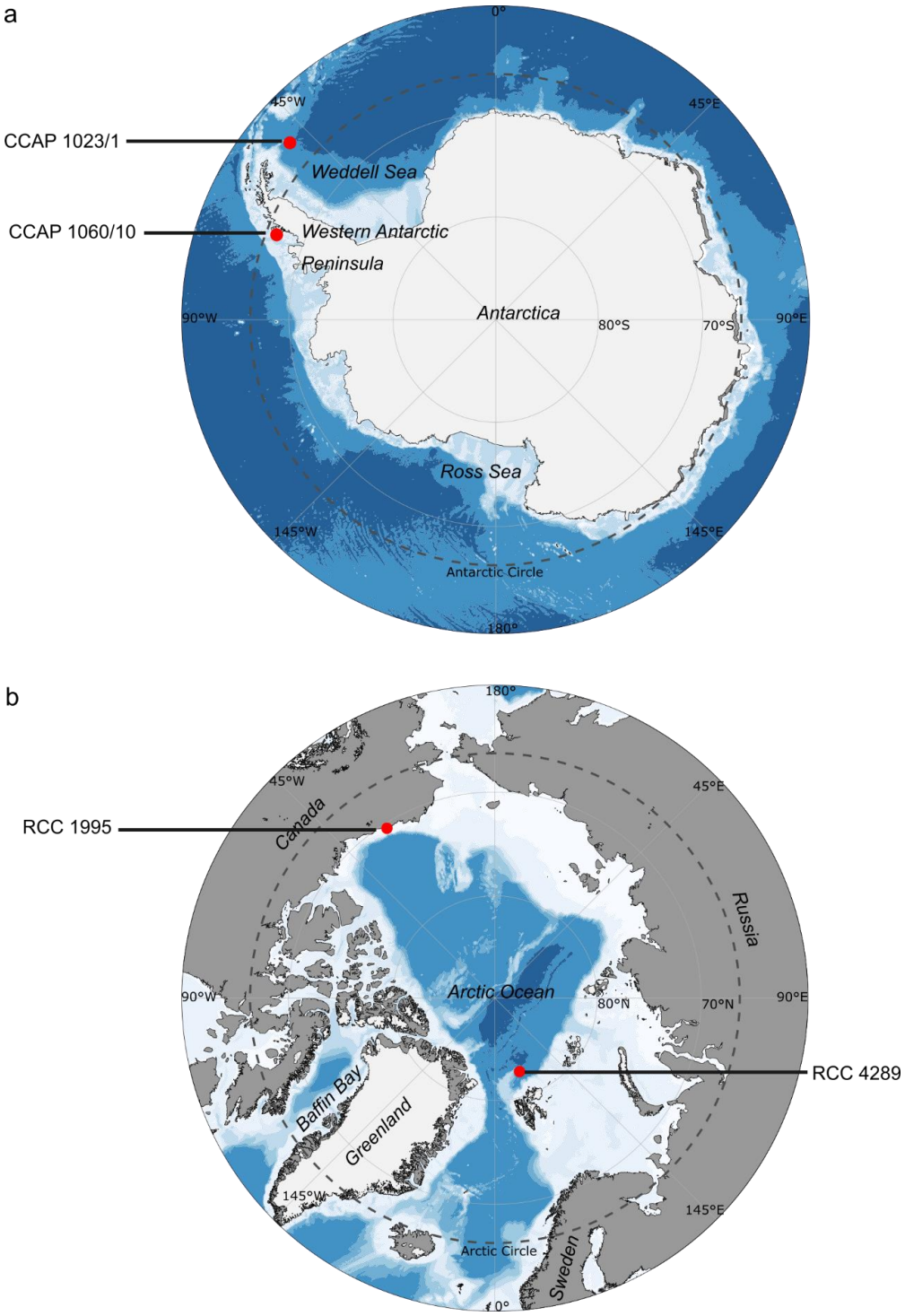

Figure 4.1 *F. cylindrus* and *P. glacialis* strain isolation locations. a) Antarctic strains and b) Arctic strains. Maps produced using the ggOceanMaps package (Vihtakari, 2021), full strain information can be found in Materials and Methods Table 2.1.

4.2 Results:

4.2.1 Establishing a broad thermal tolerance

To begin investigating the thermal tolerance of Arctic and Antarctic strains of *F. cylindrus* and *P. glacialis,* which are used throughout this chapter (Fig. 4.1, Table 2.1 in Materials and Methods), a preliminary experiment utilising 96-well microtitre plates at a range of temperatures (1°C - 18°C) was carried out (Materials and Methods Section 2.3.1). Growth was measured using optical density, indicating an increase in cell numbers. Neither strain of both species survived at 15°C or 18°C (Fig. 4.2). *F. cylindrus* strains showed a differing response over the temperature range (Fig. 4.2a and b). The Antarctic *F. cylindrus* (1023/1) was unable to grow at temperatures above 7°C (Fig. 4.2a) whereas the Arctic strain (4289) was able to grow up to 12°C (Fig. 4.2b). At 1°C, 4°C and 7°C both *F. cylindrus* strains exhibited similar growth responses. Both *P. glacialis* strains showed growth at the same temperatures (1°C-12°C, Fig. 4.2c and d) however, the Arctic strain (1995) exhibited a lower final density based on optical density (750 nm) at all temperatures tested (Fig. 4.2d).

4.2.2 Growth at cold temperatures relevant to the polar regions

Although the assay described in Section 4.2.1 provided a broad indication of the thermal tolerance of the strains, it was difficult to shed light on the growth at ecologically relevant temperatures. This was due mainly to incubators being unable to reach and maintain such cold temperatures (below 4°C). Moreover, the small volumes of 200 µl cultures and the use of OD 750 nm meant that measurements of cell numbers were approximate. Therefore, to investigate growth characteristics at temperatures relevant to the polar environment (-1°C - 4°C), further experiments utilising Cryopharos bioreactors from Xanthella Ltd were carried out. These bioreactors allowed for better control of temperature and light as well as increasing the culture volume, thus enabling cell counts to be performed. Over the temperature range tested (-1°C - 4°C) the two *F. cylindrus* strains showed very different responses (Fig. 4.3a and b). The Antarctic strain exhibited differences in growth between the different temperatures (Fig. 4.3a), as opposed to the Arctic strain which grew similarly over all temperatures (Fig. 4.3b). Average growth rates significantly differed ($p<0.001$) between strains in the -1°C treatment, which is evident by the poor growth of the Antarctic strain at this temperature (Table 4.1 and Fig. 4.3). There were no significant differences ($p>0.05$)

between the average growth rates at the other temperatures tested (Table 4.1). The two *P. glacialis* strains showed similar growth responses over the four temperatures both showing the highest response at 4°C (Fig. 4.3c and d). Average growth rates of both strains increased with increasing temperature and the Arctic strain showed a small but significant increase in growth rate at 0°C (Table 4.1). In the 2°C treatment the Arctic strain showed a significantly higher growth rate compared to the Antarctic strain (Table 4.1).

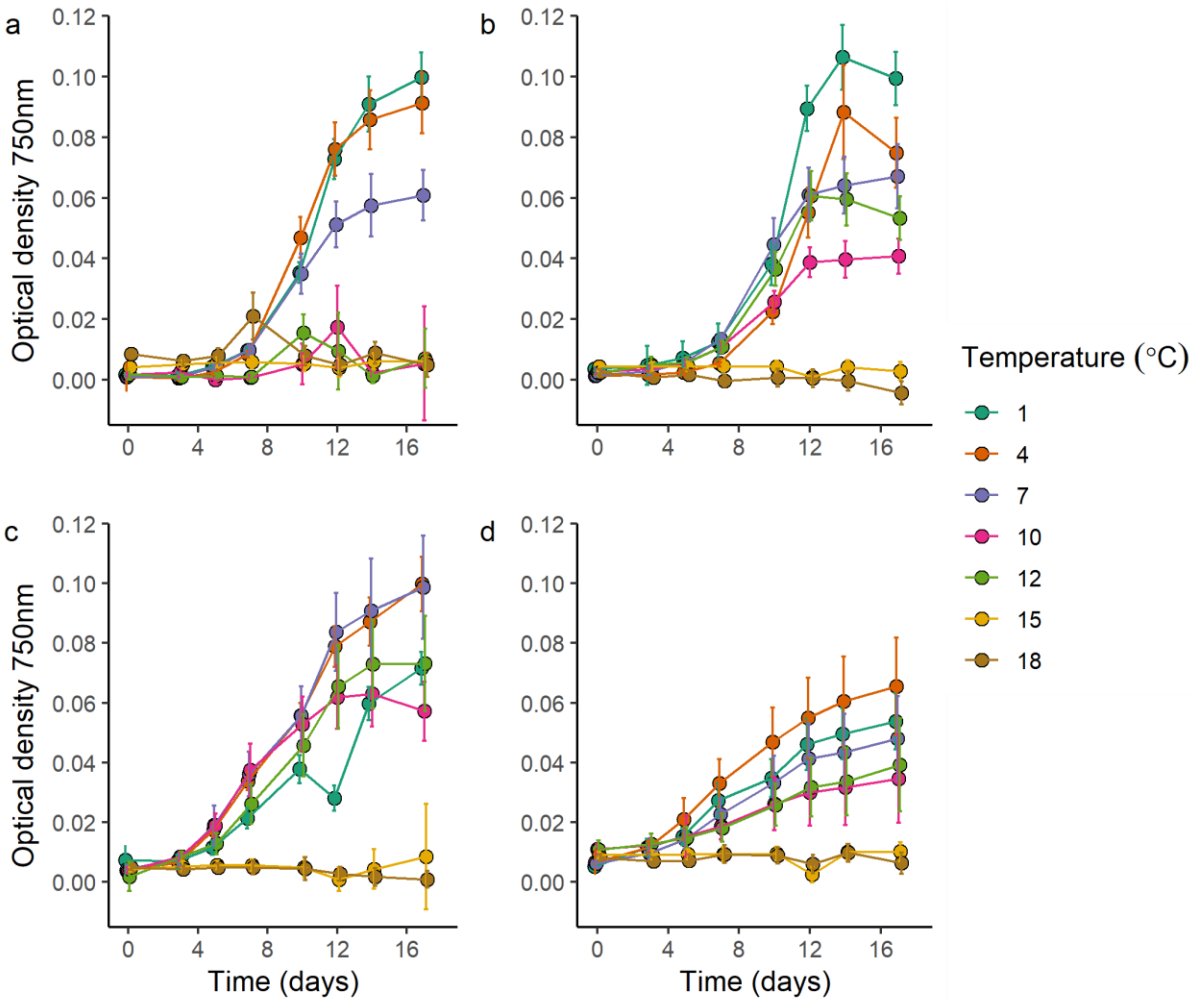

Figure 4.2 Growth assay of *F. cylindrus* and *P. glacialis* strains in microtitre plates at different temperatures. a) Antarctic *F. cylindrus* b) Arctic *F. cylindrus* c) Antarctic *P. glacialis* d) Arctic *P. glacialis*. Error bars ±SD, N = 1.

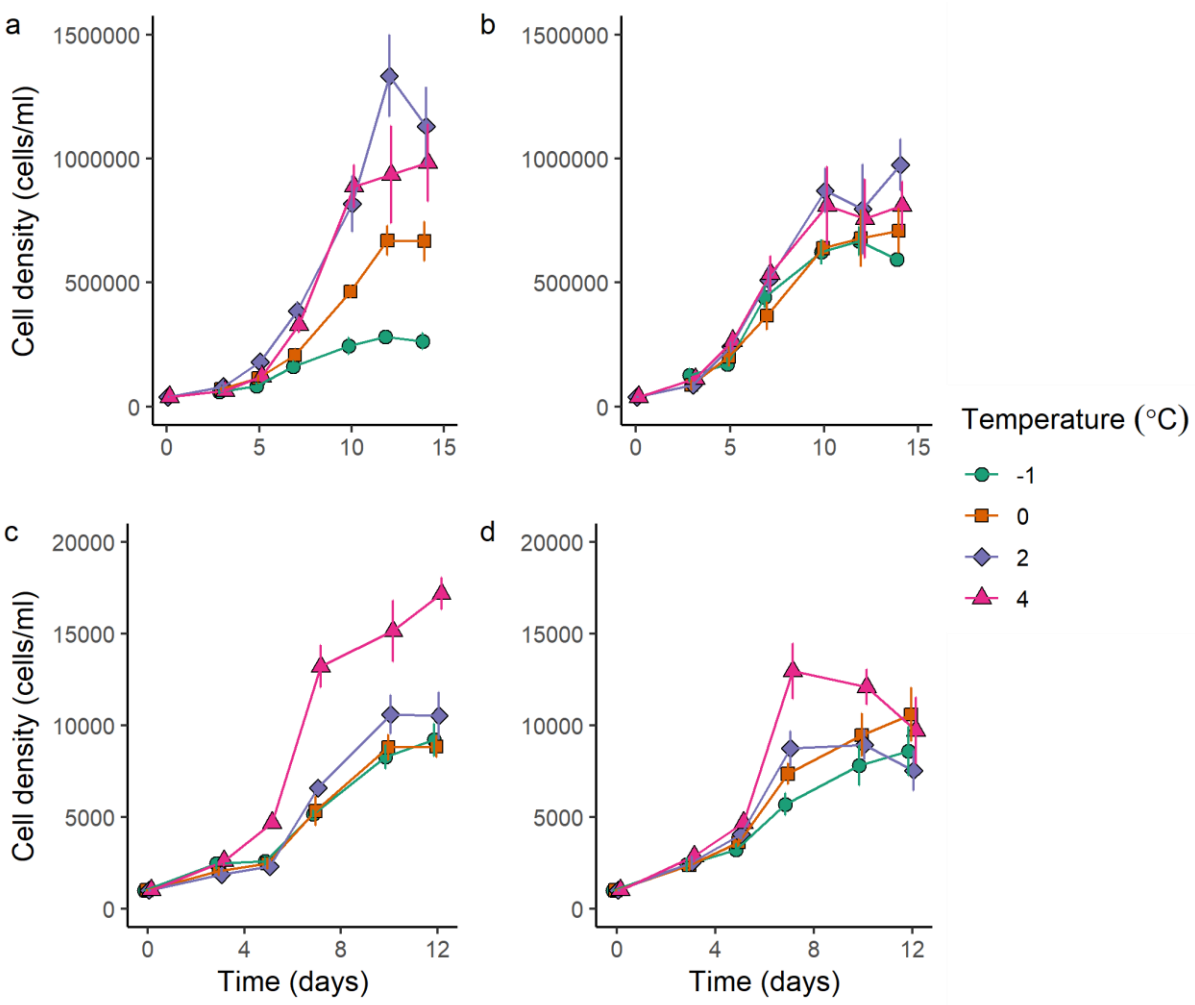

Figure 4.3 Growth assay of *F. cylindrus* and *P. glacialis* strains over cold temperatures using Cryopharos bioreactors. a) Antarctic *F. cylindrus* b) Arctic *F. cylindrus* c) Antarctic *P. glacialis* d) Arctic *P. glacialis*. Error bars ±SD, N = 3.

Table 4.1 Average growth rates of *F. cylindrus* and *P. glacialis* at cold temperatures. Within strain comparisons are denoted by letters indicating statistical significance T test - p<0.05. ns – not significant

F. cylindrus	**Temperature (°C)**			
	-1	**0**	**2**	**4**
Antarctic	0.183^{a}	0.235^{b}	0.293^{c}	0.312^{c}
Arctic	0.277^{a}	0.278^{ab}	0.310^{b}	0.303^{b}
T-test	<0.001	ns	ns	ns
P. glacialis				
	-1	**0**	**2**	**4**
Antarctic	0.210^{a}	0.213^{ab}	0.235^{b}	0.376^{c}
Arctic	0.200^{a}	0.237^{b}	0.327^{c}	0.354^{d}
T-test	ns	<0.05	<0.001	ns

4.2.3 Validating growth at elevated temperatures

Optical density as a proxy for growth in the initial experiment (Section 4.2.1) can create inaccuracies for instance due to biofilm formation and having utilized the Xanthella Cryopharos bioreactors in Section 4.2.2 it was decided to repeat the thermal tolerance over the broader temperature range (-1°C - 12°C). This was done to validate the findings from Section 4.2.1 under more controlled parameters and utilizing cell counts as a more accurate measurement.

The growth responses of both *F. cylindrus* strains were similar to the previous two experiments. The Antarctic strain showed large differences in growth over the temperature range, exhibiting no growth at 12°C, low growth at -1°C and similar growth at 4°C and 8°C (Fig. 4.4a). In contrast, the Arctic strain again showed similar growth responses over the four temperatures (Fig. 4.4b), a trait exhibited at the colder temperatures also (Fig. 4.3b). The Arctic strain consistently had higher growth rates compared to the Antarctic strain, but both showed increased growth rates as temperature increased (Table 4.2). At 8°C the Arctic strain had a significantly higher growth rate compared to the Antarctic strain (Table 4.2).

Both *P. glacialis* strains exhibited highest growth at 4°C and grew slowly at -1°C (Fig. 4.4c and d). The Arctic strain however, showed poor growth at the elevated temperatures of 8°C and 12°C, similar to what was shown in Fig. 4.2d. The Antarctic strain, however, was able to grow at these elevated temperatures which again validates the growth curves in Fig. 4.2c. Growth rates increased up to 8°C and 4°C in the Antarctic and Arctic strain respectively, after which

growth rates decreased (Table 4.2). The Antarctic strain had significantly higher growth rates at all temperatures except for 4°C where both strains had similar growth rates (Table 4.2).

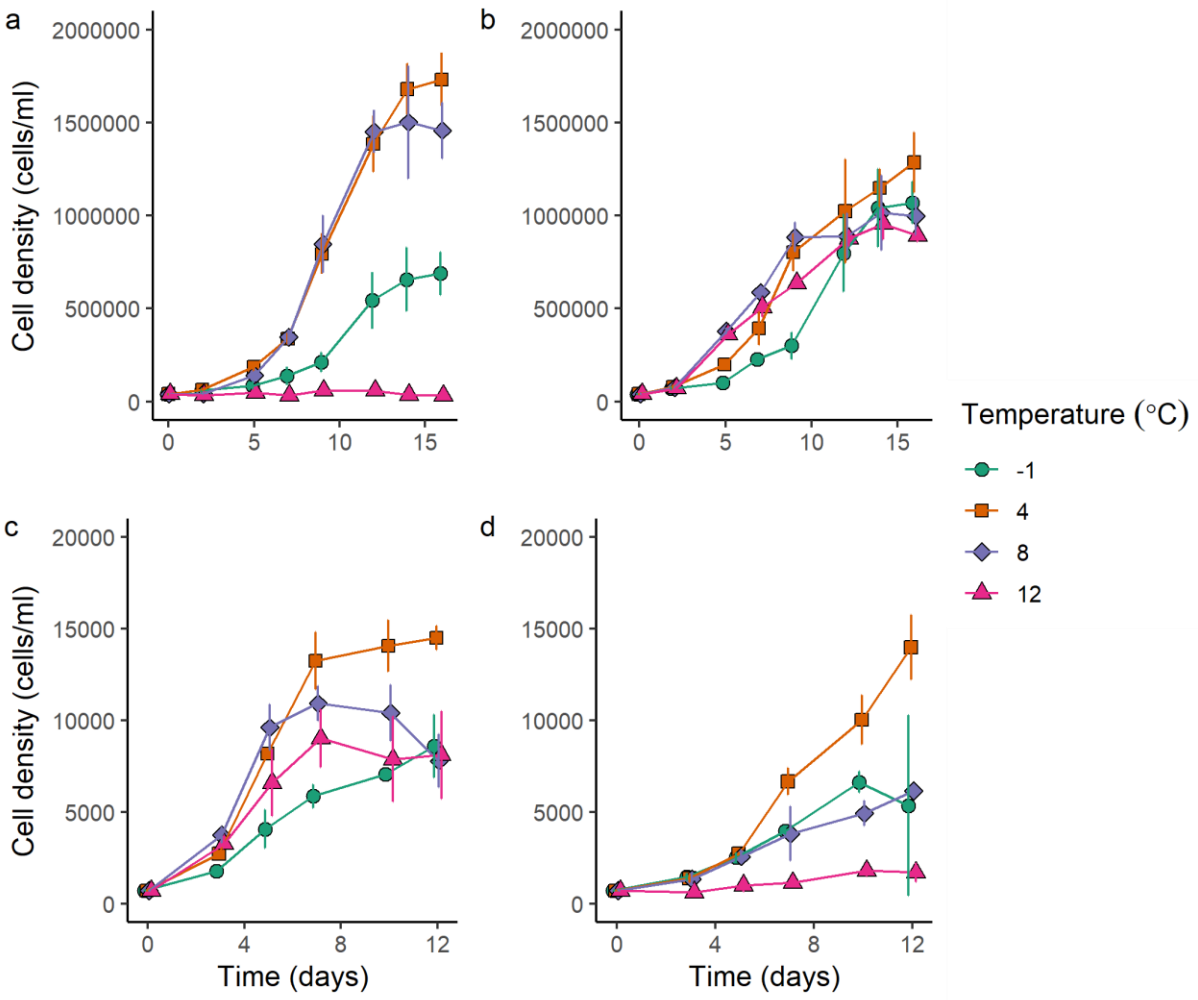

Figure 4.4 Growth assay validation of *F. cylindrus* and *P. glacialis* strains over temperatures. a) Antarctic *F. cylindrus* b) Arctic *F. cylindrus* c) Antarctic *P. glacialis* d) Arctic *P. glacialis*. Error bars ±SD, N = 3.

Table 4.2 Average growth rates of *F. cylindrus* and *P. glacialis* during thermal validation experiment. Within strain comparisons are denoted by letters indicating statistical significance p<0.05, ns – not significant.

F. cylindrus	**Temperature (°C)**			
	-1	**4**	**8**	**12**
Antarctic	0.215^{a}	0.307^{b}	0.355^{c}	n/a
Arctic	0.247^{a}	0.333^{b}	0.442^{c}	0.395^{d}
T-test	ns	ns	<0.01	n/a
P. glacialis				
	-1	**4**	**8**	**12**
Antarctic	0.302^{a}	0.359^{ab}	0.373^{b}	0.317^{b}
Arctic	0.225^{ac}	0.321^{b}	0.282^{abc}	0.152^{a}
T-test	<0.01	ns	<0.05	<0.01

4.2.4 Modelling thermal performance curves

In order to understand how both species and strains grew over the different temperatures the TPC was modelled using the rTPC package in R (Padfield *et al.*, 2021) and as described in Materials and Methods Section 2.3.3.

Assessment of the models identified three for further analysis. The three models guassian, quadratic and sharpeschoolfull were assessed based on the AICc score and the best model was the Sharpeschoolfull (Schoolfield *et al.*, 1981), therefore this model was used in both species (Table 4.3). The shapes of the TPCs were similar in both *F. cylindrus* strains (Arctic and Antarctic), which showed an increase in growth rate as temperature increased up to a maximum, after which there was a rapid decline (Fig. 4.5a). The Antarctic strain showed a narrower TPC as this strain was unable to grow at 12°C, whereas the Arctic strain could (Fig. 4.5a). The thermal optimum (T_{opt}) of the Antarctic strain was calculated at 7.194°C which is ~3.5°C lower than the calculated T_{opt} of the Arctic strain of 10.371°C. In both strains there was a rapid decline in growth rate after the T_{opt}.

Table 4.3 Thermal performance model selection. Selection of the best fitting thermal performance curve model using the rTPC package (Padfield *et al.*, 2021) for both *F. cylindrus* and *P. glacialis*. Models were assessed using AICc scores with the lowest scoring model selected as the best fit.

F. cylindrus	**Model**		
	Guassian	**Quadratic**	**Sharpeschoolfull**
Antarctic	7.34	8.61	-135
Arctic	12.6	9.97	-133
P. glacialis			
	Guassian	**Quadratic**	**Sharpeschoolfull**
Antarctic	8.57	5.52	-128
Arctic	-6.72	-9.24	-133

The two *P. glacialis* strains (Arctic and Antarctic) showed different TPC shapes (Fig. 4.5b). The Antarctic strain showed a similar shape to the two *F. cylindrus* strains, exhibiting a gradual increase in growth rate and then a rapid decline. The Arctic strain showed a rapid increase in growth rate as temperature increased and then a gradual decline at higher temperatures (Fig. 4.5b). The calculated T_{opt} was 10.050 for the Antarctic strain which is ~5.5°C higher than the Arctic strain which had a T_{opt} of 4.475°C (Fig. 4.5b).

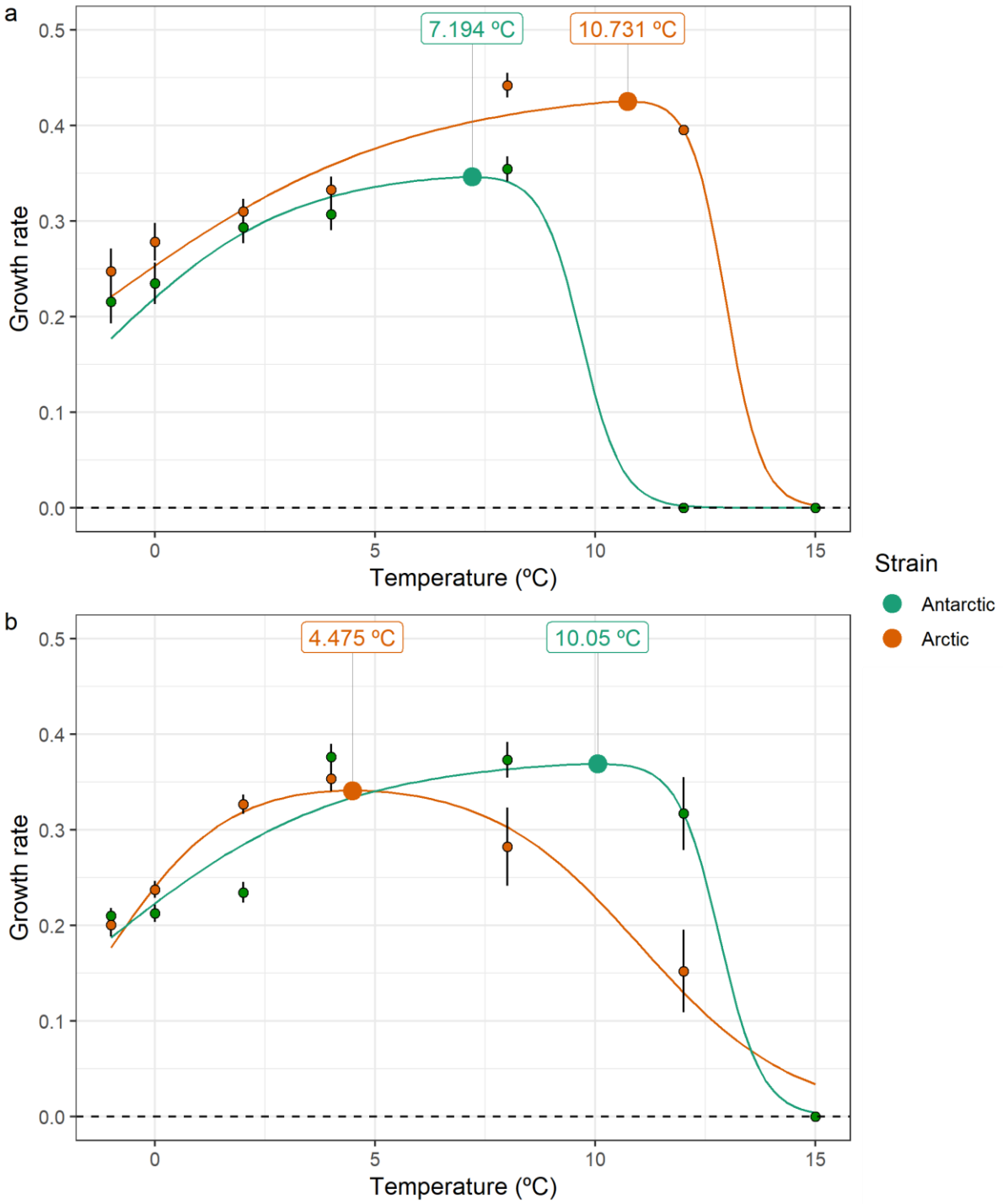

Figure 4.5 Thermal performance curves modelled via rTPC. TPC of bipolar species displaying thermal optima. a) *F. cylindrus* and b) *P. glacialis.* Error bars ±SD, N = 3.

4.2.5 Investigating thermal tolerance in newly isolated strains

The Antarctic F. cylindrus strain used in the experiments above (CCAP 1023/1) came from CCAP in Oban and had been in culture for 42 years at 4°C. To investigate whether the long-term culturing of strains affected the thermal tolerance of *F. cylindrus*, two newly isolated strains from Antarctica described in Chapter 3 were used (1023/10 – SC48 and 1023/11 – SC52, referred to as SC48 and SC52 respectively (Coffin *et al.*, submitted)).

SC48 showed a very similar response to the 1023/1 strain exhibiting an inability to grow at 12°C and strong growth at 4°C and 8°C (Fig. 4.6a and 4.4a respectively). Similar to the 1023/1 strain, SC48 showed a longer lag phase at 0°C but was able to reach a similar cell density to the higher temperatures of 4°C and 8°C (Fig. 4.6a). SC52 however, showed similar growth at 0°C but showed reduced growth at the higher temperatures of 8°C & 12°C (Fig. 4.6b). Moreover, SC52 was able to grow at 12°C, whereas neither of the other Antarctic strains could. Growth at 12°C appeared around day 20 after an extended lag phase (other temperatures showed growth from day 5) to reach a cell density of ~$3x10^5$ (Fig. 4.6b). Growth rates were significantly lower in SC52 compared to SC48 at all temperatures (Fig. 4.7 and Table 4.4). SC48 showed similar growth rates at 0°C and 4°C compared to the 1023/1 strain. Likewise, SC52 had similar rates to 1023/1 at 0°C but showed significantly lower growth rates at 4°C (Fig. 4.7 and Table 4.4). Both newly isolated strains showed significantly lower growth rates at 8°C compared to the 1023/1 strain. Growth rates of SC48 and SC52 remained largely stable with temperature, in contrast to 1023/1 which showed an increase with increasing temperature (Table 4.4, Fig. 4.7).

Table 4.4 Growth rate comparisons between Antarctic *F. cylindrus* strains. Within strain comparisons are denoted by letters indicating statistical significance p<0.05.

F. cylindrus	**Temperature (°C)**			
	0	**4**	**8**	**12**
SC48	0.261^a	0.290^b	0.264^a	n/a
SC52	0.200^a	0.233^a	0.218^a	0.196^a
1023/1	0.235^a	0.307^b	0.355^c	n/a
SC48:SC52	<0.001	<0.05	<0.05	n/a
SC48:1023/1	ns	ns	<0.001	n/a
SC52:1023/1	ns	<0.01	<0.01	n/a

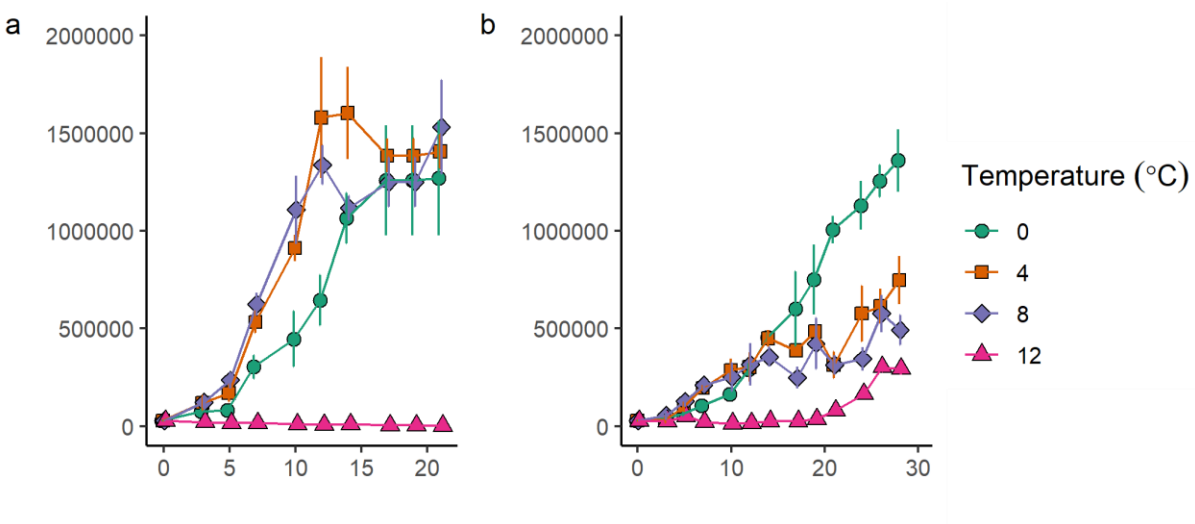

Figure 4.6 Growth assay of newly isolated *F. cylindrus* strains. Newly isolated strains grown between -1°C and 12°C. a) SC48 b) SC52. Error bars ±SD, N = 3.

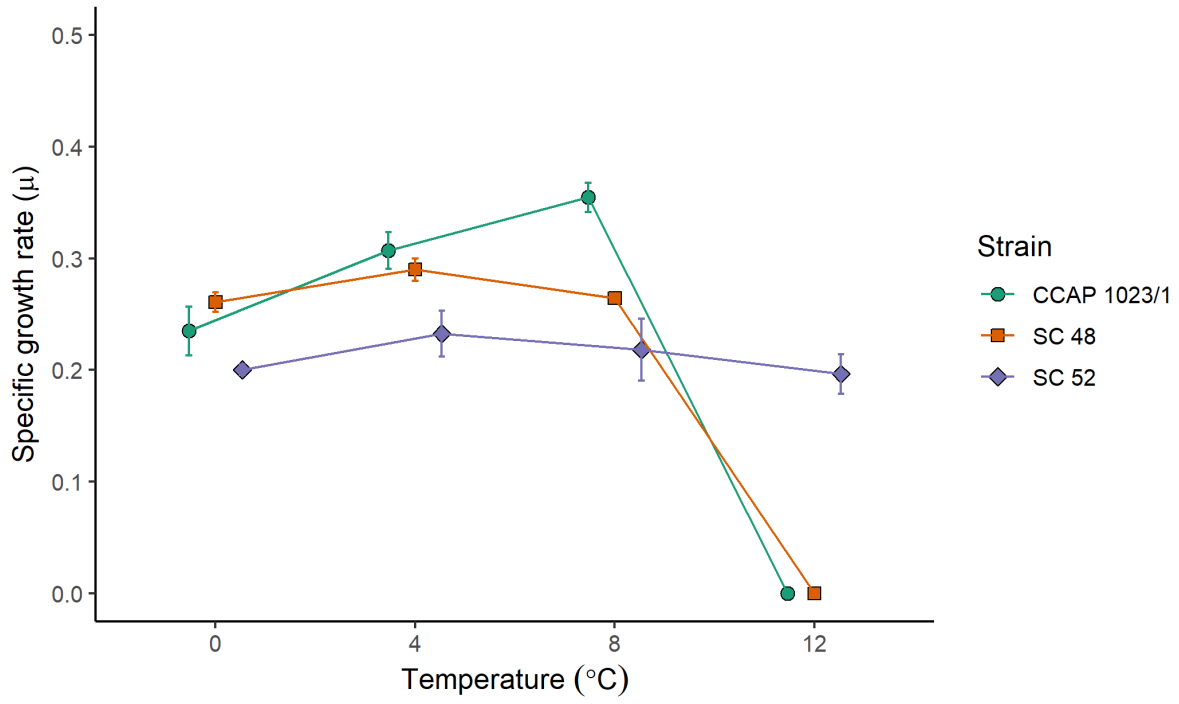

Figure 4.7 Average growth rate comparisons between Antarctic *F. cylindrus* strains. Newly isolated strains SC48 and SC52 compared to the laboratory strain CCAP 1023/1. Error bars ± SD, N = 2.

4.2.6 Using Fourier transform – infrared spectroscopy (FT-IR) to produce basic metabolic fingerprints

In this section, metabolic characteristics including metabolic fingerprinting, pigment analysis and fatty acid analysis of cultures from Section 4.2.2 grown under cold temperatures were investigated. FT-IR was used to fingerprint the basic metabolic composition of strains to investigate whether there were differences within strains and temperatures. Principal component analysis was used to discriminate groups based on a filtered dataset of FT-IR spectra (Fig. 4.8 and Table 4.5). Spectra of *F. cylindrus* strains are presented in Fig. 4.8 which shows the peaks and assigned numbers of compound groups described in Table 4.5. The Aluminium foil which was used as substrate for FT-IR analysis (Materials and Methods Section 2.4.3) was easily identifiable between 1900-2300 cm^{-1} and did not absorb at any wavelength comparable to biological compounds (Fig. 4.8 and Table 4.5). Neither species, strain nor temperature could be discriminated based on FT-IR spectra (Fig. 4.9a and b). Temperature within strains did show groupings in Antarctic *F. cylindrus* and *P. glacialis* but not in Arctic *P. glacialis* (Fig. 4.10), however none of the differences exhibited were statistically significant (ANOVA $p>0.05$). Within all PCA analyses most of the variance was explained by the silica peak at 1076 cm^{-1} (1, Fig. 4.8). PCA biplots are presented in Appendix 7 and indicates silica as the prominent factor influencing the PCA.

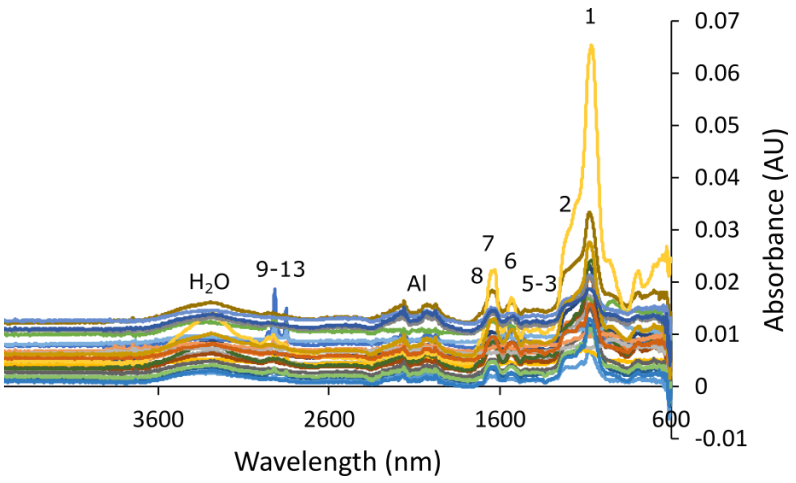

Figure 4.8 Example FT-IR spectra and peak numbers. FT-IR Spectra of all *F. cylindrus* samples and the peaks identified using FT-IR.

4.2.7 Assessing basic pigment composition of strains at cold temperatures

Pigments were extracted in DMF and first analysed via UV spectrometry (Section 2.4.1 in Materials and Methods) to give concentrations of chlorophyll *a*, chlorophyll c_1 + c_2, total chlorophyll and carotenoids all showed an increased from -1°C to 0°C in *F. cylindrus* strains (Fig. 4.11). There were significantly lower values of chlorophyll *a*, total chlorophyll, and total carotenoids at -1°C compared to the other three temperatures (ANOVA, Df, 3(16), F = 13.424, 9.654 and 13.900 respectively, $p<0.001$). The Arctic strain showed slightly higher concentrations in all pigments compared to the Antarctic strain, but there were no significant differences between strains within temperatures (Fig. 4.11, ANOVA, Df 3(16), F = 0.024, 0.530, 0.100 and 0.350 respectively, $p>0.5$).

Table 4.5 FT-IR wavelength and associated compound. Compound peaks were based on peaks identified in Driver et al., (2015) and Rüger et al., (2016).

Peak Number	Wavelength (cm^{-1})	Compound group
1	1076	Silica
2	1160	Carbohydrates
3	1236	Nucleic acids
4	1388	Proteins
5	1455	Proteins and lipids
6	1545	Amide I
7	1655	Amide II
8	1736	Lipids
9	2852	Lipids
10	2872	Lipids
11	2920	Lipids
12	2957	Lipids
13	3014	Lipids
Al	1900-2300	Aluminium foil
H_2O	3000-3600	Water

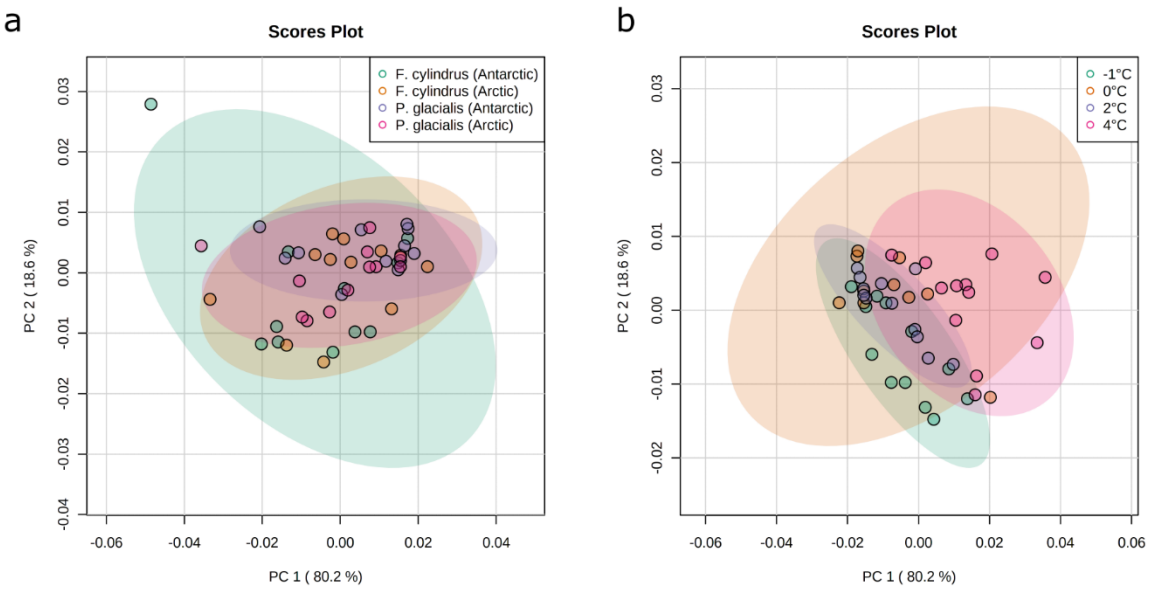

Figure 4.9 PCA analysis of FT-IR metabolic fingerprints in *F. cylindrus* and *P. glacialis*. PCA analysis of a) Species and strain and b) Temperature. Analysis conducted using MetaboAnalyst 5.0 (Pang *et al.*, 2021).

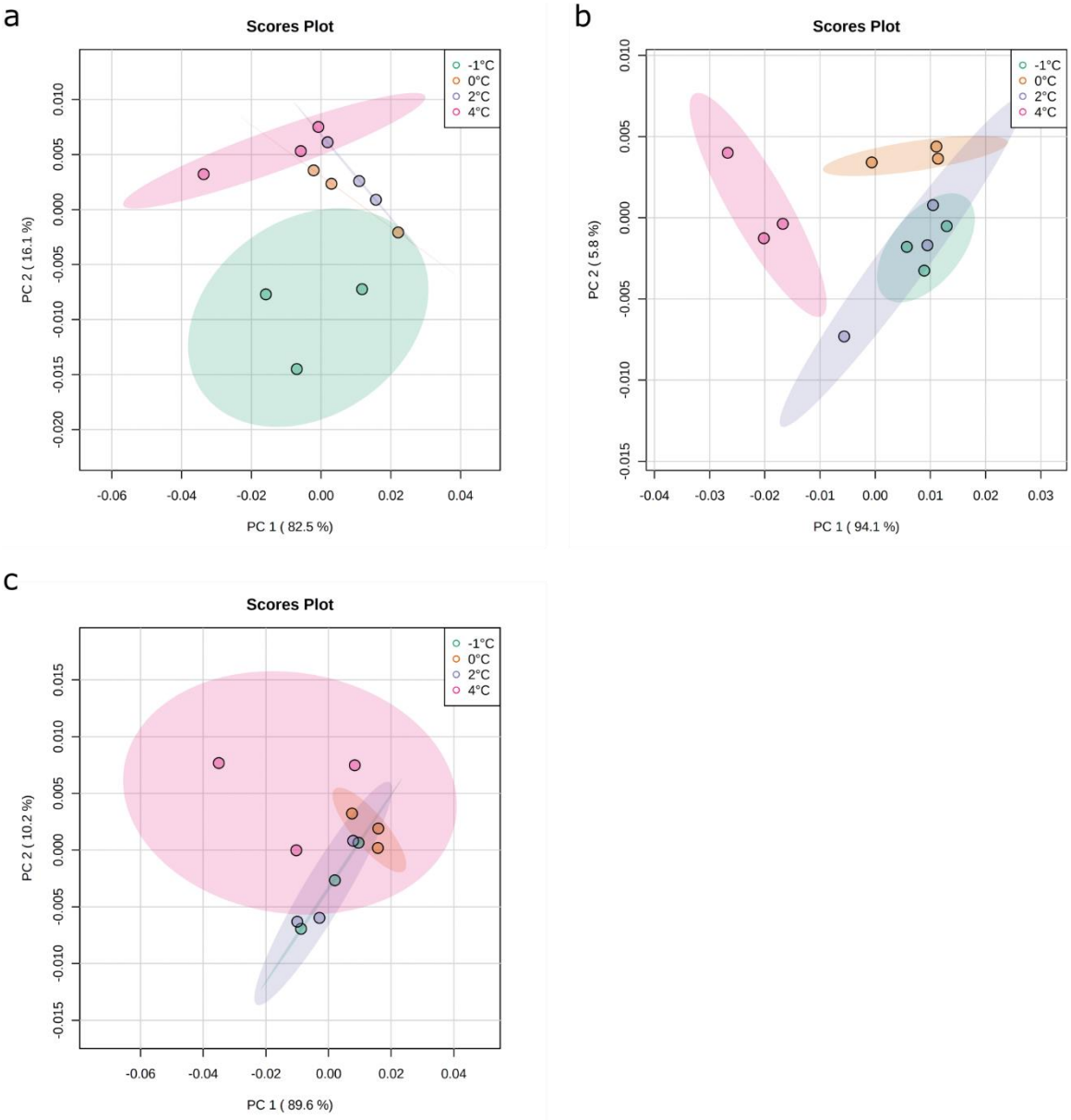

Figure 4.10 PCA analysis of FT-IR metabolic fingerprints in *F. cylindrus* and *P. glacialis* strains and temperature. a) Arctic *F. cylindrus* b) Antarctic *P. glacialis* c) Arctic *P. glacialis*. Analysis conducted using MetaboAnalyst 5.0 (Pang *et al.*, 2021). Antarctic *F. cylindrus* was not analysed due to low sampling number.

The Antarctic *P. glacialis* showed similar pigment concentrations between temperatures (Fig. 4.12). The Arctic strain however, showed an increase in pigments as temperature increased (Fig. 4.12). There were no significant differences in chlorophyll c_1 + c_2 and total carotenoids between strains (Fig. 4.12b and c, ANOVA, Df = 3(15), F = 3.584 and 1.001 respectively, $p>0.5$). However, there was a significant difference in chlorophyll *a* and total chlorophyll concentrations between strains at 4°C, with increased values in the Arctic strain ($p<0.05$, Fig. 4.12a and c). In all pigments excluding total carotenoids there was a significant increase in concentrations at 4°C compared to -1°C in the Arctic strain ($p<0.05$, Fig. 4.12a, b and c) and although not significant ($p>0.05$), chlorophyll does show an increase with increasing temperature (Fig. 4.12a, b, and c).

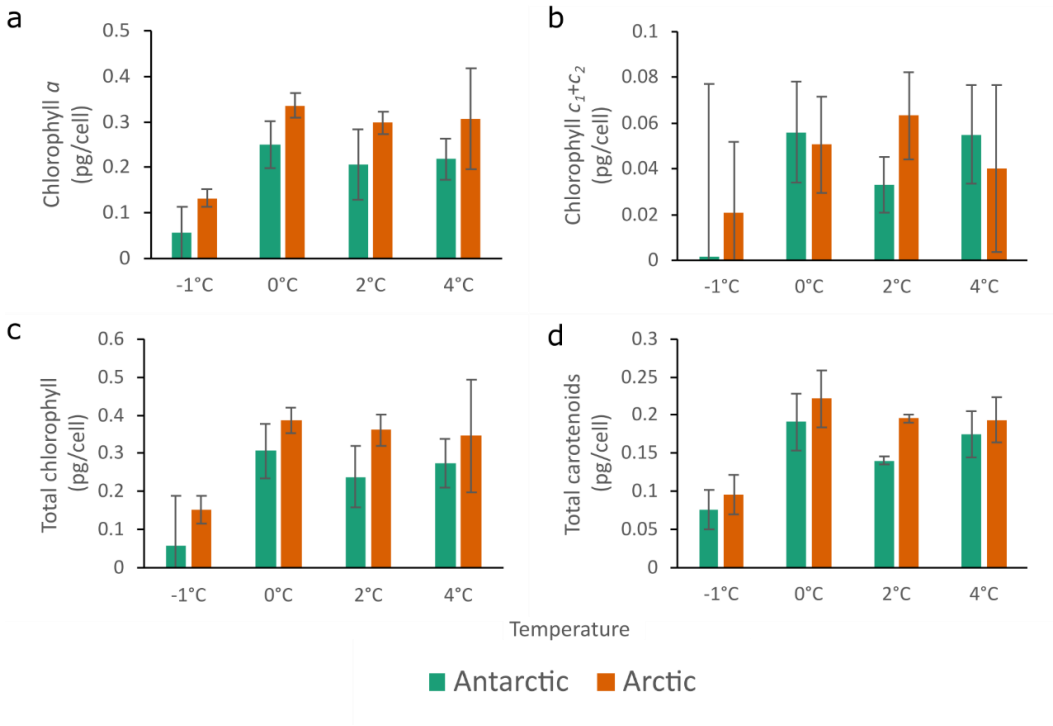

Figure 4.11 *F. cylindrus* – UV spectrometry pigment analysis. a) Chlorophyll a b) Chlorophyll c1 + c2 c) Total chlorophyll d) Total carotenoids. Error bars ±SD, N = 3.

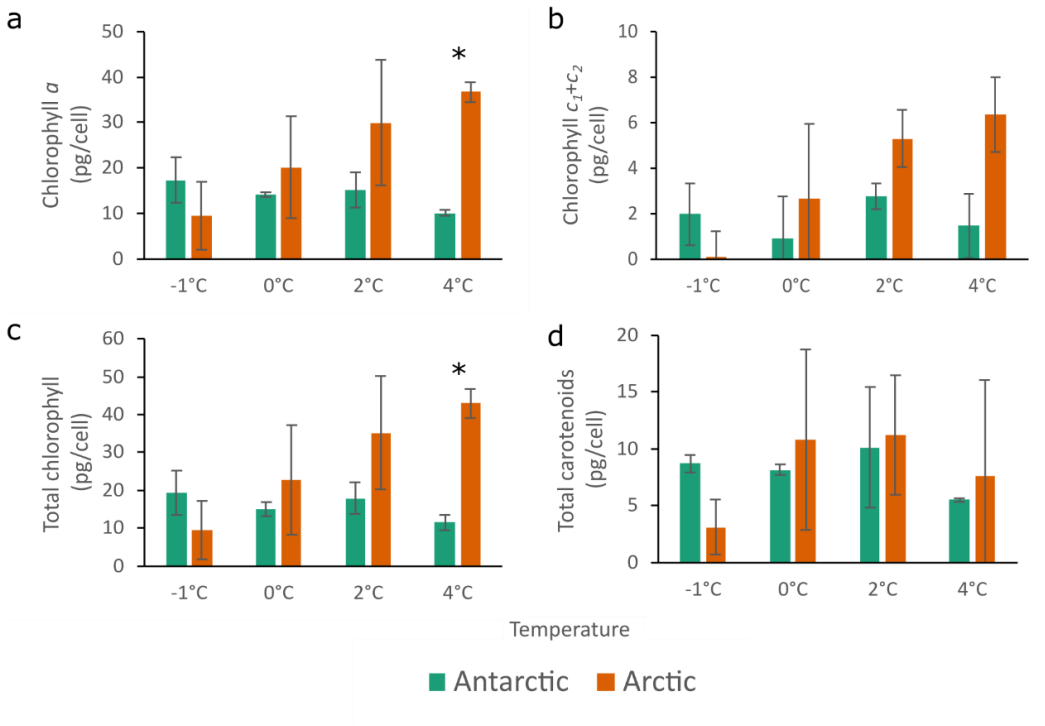

Figure 4.12 *P. glacialis* – UV spectrometry pigment analysis. a) Chlorophyll a b) Chlorophyll c1 + c2 c) Total chlorophyll d) Total carotenoids. Error bars ±SD, * denotes p<0.05. N = 3.

4.2.8 Specific analysis of pigment composition using High Performance Liquid Chromatography (HPLC)

After spectrophotometric analysis of pigments, extracts were analysed via HPLC (Section 2.4.2 in Materials and Methods) and identified four dominant pigments. These were fucoxanthin, diadinoxanthin (Dd), diatoxanthin (Dt) and chlorophyll *a* (Fig. 4.13). All four pigments could be resolved in chromatograms of extracts from *F. cylindrus* strains (Fig. 4.14). Fucoxanthin, diadinoxanthin, and chlorophyll *a* concentration remained stable over the four temperatures in the Antarctic strain (Fig. 4.14a, b and d). Fucoxanthin and diadinoxanthin showed small but significant increases from -1°C to 2°C in the Arctic strain ($p<0.05$, Fig. 4.14a and b) and chlorophyll *a* remained stable ($p>0.5$, Fig. 4.14d). There were no significant differences between strains within temperatures in any of the pigments (ANOVA, Df = 3(16), F = 0.574, 0.612, 0.696 and 0.136 respectively, $p>0.5$). There were small increases in diatoxanthin as temperature increased in both strains, but these were not significant (ANOVA, Df = 3(16), F = 0.136, $p>0.5$, Fig. 4.14c).

Only three of the four pigments could be resolved in *P. glacialis* strains, with no diatoxanthin being detected (Fig. 4.15). There were no significant changes in pigment concentrations over the different temperatures or between different strains (ANOVA, p>0.5). Differences in pigments were largely within the standard deviation, which is likely due to low sample number.

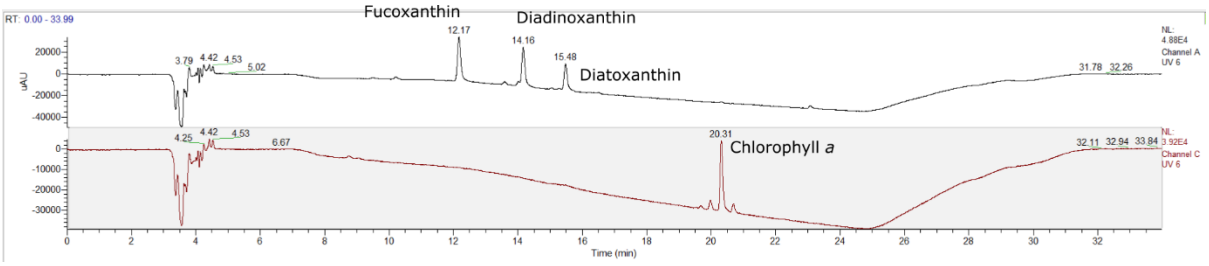

Figure 4.13 HPLC chromatogram showing the resolution of carotenoids and chlorophyll *a*. Pigments were resolved using the method described in Section 2.4.2 of Materials and Methods. Top panel displaying carotenoids and bottom panel displaying chlorophyll *a* detected. Y axis is absorbance units.

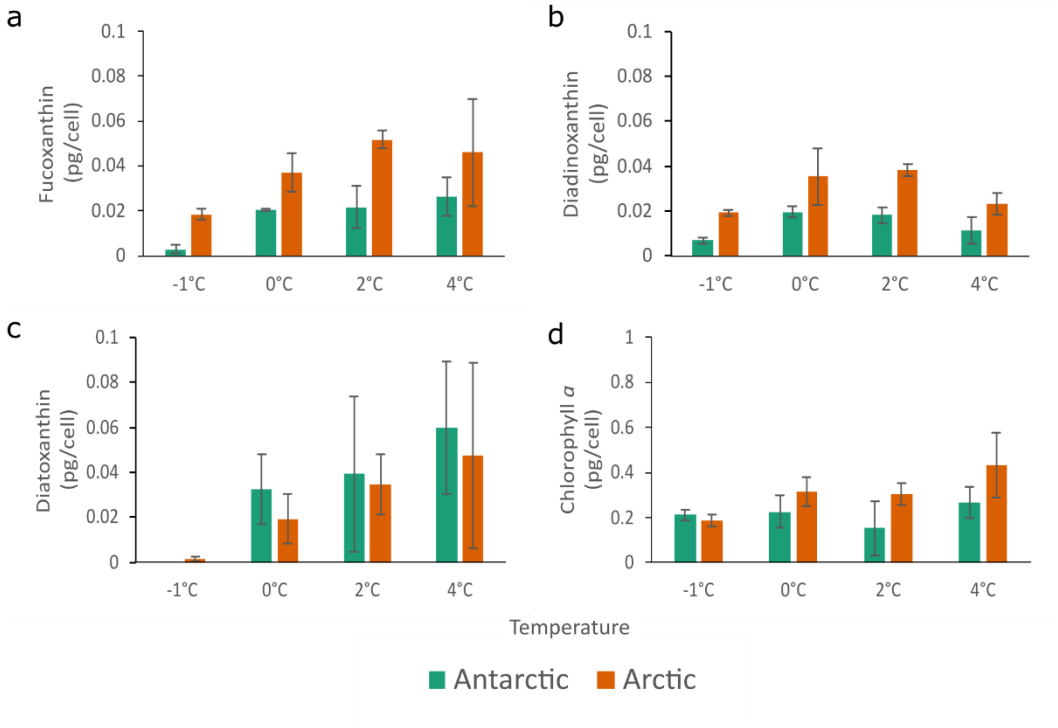

Figure 4.14 *F. cylindrus* – HPLC pigment analysis. a) Fucoxanthin b) Diadinoxanthin c) Diatoxanthin d) Chlorophyll a. Error bars ±SD. N = 3.

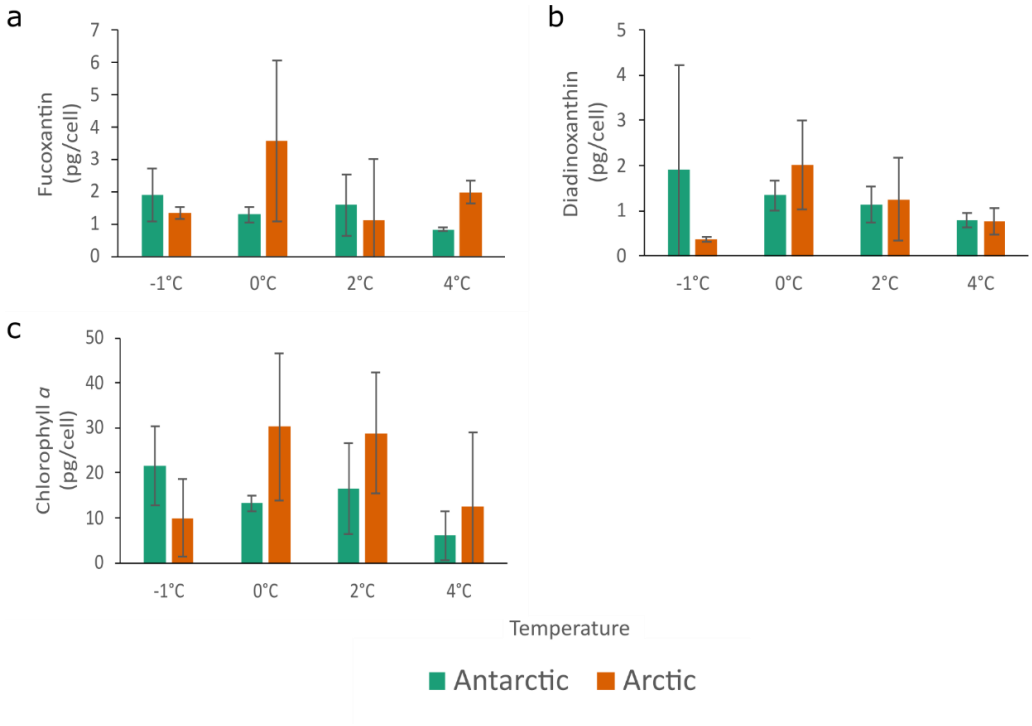

Figure 4.15 *P. glacialis* – HPLC pigment analysis. a) Fucoxanthin b) Diadinoxanthin c) Chlorophyll a. Error bars ±SD. N = 3.

4.2.9 Higher temperatures increased light protecting pigments in *F. cylindrus*

The de-epoxidation state (DES) was calculated with the following equation Dt/(Dt+Dd) (Lavaud *et al.*, 2012) and was used to determine photo stress in cultures. The DES could only be calculated in *F. cylindrus* strains due to there being no measurable diatoxanthin in *P. glacialis*. In both *F. cylindrus* strains there was an increase in diatoxanthin with increasing temperature (Fig. 4.14c). Both strains showed small increases in DES as temperature increased and this was significant between -1°C and 0°C (ANOVA, Df = 3(16), F = 8.427, $p<0.01$, Fig. 4.16). There were no significant differences between strains within temperatures (ANOVA, Df = 3(16), F = 1.037, $p>0.1$).

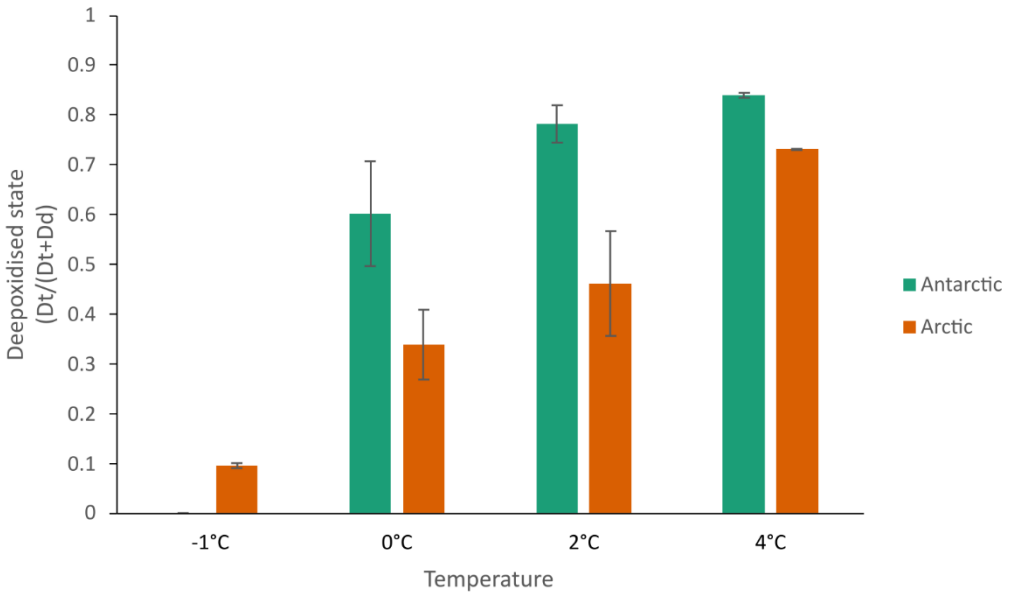

Figure 4.16 De-epoxidation state (DES) of *F. cylindrus strains*. DES state of *F. cylindrus* at cold temperatures. Error bars ±SD. N = 3.

4.2.10 Free fatty acid analysis (FFA)

Lipid extractions analysed via gas-chromatography – flame ionization detection (GC-FID) showed no changes in FFA between temperatures (ANOVA, Df = 3(16), F = 1.468, p>0.1) or strain (ANOVA, Df = 3(16), F = 0.423, p>0.5) in either *F. cylindrus* (Fig. 4.17). *P. glacialis* in contrast showed a very small but significant increase in FFAs at 4°C compared to -1°C (ANOVA, Df = 3(16), F = 4.614, p<0.05, Fig. 4.17). There were no significant differences between the same temperatures between strains (p>0.5). Further analysis of fatty acid methyl esters (FAME) could not be carried out due to lipid breakdown during extended storage during Covid-19.

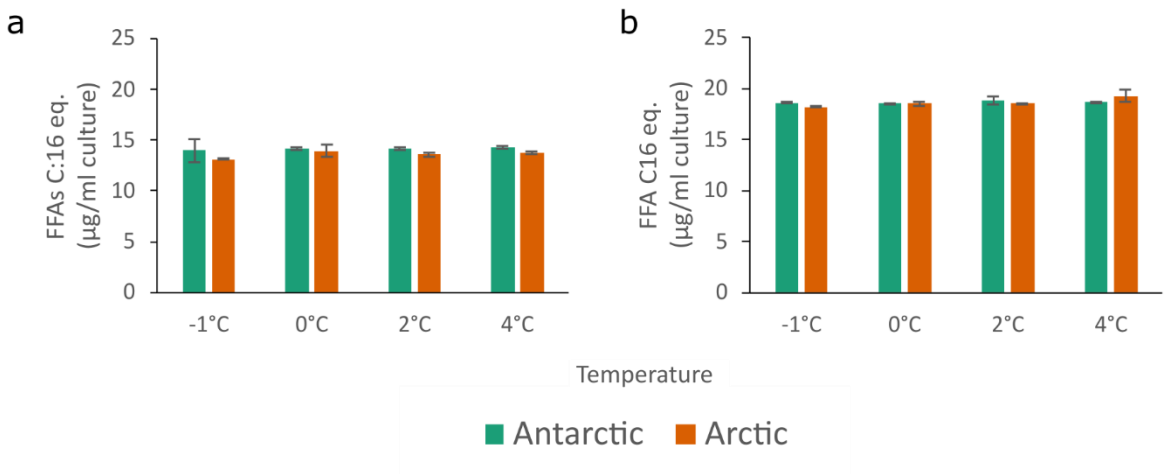

Figure 4.17 Free fatty acid (FFA) concentrations in *F. cylindrus* and *P. glacialis* strains. FFA content derived through GC-FID analysis. a) *F. cylindrus* b) *P. glacialis*. Error bars ±SD. N = 3.

4.3 Discussion:

In this chapter I have presented the thermal tolerance of two key bipolar diatom species and presented some basic metabolic characteristics of these. Previous studies have alluded to the characteristic that Arctic diatoms have a higher thermal tolerance compared to Antarctic diatoms (Coello-Camba & Agustí, 2017). Here, although I show that the Arctic *F. cylindrus* has a higher thermal tolerance compared to the Antarctic strain (Fig. 4.5a), the opposite was found in *P. glacialis* (Fig. 4.5b). Concerning *F. cylindrus*, the results are in line with previous reports of thermal tolerance. Newly isolated strains of *F. cylindrus* investigated by Fiala & Oriol, (1990) had a T_{opt} of 5°C and were unable to survive past 9°C. Antarctic *F. cylindrus* has also shown growth at 7°C (Mock & Hoch, 2005) and showed highest growth rates at 6°C (Jabre & Bertrand, 2020). Similarly, here I report the T_{opt} as 7.1°C (Fig. 4.5a) calculated by modelling the TPC using the Sharpeschoolfull model (Schoolfield *et al.*, 1981) within the rTPC package (Padfield *et al.*, 2021). Previous reports of Arctic *F. cylindrus* strains showed an optimal growth at 8°C but no temperatures above this were tested (Pančić *et al.*, 2015). The optimal temperature was estimated at 10.7°C in the current work, although similar growth was seen at 12°C (Fig. 4.5a). Contrary to *F. cylindrus,* most work on *P. glacialis* has been carried out on the Arctic population and focused on biotechnology. No study directly reported on the thermal tolerance in *P. glacialis* but Arctic isolates have been grown from -2 - 12°C (Huseby *et al.*, 2013; Svenning *et al.*, 2019). Unlike the *F. cylindrus* strains, both *P.*

glacialis strains were able to grow at the same temperatures but there was a larger disparity between T_{opt} (Fig. 4.5b).

Intraspecific differences are not unknown for marine diatoms in response to temperature, for instance, the cosmopolitan diatom *Cylindrotheca closterium* has shown high variability in thermal niche dependent on isolation location (Stock *et al.*, 2019). Stock *et al.*, (2019) did however show that the one Arctic and four Antarctic strains tested exhibited a similar thermal niche, suggesting that thermal niche in this species could well be a conserved trait in similar environments. This finding also agrees with the prediction that these environments would lead to a similar metabolic niche. Pančić *et al.*, (2015) found that the three isolates of Arctic *F. cylindrus* responded similarly in the three temperatures tested, exhibiting differences only in the rate of growth. Furthermore, three isolates of *Actinocyclus actinochilus* from Antarctica showed similar TPCs over a temperature range of -2.5-7.5°C with T_{opt} in the range of 3-4.5°C. This is contrary to the results presented in this chapter whereby both species showed large differences between the polar regions and the finding that a freshly isolated Antarctic *F. cylindrus* strain was able to grow at 12°C (Fig. 4.7). As previously mentioned in Section 4.1, the Arctic and Antarctic have very different evolutionary histories in terms of the length of time they have been under freezing conditions. These differences between the two regions have previously been suggested as a possible explanation for different thermal niches in benthic diatoms as a result of high endemism in the Antarctic (Karsten *et al.*, 2006). Building upon this, species living in Antarctica would have been subjected to these freezing temperatures far longer than those in the Arctic, which could have led to a narrowing of the thermal niche. Moreover, the Antarctic is considered as an isolated continent due to the ACC, which circumnavigates the continent (Rintoul *et al.*, 2001). The ACC prevents the mixing of the Southern Ocean with warmer water from the three ocean basins to which it connects: Atlantic, Pacific and Indian Oceans. Previously *F. kerguelensis* has shown divergent ecotypes across this ACC gradient (Postel *et al.*, 2020). In contrast, the Arctic is narrowly connected to the Pacific Ocean and largely connected to the Atlantic, which is a source of warmer water into the region (Jones *et al.*, 1998). This means that organisms in the Arctic could be subjected to more variable temperatures, and this is supported by higher SST in the Norwegian and Greenland Seas (Carvalho & Wang, 2020). The current results suggest that within the same species, the response to climate change

may differ depending on which polar region it resides in. For *F. cylindrus,* Arctic strains may be able to cope better with increasing SST compared to the Antarctica strain, and *vice versa* for *P. glacialis*. However, this is only a comparison between one strain from either region, therefore future efforts should look at increasing the number of isolates to capture intraspecific variability. This is more evident by the finding that one of the freshly isolated Antarctic strains was able to grow at 12°C, suggesting that there are potential ecotypes of *F. cylindrus* which are able to tolerate higher temperatures in Antarctica. Moreover, the Arctic diatom *Thalassiosira hyalina* has shown intraspecific variation in response to both temperature and carbon dioxide concentrations (Wolf *et al.*, 2019). Therefore, discerning how a species may respond to future warming can be problematic without considering intraspecific variation.

The metabolic characteristics used in this chapter could not identify any differences between strains or between temperatures. This suggests that under these low temperatures there is conservation between polar regions in respect of these basic metabolic characteristics. Previously intraspecific differences have been identified in response to temperature. Metabolic fingerprinting has identified differences between Northern and Southern strains of the diatom *Chaetoceros socialis* (Huseby *et al.*, 2012) and metabolic differences have also been found between Arctic and Antarctic strains of fungi (Sazanova *et al.*, 2019). Furthermore, FT-IR has shown the ability to resolve various biochemical properties of algae (Murdock & Wetzel, 2009), and has previously been used to discriminate different culture stages (Rüger *et al.*, 2016) and life stages (Davey *et al.*, 2019). FT-IR analysis of Arctic and Antarctic strains presented here indicates that these strains are biochemically similar and that this does not differ with temperature (Fig. 4.9 and 4.10). FT-IR however, only resolves large compound groups and does not identify changes in specific metabolites. GC-FID analysis of free fatty acids also showed no differences between strain or temperature (Fig. 4.17). These results show that under environmentally relevant temperatures, Arctic and Antarctic isolates of the same species have similar metabolic properties, highlighting similar adaptations to these cold environments. One concern with increasing temperatures is changes in biochemical composition in prey for higher trophic levels. Omega-3 fatty acids such as docosahexaenoic acid (DHA) and eicosapentaenoic acid (EPA) are vitally important for many trophic levels and diatoms are one of the biggest producers of these (Brett & Müller-

Navarra, 1997). Recently, omega-3 production by phytoplankton was predicted to decrease with increasing temperatures as a result of climate change (Hixson & Arts, 2016). Recent mesocosm experiments have shown no detrimental changes in the fatty acid profile in Antarctic phytoplankton, but have shown an increase in diatom abundance in response to elevated temperature (6°C) and lower salinity (Hernando *et al.*, 2018), whereas in the natural environment, a reduction in diatom abundance has been shown primarily in response to lower salinity and water column stratification (Moline *et al.*, 2004; Rozema *et al.*, 2017). Unfortunately, the compositional analysis of fatty acids in the diatom extracts analysed here was not possible due to extensive lipid degradation during long term storage, therefore despite FFAs being unchanged with increasing temperature this does not mean there is no change in omega-3s. This should be a priority for future work.

Pigments also remained relatively stable over temperature in both species, but large error and low sample number make it difficult to determine any definitive conclusions. Interestingly there was an increase in the DES in both *F. cylindrus* strains with increasing temperature (Fig. 4.16), although care should be taken when interpreting this as the standard deviations around diatoxanthin concentrations were large (Fig. 4.14c). DES is an outcome of the xanthophyll cycle which is an important photoprotective mechanism (Wilhelm *et al.*, 2006). In diatoms this involves the de-epoxidation of diadinoxanthin to diatoxanthin. This apparent trend indicates that under increasing temperature there may have been an increasing stressor from light irradiance. Light levels used in these experiments were kept low at 40µmol m^{-2} s^{-1} and *F. cylindrus* has previously shown an increase in DES at 2°C with increasing light irradiance (Kropuenske *et al.*, 2009). Recently, the synergistic effect of light and temperature has been identified as a key determinant to the temperature tolerance in a cold adapted nano diatom. Kling *et al.*, (2021) report how a cold adapted nano diatom was able to survive at increased temperatures under lower light levels compared to higher light levels. However, the temperatures compared were 4°C and 16°C, much larger than the range used in the current work and well above the ambient temperatures experienced at the poles. Diatoxanthin was not present in any of the *P. glacialis* strains indicating that this protective mechanism was not being utilized under the experimental conditions. Further work would be needed to investigate whether this is a real biological phenomenon and not the result of sampling error.

The Kling *et al.*, (2021) work does highlight the critical importance of light on the thermal tolerance in diatoms. Culturing cells over a temperature range at only one light irradiance could miss the effects of decreasing or increasing light levels on thermal tolerance. Therefore, in the future, it would be important to factor in different light irradiances when determining the thermal tolerance of species. Although light levels may remain stable in the polar environments in the future, if temperatures were to increase to the point at which light stress becomes deleterious then this could have large impacts on diatom composition and diversity. Clearly a lot more work is needed to elucidate the complexity of the ecophysiological and metabolic response of diatoms to climate change. Despite this, the expected temperature increases in both the Arctic and Antarctic are unlikely to affect the two species used in this work as a single factor. However, studies reporting a decrease in diatom abundance as a result of sea water freshening and reduced stratification (Moline *et al.*, 2004; Rozema *et al.*, 2017) stresses the importance of understanding the indirect effects as much as the direct effects.

Chapter 5 - Polar opposites: B_{12} dependency in *Fragilariopsis cylindrus*

All of the work in this chapter was carried out by myself, with the exception of the data-mining and analysis carried out in Section 5.2.1, which represents a collaboration with four PhD students within the Plant Metabolism group at the University of Cambridge: Shelby Newsad, Dominic Absolon, Ellen Harrison and Nhan-An Tran.

5.1. Introduction:

Cobalamin, more commonly known as vitamin B_{12}, is an important micronutrient for metabolic processes throughout the Tree of Life. In bacteria and eukaryotes (excluding plants and fungi) vitamin B_{12} is required as a cofactor for the B_{12}-dependent enzyme, methionine synthase (METH). Methionine is an essential amino acid produced via METH, through the transfer of a methyl group from methyl-tetrahydrofolate to homocysteine. Land plants and major fungal groups produce methionine through the B_{12}-independent methionine synthase (METE) which does not use cobalamin as a cofactor, so they are independent of B_{12}. However, recent work has demonstrated that some early diverging fungi do encode some B_{12}-dependent enzymes, including METH, methylmalonyl-CoA mutase (MCM), and ribonucleotide reductase class II (RNR) whilst also encoding METE (Orłowska *et al.*, 2021). Mammals possess METH only, and so are dependent on an external source of this compound in their diet. Looking more broadly across the eukaryotic Tree of Life, there is a much more patchwork distribution of METE and METH, particularly within the algal lineages (i.e., those that are photosynthetic, described in Section 1.2.1 within the Introduction). From studies of algal growth requirements (Croft *et al.*, 2005), over 50% of surveyed algal species exhibited an obligate requirement for vitamin B_{12}, indicating that these taxa did not encode a functional METE but instead utilized METH only. Analysis of sequenced genomes indicated that some other species had just METE, whist others encoded both enzymes, including the model green alga *C. reinhardtii* and the diatom *P. tricornutum* (Helliwell *et al.*, 2011). Closely related species to *C. reinhardtii* and *P. tricornutum* however do not possess METE and are therefore B_{12} dependent: *Ostreococcus tauri* (Helliwell *et al.*, 2011) and *Pseudo-nitzschia*

granii (Ellis *et al.*, 2017) respectively. The apparent randomness of B_{12} auxotrophy within the algae has led to work focusing on how B_{12} dependency has evolved. In diatoms this has led to the identification of the cobalamin acquisition protein 1 (CBA1) in *T. pseudonana* and *P. tricornutum* which is involved in cobalamin uptake (Bertrand *et al.*, 2012). Furthermore, unlike land plants which are independent of B_{12} encoding METE only, no algal species has shown a loss of METH (Helliwell *et al.*, 2011) and this may be due to the differing nutrient requirements e.g., zinc and nitrogen of the two enzymes (Bertrand *et al.*, 2013). Bertrand *et al.*, 2013) identified a greater requirement for zinc and nitrogen by METE over METH and nitrogen for CBA1. A hypothetical scenario of a diatom encoding METE only, indicates that under B_{12} replete conditions there is a higher nutrient cost but under B_{12} deplete conditions there is a saving (Bertrand *et al.*, 2013).

In 1992, Gonzalez *et al.*, reported that the METE enzyme from *E. coli* had a less efficient catalytic turnover compared to METH, implying that if B_{12} is present, METH will be preferentially used. This finding has been supported by the work of Croft *et al.*, (2005) who found *METE* was not expressed in the presence of B_{12} in *C. reinhardtii*. The suppression of *METE* has also been shown in *P. tricornutum* (Helliwell *et al.*, 2011) as well as the absence of METE proteins in the presence of B_{12} (Bertrand *et al.*, 2012). In *F. cylindrus,* Ellis *et al.*, (2017) also showed that the presence of B_{12} leads to a reduction in *METE* expression, the addition of which, to deplete cultures resulted in a 107-fold decrease in *METE* (Ellis *et al.*, 2017).

In this chapter I wanted to explore the relationship between environment and geography on the prevalence of B_{12} auxotrophy in algal lineages. The chapter reports on two lines of work which were investigated in parallel based on initial results presented in Fig. 5.3 which shows the geographical difference in B_{12} dependency of *F. cylindrus* strains. I, therefore questioned whether biogeography could explain patterns in B_{12} auxotrophy in other algae. Since the publication of Croft *et al.*, (2005) several other publications have elaborated on B_{12} dependency in algae, finding that specific algal groups are largely B_{12} dependent including, dinoflagellates (Tang *et al.*, 2010) and haptophytes (Nef *et al.*, 2019). Much of the recent work used the presence or absence of *METE* as an *a priori* method to determine B_{12} auxotrophy, where lack of *METE* suggests B_{12} dependency (Helliwell *et al.*, 2011; Ellis *et al.*, 2017; Nef *et al.*, 2019). The advent of large-scale genomic projects such as the Marine Microbial Eukaryotic Transcriptome Sequencing Project (MMETSP, Keeling *et al.*, 2014) and

TaraOceans (https://oceans.taraexpeditions.org/en/m/about-tara/les-expeditions/tara-oceans/), has led to the ability to interrogate a larger number of species for particular genes. Utilizing the MMETSP dataset, Ellis *et al.*, (2017) described a biogeographical pattern in the distribution of *METE* in diatoms, with a higher proportion of Southern Ocean diatoms possessing the gene compared to non-Southern Ocean diatoms.

B_{12} auxotrophy has arisen independently several times within algal lineages (Croft *et al.*, 2005; Helliwell *et al.*, 2011) and without a clear phylogenetic relationship between dependent algae, the environment is a likely factor contributing to the selection of this trait. With this in mind, it was decided to combine the various published data on algal B_{12} dependency with a focus of extracting isolation location and habitat information. This work was done in collaboration with four other PhD students within the Plant Metabolism group at the University of Cambridge, Dominic Absolon, Ellen Harrison, Shelby Newsad and Nhan-An Tran.

Second, I took a deeper dive into B_{12} auxotrophy biogeography by investigating strains within the two polar regions. In the previous chapter I presented work detailing the thermal tolerance of Arctic and Antarctic *F. cylindrus* strains, and how the Arctic strain exhibited a higher thermal tolerance with sufficient growth at 12°C. These results prompted me to investigate the B_{12} dependency in these strains as it has previously been suggested that the B_{12}-dependent methionine synthase enzyme could offer an advantage under heat stress (Xie *et al.*, 2013). Xie *et al.*, (2013) reported that *C. reinhardtii* was able to tolerate higher temperatures of 42°C when exogenous B_{12} was supplied either through direct addition to the media or through a symbiotic interaction with B_{12} producing bacteria. When B_{12} was not present *C. reinhardtii* was unable to grow at the higher temperature (Xie *et al.*, 2013). It is common practice to include vitamin B_{12} into the media even if a species does not require it, due to the widespread B_{12} dependency of algae. Previous reports on the thermal tolerance of *F. cylindrus* (including my own in chapter 4) include vitamin B_{12} in the media. The inclusion of B_{12} means it is not possible to identify whether the thermal optimum (T_{opt}) is altered as a result.

REDACTION: Sentence describing unpublished results removed for copyright reasons. Copyright holder is Catalina Albury.

I therefore hypothesised that the increased thermal tolerance could potentially be the result of a differing response to B_{12} in the strains. The observation that Southern Ocean diatoms display a higher proportion of species retaining the *METE* gene over non-Southern Ocean diatoms, suggested that different selection pressures between environments may have led to differing B_{12} dependencies (Ellis *et al.*, 2017). Despite the Arctic and Antarctic sharing many environmental characteristics, they do present two different environments which are significantly isolated from one another. It is also not unheard of for multiple strains within the same species to have different B_{12} requirements (Lewin & Lewin, 1960; Tang *et al.*, 2010).

5.2 Results

5.2.1 Assessment of algal B_{12} dependency over latitude and habitat type

To determine the location coordinates and habitat of strains classified as B_{12}-dependent or independent on the basis of culture requirements, data were extracted from the Supplementary Table 1 presented in Croft *et al.*, (2005) and the original reference of Provasoli & Carlucci, (1974 and references therein). Isolation location was noted either directly from the specific reference or, if necessary, through accessing the strain information via culture collections. In some cases, the isolation description was very broad e.g., South Finland, in such cases non-specific coordinates were used. If the original paper did not describe the habitat from which the strain was isolated, we carried out a search of the species on Algaebase (https://www.algaebase.org/) or Marine Worms databases (https://www.marinespecies.org/) to check the general habitat and also update species nomenclature. In addition to the Croft *et al.*, (2005) strain list, we also included data from more recent publications incorporating both genetic and physiological characterization of B_{12} dependency (Tang *et al.*, 2010; Helliwell *et al.*, 2011; Ellis *et al.*, 2017; Nef *et al.*, 2019, 2020).

The B_{12} dependency status of an additional 130 algal strains were acquired through (Tang *et al.*, 2010; Helliwell *et al.*, 2011; Ellis *et al.*, 2017; Nef *et al.*, 2019, 2020), resulting in a total of 456 strains. Of these, we found that 268 required B_{12} (58.8%) and 188 do not require B_{12} (41.2%). We found that B_{12} dependency varied amongst algal groups and that the majority of algal groups had over 50% auxotrophy with the exception of the Chlorophyta (Table 5.1a). Of

the 456 strains assessed, 78.7% of strains were characterized through physiological experimentation, 16.9% through genetic analysis alone and 4.4% through both physiological and genetic analysis (Table 5.1b).

Table 5.1 Survey of B_{12} dependency in algae. a) B_{12} dependency in algal groups and b) method at which B_{12} dependency was determined.

a

Phylum	Species Surveyed	Require B_{12}	% Require B_{12}	Do not require B_{12}	% Do not require B_{12}
Chlorophyta	134	40	29.9%	94	70.1%
Charophyta	27	14	51.9%	13	48.1%
Cryptophyta	9	8	88.9%	1	11.1%
Euglenozoa	15	13	86.7%	2	13.3%
Glaucophyta	1	1	100.0%	0	0.0%
Haptophyta	40	31	77.5%	9	22.5%
Myzozoa	59	51	86.4%	8	13.6%
Ochrophyta	157	98	62.4%	59	37.6%
Rhodophyta	14	12	85.7%	2	14.3%
Total	**456**	**268**	**58.8%**	**188**	**41.2%**

b

Characterisation type	Counts	Percentage
Physiological	359	78.7%
Genetic	77	16.9%
Physiological and Genetic	20	4.4%

To investigate whether B_{12} dependency showed a spatial pattern, we assessed the location and habitat information of algal strains based on their B_{12} dependency status via a binomial general linear model (GLM). The location information was identified in 315 strains and the majority of strains were isolated from North America and Europe (Fig. 5.1). There was no significant effect of latitude on B_{12} dependency (p-value>0.05), however, there was a significant effect of habitat type (Chisq = 78.428, Df (3, 310), p<0.001).

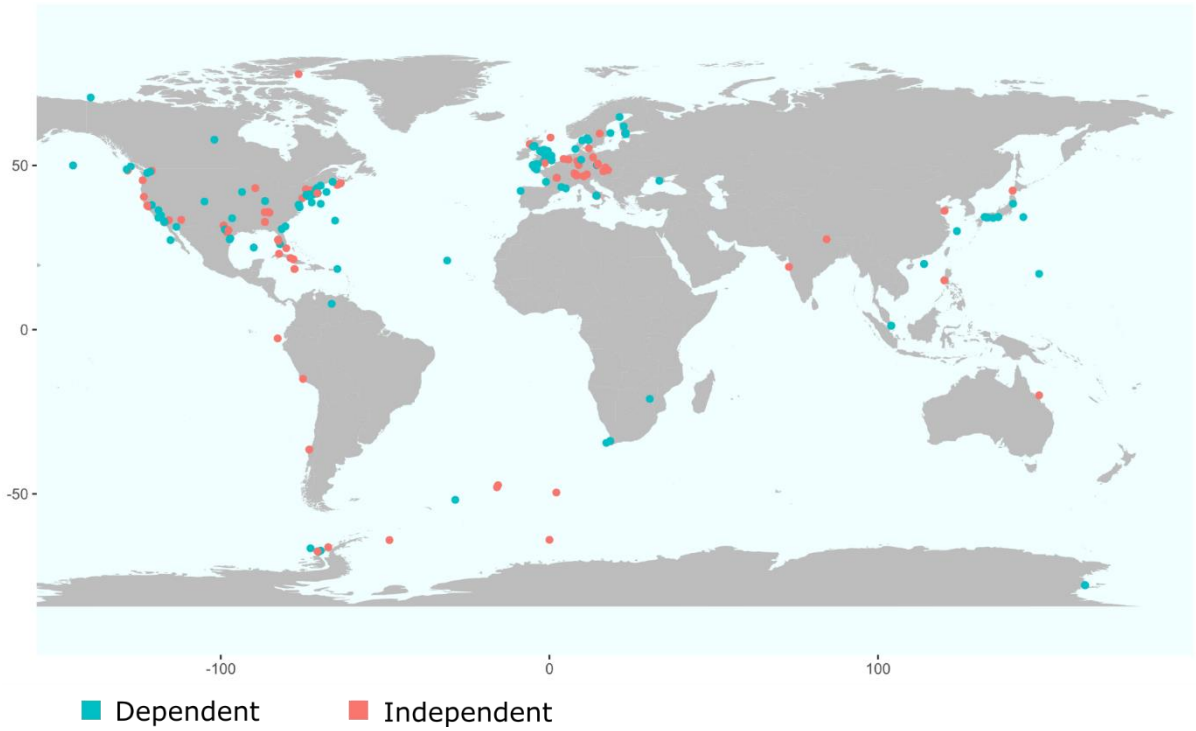

Figure 5.1 Biogeography of algal B_{12} dependency. Coordinate positions of algal strains used for B_{12} auxotrophic analysis and their B_{12} dependency state.

We followed up the significant effect of habitat type by excluding the latitude factor in the analysis, resulting in a total of 449 strains with habitat type information. A binomial GLM found habitat type to be a significant factor influencing the B_{12} dependency in algae (Chisq = 82.112, Df (3, 444), $p<0.001$). The effect of individual habitats was investigated via *a priori* contrasts. Over 50% of tested strains were marine and within the marine habitat the number of B_{12} dependent strains was significantly higher (76.28%, n = 238, $p<0.001$, (Fig. 5.2)).The number of B_{12} dependent strains decreased in a stepwise fashion in the remaining habitats with habitats becoming increasingly B_{12} independent; estuarine (55.95% dependency, n = 27, $p<0.05$), freshwater (44.9% dependency, n = 71, $p<0.001$) and terrestrial (13.03% dependency , n = 41, $p<0.001$). There was a significant difference in B_{12} dependency within the terrestrial habitat, with more strains being B_{12} independent (86.97% independency, n = 41, $p<0.001$ (Fig. 5.2)). There was no significant difference in B_{12} dependency within estuarine and freshwater habitats ($p>0.1$ for both habitats) and there was no significant difference between the two habitats ($p>0.1$). Within the terrestrial habitat 95% of strains were within the Chlorophyta.

As much of the data were within North America and Europe, a subset of the data between 30°N and 60°N classified as "Northern Temperate" was analysed. There remained no effect of latitude on B_{12} dependency ($p>0.5$), but marine and terrestrial habitats again showed significant effects ($p<0.05$). The number of strains tested within this region was 247 of which 147 were B_{12} auxotrophic (59.1%). All the other regions are represented by only 66 strains and of these 34 were B_{12} auxotrophic (51.5%).

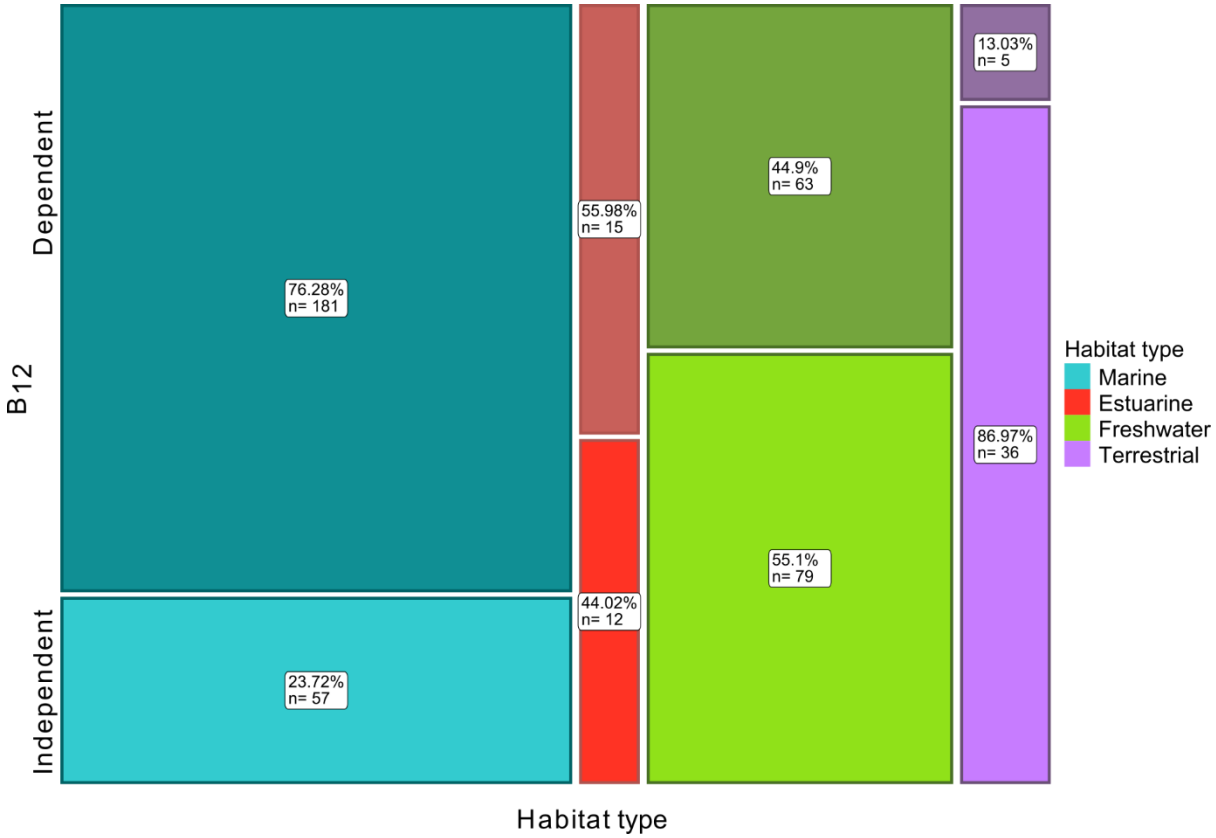

Figure 5.2 Algal B_{12} dependency as a factor of habitat type. Habitat analysis of algal strains used for B_{12} auxotrophic analysis. Box width corresponds to the number of strains analysed within each habitat type and height corresponds to the number of strains dependent or independent for B_{12}.

5.2.2 Determing vitamin requirments in *F. cylindrus* strains using microtitre assays

Initial experiments identified that the Arctic strain (RCC 4289) of *F. cylindrus* exhibited reduced growth when the *f*/2 B vitamin mix was omitted from the media, whereas the Antarctic strain showed no difference (Fig. 5.3). Previously the Antarctic strain (CCAP 1023/1) was shown to have no requirement for biotin (B_7), thiamine (B_1), or cobalamin (B_{12}) (Helliwell *et al.*, 2011). I next set out to determine the vitamin preferences of *F. cylindrus* strains from both polar regions through physiological experimentation and genetic analysis of methionine synthase genes. To assess whether the B_{12} dependent and independent phenotypes are characteristic of the Arctic and the Antarctic, additional strains from both regions were acquired. Care was taken to select strains from different regions of the poles so to capture regional variability (Fig. 5.4). These additional strains will also increase the number of strains analysed for B_{12} dependency in the polar regions which is low (Fig. 5.1).

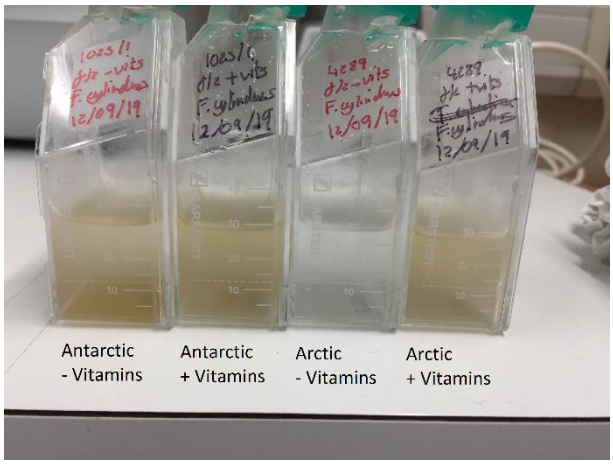

Figure 5.3 Requirement for B vitamins in the Arctic *F. cylindrus* strain. Cultures of the Antarctic and Arctic strains of F. cylindrus after two transfers with or without B vitamins.

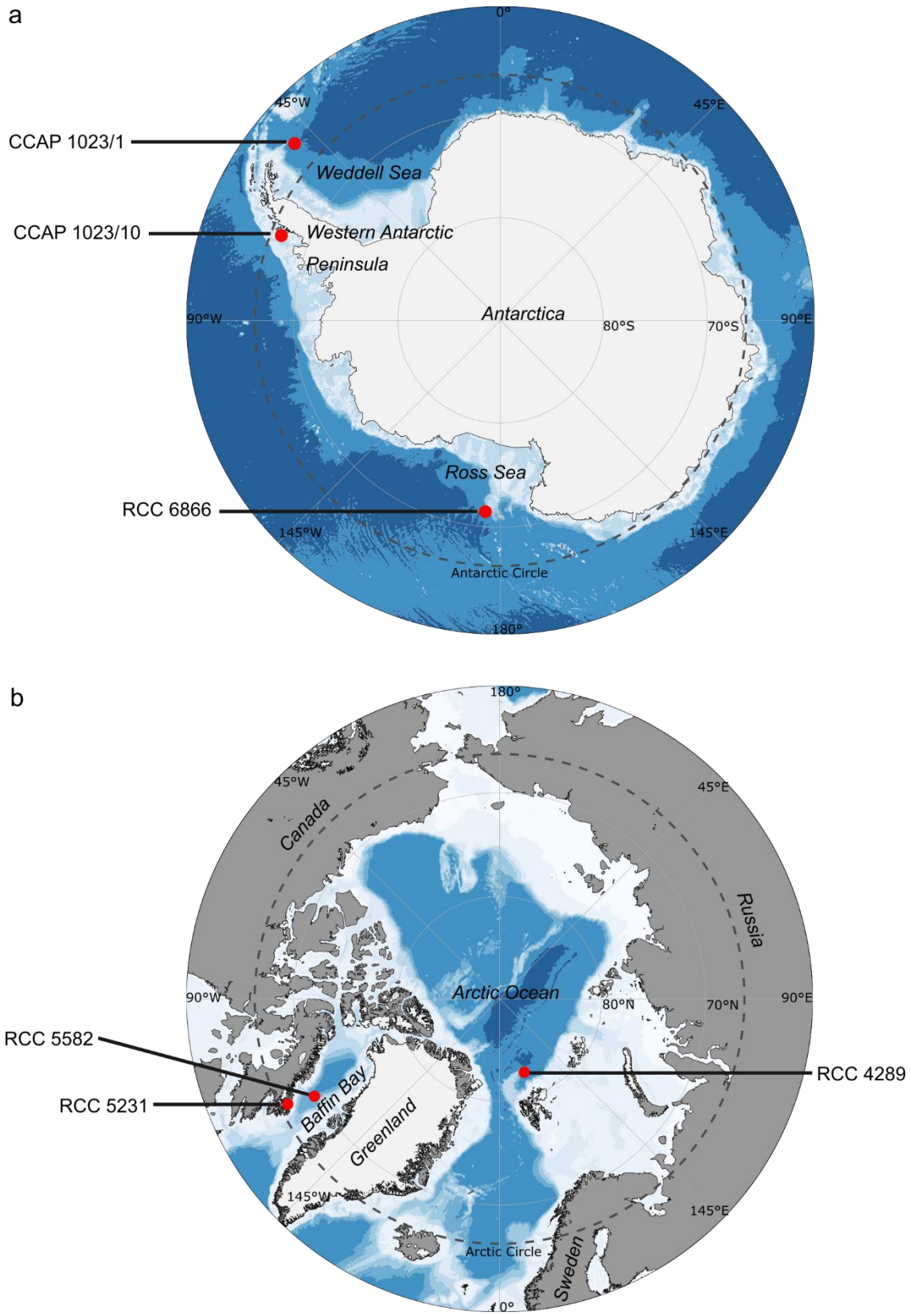

Figure 5.4 *F. cylindrus* strain isolation locations. a) Antarctic strains and b) Arctic strains. Maps produced using the ggOceanMaps package (Vihtakari, 2021).

5.2.2.1 B vitamin requirements of *F. cylindrus* during the 1st subculture

To understand the lack of growth in the Arctic *F. cylindrus* strain (RCC 4289), a vitamin growth assay (see 2.5.1 in Materials and Methods) was utilized in all strains to distinguish which of the three vitamins present in the *f*/2 vitamin solution were required for growth. Cells were washed with sterile seawater (Section 2.5.1) and transferred into the microtitre plate with vitamin treatments (Fig. 2.1). All three Arctic strains showed growth in all vitamin combinations (Fig. 5.5), but strains 4289 and 5582 showed reduced growth in treatments where 500 ng/L B_{12} was omitted (Fig. 5.5e-h, Appendix 8). Strain 5231 showed slightly faster growth or higher carrying capacities compared to the other two strains and did not show the reduced growth where B_{12} was omitted (Fig. 5.5, Appendix 8). The omission of B_1 and B_7 in Arctic strains did not result in a reduction of growth in the presence of B_{12}, indicating that these strains do not require either of these two vitamins (Fig. 5.5a-e). This is further confirmed by the similar growth shown between *f*/2 vitamins (including all B vitamins) and B_{12} alone demonstrating the lack of requirement for exogenous B_1 and B_7 in Arctic strains (Fig. 5.5a and b respectively).

In treatments where B_{12} was omitted, growth was lowest in 4289 and highest in 5231 and growth rates between strains were all significantly different (Table 5.2, ANOVA Df = 2(66), F = 123.691, $p<0.001$, Tukey posthoc tests $p<0.001$). All three strains showed lower growth rates where B_{12} was not present and there was a significant effect of the presence of B_{12} on growth rate (Table 5.2, ANOVA Df, 3(66), F = 8.017, $p<0.001$). Posthoc testing revealed that strain 4289 showed significantly lower growth rates in treatments without B_{12} ($p<0.01$), whereas strains 5231 and 5582 showed slightly lower growth rates but these were not significant ($p>0.5$ and >0.1 respectively).

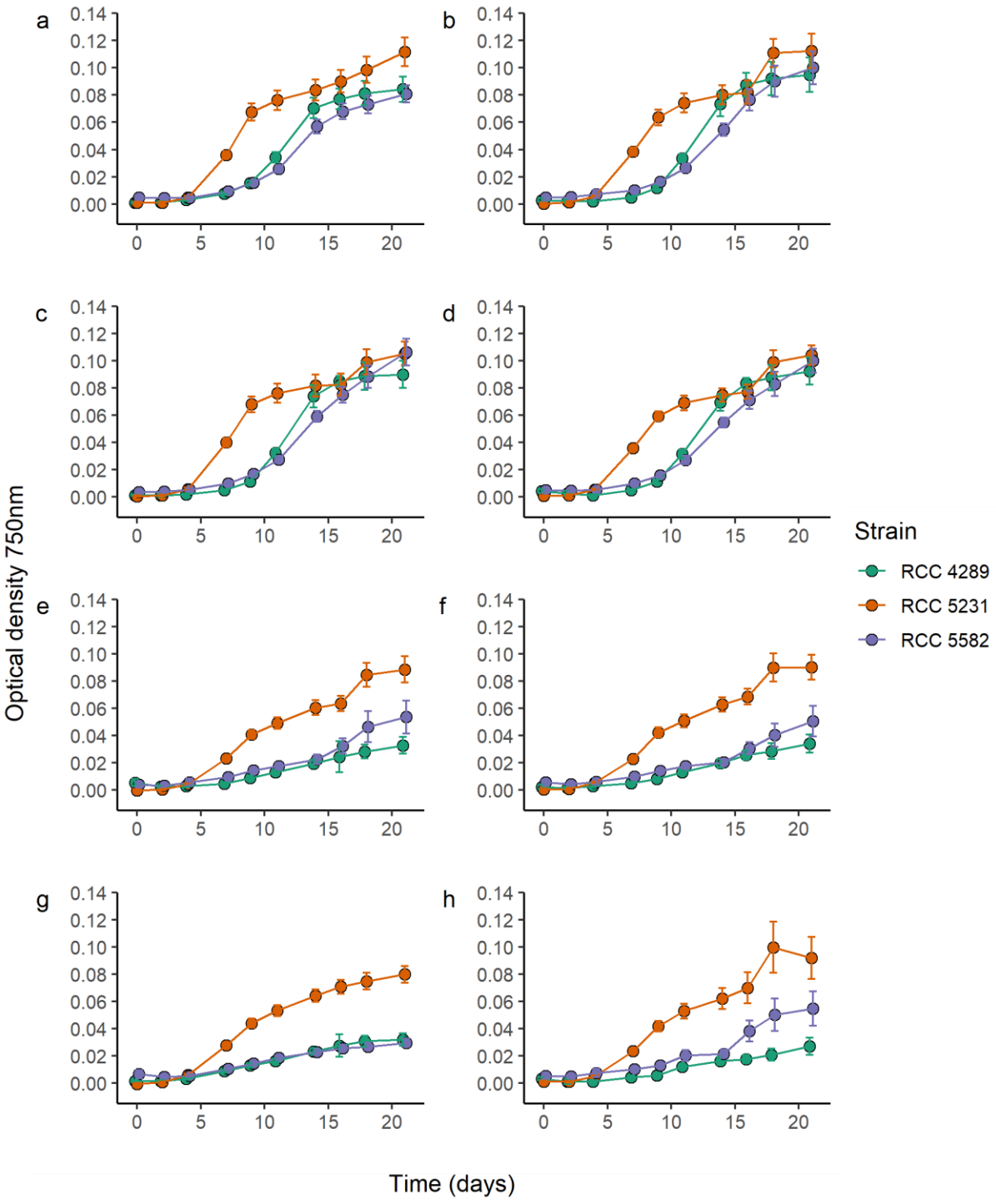

Figure 5.5 Vitamin growth assay in Arctic *F. cylindrus* strains – 1st subculture. a) *f*/vitamins b) B_{12} c) B_{12} + B_1 d) B_{12} + B_7 e) B_1 f) B_7 g) B_7 + B_1 and h) no vitamins. Errors bars ±SD. Cultures grown at 4°C at a starting inoculation of $17.6x10^3$ cells/ml in 200 µl of treatment media. Concentrations of vitamins were: B_{12} – 500 ng/L, B_1 – 100 µg/L and B_7 – 500 ng/L. N = 3.

Table 5.2 Growth rates in *F. cylindrus* strains grown with or without vitamin B_{12} during the 1st subculture.

Strain	Average growth rate	
Arctic Strains	**+B_{12}**	**-B_{12}**
4289	0.257	0.129
5231	0.592	0.529
5582	0.393	0.315
Antarctic Strains		
1023/1	0.228	0.243
1023/10 – SC48	0.261	0.272
6866	0.270	0.268

Conversely, the three Antarctic strains exhibited similar growth in all vitamin combinations with or without B_{12} (Fig. 5.6, Appendix 9). Growth rates significantly differed between strains (Table 5.2, ANOVA Df = 2(66), F = 4.594, $p<0.05$) with 1023/1 showing significantly lower values compared to 1023/10 – SC48 ($p<0.05$) and 6686 ($p<0.05$). There was no significant difference between 1023/10 – SC48 and 6866 ($p>0.5$). Within strains, there were no significant differences between growth rates in treatments with or without the presence of B_{12} (Table 5.2, ANOVA, Df = 3(66), F = 0.399, $p>0.5$).

5.2.2.2 A requirement for B_{12} in Arctic strains revealed in the 2nd subculture

Although cells were washed to remove excess vitamins before experimental cultures were acclimated, cells are likely to have internal stores of B_{12} which they utilize in periods of B_{12} scarcity. Internal stores may be evidenced by the growth of all three Arctic strains during the first subculture, but this may also be due to an ability to grow without the vitamin (Fig. 5.5). Another potential factor which could explain the growth shown in Arctic strains is B_{12}-producing bacteria. Strains were not made axenic prior to experimentation, and bacteria could supply the B_{12} needed for the cells to grow. To confirm the exhibited growth in Arctic strains, a sub-culture was made into fresh media, termed the "2nd subculture" and the assay re-run. Therefore, any growth present in these second cultures would most likely be the result of bacterial B_{12} production or an independence for the vitamin, likewise a lack of growth would imply a dependence for the vitamin.

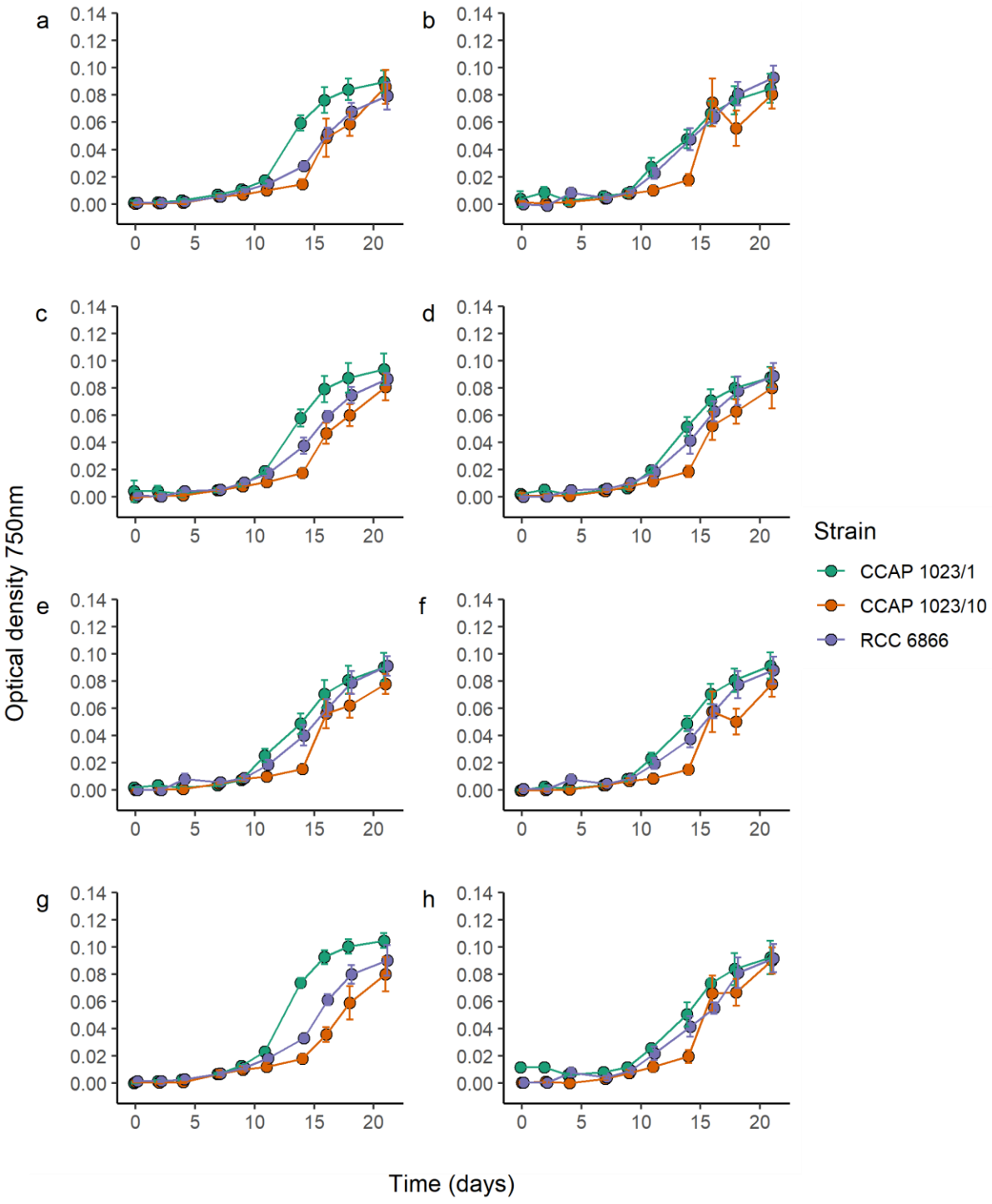

Figure 5.6 Vitamin growth assay in Antarctic *F. cylindrus* strains – 1st subculture. a) *f*/vitamins b) B_{12} c) B_{12} + B_1 d) B_{12} + B_7 e) B_1 f) B_7 g) B_7 + B_1 and h) no vitamins. Errors bars ±SD. Cultures grown at 4°C at a starting inoculation of 17.6x10^3 cells/ml in 200 µl of treatment media. Concentrations of vitamins were: B_{12} – 500 ng/L, B_1 – 100 µg/L and B_7 – 500 ng/L. N = 3.

In the 2nd subculture, Arctic strains showed similar responses over the eight vitamin treatments (Fig. 5.7). All three strains exhibited no growth in treatments which did not contain B_{12} (Fig. 5.7e-h, Appendix 10), indicating that internal stores were depleted, and that any bacterial contamination was not producing B_{12}. All three strains showed similar growth in treatments with B_{12} however, 5231 showed slightly reduced growth in the "*f*/2 vitamins" treatment which contained all three B vitamins (Fig. 5.7a). Due to the lack of growth in treatments without B_{12}, growth rates could not be calculated (Table 5.3). Growth rates varied between strains within treatments with B_{12} but there were no significant differences (Table 5.3, ANOVA Df =2(66), F = 2.488, $p>0.05$).

Antarctic strains grew similarly between all treatments in the 2nd subculture (Fig. 5.8, Appendix 11) and there were no significant differences between the growth rates in treatments with or without B_{12} (Table 5.3, ANOVA Df = 3(66), F = 0.068, $p>0.5$). There was a significant effect of strain on growth rates (ANOVA, Df = 2(66), F = 6.382, $p<0.01$) with 1023/1 again showing the slowest growth, which was significantly different to 1023/10 – SC48 ($p<0.01$) but not significant compared to 6866 ($p>0.05$). There was no significant difference in growth rate between 1023/10 – SC48 and 6866 ($p>0.1$).

Table 5.3 Growth rates in *F. cylindrus* strains growth with or without vitamin B_{12} during the 2nd subculture.

Strain	Average growth rate	
Arctic Strains	**+B_{12}**	**-B_{12}**
4289	0.341	n/a
5231	0.364	n/a
5582	0.322	n/a
Antarctic Strains		
1023/1	0.321	0.312
1023/10 – SC48	0.373	0.377
6866	0.357	0.353

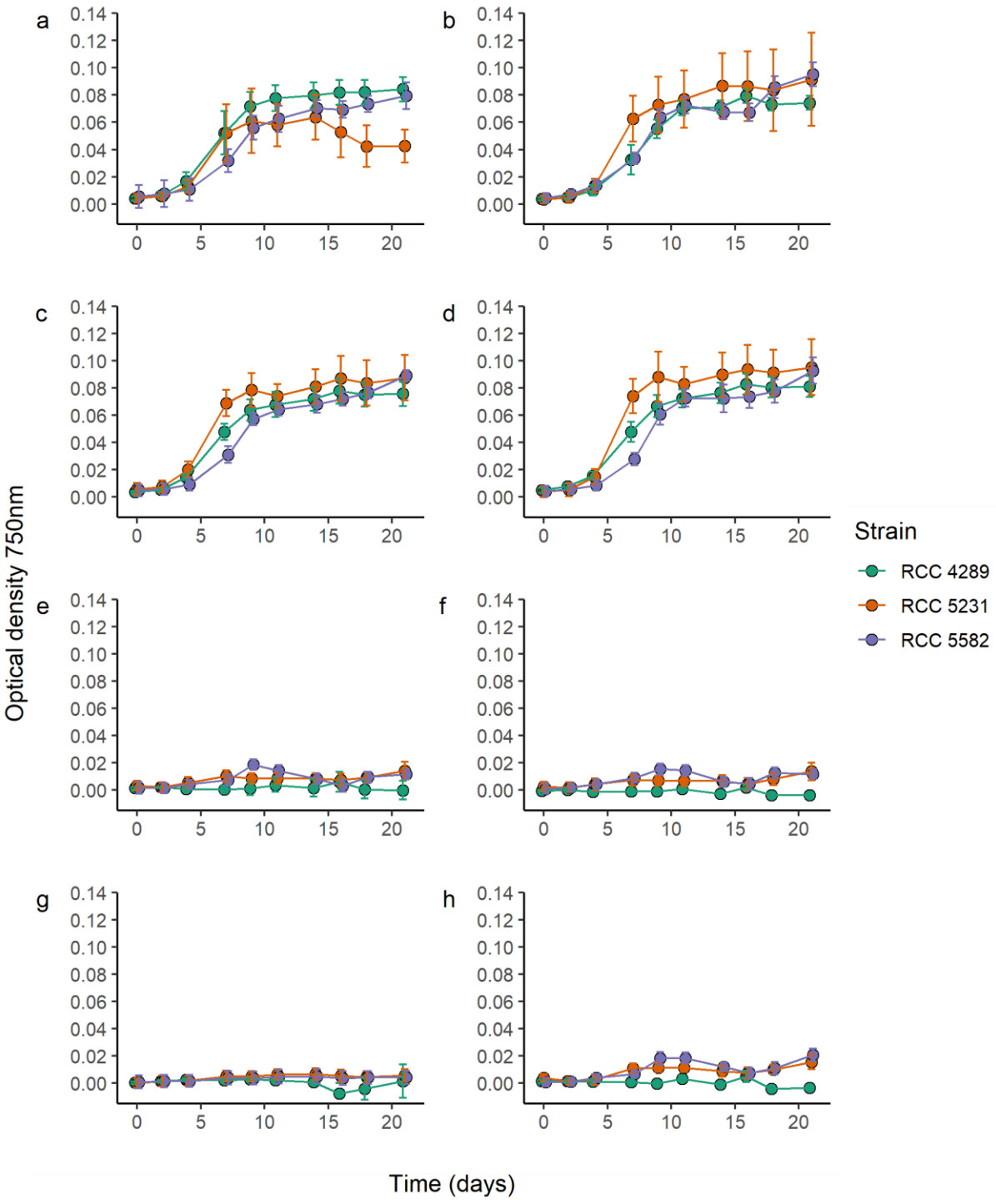

Figure 5.7 Vitamin growth assay in Arctic *F. cylindrus* strains – 2nd subculture. a) *f*/vitamins b) B_{12} c) B_{12} + B_1 d) B_{12} + B_7 e) B_1 f) B_7 g) B_7 + B_1 and h) no vitamins. Errors bars ±SD. Cultures grown at 4°C after being subcultured 1/10 into fresh 200 µl of treatment media. Concentrations of vitamins were: B_{12} – 500 ng/L, B_1 – 100 µg/L and B_7 – 500 ng/L. N = 3.

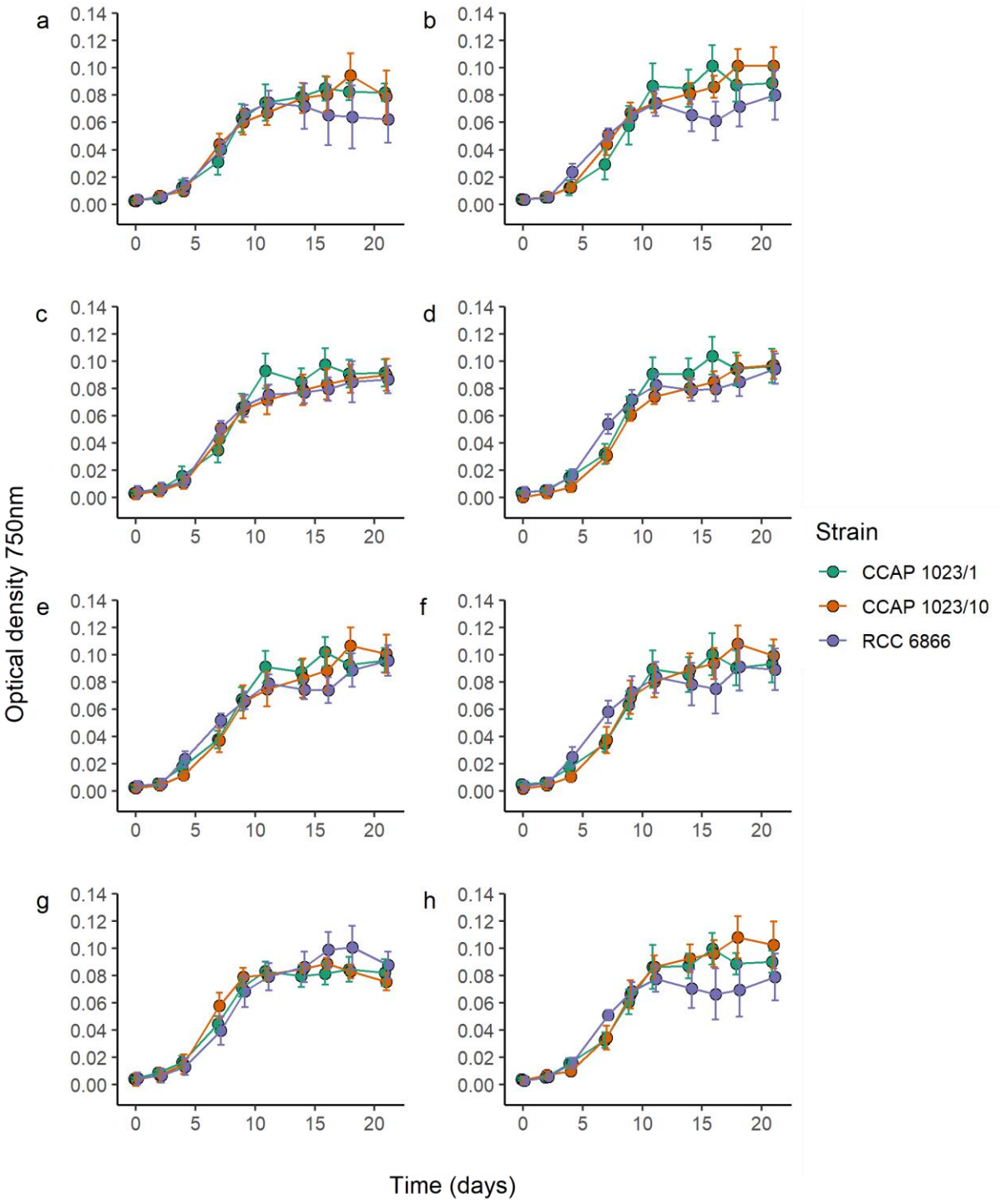

Figure 5.8 Vitamin growth assay in Antarctic *F. cylindrus* strains – 2nd subculture. a) *f*/vitamins b) B_{12} c) B_{12} + B_1 d) B_{12} + B_7 e) B_1 f) B_7 g) B_7 + B_1 and h) no vitamins. Errors bars ±SD. Cultures grown at 4°C after being subcultured 1/10 into fresh 200 µl of treatment media. Concentrations of vitamins were: B_{12} – 500 ng/L, B_1 – 100 µg/L and B_7 – 500 ng/L. N = 3.

5.2.2.3 Cell density at the end of the 1st and 2nd subcultures

Representative cell counts taken at the end of the 1st and 2nd subcultures (day 21), show a significant decrease in cells at the end of the 1st subculture in -B_{12} treatments in all Arctic strains (Fig. 5.9, ANOVA Df = 3(66), F = 211.95, $p<0.001$) and there was a significant difference between strains (ANOVA, Df 2(66), F = 17.61, $p<0.001$). No cells were present at the end of the second subculture. Antarctic strains on the other hand showed no significant differences in cell densities between B_{12} treatments in the 1st and 2nd subcultures (Fig. 5.10, ANOVA Df = 3(66), F = 0.653, $p>0.5$ and Df = 3(66), F = 0.553, $p>0.5$ respectively). In both Arctic and Antarctic strains, there were small but significant differences in cell densities between strains (ANOVA Df = 2(66), F = 137.653, $p<0.001$ and 2(66), F = 20.014, $p<0.001$ respectively). In the 1st subculture, average cell densities decreased by 61 - 82% in Arctic strains when B_{12} was omitted, whereas Antarctic strains showed decreases of only 2 - 5%. In the 2nd subculture, there were no cells visible in the Arctic isolates and Antarctic strains showed a varied response with 1023/1 showing a 1.1% increase in treatments excluding B_{12} and 1023/10-SC48 and 6866 showing reductions of 2.9% and 7.9% respectively. Conducting cell counts was a useful way to get another measure of growth, as although the Arctic 5231 showed similar OD readings between +B_{12} and -B_{12} treatments in the 1st subculture (Fig. 5.5, Appendix 8), cell counts show that the strain was in fact detrimentally impacted by the lack of B_{12} (Fig. 5.9). Although microtitre assays are a useful method, reading errors can occur due to biofilm formation and inadequate mixing and it is useful to confirm results at larger volumes.

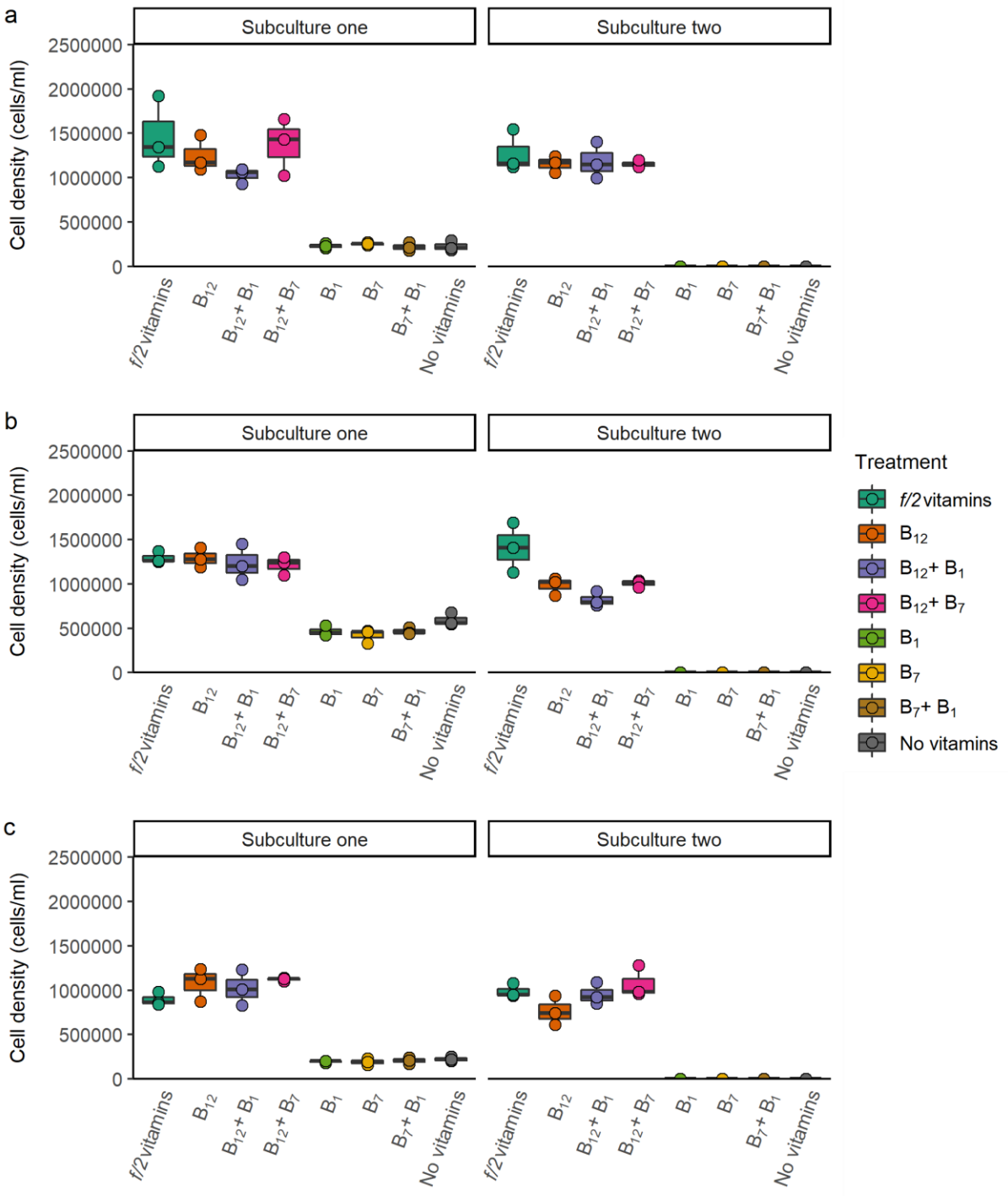

Figure 5.9 Cell densities of Arctic F. cylindrus strains on day 21 in 1st and 2nd subcultures. a) RCC 4289 b) RCC 5231 c) RCC 5582.

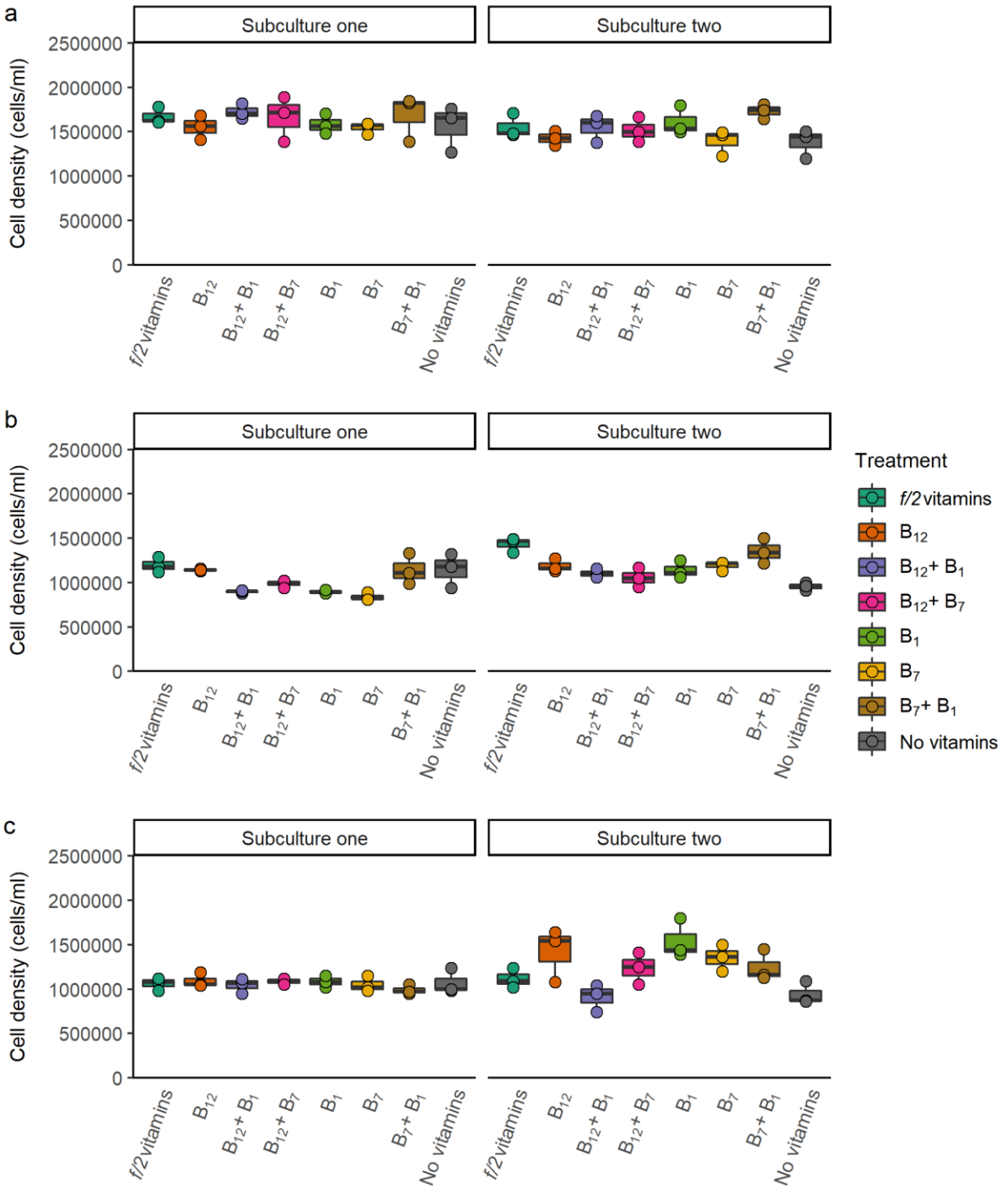

Figure 5.10 Cell densities of Antarctic *F. cylindrus* strains on day 21 in 1st and 2nd subcultures. a) CCAP 1023/1 b) CCAP 1023/10 – SC48 c) RCC 6866.

5.2.3 Rescuing growth in Arctic *F. cylindrus* strains after B_{12} depletion.

The vitamin assay was able to determine that the Arctic strains required B_{12} in order to grow, which suggests they have an obligate requirement for exogenous B_{12}. To validate these findings and to also investigate whether the addition of B_{12} could rescue growth in the Arctic strains, a further experiment adding B_{12} back into B_{12} deprived cultures was carried out (Section 2.5.2 in Materials and Methods). The Arctic 4289 strain was inoculated from a replete (500 ng/L) or deplete (no B_{12}) culture at $5x10^4$ cells/ml into *f*/2 medium with and without B_{12} respectively. The latter exhibited reduced growth in the B_{12} deprived treatment after 4 - 5 days, but addition of 500 ng/L B_{12} at day 6, led to a gradual increase in growth to almost the same rate as the replete culture from day 12 (Fig. 5.11). Growth rate recovered to 0.301 which was slightly lower than the growth rate of 0.401 in the B_{12} replete treatment. After the addition of B_{12} at day 6, the replete culture of 4289 appeared to crash and plateau within two days, after which growth steadily increased (Fig. 5.11). The Antarctic 1023/1 strain exhibited no difference in growth between B_{12} replete or deplete cultures upon the re-addition of B_{12} (Fig. 5.11). Specific growth rates between replete and deplete cultures were also similar (replete = 0.359, deplete = 0.339), providing further evidence that the Antarctic *F. cylindrus* does not require exogenous B_{12}.

To validate this phenotype in the Arctic strain, the same experiment was repeated in the additional Arctic isolates. These experiments followed the same design described above, however the inoculated cell densities were $2.5x10^4$ cells/ml due to lower cell densities in the B_{12} deplete starter cultures. After B_{12} resupply on day 6, strains 5231 and 5582 both showed an increase in cell number on day 12 like the 4289 strain, although exponential growth was not seen until day 16 for 5231 and day 19 for 5582 (Fig. 5.12). This longer lag phase is likely due to the lower inoculation density used in these repeat experiments ($2.5x10^4$) compared to the first experiment ($5x10^4$). The additional B_{12} added on day 6 to the strains growing in replete conditions, which increased concentration from 500 ng/L to 1000 ng/L, did not influence the growth of either Arctic strain (Fig. 5.12).

These experiments demonstrate that the Arctic strains are dependent on B_{12} and are able to utilize the compound upon re-addition. The rapid plateau shown in 4289 upon the additional B_{12} supplement (Fig. 5.11) was not replicated in the other two strains, evidenced by the replete control (which did not receive an additional B_{12} supplement) growing similarly to the

replete cultures which did receive additional B_{12} (Fig. 5.12). The plateau shown in Fig. 5.11 is therefore unlikely to be a result of this additional B_{12}. The B_{12} deplete control indicates that the bacteria present in these cultures were not producing B_{12} or at least not producing it to an extent to which the Arctic *F. cylindrus* could survive.

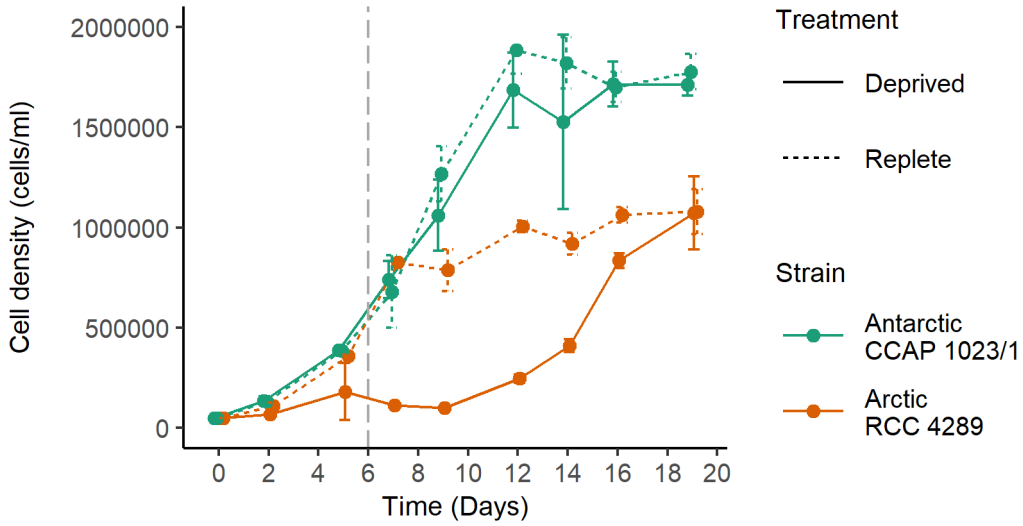

Figure 5.11 Recovery of B_{12} depleted cultures upon B_{12} addition. B_{12} replete and deplete cultures were inoculated at 5x10^4 cells/ml into media containing B_{12} or no B_{12} respectively and grown at 4°C. Vertical dashed line denotes the addition of B_{12} (500 ng/L) on day 6. Error bars ±SD. N = 3.

5.2.4 Vitamin B_{12} dose response

Although many diatoms, including the Antarctic *F. cylindrus* strains investigated here, do not require B_{12}, there still may be a growth advantage when B_{12} is present. Therefore, an experiment to monitor the growth of the Antarctic 1023/1 and Arctic 4289 strains across a range of B_{12} concentrations was carried out. B_{12} deplete cultures (Section 2.5.1) were sub-cultured into 96-well microtitre plates with a range of B_{12} concentrations serially diluted from 2000 ng/L to 1.9 ng/L. The lowest concentration at which the Arctic 4289 strain was able to grow at a measurable rate was 62 ng/L (Fig. 5.13a). At concentrations above 62 ng/L the Arctic strain showed similar growth responses and specific growth rates ranging between 0.212-0.249 (Df = 6, Chisq = 10.065, p>0.1). The Antarctic strain which does not require B_{12} showed similar growth responses over the whole range tested, with slight reductions in growth shown only in the 2000 ng/L and no B_{12} control treatments based on optical density

(Fig. 5.13b). Specific growth rates were similar over all B_{12} concentrations but there was a significant difference between concentrations (Df = 11, Chisq = 23.217, $p<0.05$); maximum = 0.295 (no B_{12} treatment), minimum = 0.243 (3.9 ng/L treatment) and median = 0.275 (62 ng/L treatment). Growth at 3.9 ng/L and 7.8 ng/L was statistically the same ($p>0.5$), but both were significantly lower than no B_{12}, 15.6, 31 and 1000 ng/L ($p<0.05$).

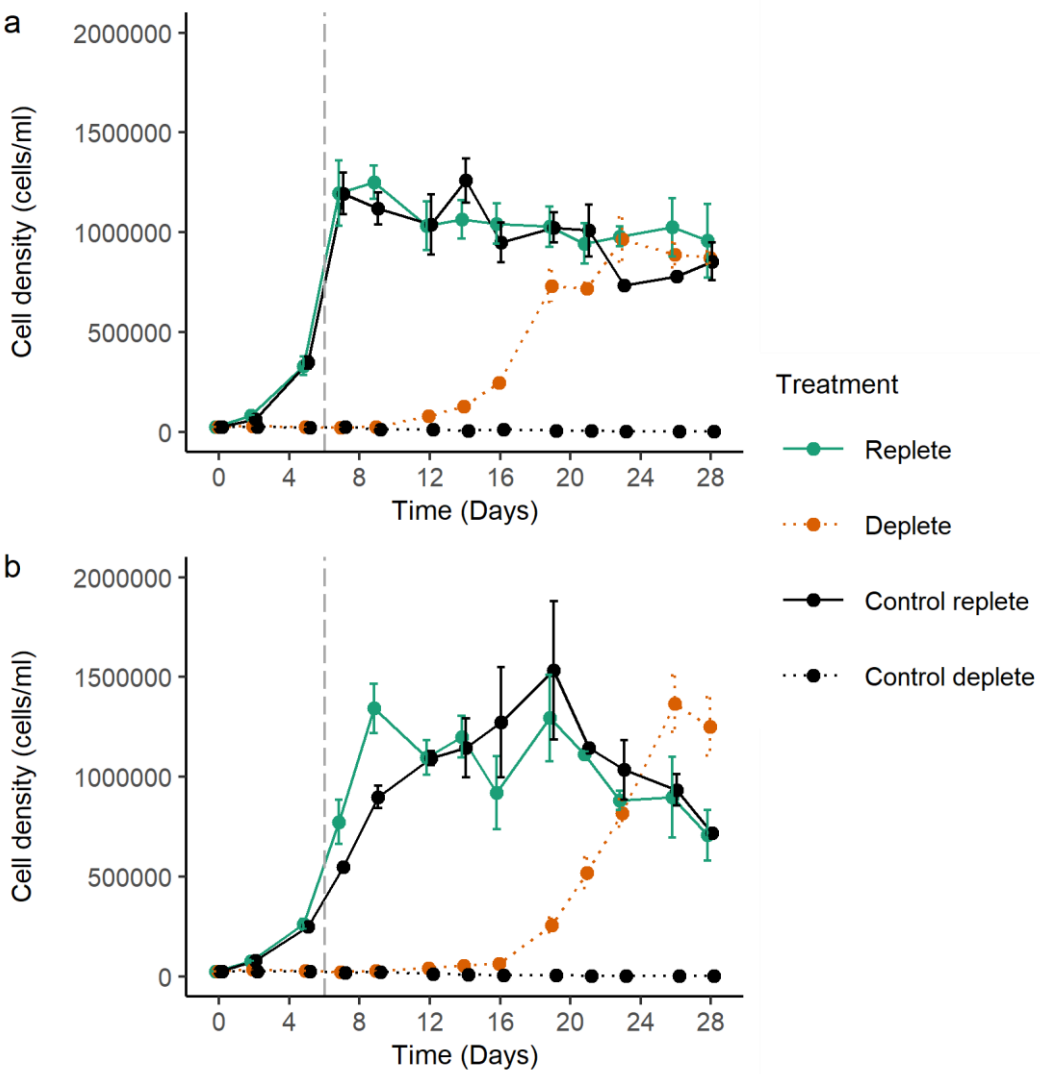

Figure 5.12 Recovery of B_{12} depleted cultures upon B_{12} addition in additional Arctic strains. a) RCC 5231 b) RCC 5582. B_{12} replete and deplete cultures were inoculated at 2.5x10^4 cells/ml into media containing B_{12} or no B_{12} respectively and grown at 4°C. Vertical dashed line denotes the addition of B_{12} (500 ng/L) on day 6. Control cultures represent replete and deplete cultures which did not receive the additional B_{12}. Error bars ±SD, N = 3.

To analyse the response of the Arctic strain further, a dose response curve was modelled using the "drc" package in R (Ritz *et al.*, 2015). Specific growth rates were calculated for each concentration, and the best model (based on AIC score) was evaluated using an inbuilt function "mselect", which tests a range of models for goodness of fit. The model selected was the Weibull type 2 with 4 parameters (W2.4) and the output is presented in Fig. 5.14. The value at which the growth rate is half the maximum shown (the ED50 value) was estimated at of 76.9 ±3.1 ng/L. The figure of 76.9 ±3.1 ng/L equated to 56.7 pM ± 2.3.

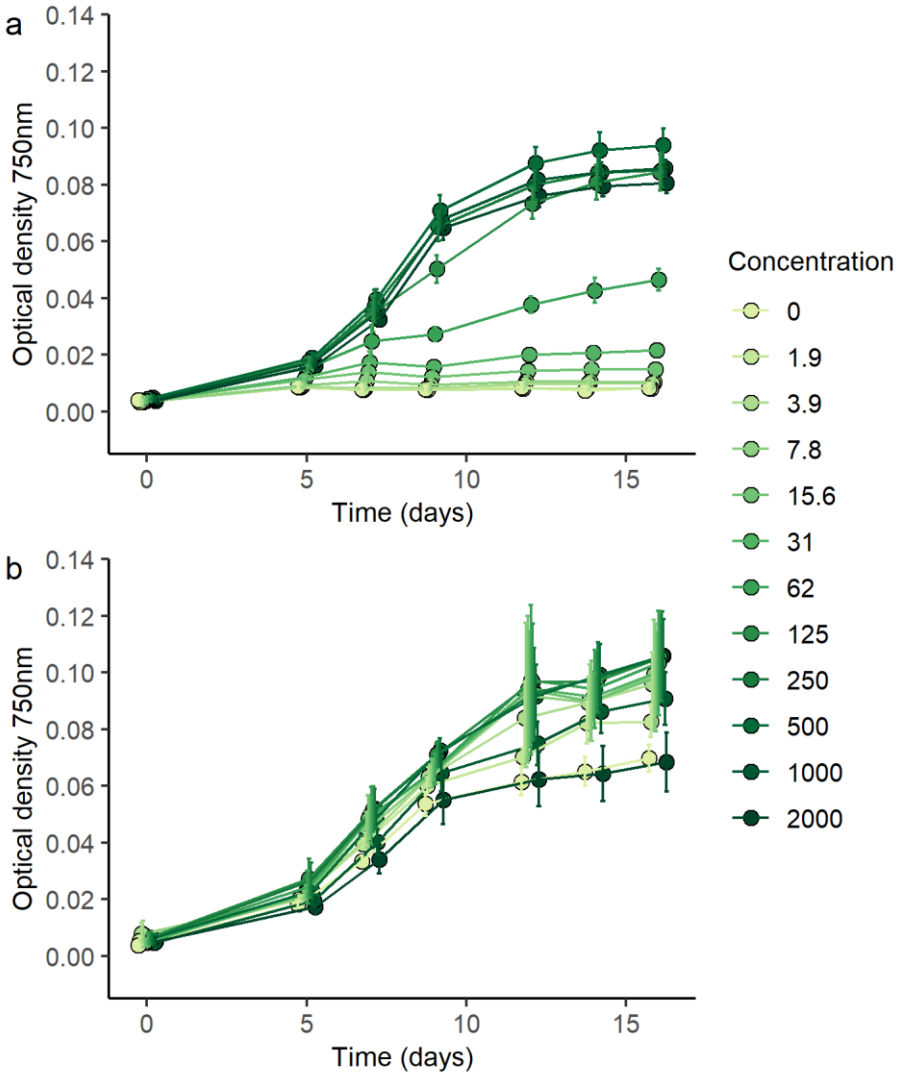

Figure 5.13 Growth responses of *F. cylindrus* over B_{12} concentrations. a) Arctic RCC 4289 and b) Antarctic CCAP 1023/1. Deplete cultures were inoculated at a dilution of 1/10 into 200 µl *f*/2 media containing B_{12} which was serially diluted from 2000 ng/L to 1.9 ng/L and cultured at 4°C. Error bars ±SD. N = 2.

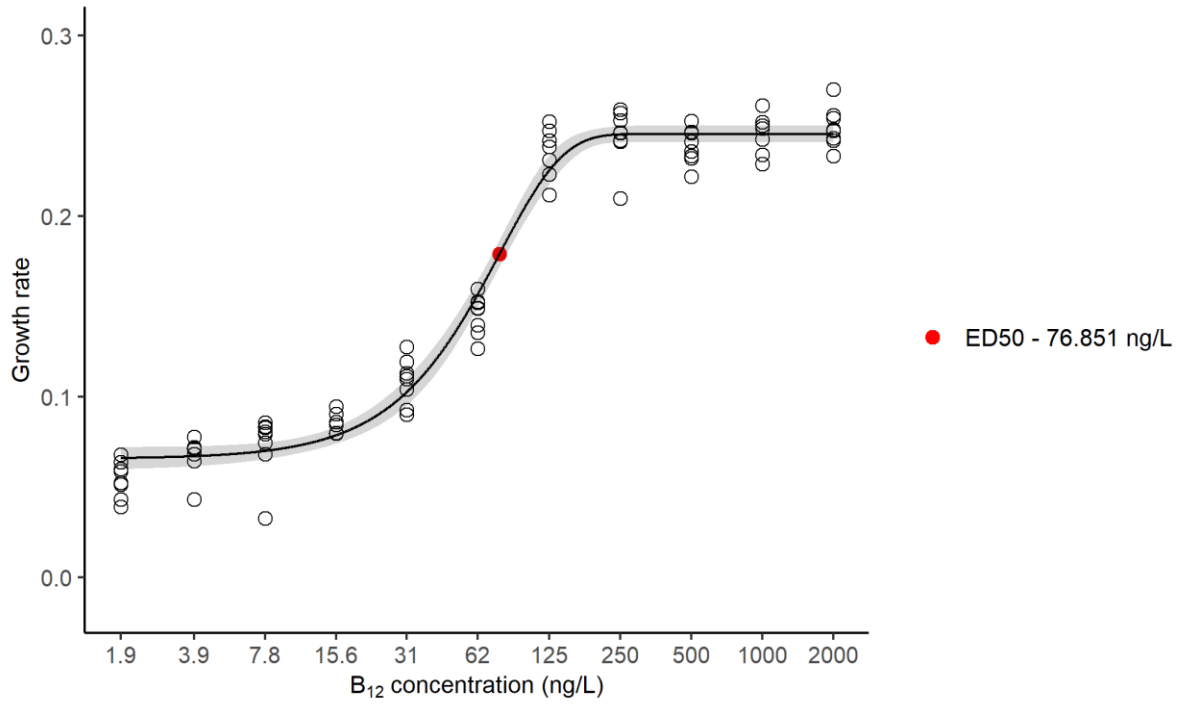

Figure 5.14 B_{12} dose response model in the Arctic *F. cylindrus* (RCC 4289). Growth of the Arctic strain was modelled using the Weibull type 2 with 4 parameters (W2.4) using the drc package in R (Ritz et al., 2015).

5.2.5 Investigating the genetic characteristics of B_{12} dependency in *F. cylindrus* strains

As previously mentioned in 5.1, the *METH* and *METE* genes are important determinants of B_{12} dependency in algae, with the absence of the latter resulting in B_{12} auxotrophy. Helliwell *et al.*, (2011) identified both genes in the Antarctic *F. cylindrus* genome, although only a small fragment of the *METE* gene was found, but later the full gene sequence was confirmed from a refined version of the genome (Mock *et al.*, 2017). The finding that three Arctic strains were all B_{12} dependent prompted the investigation of *METH* and *METE* in all strains.

5.2.5.1 *METE*

It was hypothesised that the three Arctic strains have a defect or lack of the *METE* gene so that no functional METE protein is produced and leading to B_{12} dependency. Primers were designed using the *METE* gene extracted from the Antarctic *F. cylindrus* genome (Mock *et al.*, 2017, Fig. 2.2b, Appendix 4). In order to cover the entire *METE* gene, an extended PCR was used, with primers anchored in the two adjacent genes. A total of nine different primer pairs

were used to amplify the *METE* gene (Fig. 2.2b, Appendix 4), none of which resulted in products in the Arctic strains (data not shown). A final primer pair rooted in the 5′ and 3′ UTR of the *METE* gene was used, and this would be expected to generate a 3277 bp product (Fig. 5.15b).

The expected product was found in all three Antarctic strains, but there were no products amplified in the Arctic strains (Fig. 5.16a). Although these results do not prove that *METE* is absent in the genome of the Arctic strains, it implies that any gene resembling *METE*, if present, has likely undergone significant changes so that it cannot be amplified with the primer pairs. This is likely to have resulted in it becoming non-functional. A lack of amplification in all three Arctic strains, suggests that the potential loss/mutation of *METE* in the Arctic *F. cylindrus* is a region-specific characteristic and not strain specific.

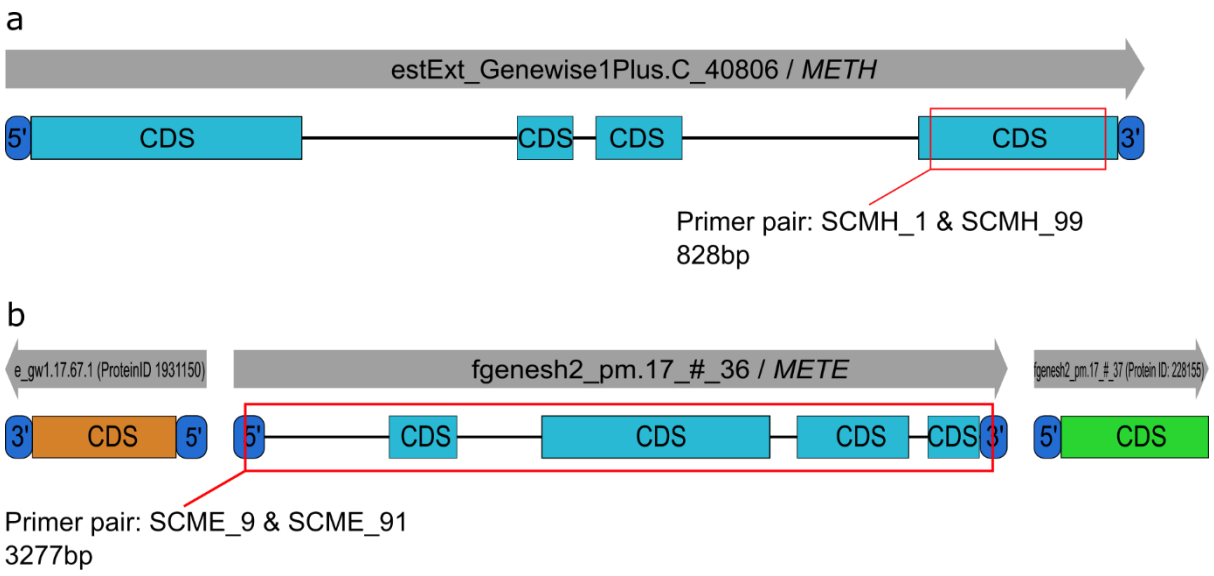

Figure 5.15 Schematic of F. cylindrus methionine synthase genes. a) *METH* and b) *METE*. Red boxes indicate the positioning of primers used to amplify each gene. Primer information can be found in Appendix 4.

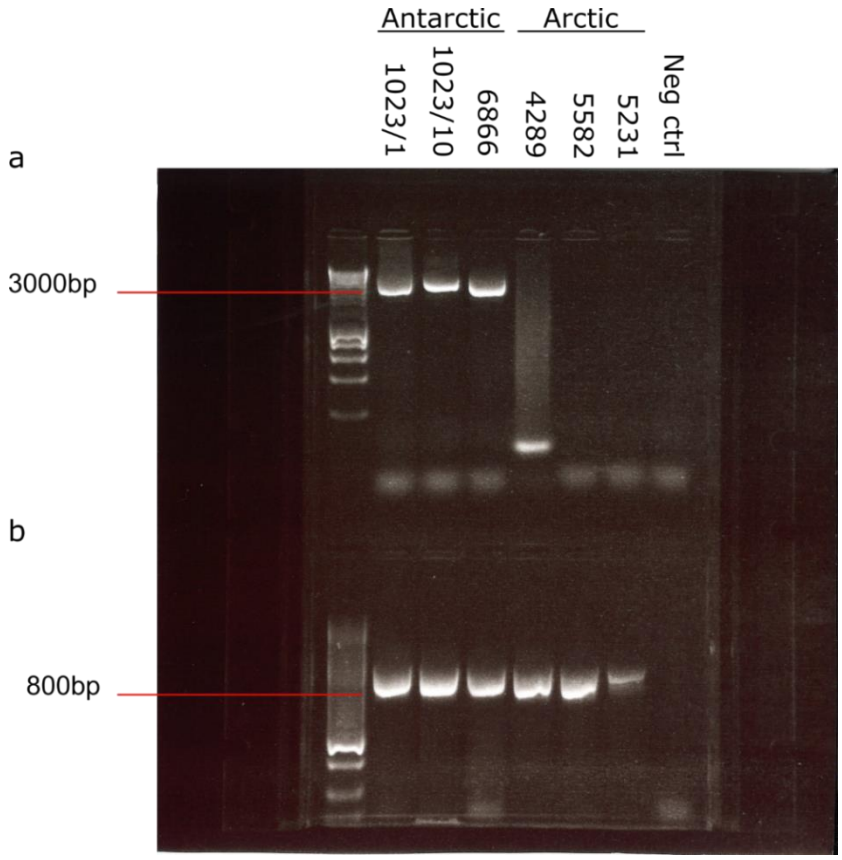

Figure 5.16 Amplification of *METE* and *METH* genes in F. cylindrus strains. a) *METE* and b) *METH*. Primer pairs used are outlined in Fig. 5.15 and Appendix 4).

5.2.5.2 *METH*

As all three Arctic *F. cylindrus* strains were able to grow in the presence of B_{12}, it was hypothesised that the *METH* gene was present and functional. *METH* was amplified in all six *F. cylindrus* strains (Fig. 5.16b) using the primer pair detailed in Fig. 5.15a. These *c*800 bp products were sequenced and confirmed to encode the region of *METH* for which the primers were designed. However, 29 single nucleotide polymorphisms (SNP, Appendix 12) were identified in Arctic strains, 13 of which resulted in eight amino acid substitutions between the Arctic and Antarctic strains (Fig. 5.17). In the Antarctic RCC 6866 strain, a single conservative amino acid substitution was identified at position 885 where an alanine was substituted for a threonine. In all strains except the genome reference strain (CCAP 1023/1), glutamine was substituted for lysine at position 1019. Conversely, no inter-strain variation was identified in the Arctic strains, which showed a total of eight amino acid substitutions compared to the Antarctic strains, half of which were conservative (Phe854Met, Thr879Ser,

Gln938Lys, and Gln980Lys) and half were non-conservative (Pro832His, Asp839Ala, Cys860Val, and Asp983Cys (Fig 5.17). Heterozygote base calls in the nucleotide sequence resulted in two possible amino acids at position 942 in 4289 and 5231 (alanine (A) or aspartic acid (D)). Further heterozygote base calls at position 980 in 4289 resulted in two possible amino acids (glutamic acid (E) or lysine (K)). Helliwell (2011) performed an alignment of *METH* genes from various organisms and found that the 3' region is highly variable between species, suggesting that changes in this region and subsequent protein C-terminus, may not influence protein function. In fact, an alignment of diatom *METH* sequences including the strains presented here indicates that the position of the amino acid differences in Arctic strains align well with variations shown in other species (Fig. 5.18), i.e., these represent highly variable positions and therefore are unlikely to affect function.

5.2.6 Genetic barcoding reveals genetic divergence between Arctic and Antarctic strains

To investigate this variability within strains further, molecular barcoding using 18S and *rbc*L as nuclear and chloroplast genome markers respectively were used (3p-*rbc*L, Hamsher *et al.*, 2011; and 18S V4, Zimmermann *et al.*, 2011).

Barcoding the six *F. cylindrus* strains identified no differences within the V4 region of the 18S ribosomal gene but did identify differences within the 3P-*rbc*L barcode (Fig. 5.19). Newly isolated strains described in Chapter three were also included in the analysis and showed 100% identity to all three Antarctic strains used in this chapter. The 3P-*rbc*L barcode showed 11 nucleotide differences between Arctic and Antarctic strains equating to 98.6% identity. P-distances were 0.014 nucleotide substitutions between Arctic and Antarctic strains, which is in the region of both intraspecific and interspecific divergence in diatoms (0-0.11, MacGillivary & Kaczmarska, 2011). Compared to *F. cylindrus* strains*, F. kerguelensis* showed 0.071 nucleotide substitutions (92.9% identity). Upon translation, none of these differences resulted in amino acid substitutions so that the amino acid sequences were 100% identical.

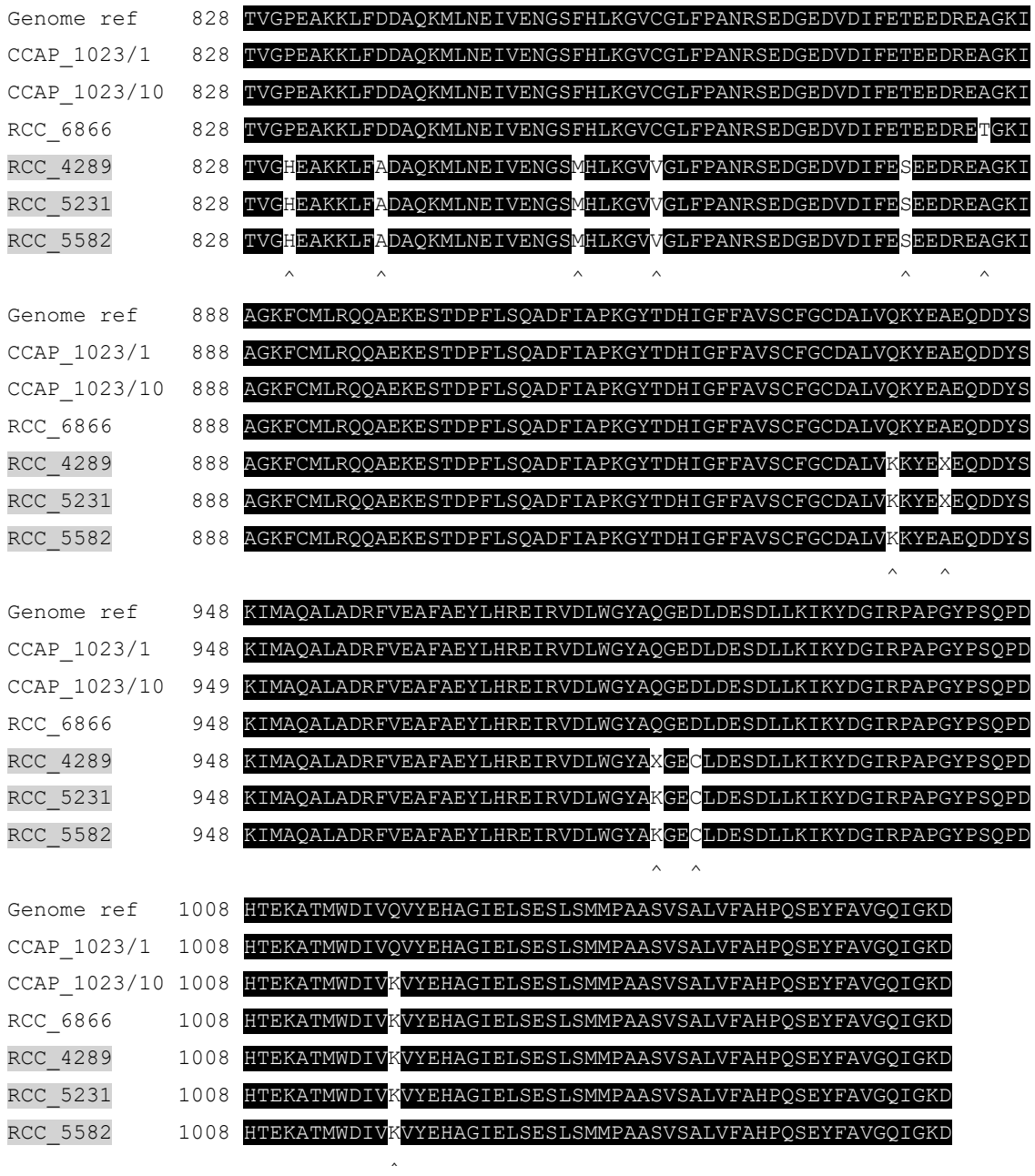

Figure 5.17 *F. cylindrus* METH protein alignment. Alignment of protein sequences aligned using MAFFT (Katoh et al., 2019). Similarity shading was created using BoxShade (https://embnet.vital-it.ch/software/BOX_form.html). Grey shading denotes Arctic strains, and no shading Antarctic strains.

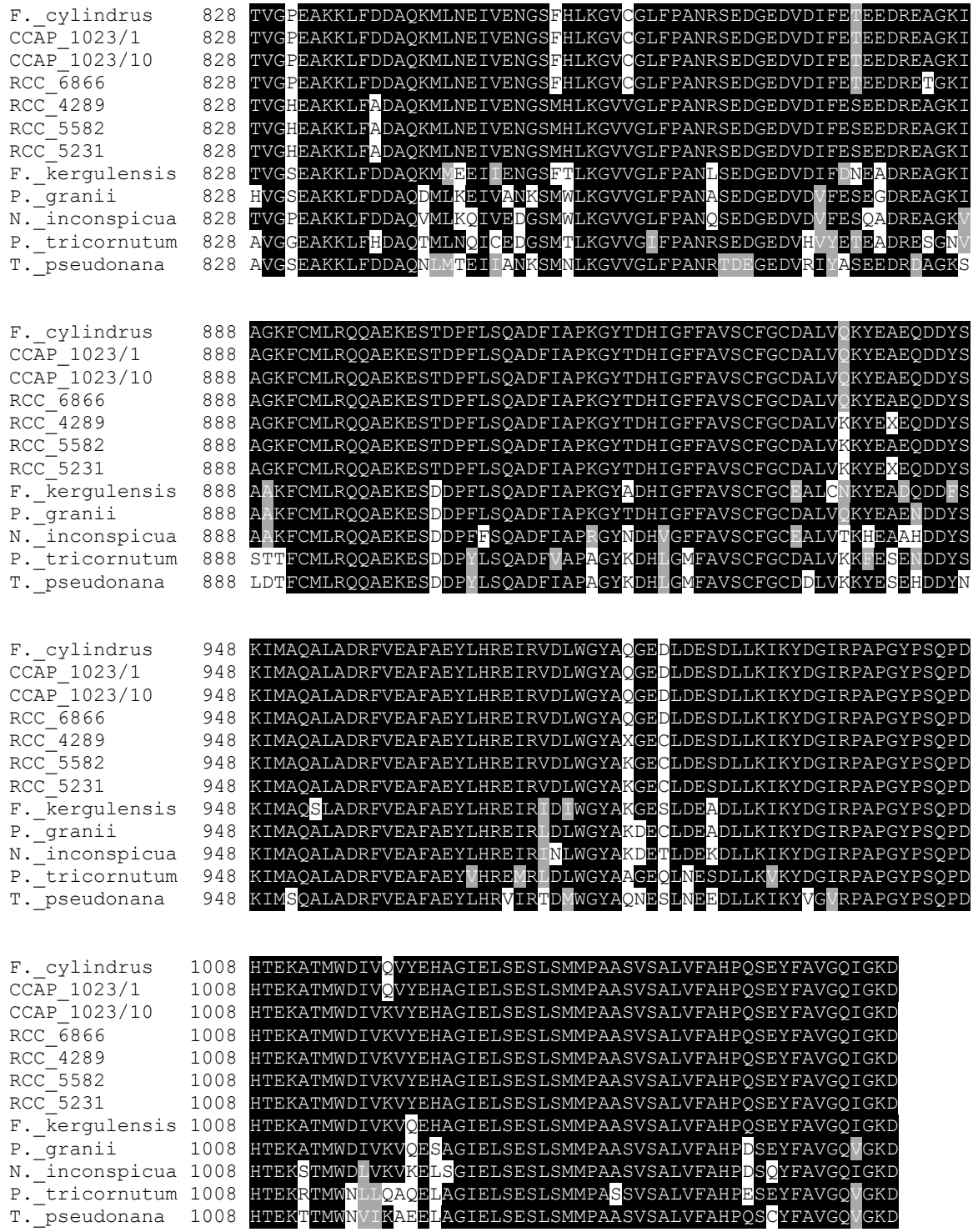

Figure 5.18 Multiple sequence alignment of diatom *METH* sequences. Alignment of protein sequences aligned using MAFFT (Katoh et al., 2019). Similarity shading was created using BoxShade (https://embnet.vital-it.ch/software/BOX_form.html). Grey shading denotes Arctic strains, and no shading Antarctic strains.

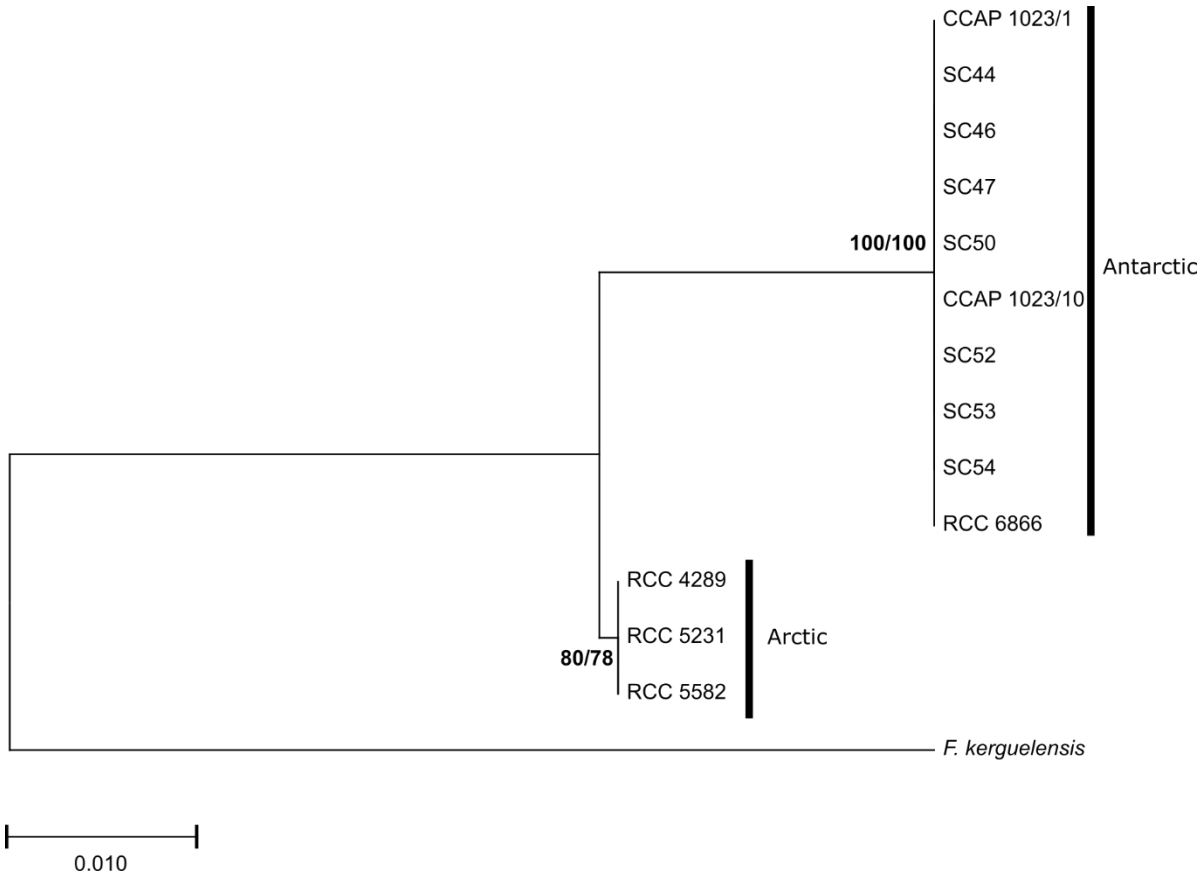

Figure 5.19 Phylogenetic analysis of the 3P-*rbc*L barcode in *F. cylindrus* strains. Maximum likelihood (ML) tree was built using the general time reversal (GTR) model with gamma distribution (G) and proportion of invariable sites (I) in MEGA X (Kumar *et al.*, 2018). The numbers at each node are values for ML/neighbour joining bootstraps respectively and are a result of 1000 replications. Scale bar denotes substitutions per site.

5.3 Discussion

5.3.1 Biogeography of B_{12} auxotrophy in algae

In the first part of this chapter, the effect of biogeography and habitat types was investigated in relation to B_{12} auxotrophy in algae. Through collating the data from relevant publications the number of strains analysed was 456 which is an increase of 130 (28.5%) on the dataset of (Croft *et al.*, 2005). More importantly, this study provides higher representation of other algal groups such as, Haptophyta, Myzozoa, and Ocrophyta which were largely underrepresented in the original list. The percent of algal strains that show B_{12} auxotrophy increased from the reported figure of 52% (Croft *et al.*, 2005) to nearly 59%, further emphasising how widespread the dependence for the vitamin is within photosynthetic microbial eukaryotes. Despite B_{12} auxotrophy showing variability across these diverse lineages, seven out of the

nine phyla analysed showed B_{12} auxotrophy in >60% of strains. The majority of the strains were characterized via physiological experimentation alone (Croft *et al.*, 2005; Tang *et al.*, 2010), however the more recent studies have focused on the genetic identification of B_{12} dependency (Ellis *et al.*, 2017; Nef *et al.*, 2019). Although the presence of *METE* does indicate B_{12} autotrophy it cannot always be a trusted approach depending on the sequencing method used. For instance, transcriptomes are a snapshot of the genetic architecture being transcribed at a particular point of time. As *METE* has previously been downregulated when B_{12} is present (Croft *et al.*, 2005; Helliwell *et al.*, 2011), it is possible that in B_{12} replete conditions the expression of *METE* could be repressed and go undetected. If the presence of *METE* is confirmed through genome sequencing, then there is a higher likelihood that the strain would be B_{12} auxotrophic. Conversely, genome sequencing is still labour-intensive and expensive, and identification of a putative coding sequence does not necessarily indicate that the gene encodes a functional enzyme. Physiological characterization of B_{12} dependency thus remains a vital method in determining or confirming B_{12} auxotrophy. In an ideal world the combination of both should be utilized.

Latitude had no influence on the B_{12} auxotrophic state of algal strains. However, it must be stressed that there were significant biases in the data towards North America and Europe, and when this region termed "Northern Temperate" was analysed alone, the percentage of strains showing B_{12} auxotrophy was the same to the full data set (59%), implying that this region is biasing the dataset. Only 66 strains represented regions outside of the "Northern Temperate" and the percentage that were B_{12} auxotrophic (51.5%) was similar to the original figure of 52.5% (Croft *et al.*, 2005). This observation indicates that the biogeographical pattern reported by Ellis *et al.*, (2017) in marine diatoms does not translate across algal lineages as a whole, although this is not to say that particular groups do not show a geographical pattern. Instead, more data are clearly needed from under-represented regions and habitats.

Despite improving the representation of certain algal groups within the analysis there was a bias towards marine strains. This bias could account for the increase seen in the total number of strains showing B_{12} auxotrophy because 76% of marine strains were B_{12} dependent. Different habitats will have different selection pressures and variable B_{12} concentrations, especially aquatic versus terrestrial habitats. Terrestrial habitats could be considered as

sedentary as they do not have the mixing and homogenous properties to which aquatic habitats are subject. Therefore, it could be hypothesized that terrestrial habitats would lead to a higher incidence of B_{12} dependency if B_{12} concentrations are less changeable. Bacterial biomass in the top soil is highest in high latitudes and around the equator; between 15°N and 45°N there is lower bacterial biomass (He *et al.*, 2020). Moreover, 70% of bacterial isolates tested within soil have demonstrated the ability to synthesise vitamin B_{12} (Lochhead & Thexton, 1951) suggesting that where bacterial biomass is high, B_{12} concentrations may also be high. In the present study and in contrast to the marine habitat, the number of terrestrial strains showing auxotrophy was only 13%. The majority of terrestrial strains were within the Chlorophyta, which are an early diverging group relative to land plants. Plants are primarily terrestrial and they neither synthesise nor require vitamin B_{12} (Smith *et al.*, 2007). It could therefore be possible that the implementation of a terrestrial life strategy may select for B_{12} independence, but to test this hypothesis additional work would need to be carried out on a higher number of terrestrial strains. Phylogenetics of *METH* indicates that B_{12} independence is likely a result of independent gene loss in some Chlorophyta and land plants (Helliwell *et al.*, 2011). As mentioned previously (Section 5.1), METH is more catalytically efficient than METE (Gonzalez *et al.*, 1992), which makes the evolutionary loss of *METH* a puzzling occurrence.

This work further demonstrates the high occurrence of vitamin B_{12} auxotrophy within algae. Combining both physiological characterization with modern genetic analyses, the number of strains evaluated for B_{12} auxotrophy has improved, but some taxa, regions, and habitats are still under-represented. However, even with limitations, the current dataset has highlighted how ecological factors have influenced B_{12} dependency in algae.

My study of polar diatoms offered the means to address the fact that there were limited polar strains in the analysis above. Accordingly, I investigated the vitamin B_{12} dependency of *F. cylindrus* strains from the Antarctic and Arctic regions. My physiological experiments have shown that Arctic *F. cylindrus* strains have an obligate requirement for exogenous vitamin B_{12} whereas, the Antarctic strains have no such requirement. These results are corroborated by the inability to amplify the B_{12}-independent methionine synthase (*METE*) gene in Arctic strains. Although there might be other explanations for the lack of amplification in the

absence of a full-genome sequence, it would provide an explanation for the B_{12} dependency shown.

5.3.2 Physiological characterization of B_{12} dependency in *F. cylindrus*

Growth assays demonstrated that the Arctic strains were unable to grow after two transfers in B_{12} omitted media (Fig. 5.5 and 5.7). Rapid declines in growth after two transfers in B_{12} omitted media have been shown in *Volvox carteri* f. *nagariensis*, *Ostreococcus* sp. and *Micromonas pusilla* (Helliwell *et al.*, 2011). Helliwell *et al.*, (2011) demonstrated that the Antarctic *F. cylindrus* had comparative growth rates over three transfers with or without the presence of exogenous B_{12}. The current work shows that all three Antarctic strains show comparable growth with or without B_{12} over two transfers (Fig. 5.6 and 5.8). It was not felt necessary to complete a third transfer (as per Helliwell *et al.*, (2011)) based on previous results and the comparable growth shown between transfers.

Vitamin B_{12} is thought to be produced only by prokaryotes (Warren *et al.*, 2002) and because of this, environments could see variable B_{12} concentrations depending on prokaryotic biomass. Therefore, B_{12} dependent organisms would be able to rapidly utilise vitamin B_{12} upon more favourable concentrations. In fact, large scale studies of the impact of supplying exogenous B_{12} alone did not lead to an increase in phytoplankton growth, whereas they have identified co-limitation properties between B_{12} and other nutrients e.g., iron (Fe) and nitrate (Panzeca *et al.*, 2006; Sañudo-Wilhelmy *et al.*, 2006; Bertrand *et al.*, 2007, 2015; Koch *et al.*, 2011). However, there were reductions in gene transcripts related to B_{12} deprivation e.g., reduction of *METE* upon addition of B_{12} (Bertrand *et al.*, 2015). It would be expected to see a decrease in gene transcripts related to B_{12} deprivation when B_{12} is present as METH is catalytically more efficient than METE (Gonzalez *et al.*, 1992).

It is very unlikely that marine diatoms would be in a position where there is no B_{12} available, more credibly, B_{12} concentrations are likely to be sub-optimal as shown in Croft *et al.*, (2005). However, to further demonstrate that B_{12} was fundamentally required in the Arctic strains, a B_{12}-rescue experiment was carried out. Upon re-addition of B_{12} to deplete cultures, all Arctic strains showed a recovery of growth to reach a similar carrying capacity to that of replete cultures (Fig. 5.11 and 5.12). Ellis *et al.*, (2017) demonstrated that the re-addition of B_{12} was

able to positively affect growth of the B_{12} dependent diatom *Pseudo-nitzschia granii*. However, my results show that the recovery of growth in the Arctic strains is not seen until 6-10 days after B_{12} re-addition, indicating that there is a delayed response to recover from B_{12} stress. B_{12} re-addition could have been performed earlier which would have likely resulted a faster ability to recover, similar to the results of Ellis *et al.*, (2017). Recovery is consistent with previous work carried out on the B_{12} dependent strain of *C. reinhardtii* where growth was recovered by a symbiotic interaction with B_{12} producing bacteria (Helliwell *et al.*, 2015). Ellis *et al.*, (2017) further demonstrated that the Antarctic *F. cylindrus* was not impacted by the re-addition of B_{12}. My experiments show the same result in all three Antarctic strains, whereby the presence, absence, or re-addition of B_{12} had no impact on growth.

Although the presence of *METE* allows an alga to grow without exogenous B_{12}, *P. tricornutum* showed a slight increase in growth in the presence of B_{12} over no B_{12} (Bertrand *et al.*, 2013). In my current work, during the vitamin requirement assays there was no demonstrable benefit in $+B_{12}$ treatments over $-B_{12}$ treatments in the Antarctic strains (Fig. 5.6 and 5.8, Appendix 9 and 10). During the B_{12} dose response of the Antarctic CCAP 1023/1 strain (Fig. 5.13), growth rates remained comparable over all 12 concentrations with a maximum rate of 0.295 (no B_{12}) and a minimum of 0.243 (3.9 ng/L). The growth curves did show that in the culture with no B_{12} there was a lower carrying capacity based on optical density than for most supplementation conditions. The exception was for 2000 ng/L which showed reduced growth, the reason for this is unknown. These results signify that the presence of exogenous B_{12} does not provide a growth advantage in terms of the growth rate, although further work would be needed to investigate this if it enables an increase biomass or carrying capacity in Antarctic *F. cylindrus*.

Despite efforts to create axenic cultures through filtering, washing, differential centrifugation, and antibiotic treatment, bacteria remained in all cultures. As previously mentioned, bacteria are important producers of vitamin B_{12} and symbiotic relationships with algae have been identified as a key source of the micronutrient (Croft *et al.*, 2005; Kazamia *et al.*, 2012) as well as other nutrients such as Fe. Nonetheless, the lack of growth shown in cultures excluding B_{12} and the additional control treatments used in the rescue experiments (Fig. 5.12) indicated that the bacteria present were not producing B_{12} or at least to the extent needed for growth.

A lack of growth after only two subcultures in Arctic strains shows how reliant some algal strains are on vitamin B_{12} and suggests internal stores can quickly be depleted when B_{12} is not available. Currently we do not understand where B_{12} is stored in diatom cells and at what concentration. However, research on edible algae show that some species of macroalgae e.g. *Porphyra spp.* can have high levels of B_{12} whilst others e.g. *Laminaria spp.* have very little (Watanabe *et al.*, 2002, 2014). Edible microalgae *Chlorella spp.* and *Spirulina spp.* have shown varied concentrations of B_{12} but in the case of the latter, B_{12} content is made of pseudocobalamin and cyanocobalamin (Edelmann *et al.*, 2019). Understanding the way B_{12} is stored and utilized would help to understand how species cope with B_{12} limitation in the environment.

5.3.3 Genetic basis of B_{12} dependency in Arctic strains

Vitamin B_{12} dependency in algae has been identified to be a result of the presence or absence of two genes, the B_{12}-dependent *METH* and the B_{12}-independent *METE* (Croft *et al.*, 2005). The lack of *METE* results in an obligate requirement for exogenous B_{12} and various studies of B_{12} dependent algae have shown an absence of *METE* in the genome but presence of *METH* (Croft *et al.*, 2005; Helliwell *et al.*, 2011; Ellis *et al.*, 2017). Here, I have shown that three Arctic *F. cylindrus* strains require B_{12} and *METE* could not be found via PCR amplification. Nine primers were created based on the sequenced genome of the Antarctic 1023/1 strain (Mock *et al.*, 2017) to identify *METE*, none of which were successful in the Arctic strains. Previously Helliwell (2011), found *METH* to be more conserved than *METE* in algal species which could explain why *METE* was not identified in Arctic strains if there was significant divergence in sequence between the reference genome used for primer design and the strains under study. In addition, primers designed to conserved genes adjacent to the *METE* gene failed to amplify this region in *F. cylindrus* indicating a potential rearrangement in gene order between the Arctic and Antarctic strains.

B_{12} dependency is hypothesised to arise through the loss of a functional *METE* and the generation of a B_{12} dependent strain of *C. reinhardtii* supported this (Helliwell *et al.*, 2015). Helliwell *et al.*, (2015) reported the creation of a B_{12} dependent strain of *C. reinhardtii* after ~600 generations in high B_{12} conditions (1000 ng/L). A transposable element inserted into the *METE* gene was identified as the cause resulting in *METE* being non-functional. To

elucidate the state of *METE* and offer explanations to the genetic basis of B_{12} dependency in Arctic *F. cylindrus* isolates it would be necessary to obtain further sequence data from these strains. Further to this, *METH* in Arctic strains had various SNPs leading to amino acid substitutions (Fig. 5.17), and these changes occur in the B_{12} activation domain at the 3'end (Helliwell, 2011). A sequence alignment performed by Helliwell (2011), with additional data from this work (Fig. 5.18) showed that this B_{12} activation domain is highly varied amongst different organisms and within algal species. This suggests that mutations in this region are not detrimental to protein function and are likely a result of natural mutations acting on the same ancestral gene. These mutations, however, do bring into question the extent of divergence between the Arctic and Antarctic *F. cylindrus* strains and the selective pressures acting on them. Such potential divergence is also suggested by the presence of synonymous mutations shown in the 3' end of the *rbc*L gene between Arctic and Antarctic strains (Fig. 5.19). It is expected for two geographically isolated populations to diverge because of the allopatric speciation model due to a lack of gene flow. If selection pressures are different in the two environments, then mutations leading to phenotypic variations may arise which could be an explanation for the B_{12} dependency shown here and habitat has shown a strong link to B_{12} dependency (Fig. 5.2).

REDACTION: Sentence describing unpublished results removed for copyright reasons. Copyright holder is Amanda Hopes.

Lundholm & Hasle, (2008) reported morphological and genetic differences in ITS2 between *F. cylindrus* and a similar species *F. nana*. Their analysis concluded that although *F. nana* has often been misidentified as *F. cylindrus*, both species show a bipolar distribution. Both the current work and the two studies mentioned above highlight the need to investigate the genomes of Arctic and Antarctic strains of *F. cylindrus* further.

5.3.4 The intraspecific variation of B_{12} dependency

Over 50% of algal strains were found to have a requirement for vitamin B_{12} (Table 5.1, Croft *et al.*, 2005), but what was not reported within that study and the resource used to develop the list (Provasoli & Carlucci, 1974) was the occurrence of intraspecific variation in B_{12} dependency. The occurrence of strains of the same species having differing B_{12} dependencies is not a new observation. In 1960, Lewin & Lewin found that three marine diatoms isolated

from different regions within North America, *Amphora coffaeiformis*, *Navicula fusiformis* and *Nitzschia closterium*, showed intraspecific variation in regards to B_{12} dependency. Four out of the ten *A. coffaeiformis* strains, two out of the six *N. fusiformis* strains and one out of the four *N. Closterium* strains were B_{12} dependent (Lewin & Lewin, 1960). Moreover, two of the *A. coffaeiformis* strains showing differing B_{12} dependency were isolated from the San Diego region indicating that B_{12} dependency can differ within species over small spatial scales. Previous efforts have highlighted the random pattern of B_{12} auxotrophy shown in algal lineages (Croft *et al.*, 2005; Helliwell *et al.*, 2011; Bertrand & Allen, 2012) and B_1 auxotrophy (McRose *et al.*, 2014). However, the most probable hypothesis to the development of B_{12} dependency is adaptation to local environments, primarily to B_{12} concentrations.

B_{12} concentrations in the natural environment can be facilitated by the presence of B_{12} producing bacteria and the abundance of relevant precursors to biosynthesis. B_{12} concentrations are highly varied amongst marine environments; Cowey, (1956) reported 0.7-4.4 pM and Panzeca *et al.*, (2009) reported figures of 0.1-22 pM. In specific ocean basins, concentrations are low with reported figures of 0.4-4 pM (Southern Ocean) and 0.1-2 pM (North Atlantic, (Panzeca *et al.*, 2009)), 0.1-2.5 pM (North West Pacific, (Natarajan, 1970)), 2.2-446 pM (North West Atlantic, (Okbamichael & Sañudo-Wilhelmy, 2004)) and 0.5-6.2 pM (Mediterranean, (Bonnet *et al.*, 2013)). At present there are no figures for B_{12} concentrations within the Arctic. My analysis demonstrates that the Arctic 4289 requires a minimum of 22-46 pM B_{12} for growth, which would not be met in most global regions based on the above concentrations. As cobalt is required for the biosynthesis of B_{12} it may be hypothesised that vitamin B_{12} concentrations might reflect cobalt concentrations. However, B_{12} and cobalt concentrations showed no such relationship in the majority of coastal stations tested (Panzeca *et al.*, 2009) and cobalt is thought not to limit B_{12} production in the Ross Sea (Bertrand *et al.*, 2007). The addition of cobalt did not lead to an increase in phytoplankton in the North Atlantic but did lead to an increase in B_{12} concentrations only where cobalt was low (Panzeca *et al.*, 2008).

In the Ross Sea, Antarctica the addition of B_{12} and cobalt individually did not lead to an increase in phytoplankton growth (Bertrand *et al.*, 2007), although they did find that when B_{12} or cobalt were combined with Fe an increase in phytoplankton growth was seen indicating that Fe was the main growth limiting nutrient. Interestingly, the most northerly

sample site in the North Atlantic (Eastern coast of Iceland) had the highest average cobalt (19 pM) and vitamin B_{12} concentrations (1.4 pM, (Panzeca *et al.*, 2008)). Recently, high concentrations of cobalt have been measured in the Arctic with total dissolved cobalt concentrations in the range of 25 - 1900 pM and labile cobalt in the range of 1-600 pM (Bundy *et al.*, 2020). The maximum levels are much higher than the reported figures of dissolved cobalt in Antarctic waters: Ross Sea, 8.4-30.1 pM (Bertrand *et al.*, 2007), 19-71 pM (Saito *et al.*, 2010) and other Antarctic regions ranging between 5-172 pM (Bown *et al.*, 2011 and references therein). The high cobalt in the Arctic is also thought to act as a source of cobalt for the North Atlantic and may explain the higher levels seen in that area (Bundy *et al.*, 2020).

Both bacteria and cyanobacteria have been reported to be in low abundance in the Antarctic (Carlson *et al.*, 1998; Ducklow, 2000; Caron *et al.*, 2000; Ducklow *et al.*, 2001), although cyanobacteria have been found to mainly produce the less bioavailable form of B_{12} known as pseudocobalamin (Helliwell *et al.*, 2016; Heal *et al.*, 2019). In the Arctic there is much less information, but bacterial abundances directly compared between the Western Arctic and the Ross Sea showed similarly low biomass values (Kirchman *et al.*, 2009). Moreover, the heterotrophic eubacterial communities in both polar regions are dominated by α- and γ-proteobacteria in sea ice (Brinkmeyer *et al.*, 2003) and open water (Ghiglione *et al.*, 2012; Cao *et al.*, 2020), both of which are key B_{12} producing groups (Bertrand *et al.*, 2011; Sañudo-Wilhelmy *et al.*, 2014; Heal *et al.*, 2017). It should be noted however, that the studies focusing on bacterial abundance in the Antarctic attribute the lower biomass to concentrations of dissolved organic matter (DOM) rather than temperature, which had previously been suggested as the main driver of abundance (Carlson *et al.*, 1998; Church *et al.*, 2000; Kirchman *et al.*, 2009). Therefore, in terms of eubacterial biomass there seems to be similarities between the two regions.

Although the Arctic and Antarctic show taxonomic similarities in a dominance of α- and γ-proteobacteria, they can differ extensively in other taxonomic groups. Higher taxonomic diversity was found in the Arctic compared to the Antarctic and was linked to freshwater sources (Brinkmeyer *et al.*, 2003). Ghiglione *et al.*, (2012) reported that 85% of operational taxonomic units (OTUs) were not shared between the two polar regions. This higher diversity in the Arctic was also shown by Cao *et al.*, (2020) who found functional differences including

an increase in genes related to antibiotic resistance in the Arctic and DNA recombination in the Antarctic. So, despite eubacterial abundance being similar between the two regions, taxonomically and functionally there are differences which may lead to differing biosynthetic capacities for B_{12} between the regions. More recently, a new group of B_{12} producing Archaea called *Thaumarchaeota* was identified as an important producer of the vitamin in the World's oceans (Doxey *et al.*, 2015). Moreover, Doxey *et al.*, (2015) showed that the contribution to cobalamin production was primarily from *Thaumarchaeota* and Proteobacteria in the colder, higher latitudes with Cyanobacteria replacing *Thaumarchaeota* in the warmer, lower latitudes. Without direct measurements of vitamin B_{12} in the Arctic it is difficult to elucidate whether the B_{12} dependency shown in *F. cylindrus* is a direct result of higher B_{12} concentrations in the region. *F. cylindrus* is an ice diatom, forming blooms under the sea ice and within it. It is likely that these blooms will promote the formation of biofilms consisting of B_{12} producing prokaryotes. What this does not explain though, is why Arctic and Antarctic isolates differ, despite residing in similar environments and occupying the same biological niche and ecology. The evolution of B_{12} dependency as a result of high B_{12} concentrations has already been described in *C. reinhardtii* (Helliwell *et al.*, 2015). Therefore, it is quite possible that the Arctic *F. cylindrus* populations have experienced selection pressure (due to high B_{12} and cobalt concentrations and a greater number of B_{12} producing bacteria) from the environment resulting in B_{12} dependency. Indeed, there seems to be a selection for retaining *METE* in Southern Ocean marine diatoms with 62% possessing the gene compared to only 11% in non-Southern Ocean diatoms (Ellis *et al.*, 2017). Clearly more work is required to identify the complex relationships and interactions between diatoms and bacteria.

Chapter 6 - Potential for use of polar diatoms in biotechnology

6.1 Introduction

Diatoms are an attractive resource for several different industries including nutrition/food, waste management, pharmaceuticals, nutraceuticals, medicine, and biofuels. For example, currently diatoms and other microalgae are used at large scale for aquafeed (Couteau, 1996) and have been suggested as potential sources of lipids for biofuels (Griffiths & Harrison, 2009; Hildebrand *et al.*, 2012). Diatoms have also shown potential for high polyunsaturated fatty acid synthesis (PUFAs, Dunstan *et al.*, 1993) which are important for human nutrition (Swanson *et al.*, 2012), making diatoms an attractive sustainable replacement to fish oils. Moreover, diatoms produce a range of pigments, the most dominant being carotenoids which have shown to have bioactive properties (Kuczynska *et al.*, 2015). The carotenoid fucoxanthin is the main accessory pigment in diatoms and is a compound of interest due to its bioactivity against cancer and other diseases (Stahl & Sies, 2005 and references therein). In addition to the products which diatoms can provide, they are also seen as an environmentally clean resource due to being phototrophic.

However, the large-scale production of diatoms remains problematic (Grobbelaar, (2010) and Slade & Bauen, (2013)). Most diatom species used in biotechnology have an optimal growth temperature of >20°C, which limits production to warmer climates or requires the expenditure of energy to heat and illuminate algal cultures. This is costly and often relies on fossil fuels. It is therefore difficult to efficiently run biotechnological processes in cold climates or in the winter months of temperate regions due to low temperatures and low light irradiance. Moody *et al.*, (2014) modelled the production of *Nannochloropsis* (a commonly grown alga) in closed photobioreactors around the globe and identified reduced growth and lipid production in cold climates. This was confirmed by Quinn *et al.*, (2012) who modelled the growth of *Nannochloropsis* across North America and found poor growth and lipid production in the colder Northern states. Both studies attributed low temperatures and low light irradiance for the decreased productivity and lipid production and concluded that algal biotechnology in its current state is not economically feasible in cold climates and during winter months.

For biotechnology to be economical, processes must be able to run year-round with high yields. One of the potential solutions to this lack of productivity in colder climates and in winter months is the effective partnership with other industries, utilising waste products such as low-grade heat and CO_2 emissions to increase productivity (Baliga & Powers, 2010). Modelling the production of biodiesel in New York, Baliga & Powers, (2010) showed how coupling algal production to power plants providing waste heat and CO_2 required half the energy needed compared to producing the heat in house and that heat was dominant energy consumer. The limitation of this solution, however, is that biotechnological businesses will be limited by the availability of other industries providing waste products. Furthermore, enhanced processes may be needed to ensure such waste products are not toxic and detrimental to algal cultures. Emissions from power stations for instance may have high levels of SOx and NOx. Another solution is the use of specialised reactors to cope with challenging conditions. Pankratz *et al.*, (2017) identified nine means of algal production that could potentially be used in Northern Canada including open and closed photobioreactors. However, the costs of these specialised setups would require large capital investment, which may be beyond the scope of many companies. Furthermore, the cost per tonne of algae for biomass is reported at between 3000-20000 $/tonne in open photobioreactors and 3500-95000 $/tonne in closed photobioreactors, which are significantly higher than the traditional feedstocks e.g., soybean 623 $/tonne (Pankratz *et al.*, 2017). Various bioreactor types and associated costs have previously been reviewed by Gupta *et al.*, (2015), which highlighted the large costs involved in producing and running photobioreactors. In recent years, scientists have begun looking at the potential for utilising polar, cold adapted algal species as a way of reducing the need for extensive energy expenditure for heat and light or specialised bioreactors in colder climates. There is also interest in cold-adapted species for the identification and production of novel metabolites resulting from local adaptation to extreme environments (e.g., the polar regions).

The potential of polar algae for biotechnological exploitation has previously been identified. For example, terrestrial snow algae produce high levels of the high value compound, astaxanthin (a high value compound used for dietary and industrial purposes, (Remias *et al.*, 2005)) and show high growth and lipid production at low temperatures (Hulatt *et al.*, 2017). The polar diatom *Chaetoceros brevis* has shown high production of EPA (a beneficial omega-

3 fatty acid important for human diet) at low temperatures (3°C and 7°C) under low light irradiance (Boelen *et al.*, 2013). Compared to a temperate diatom grown at 16°C, *C. brevis* produced higher levels of EPA under low light irradiance (10 µmol m^{-2} s^{-1}) and low temperature (7°C) but showed the same specific growth rate (Boelen *et al.*, 2013). In addition, cold adapted species are predicted to produce high levels of membrane lipids e.g., PUFAs (which include omega-3s), as these have been identified as key components to cell membrane fluidity, a necessary adaptation to the cold (Nichols *et al.*, 1993; Russell & Nichols, 1999; Chintalapati *et al.*, 2004). Polar algae have also been shown to produce a variety of bioactive compounds which may have significant benefits to human society e.g., antibacterial, and anticancer compounds (Ingebrigtsen *et al.*, 2016, 2017)).

Despite polar diatoms showing high potential for growth in cold temperatures, low light conditions and the production of compounds with existing economic markets, there is currently little research into how they can be incorporated into biotechnology. A recent literature search found one article that focused on assessing the performance of polar diatoms in ambient conditions in cold climates. Steinrucken *et al.*, (2018) investigated two cold adapted Norwegian strains and a temperate strain of *P. tricornutum* under ambient conditions in Norway but found no difference in growth with lower EPA production in polar strains. Fig. 6.1 shows the average winter surface temperatures in the Northern Hemisphere, which identifies 40°N as the minimum latitude that should be targeted for the growth of polar strains based on all investigated strains so far having optimal growth below 10°C.

This chapter aimed to scope the potential of a variety of polar diatom strains for biotechnology, primarily focusing on biomass production under winter conditions in the UK. Growth was compared to the temperate species *P. tricornutum* which has been successfully used in algal biotechnology projects for production of lipids and fucoxanthin (Kim *et al.*, 2012 and references therein) and has optimal growth between 20-22°C (Nur *et al.*, 2019).

REDACTION: Image showing the average winter temperatures in the Northern Hemisphere removed for copyright reasons. Copyright holder is National Geographic.

6.2 Additional materials and methods

Two experiments were conducted in the algal innovation centre (AIC) greenhouse at the University Botanic Garden in Cambridge, UK between January-March 2018. Antarctic strains were assessed in January-February and Arctic strains assessed in February-March that year. Antarctic strains *Fragilariopsis* sp. (CCAP 1023/6), *P. glacialis* (CCAP1060/10), and *T. antarctica* (CCAP 1085/25) and Arctic strains *Fragilariopsis* sp. (CCAP 1023/3), *T. gravida* (CCAP 1085/24) and *P. tricornutum* (CCAP 1055/9) were used together with a temperate strain, *P. tricornutum* (UTEX 646). Starter cultures (1 L) were grown at 4°C for polar strains and room temperature for the temperate strain and then used to inoculate 10L bubble column reactors. Starter cultures were acclimated to the experimental conditions for one week before experiments began and were inoculated at a cell density of $4.8x10^5$/L in the January/February experiment and $1.5x10^6$L in the February/March experiment. Sea water was made as previously described in Appendix 1, however due to the large volumes required the water could not be filtered sterilised but was used directly from the tap. Three biological replicates were used per strain and the temperate *P. tricornutum* strain was used as a reference to compare with the performance of the polar strains. Cultures were bubbled with 0.2 µm filtered (Whatman, Maidstone, UK) air delivered by an air compressor at a flow rate of 8 L per minute to provide CO_2 and adequate mixing. Light and temperature were not controlled, so ambient conditions were measured using a Sirius weather station measuring light intensity every 10 minutes.

Water temperature was measured in one bubble column every 15 minutes using an Elitech RC-4W temperature logger (Elitech, UK) and pH was measured once a week. Experiments lasted 24 days.

Dry weight was conducted following a slightly modified protocol of Zhu & Lee, (1997), in brief; 30 ml of algal culture was filtered onto pre-heated (48 hours at 80°C), pre-weighed Whatman 0.45 µm filter paper. The filter paper was washed with 15 ml 0.5M ammonium formate and dried in an oven for 48 hours at 80°C. The dried filter paper was then re-weighed, and the start value subtracted from the end value to get the dry mass. Seawater controls were used to account for any influence from the sea water.

6.3 Results

6.3.1 Growth of Antarctic diatom strains

Growth curves of the Antarctic strains investigated in January/February 2018 are shown in Fig. 6.2a. Strains showed a long lag phase after inoculation until day 13 when temperate *P. tricornutum* and *T. antarctica* showed an increase in optical density (Fig. 6.2a) and became visible in the bubble columns (Appendix 13). *P. tricornutum* continued to show exponential growth until the end of the experiment whereas *T. antarctica* exhibited a stable, flat rate of growth. *P. glacialis* did not show signs of growth until day 20, after which it grew exponentially and reached the same optical density of *T. antarctica* (Fig. 6.2a). *Fragilaria* sp. did not show any growth during the period of the experiment. Antarctic strains and temperate *P. tricornutum* showed low but similar specific growth rates (Table 6.1) with *P. glacialis* showing the fastest rate in the exponential phase. However, there were no statistical differences between the growth rates of the three strains (Table 6.2). Average pH levels at the end of the experiment varied between species but were considerably higher than the starting pH of 8.1 (Table 6.1).

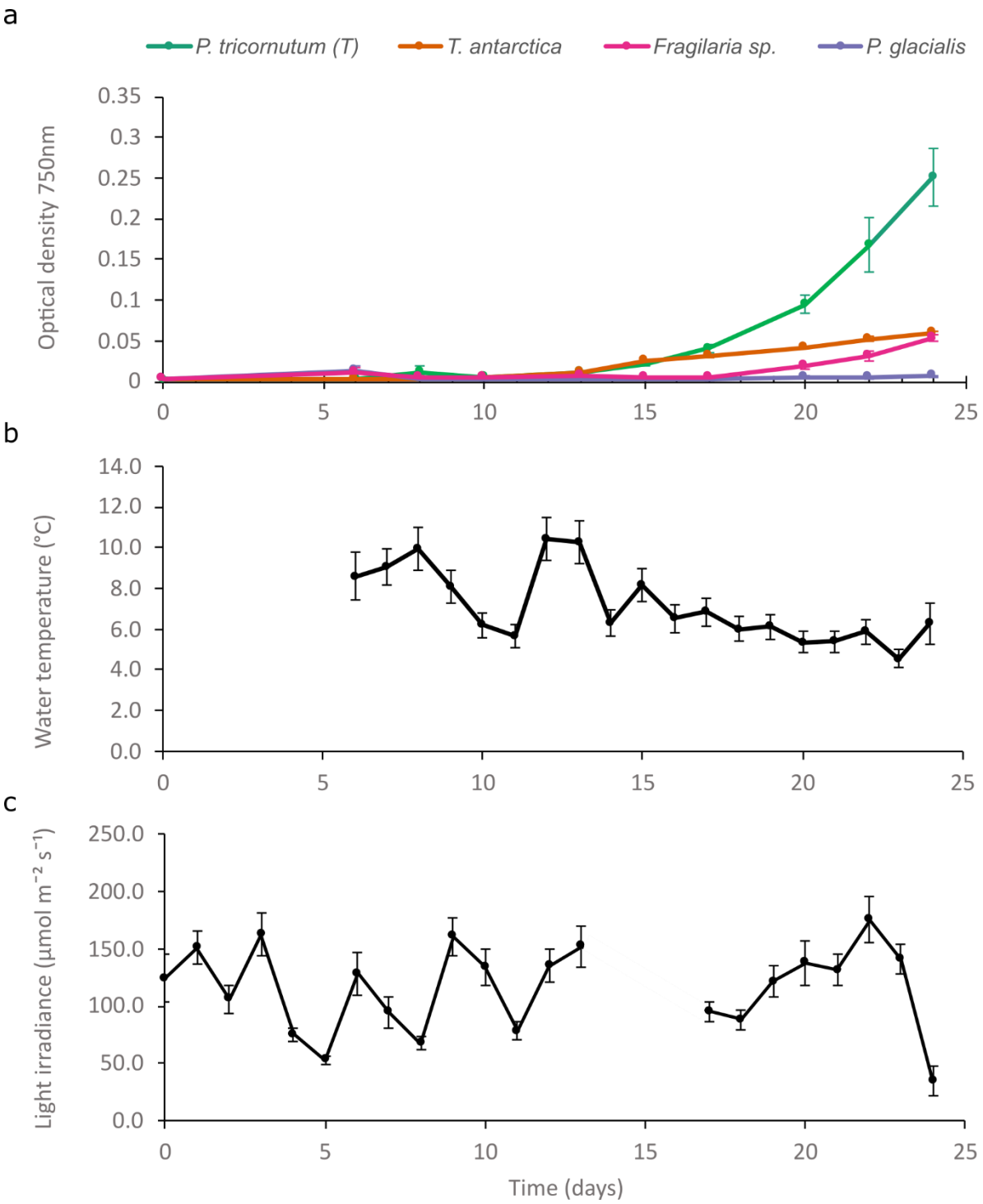

Figure 6.1 Growth of Antarctic strains grown under ambient temperature and light in January/February 2018. a) Growth curves of Antarctic strains and the temperate *P. tricornutum* (T) strain, N = 3, mean ±SD. b) Average daily water temperature, mean ±SE (data unavailable for the first five days). c) Average daily light irradiance, mean ±SE.

Table 6.1 January/February 2018 growth rates. Specific growth rates and final culture media pH values of Antarctic strains compared to a temperate *P. tricornutum* (T) strain grown under ambient conditions during January/February 2018.

January/February 2018	Specific growth rate (μ OD750)	Average final Ph
P. tricornutum (T)	0.264	8.73
T. antarctica	0.268	8.96
P. glacialis	0.313	8.53

The average daily water temperatures were consistently below 10°C except for days 12 and 13 and there was no pattern between water temperature and the growth curves (Fig. 6.2b). Water temperature data for the first six days was unavailable, however light intensity (Fig. 6.2c) and ambient temperature (data not shown) did not vary substantially during the experiment and therefore water temperature was unlikely to differ.

During the experiment, water temperatures exceeded 10°C for 16% of the measured time and reached a maximum of 14°C, but the rate of temperature change was often very rapid. The average water temperature for the duration of the experiment was 7.1°C. Light irradiance during the day was approximately the same throughout (Fig. 6.2c), with average daily light intensity of 118 μmol m^{-2} s^{-1} although day length increased by 1 hour (h) 17 minutes (min) between the start (8h 18min) and end (9h 35min) of the experiment. There was no pattern shown between the growth curves and average daily light irradiance (Fig. 6.2a and c).

Table 6.2 January/February growth statistics. Statistical analysis of specific growth rates of polar diatoms and the temperate *P. tricornutum* (T).

January/February 2018	t test statistics		
	t	**Df**	***P***
P. tricornutum (T) + *T. antarctica*	-0.326	2.604	>0.05
P. tricornutum (T) + *P. glacialis*	-1.376	2.149	>0.05
T. Antarctica + *P. glacialis*	-1.103	2.914	>0.05

6.3.2 Growth of Arctic diatom strains

Growth curves of the Arctic strains investigated during February/March 2018 are shown in Fig. 6.3a. As before, strains showed a long lag phase post inoculation with growth starting around day 10 for *Fragilariopsis* sp. and day 15 for the other strains including the temperate *P. tricornutum* (Fig. 6.3a and Appendix 14). *Fragilariopsis* sp. exhibited steady growth until day 19 where it plateaued and began to decrease. Both the Arctic (CCAP 1055/9) and temperate (T) *P. tricornutum* strains exhibited similar growth, showing exponential growth until day 24 when both started to plateau. *T. gravida* exhibited a delayed growth, only showing growth towards the end of the experiment based on optical density (Fig. 6.3a and Appendix 14). Specific growth rates were low but were higher compared to the January/February 2018 Antarctic experiment (Table 6.3). Both the Arctic and temperate *P. tricornutum* strains had the highest growth rates with no statistical difference between the two ($p>0.05$). There was a significant difference between *T. gravida* and the other three strains ($p<0.05$, Table 6.4), with *T. gravida* showing a significantly lower specific growth rate. The specific growth rate of *Fragilariopsis* sp. was significantly lower than the temperate *P. tricornutum*, but there was no significant difference between *Fragilariopsis* sp. and the Arctic *P. tricornutum* strain (Table 6.4). As in the first experiment, pH values had increased by the end of the experiment (Table 6.3).

Table 6.3 February/March 2018 growth rates. Specific growth rates and final culture media pH values of Arctic strains compared to a temperate *P. tricornutum* (T) strain grown under ambient conditions during February/March 2018.

February/March 2018	Specific growth rate (μ OD 750)	Average final pH
P. tricornutum (T)	0.369	9.50
T. gravida	0.232	8.73
P. tricornutum	0.340	9.76
Fragilariopsis sp.	0.306	8.86

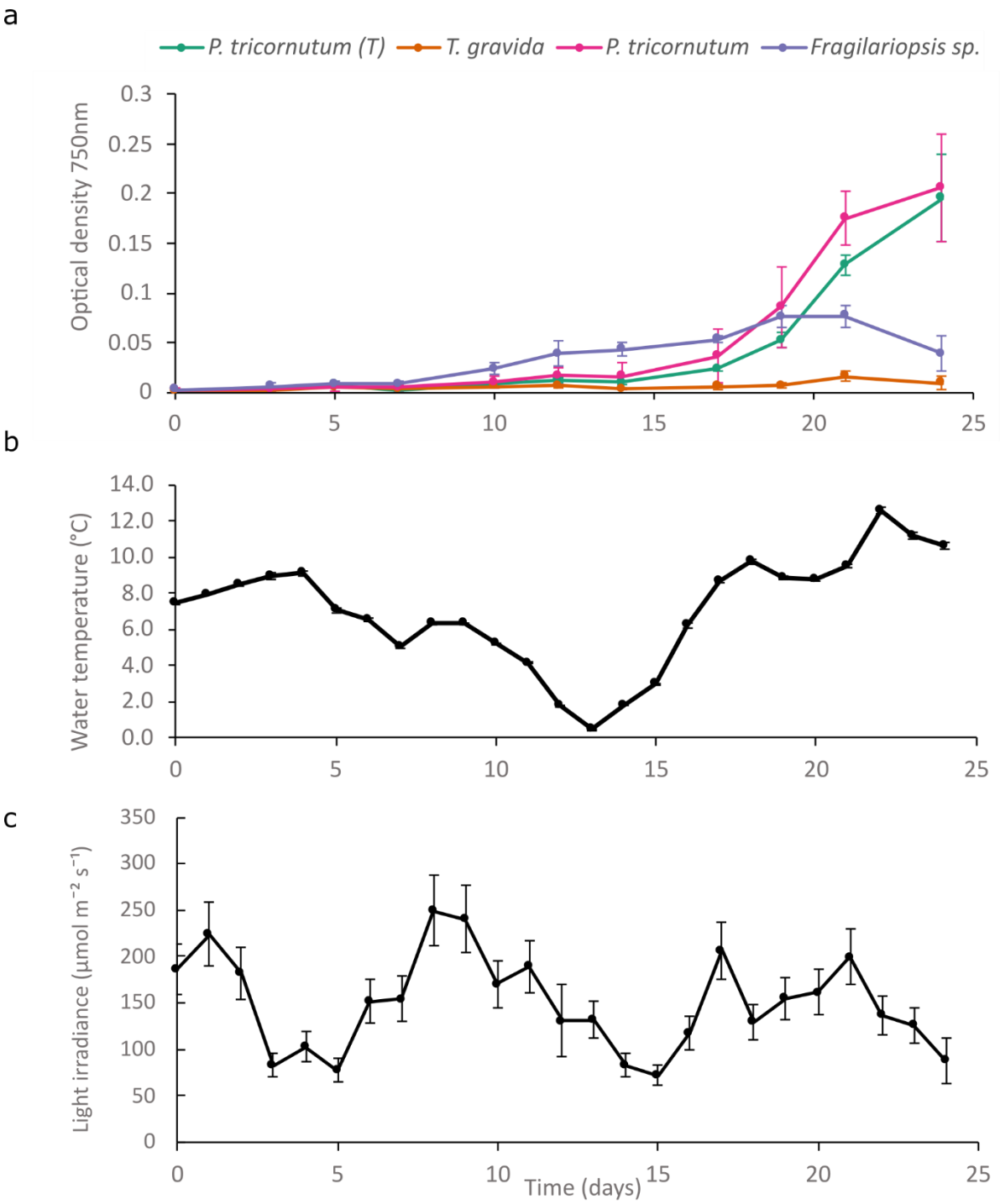

Figure 6.2 Growth of Arctic strains grown under ambient temperature and light in February/March 2018. a) Growth curves of Arctic strains and the temperate *P. tricornutum* (T) strain, N = 3, mean ±SD. b) Average daily water temperature, mean ±SE. c) Average daily light irradiance, mean ±SE.

Average water temperatures were consistently below 10°C for the majority of the experiment with an average for the whole experiment of 7.0°C. The February/March 2018 experiment was characterised by a severe cold period between days nine and 15, with temperatures falling to a minimum of -1.1°C after which average water temperatures rose significantly (Fig. 6.3b). Water temperatures exceeded 10°C for 25% of the experiment and water temperatures consistently rose to >13°C by mid-afternoon reaching a maximum of 16.5°C in the last three days. Similar to the first experiment, the temperature change was often rapid, specifically around midday. The cold period between days nine and 15 was also characterised by low light, but intensity remained medium/high with an average intensity of 135 µmol m^{-2} s^{-1} for the experimental duration (Fig. 6.3c). Day length providing light irradiance was 27 minutes longer at the start of the February/March 2018 experiment compared to the end of the January/February 2018 experiment. Over the course of the experiment day length increased by 1h 35 min from the start (10h 2 min) to the end (11h 35 min).

6.3.3 Dry weight of polar strains

Final dry weights of Antarctic and Arctic strains are presented in Fig. 6.4a and b respectively. The Antarctic strains *T. antarctica* and *P. glacialis* showed a similar final dry weight of ~1 g/L, and this was much lower than the temperate *P. tricornutum* strain which had a final dry weight of 1.7 g/L (Fig. 6.4a). There was no significant difference between the three strains ($p>0.05$). *Fragilaria* sp. was not analysed for dry weight due to a lack of growth during the experiment. The Arctic strains showed less disparity in final dry weight to the temperate strain (Fig. 6.4b).

Table 6.4 February/March 2018 growth statistics. Statistical analysis of specific growth rates of polar diatoms and the temperate *P. tricornutum* (T).

February/March 2018	t test statistics		
	t	**Df**	***P***
P. tricornutum (T) + *T. gravida*	6.774	2.075	**<0.05**
P. tricornutum (T) + *P. tricornutum*	1.954	1.082	>0.05
P. tricornutum (T) + *Fragilariopsis* sp.	4.088	2.154	**<0.05**
T. gravida + *P. tricornutum*	-4.532	2.996	**<0.05**
T. gravida + *Fragilariopsis* sp.	-3.216	3.578	**<0.05**
P. tricornutum + *Fragilariopsis* sp.	1.596	2.714	>0.05

The Arctic and temperate strains of *P. tricornutum* showed a similar dry weight of ~1.3 g/L, however *T. gravida* despite showing poor growth (Fig. 6.3a) had a final dry weight of 1.15 g/L. *Fragilariopsis* sp. had the lowest final dry weight of the Arctic strains (0.915 g/L). There were no significant differences between the four strains ($p>0.05$).

6.3.4 Pigment analysis

Pigments showed an increase between week 1 and experiment end in all strains (Appendix 15).

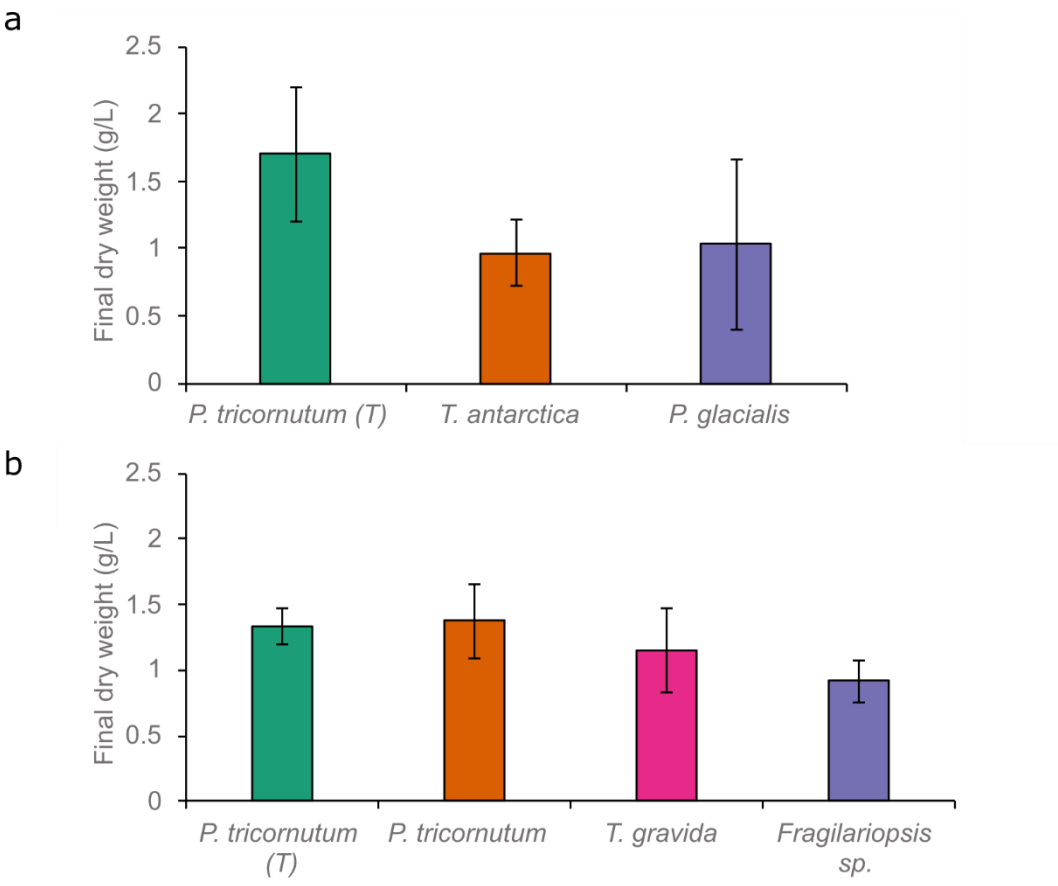

Figure 6.3 Final dry weights of polar strains. a) Antarctic strains and b) Arctic strains compared to the temperate *P. tricornutum* (T). N=3, mean ± SD.

6.4 Discussion

Polar organisms, especially algae, have come under increased interest to science for research into their evolution and adaptation but also for their potential role in biotechnology. Here a preliminary study investigating the feasibility of using polar diatoms for biotechnology in a temperate environment is presented. Grown in 10L bubble reactors in the AIC at the University of Cambridge Botanic Garden, polar diatoms were grown in ambient British winter conditions to assess growth, compared to a commonly used temperate species *P. tricornutum.* Ambient winter conditions were characterised by low temperatures and low light irradiance (Fig. 6.2b, c and Fig. 6.3b, c). Polar diatoms have previously shown high growth under low temperatures and light irradiance in controlled conditions (Hegseth, 1989; Fiala & Oriol, 1990; Longhi *et al.*, 2003). In the current experiments growth of all diatom strains tested was low using optical density as a proxy for growth (Fig. 6.2a and Fig. 6.3a), but the final biomass achieved from all strains was promising since it was equivalent to that of a temperate strain of *P. tricornutum* (Fig. 6.4). It is currently not possible to propose a single factor which explained the low growth of polar diatoms and it was likely to be a combination including photoinhibition, light irradiance, temperature stress and pH stress. Although there was no visible contamination from other protists there was bacteria present in all cultures. Bacteria was not quantified and therefore may have influenced the biomass measured.

6.4.1 Photoinhibition and light irradiance

Cell inoculations for all strains were matched at the start of each experiment, however because of the variable growth of the starter cultures, this meant that low inoculations were used for all of them. This may have resulted in cellular stress due to high light irradiance, inhibiting growth. As cell density increases it leads to "self-shading", which can protect cells from cellular stress due to high light irradiance (Barros *et al.*, 2003). Average maximum light irradiances ranged from 277 µmol m^{-2} s^{-1} (January/February) and 393µmol m^{-2} s^{-1} (February/March) and although these values were only maintained for short periods of time, they could potentially cause photoinhibition of low-density cultures. In the toxic cyanobacterium *Microcystis aeruginosa* an initial inoculation density of 1069 cells/ml (similar values to the current study) resulted in a slower growth rate and a final density 3.7 times lower than an inoculation of 6417 cells/ml (Dunn & Manoylov, 2016). Therefore, increased

inoculation densities would potentially enable growth of polar diatoms at a faster rate post inoculation and likely lead to higher final biomass.

An increase in day length during the February/March 2018 experiment is likely to be a strong factor influencing the higher growth rates shown by Arctic species (Table 6.3). A long-term experiment to assess the feasibility of algal biotechnology in Norway found that maximum growth and yield was achieved in spring when the light irradiance was highest (Steinrücken *et al.*, 2018b). The strains tested by Steinrucken *et al.*, (2018) also produced high levels of EPA throughout the experiment and even though biomass was lower during summer and autumn months the higher levels of EPA compensated this. The growth rates of *Fragilariopsis* sp., *P. glacialis*, and *P. tricornutum* were comparable or higher than reported rates at similar temperatures (7-10°C, William & Morris, 1982; Mock & Hoch, 2005; Huseby *et al.*, 2013; Pančić *et al.*, 2015). *T. gravida* showed a lower growth rate compared to reported rates (0.51 μ/day at 8.5°C, Huseby *et al.*, 2013). The disparity of the growth rates in *T. gravida* in the current experiment and reported literature could potentially be due to the omission of added vitamins to the medium in the current study. *T. pseudonana* requires vitamin B_{12} (Croft et al. 2005). *T. gravida* however grows well without the addition of vitamins at 4°C at a light irradiance of 30 μmol m^{-2} s^{-1} (personal observation) and polar strains showed signs of growth at similar times to *P. tricornutum* (Fig. 6.2a and 6.3a) which grows independently of vitamin B_{12} (Croft *et al.*, 2005). The requirement of vitamins cannot be ruled out and further work will be needed to identify the vitamin requirements of polar diatoms but light and temperature are likely to have had a larger impact on the growth. The addition of vitamins may also be beneficial for metabolite production as the addition of vitamin B_{12} to *P. tricornutum* cultures resulted in an increased production of EPA (Yongmanitchai & Ward, 1991).

6.4.2 Temperature

Although polar diatoms have shown an ability to grow at elevated temperatures (Fiala & Oriol, 1990; Longhi *et al.*, 2003; Boelen *et al.*, 2013; Huseby *et al.*, 2013), their ability to cope with daily changes in temperature is not known. Fiala & Oriol, (1990) found that the optimal growth temperature for seven Antarctic diatoms was between 3-5°C and the temperature at which it became lethal was between 6-9°C, with one species showing a lethal temperature of

15°C. In the current study all polar strains except for the Antarctic *Fragilaria* sp. were able to survive temperatures >10°C and maximum temperatures of 14°C (January/February 2018) and 16.5°C (February/March 2018) for brief periods. It is likely that the temperatures in the January/February 2018 experiment which averaged 7.1°C were above the thermal limit of *Fragilaria sp* and this is in agreement with the thermal limits shown by Fiala & Oriol, (1990) for Antarctic species. Longhi *et al.*, (2003) also found the maximal survival temperature of two benthic Antarctic diatoms to be between 7-9°C. Arctic diatom species however have shown a better ability to survive higher temperatures e.g. (Huseby *et al.*, 2013) found high growth and physiological health of six Arctic diatoms grown at 8.5°C. Eight Arctic diatom strains have also shown optimal growth between 1-20°C and seven of the eight strains could be grown at 20°C (Schlie & Karsten, 2017). Although polar strains showed an ability to grow at elevated temperatures in the current study, the rapid changes in temperature experienced may potentially have induced cyclical stress which ultimately could limit growth. Identifying species and strains which can cope with rapid fluctuations in temperature will be key for maximising the potential for biotechnology. Assessing the thermal tolerance of species, as was done in Chapter four, can be completed at small scales to identify optimal growth temperatures, enabling better selection of strains for biotechnology.

6.4.3 pH stress and culture circulation

Bubble column cultures were purged with air to create adequate mixing within the column and provide CO_2 as the sole carbon source. As cultures grew and became denser CO_2 was removed from the media and a rise in pH was shown (Table 6.1 and Table 6.3). In both experiments the final pH was dependent on the strain, but all strains showed an increase in pH. High pH has been previously shown to inhibit growth of the diatom *Skeletonema costatum* at pH ≥9 (Taraldsvik & Myklestad, 2000) and growth of *T. pseudonana* and *T. oceanica* at pH ≥8.8 (Chen & Durbin, 1994). To avoid this growth inhibition, it is common to purge cultures with CO_2 at a calculated rate to achieve optimal pH conditions and maximise growth (Behrens, 2005). Despite the sub-optimal abiotic factors discussed above, the final biomass of cultures was relatively high, with all cultures except for the Antarctic *Fragilaria* sp. reaching a final dry weight of ~1 g/L (Fig. 6.4). One problem which was identified with the bubble column reactors was the settling of cultures. The Arctic *Fragilariopsis* sp., which

showed the lowest biomass of the Arctic strains (Fig. 6.4), is a chain forming diatom and at the end of the experiment cultures had formed a dense sediment at the bottom of the column (Appendix 13). This sedimentation is likely to have led to an underestimate of the final biomass of the culture, which was measured by optical density.

Polar diatoms have been suggested as a novel resource for increased biotechnology in cold climates and temperate winter months and as a potential source of novel cold adapted metabolites. In this preliminary study, it was demonstrated that although the growth of polar diatoms was generally poorer than that of the temperate *P. tricornutum*, in spite of the issues noted above, they do show potential for high productivity and biomass under ambient conditions during the British winter. Though the growth of the temperate *P. tricornutum* may be discouraging to the prospect of polar strains, it is important to note that no optimisation of growth requirements such as temperature, light intensity, nutrients, and mixing were carried out due to limited time. These experiments presented a one-off possibility to assess polar strains under natural conditions due to limited availability of the AIC and Covid-19 repercussions. Despite this, the AIC is an ideal facility to scope strains and optimize growth conditions and although environmental conditions are difficult to control for certain parameters can be influenced e.g., additional artificial light to increase irradiance. Furthermore, biomass is not always the most important aspect to base potential on as there is the potential for metabolic products to outweigh the lower biomass e.g., lipid production in *P. tricornutum* strains grown in Norway (Steinrücken *et al.*, 2018b). Optimising salinity and light irradiance have shown the ability to alter lipid production and growth rates in the Arctic diatom *Attheya septentrionalis* grown at 10°C, showing the potential of the strain which the Authors suggest should be followed up at scale (Steinrücken *et al.*, 2018a).

The selection of a strain that produces the metabolite(s) of interest and high biomass is important in biotechnology. Therefore, future work should look to characterise specific strains based on their potential for metabolic products but also to optimise growth conditions in a biotechnology setting. Moreover, metabolic products are sometimes produced through cell stress, so by testing a range of environmental parameters will allow for the assessment of a strain under optimal and sub-optimal conditions. Growth and biomass are two important traits which should be selected and four strains which were isolated in Chapter 3 should be investigated further for their biotechnological potential:

Proboscia truncata (CCAP 1064/3), *Chaetoceros* sp. (CCAP 1010/54), *C.* cf. *flexuosus* (CCAP 1010/55), and *Synedropsis* sp. (CCAP 1063/1). Though no data of growth or biomass was completed on these strains due to time constraints, their growth observed at 0°C looks very promising. The use of polar strains for biotechnology in the literature is still relatively sparse but with increasing pressure to find alternative energy and to be more environmentally friendly, it is hoped this resource will be investigated further in the future.

Chapter 7 - Final Synthesis and future work

In this thesis, new species and strains of polar diatoms were isolated during Antarctic field work. These new isolates and culture collection strains underpinned experiments on the physiology and metabolism of key polar diatoms species. In particular, this thesis explored diatom biology in the context of two bipolar species *F. cylindrus* and *P. glacialis* and the disjunct bipolar distribution they exhibit. Bipolarity is a seldom studied phenomenon and the results in this thesis demonstrate that the two disjunct populations cannot necessarily be considered equal in terms of their physiology and metabolism, with significant differences demonstrated in thermal tolerances and B_{12} dependency between Arctic and Antarctic strains. Finally, the potential of polar diatoms for biotechnology exploitation was investigated.

7.1 Fresh isolates, a platform to build upon

One difficulty experienced in studying algal species in the laboratory is the length of time strains had been maintained in culture. Algal culture collections are an incredibly valuable resource but there are limits to what can be obtained and stored. For instance, many culture collections often do not keep more than one isolate of the same species, especially when they have been isolated in proximity to each other. Moreover, certain environments are represented to a much lesser extent compared to others particularly polar compared to temperate. For many algal physiologists, work on laboratory strains is interpreted in context to their natural environment and therein lies a fundamental issue, how representative are these strains? Like most biological sciences, the use of model species is fundamentally important to understand certain biological characteristics because they can be extensively studied due to their ease of culture and scientific reproducibility. *P. tricornutum* is one such model species, the strain upon which most of the research is based being isolated in 1956. This is also true of the two other model species *T. pseudonana* and *F. cylindrus,* which were isolated in 1958 and 1979 respectively. Considering the fast generation times of diatoms, which range from 11 hours to >10 days (Baars, 1981), looking into whether algal strains kept in culture conditions for decades behave exactly the same as their environmental

counterparts is an important question to investigate. Prior work in the Plant Metabolism group has shown just how quickly microalgae can evolve to laboratory conditions. Helliwell *et al.*, (2015) demonstrated how the green alga *C. reinhardtii* grown under replete vitamin B_{12} conditions was able to evolve a B_{12} dependent phenotype as the result of a genetic insertion of a transposable element. What is more, this phenotype was derived in just ~600 generations (6 months). Rapid evolution has also been shown in diatoms. Schaum *et al.*, (2018) demonstrated how *T. pseudonana* under various temperature regimes showed rapid evolution of both metabolic traits and genetic divergence in ~300 generations. A similar result was also presented by O'Donnell *et al.*, (2018) whereby *T. pseudonana* exhibited a shift in thermal tolerance after ~350 generations when selectively grown at 31°C compared to 16°C. Both studies demonstrate how rapidly this diatom species can adapt to changing conditions.

Investigating the effects of long-term culture and acclimation *per se* was not the focus of the present work, but rather to assemble the resources needed to be able to do this. Although culture collections are often limited in the number of strains they can maintain, many are open to the deposition of freshly isolated strains of species they already hold. Having a constant cycle of freshly isolated strains is beneficial, not just for studying intraspecific variation, but also for evaluating the responses of the different strains and the effects of culture. Logistically, the cycling of new strains is easier for temperate species and as a result polar strains, especially from the Antarctic, are often neglected. The work presented in Chapter three provides such a resource with the deposition of new strains of already available species and of new species. The Culture Collection for Algae and Protozoa at Oban, where the strains isolated in Chapter three are deposited, is a world-renowned resource for both scientific research and commercial interests. The addition of seven new species made to this collection will enable researchers to study physiological, metabolic, and genetic characteristics of these species, enhancing our knowledge of polar diatoms. This work echoes the motives of Gérikas Ribeiro *et al.*, (2020) who intended to isolate and culture phytoplankton in the Arctic and managed to obtain 193 diatom isolates that are deposited in the Roscoff culture collection. Gérikas Ribeiro *et al.*, (2020) were able to achieve such high numbers due to utilizing a range of isolation methods and employing a non-targeted approach and a similar study would be advantageous in the Antarctic. Combined, both

Gérikas Ribeiro *et al.*, (2020) and the present work have greatly improved the diversity and number of diatom strains available from the polar regions.

7.1.1 Future work

- Scanning electron microscopy analysis of morphological features to fully confirm identifications.
- Newly isolated strains would be ideal candidates to carry out experiments regarding long-term acclimation to laboratory conditions e.g., temperature and light.
- Growth and biochemical analysis of strains would provide a useful resource to help scientists and commercial partners assess the physiological and metabolic properties of strains.

7.2 Bipolar species should not be assumed to be equals

It is surprising that little work has been carried out on bipolar diatom species and in fact on bipolarity as a whole. The occurrence of bipolar distributions of *F. cylindrus* and *P. glacialis* offered a unique opportunity to study this phenomenon in diatoms. Work on both species often states their bipolar distribution but usually only report work on either an Arctic or an Antarctic strain. Below I discuss how strains from both regions do not respond similarly to temperature and vitamins and that interpretation of responses should be limited to the environment they were isolated from.

7.2.1 Response to temperature

Evaluating the thermal tolerance of polar diatoms proved to be problematic in the early stages using already available in-house equipment due to the difficulty of replicating the cold temperatures of the polar regions, especially sub-zero temperatures. The purchase of bioreactors developed by Xanthella Ltd to specified requirements were fundamental to achieving the growth of polar strains at sub-zero temperatures whilst also controlling for other factors such as light intensity and irradiance cycles.

The polar environments are both experiencing various elements of environmental change including increasing sea water temperatures. Temperature is an interesting factor to study as it not only influences the growth of diatoms, but also their metabolic rates. Chapter 4 demonstrates that the responses of the Arctic and Antarctic strains of *F. cylindrus* and *P. glacialis* differ in response to temperature. This is an important finding as studies will often utilize one strain and sometimes generalize their findings at the species level. Diatoms show a large degree of intraspecific variation so generalizing to the species level assumes a homogenous response over the whole species. This generalization is true for the model diatom species and of *F. cylindrus* where many studies perform experimental work on the Antarctic strain and then relate this response to the Arctic as well. Fig. 4.5 shows that the thermal tolerance of both species is different between the Arctic and Antarctic strains. In *F. cylindrus* the Arctic strain had a T_{opt} ~3.5°C higher than the Antarctic strain. The higher T_{opt} in the Arctic strain agrees with the hypothesis that Arctic strains may have higher thermal tolerance and also agrees with the literature which reports higher T_{opt} in Arctic phytoplankton more generally (Coello-Camba & Agustí, 2017).

In contrast, *P. glacialis* showed the opposite whereby the Arctic strain had a T_{opt} ~5.5°C lower than the Antarctic strain. Moreover, unlike *F. cylindrus*, both *P. glacialis* strains were able to grow over the same temperature range up to 12°C so the thermal niche between these two strains is similar. The thermal niche in the Antarctic *F. cylindrus* was not the same as it was unable to grow at 12°C. Focusing on these two strains alone, *F. cylindrus* in the Arctic may possess a better resilience to future warming, however this is the response of just one strain. When intraspecific variation and age of the culture was investigated in more detail, the thermal response of Antarctic *F. cylindrus* was puzzling (Fig. 4.7). The thermal response of the two newly isolated strains from Chapter three indicated two things: 1) that there are possible ecotypes in the Antarctic *F. cylindrus* population able to survive at 12°C and 2) that both newly isolated strains had optimal temperatures lower than the original strain isolated in 1979. The first of these may be a result of the vast gene pool this species exhibits (Mock *et al.*, 2017) and its plastic response to environmental changes (Sackett *et al.*, 2013). The second may be a result of the long-term culturing of that particular strain at slightly higher temperatures (4°C), which although not studied in polar species has been shown to shift the thermal tolerance in a temperate diatom (O'Donnell *et al.*, 2018; Schaum *et al.*, 2018).

The expected increase in SST in the Arctic and the Antarctic are predicted to be 3°C and 1.2°C respectively by 2100 (Iturbide *et al.*, 2021). These predicted increases were the primary reason for evaluating growth and metabolic characteristics at low temperatures (-1°C – 4°C, Chapter 4 sections 4.2.6-4.2.10). Metabolic characteristic did not show any changes within the cold temperature range and growth remained high. Various constraints including equipment availability and Covid-19 meant it was not possible to evaluate the metabolic composition further but there are several lines of further work that are possible.

7.2.1.1 Future work

- Complete targeted and untargeted metabolomic analysis in response to temperature should be carried out. Metabolomics has been used to further our understanding of diatom metabolism during different growth phases (Vidoudez & Pohnert, 2012) and in response to vitamin deprivation (Heal *et al.*, 2019). Recently, metabolomics has been used to investigate the effects of temperature and salinity on an Antarctic ice diatom *Nitzschia lecointei*. The study by Dawson *et al.*, (2020) showed that temperature (-1°C and 4°C) had a much larger effect on the metabolites compared to salinity (32PSU and 41PSU). Their work indicated that even the small temperature change studied influenced the metabolic characteristics despite growth rates remaining comparable between the two. This approach was originally intended for this study but was not possible due to time constraints and access to relevant equipment as a result of Covid-19. However, it would be interesting to elucidate the metabolic responses at these temperatures and between the two polar regions.
- Further thermal tolerance work on additional strains of each species from the two regions should be carried out. The results presented in Fig. 4.7 stress the importance of testing additional strains. The isolation of a *F. cylindrus* strain capable of growing at 12°C demonstrates that within Antarctica there are possible ecotypes of the species able to tolerate these elevated temperatures. In addition, the bioreactors used in this work are an ideal setup to take to the Arctic or Antarctica to experiment on natural communities or isolated strains that have not been exposed to artificial conditions. Recently *T. hyalina* has shown a high degree of intraspecific variation within the Arctic population, exhibiting variable responses to future temperature and

CO_2 concentrations (Wolf *et al.*, 2019). An interesting method established by Wolf *et al.*, (2019) was allele specific PCR, which was used to determine the abundance of individual genotypes within mixed cultures grown at different temperatures, to distinguish which genotype had a competitive advantage. The findings were used to predict likely outcomes in response to future climate change. Similar studies carried out in other species and different regions would be a good way of evaluating the population level response.

- "Long-term adaptation" or "artificial selection" experiments in the laboratory in response to temperature could be conducted. There have been a variety of artificial selection experiments in response to temperature conducted in algae (Schlüter *et al.*, 2014; Padfield *et al.*, 2016; Schaum *et al.*, 2017, 2018; O'Donnell *et al.*, 2018) but these have all been carried out using temperate algal strains, which have larger thermal niches. Tropical and polar species have narrower thermal niches due to the stability of their environments. An experiment on four tropical diatom species isolated from the Red Sea showed either increased thermal maxima or thermal optima in strains which had been grown at high temperatures of 30°C over time (Jin & Agustí, 2018). There has been only one of these types of studies reported for a polar strain. Benner *et al.*, (2020) showed that the polar green alga *Micromonas polaris* exhibited an increase in growth rate when selectively grown at elevated temperatures. Thermal performance curves obtained here indicated low optimal growth temperatures in polar diatoms, so it would be of considerable importance to determine if they possess the potential to rapidly adapt to warming environments, or whether they would suffer as a result of climate change.

7.2.2 Vitamin dependency in *F. cylindrus*

Vitamins are critical organic micronutrients required to some extent by all organisms on Earth. The difference in thermal tolerance between *F. cylindrus* isolates from the two poles described in Chapter four prompted the investigation of B_{12} dependency in *F. cylindrus*. The results of Chapter five show that three different Arctic *F. cylindrus* strains have an obligate requirement for vitamin B_{12} whereas the Antarctic strains do not. None of the strains tested required thiamine or biotin. Testing three strains from each region suggests that this B_{12}

dependency may be a characteristic trait of Arctic strains, although more sampling is needed to establish how widespread this is. Prior work had already revealed that the Antarctic strain CCAP 1023/1 is independent of vitamin B_{12} and possesses the *METE* gene (Helliwell *et al.*, 2011; Ellis *et al.*, 2017). Attempts to amplify the *METE* gene in Arctic strains failed, but the B_{12}-dependent *METH* could be amplified (Fig. 5.16). Although it is difficult to prove a negative, the lack of *METE* amplification suggests that the gene has changed compared to the reference strain and therefore could not be amplified by primers designed from the reference genome. The loss of *METE* and subsequent B_{12} dependency is thought to be a result of environmental selection. The analysis on habitat type described in chapter 5 Section 5.2.3 does suggest a link between the environments. Although, Helliwell, (2011) could not identify a link between environmental B_{12} concentrations and the occurrence of B_{12} dependency, they suggested that the role of biological interactions must be investigated. The Arctic has been found to have higher concentrations of cobalt which is a fundamental constituent of vitamin B_{12} (Bundy *et al.*, 2020), so this might favour B_{12}-producing bacteria. However, without direct measurements of B_{12} concentrations, any correlation between B_{12} and dependency in the Arctic is purely hypothetical. Below I propose several lines of work which would help to understand the B_{12} dependency in Arctic strains.

7.2.2.1 Future work

The direction of further work is based upon evaluation of Arctic and Antarctic strains at the molecular level. In Fig. 5.19 genetic divergence in the *rbc*L barcode was identified between the Arctic and Antarctic strains. Therefore, sequencing the genome of strains from both regions would enable a better evaluation as the comparison between Arctic and Antarctic strains would be based on much more sequence data than a single gene. It would help to distinguish if the strains from either region are in fact the same species.

REDACTION: Sentence describing unpublished results removed for copyright reasons. Copyright holder is Amanda Hopes.

Many bipolar species were first identified using morphological characteristics and this may have led to the misidentification of cryptic species e.g., *Limacina helicina* (Pteropod, Hunt *et al.*, 2010). Lundholm & Hasle, (2008) suggested that the 1023/1 strain of *F. cylindrus* is in fact *F. nana* based on morphological features and ITS2 sequencing, but this result has not been

explored further. What Lundholm & Hasle, (2008) did confirm however, is that strains identified as *F. cylindrus* were the same between polar regions.

If genome sequencing reveals that these two disjunct populations of *F. cylindrus* are the same species, then the following is proposed:

- Determine the genetic architecture of *METE*. Based on the results of Chapter five *METE* is non-functional in the Arctic strains and the reason for this could be confirmed by the genome sequence data. Absence of a complete *METE* would indicate that the functional gene was lost at some point in evolutionary history. It could potentially be truncated (i.e. a pseudogene), similar to what was found in *Volvox carteri* and *Gonium pectoral* (Helliwell *et al.*, 2011) or have a series of mutations like the transposable element which caused the B_{12} dependent phenotype in *C. reinhardtii* (Helliwell *et al.*, 2015). Or be lost altogether as in *T. pseudonana*. Understanding the architecture of *METE* would elucidate how recent B_{12} dependency occurred in Arctic *F. cylindrus*.
- Complementation of the Arctic strain with a complete *METE* gene. Genetic engineering tools have been developed in *F. cylindrus* (Hopes, 2017). Utilizing these tools to complement the Arctic *F. cylindrus* with a functional *METE* from the Antarctic strain would identify if the B_{12} independent phenotype could be restored. In addition, the opposite could be tested in Antarctic strains whereby *METE* can be knocked out or mutated to mimic the Arctic strain.
- Role of B_{12} dependency on thermal tolerance. One element which could be investigated from these genetic manipulations is whether a B_{12} dependent life strategy enables a better resilience to elevated temperatures. In *C. reinhardtii* the presence of B_{12} enabled the survival at elevated temperatures compared with when B_{12} was absent (Xie *et al.*, 2013). Therefore, temperature stress may in fact be a selective pressure leading to B_{12} dependency in algae.
- Compare the competitive advantage between strains. Culturing B_{12} dependent and independent strains together can deduce whether there is a competitive advantage. Allele-specific PCR (Wolf *et al.*, 2019) could be a useful method in determining the abundance of each strain. Alternatively, they could be transformed with different fluorescent proteins and quantified by fluorescence-activated cell sorting (FACS).

- Carry out artificial selection experiments to B_{12} concentrations. If B_{12} dependency is a result of environmental selection, then laboratory conditions can be used to create a selection pressure (Helliwell *et al.*, 2015). It is interesting as to why the Antarctic strain (1023/1) has not become B_{12} dependent in long-term culture in the presence of B_{12} supplemented media. Considering the number of B_{12} dependent diatoms species in the marine environment, it might be worthwhile carrying out an artificial selection experiment in high B_{12} concentrations as did Helliwell *et al.*, (2015). Understanding the mechanism by which B_{12} dependency is established in diatoms will be an important addition to understanding the evolution of B_{12} auxotrophy. However, this will be more challenging because the diatom genome is diploid, requiring both alleles to be mutated to express the recessive trait.
- Co-cultures of B_{12} dependent strains with B_{12} producing bacteria. The biological interaction between algae and bacteria has been identified as a key mutualism for the acquisition of vitamins (Croft *et al.*, 2005). *F. cylindrus* is an ice diatom and there is likely to be a high degree of mutualism within this environment. Mutualistic co-cultures of the Arctic strains and a B_{12} producing bacteria that have already been shown to support growth of B_{12}-dependent algae, such as *Dinoroseobacter shibae* (Cooper et al 2018) or *Halomonas* (Croft et al 2005), would establish if growth can be supported.
- Measurements of environmental B_{12} concentrations in the Arctic Ocean. Understanding the natural concentrations will help to understand the selection pressure in this region.

7.2.3 Future work on bipolar species

- Molecular tools such as genomic sequencing or multiple genetic markers will help to identify whether both diatom species used in this thesis are truly bipolar or rather represent similar cryptic species.
- Establish whether there is genetic exchange between the Arctic and Antarctic populations. Rates of evolution in genetic markers has been used previously in foraminifera (Darling *et al.*, 2000) to establish their last genetic exchange.

- Establish mating compatibility between bipolar populations through mating compatibility assays.

7.4 Polar diatoms in biotechnology

Polar species are seen as a potentially attractive source of metabolic products and for growth at cold temperatures. Efforts to reduce carbon emissions in industry, and society as whole, to become more environmentally friendly makes algal biotechnology an attractive prospect for industry exploitation. In Chapter six the growth of polar diatom strains was evaluated during British winter conditions. The results highlight that even though *P. tricornutum* may exhibit reduced growth in the UK winter it is still able to grow better than polar strains. Nonetheless, polar strains still produced high biomass.

Although the optimisation of growth would have enabled a better analysis of polar diatom potential, it can be argued that strain selection is more important in the first instance. Strain selection is a very difficult process within algal biotechnology. There is an element of bioprospecting to identify strains of interest which can then be assessed for growth and biomass production. Polar diatoms have been earmarked as potential producers of pigments such as fucoxanthin and lipids such as EPA, but the identification of these strains can be long winded. The role of culture collections in the identification of attractive strains is one possibility to maximising our knowledge of strain potential. Lang *et al.*, (2011) carried out an assessment of fatty acid profiles of >2000 strains deposited in the algal collection at the University of Göttingen (SAG), providing a resource for research to scope potential strains. Assessments of culture collections would be highly beneficial and save time and work in identifying potential strains and this method should be utilized further. The other option is to identify strains which grow well in laboratory conditions and then analyse these for metabolic products. The culturing of strains isolated in Chapter three has identified six strains that grow rapidly and form dense cultures at the maintenance temperature. The strains which are stated in Chapter six would be ideal candidates to explore further biotechnological properties.

7.4.1 Future work

- Perform growth and biochemical analysis of polar strains to identify strains of interest.
- Optimise the growth of interesting strains in the laboratory at small volumes (100-1000 ml) for both biomass production and metabolic properties.
- Investigate the potential of stressful, non-optimal conditions e.g., high light or low salinity on the metabolic composition of strains.
- Evaluate the growth of potential strains under optimal conditions established in previous experiments and to simulate or utilize natural conditions of the northern hemisphere at larger volumes (10-250 L).

References

Abelmann A. **1992**. Diatom assemblages in Arctic sea ice—indicator for ice drift pathways. *Deep Sea Research Part A. Oceanographic Research Papers* **39**: S525–S538.

Ajani PA, Petrou K, Larsson ME, Nielsen DA, Burke J, Murray SA. **2021**. Phenotypic trait variability as an indication of adaptive capacity in a cosmopolitan marine diatom. *Environmental Microbiology* **23**: 207–223.

REDACTION: Sentence describing citation to unpublished results removed for copyright reasons. Copyright holder is Catalina Albury.

Altschul SF, Gish W, Miller W, Myers EW, Lipman DJ. **1990**. Basic local alignment search tool. *Journal of Molecular Biology* **215**: 403–410.

Alvain S, Moulin C, Dandonneau Y, Loisel H. **2008**. Seasonal distribution and succession of dominant phytoplankton groups in the global ocean: a satellite view. *Global Biogeochemical Cycles* **22**: GB3001.

AMAP. **2021**. Summary for Policy-makers. In: Arctic Climate Change Update 2021: Key Trends and Impacts. Tromsø, Norway.

Archibald JM. **2009**. The puzzle of plastid evolution. *Current Biology : CB* **19**: R81–R88.

Ardyna M, Babin M, Gosselin M, Devred E, Rainville L, Tremblay J-É. **2014**. Recent Arctic Ocean sea ice loss triggers novel fall phytoplankton blooms. *Geophysical Research Letters* **41**: 6207–6212.

Armbrust EV. **2009**. The life of diatoms in the World's oceans. *Nature* **459**: 185.

Arrigo KR, van Dijken GL. **2015**. Continued increases in Arctic Ocean primary production. *Synthesis of Arctic Research (SOAR)* **136**: 60–70.

Baars JWM. **1981**. Autecological investigations on marine diatoms. 2. Generation times of 50 species. *Hydrobiological Bulletin* **15**: 137–151.

Baliga R, Powers SE. **2010**. Sustainable Algae Biodiesel Production in Cold Climates. *International Journal of Chemical Engineering* **2010**: 13.

Ban S, Burns C, Castel J, Chaudron Y, Christou E, Escribano R, Umani SF, Gasparini S, Ruiz FG, Hoffmeyer M, *et al.* 1997. The paradox of diatom-copepod interactions. *Marine Ecology Progress Series* **157**: 287–293.

Barrett P. **1996**. Antarctic Palaeoenvironment through Cenozoic Times - A Review. *Terra Antarctica* **3**: 103–119.

Barros MP, Pedersen M, Colepicolo P, Snoeijs P. **2003**. Self-shading protects phytoplankton communities against H2O2-induced oxidative damage. *Aquatic Microbial Ecology* **30**: 275–282.

Bayer-Giraldi M, Uhlig C, John U, Mock T, Valentin K. **2010**. Antifreeze proteins in polar sea ice diatoms: diversity and gene expression in the genus *Fragilariopsis*. *Environmental Microbiology* **12**: 1041–1052.

Becking LGMB. **1934**. *Geobiologie of inleiding tot de milieukunde*. WP Van Stockum & Zoon.

Behrens P. **2005**. Photobioreactors and fermentors: the light and dark sides of growing algae (R Anderson, Ed.). *Algal Culturing Techniques*: 193–194.

Benner I, Irwin AJ, Finkel ZV. **2020**. Capacity of the common Arctic picoeukaryote *Micromonas* to adapt to a warming ocean. *Limnology and Oceanography Letters* **5**: 221–227.

Bertrand EM, Allen A. **2012**. Influence of vitamin B auxotrophy on nitrogen metabolism in eukaryotic phytoplankton. *Frontiers in Microbiology* **3**: 375.

Bertrand EM, Allen AE, Dupont CL, Norden-Krichmar TM, Bai J, Valas RE, Saito MA. **2012**. Influence of cobalamin scarcity on diatom molecular physiology and identification of a cobalamin acquisition protein. *Proceedings of the National Academy of Sciences* **109**: E1762–E1771.

Bertrand EM, McCrow JP, Moustafa A, Zheng H, McQuaid JB, Delmont TO, Post AF, Sipler RE, Spackeen JL, Xu K, *et al.* 2015. Phytoplankton–bacterial interactions mediate micronutrient colimitation at the coastal Antarctic sea ice edge. *Proceedings of the National Academy of Sciences* **112**: 9938–9943.

Bertrand EM, Moran DM, McIlvin MR, Hoffman JM, Allen AE, Saito MA. **2013**. Methionine synthase interreplacement in diatom cultures and communities: Implications for the persistence of B_{12} use by eukaryotic phytoplankton. *Limnology and Oceanography* **58**: 1431–1450.

Bertrand EM, Saito MA, Jeon YJ, Neilan BA. **2011**. Vitamin B_{12} biosynthesis gene diversity in the Ross Sea: the identification of a new group of putative polar B_{12} biosynthesizers. *Environmental Microbiology* **13**: 1285–1298.

Bertrand EM, Saito MA, Rose JM, Riesselman CR, Lohan MC, Noble AE, Lee PA, DiTullio GR. **2007**. Vitamin B_{12} and iron colimitation of phytoplankton growth in the Ross Sea. *Limnology and Oceanography* **52**: 1079–1093.

Beszczynska-Möller A, Fahrbach E, Schauer U, Hansen E. **2012**. Variability in Atlantic water temperature and transport at the entrance to the Arctic Ocean, 1997–2010. *ICES Journal of Marine Science* **69**: 852–863.

Biersma EM, Jackson JA, Hyvönen J, Koskinen S, Linse K, Griffiths H, Convey P. **2017**. Global biogeographic patterns in bipolar moss species. *Royal Society Open Science* **4**: 170147.

Blakey RC. **2008**. Gondwana paleogeography from assembly to breakup—A 500 my odyssey. *Geological Society of America Special Papers* **441**: 1–28.

Bligh EG, Dyer WJ. **1959**. A rapid method of total lipid extraction and purification. *Canadian Journal of Biochemistry and Physiology* **37**: 911–917.

Boelen P, van Dijk R, Sinninghe Damsté JS, Rijpstra WIC, Buma AG. **2013**. On the potential application of polar and temperate marine microalgae for EPA and DHA production. *AMB Express* **3**: 26.

Bonnet S, Tovar-Sanchez A, Panzeca C, Ortega-retuerta E, Duarte C, Sanudo-Wilhelmy S. **2013**. Geographical gradients of dissolved Vitamin B_{12} in the Mediterranean Sea. *Frontiers in Microbiology* **4**: 126.

Bopp L, Aumont O, Cadule P, Alvain S, Gehlen M. **2005**. Response of diatoms distribution to global warming and potential implications: A global model study. *Geophysical Research Letters* **32**: L19606.

Bowler C, Vardi A, Allen AE. **2010**. Oceanographic and Biogeochemical Insights from Diatom Genomes. *Annual Review of Marine Science* **2**: 333–365.

Bown J, Boye M, Baker A, Duvieilbourg E, Lacan F, Le Moigne F, Planchon F, Speich S, Nelson DM. **2011**. The biogeochemical cycle of dissolved cobalt in the Atlantic and the Southern Ocean south off the coast of South Africa. *Marine Chemistry* **126**: 193–206.

Boyd PW, Rynearson TA, Armstrong EA, Fu F, Hayashi K, Hu Z, Hutchins DA, Kudela RM, Litchman E, Mulholland MR, *et al.* 2013. Marine phytoplankton temperature versus growth responses from polar to tropical waters – outcome of a scientific community-wide study (H Browman, Ed.). *PLoS ONE* **8**: e63091.

Bozarth A, Maier U-G, Zauner S. **2009**. Diatoms in biotechnology: modern tools and applications. *Applied Microbiology and Biotechnology* **82**: 195–201.

Brett M, Müller-Navarra D. **1997**. The role of highly unsaturated fatty acids in aquatic foodweb processes. *Freshwater Biology* **38**: 483–499.

Brinkmeyer R, Knittel K, Jürgens J, Weyland H, Amann R, Helmke E. **2003**. Diversity and structure of bacterial communities in arctic versus Antarctic pack ice. *Applied and Environmental Microbiology* **69**: 6610–6619.

Brody JR, Kern SE. **2004**. Sodium boric acid: a Tris-free, cooler conductive medium for DNA electrophoresis. *BioTechniques* **36**: 214–216.

Budge SM, Wooller MJ, Springer AM, Iverson SJ, McRoy CP, Divoky GJ. **2008**. Tracing carbon flow in an arctic marine food web using fatty acid-stable isotope analysis. *Oecologia* **157**: 117–29.

Bundy RM, Tagliabue A, Hawco NJ, Morton PL, Twining BS, Hatta M, Noble AE, Cape MR, John SG, Cullen JT, *et al.* 2020. Elevated sources of cobalt in the Arctic Ocean. *Biogeosciences* **17**: 4745–4767.

Cao S, Zhang W, Ding W, Wang M, Fan S, Yang B, Mcminn A, Wang M, Xie B, Qin Q-L, *et al.* 2020. Structure and function of the Arctic and Antarctic marine microbiota as revealed by metagenomics. *Microbiome* **8**: 47.

Carlson CA, Ducklow HW, Hansell DA, Smith WO. **1998**. Organic carbon partitioning during spring phytoplankton blooms in the Ross Sea polynya and the Sargasso Sea. *Limnology and Oceanography* **43**: 375–386.

Caron DA, Dennett MR, Lonsdale DJ, Moran DM, Shalapyonok L. **2000**. Microzooplankton herbivory in the Ross Sea, Antarctica. *Deep Sea Research Part II: Topical Studies in Oceanography* **47**: 3249–3272.

Carvalho KS, Wang S. **2020**. Sea surface temperature variability in the Arctic Ocean and its marginal seas in a changing climate: Patterns and mechanisms. *Global and Planetary Change* **193**: 103265.

Casteleyn G, Leliaert F, Backeljau T, Debeer A-E, Kotaki Y, Rhodes L, Lundholm N, Sabbe K, Vyverman W. **2010**. Limits to gene flow in a cosmopolitan marine planktonic diatom. *Proceedings of the National Academy of Sciences* **107**: 12952–12957.

Cermeno P, Falkowski PG. **2009**. Controls on diatom biogeography in the ocean. *Science* **325**: 1539–1541.

Cermeño P, Falkowski PG, Romero OE, Schaller MF, Vallina SM. **2015**. Continental erosion and the Cenozoic rise of marine diatoms. *Proceedings of the National Academy of Sciences* **112**: 4239–4244.

Chen CY, Durbin EG. **1994**. Effects of pH on the growth and carbon uptake of marine phytoplankton. *Marine Ecology Progress Series* **109**: 83–94.

Cheregi O, Ekendahl S, Engelbrektsson J, Strömberg N, Godhe A, Spetea C. **2019**. Microalgae biotechnology in Nordic countries – the potential of local strains. *Physiologia Plantarum* **166**: 438–450.

Chintalapati S, Kiran MD, Shivaji S. **2004**. Role of membrane lipid fatty acids in cold adaptation. *Cellular and Molecular Biology* **50**: 631–642.

Church MJ, Hutchins DA, Ducklow HW. **2000**. Limitation of bacterial growth by dissolved organic matter and iron in the Southern Ocean. *Applied and Environmental Microbiology* **66**: 455–466.

Clark DL. **1990**. Arctic Ocean ice cover; Geologic history and climatic significance. In: Grantz A, Johnson L, Sweeney JF, eds. The Arctic Ocean Region. Geological Society of America.

Clarke A, Crame A. **1992**. The Southern Ocean benthic fauna and climate change: a historical perspective. *Philosophical Transactions of the Royal Society of London. Series B: Biological Sciences* **338**: 299–309.

Clarke A, Gaston KJ. **2006**. Climate, energy and diversity. *Proceedings of the Royal Society B: Biological Sciences* **273**: 2257–2266.

Clarke A, Meredith MP, Wallace MI, Brandon MA, Thomas DN. **2008**. Seasonal and interannual variability in temperature, chlorophyll and macronutrients in northern Marguerite Bay, Antarctica. *Deep Sea Research Part II: Topical Studies in Oceanography* **55**: 1988–2006.

Cleary A, Durbin E, Casas M. **2018**. Feeding by Antarctic krill *Euphausia superba* in the West Antarctic Peninsula: differences between fjords and open waters. *Marine Ecology Progress Series* **595**: 39–54.

Coello-Camba A, Agustí S. **2017**. Thermal thresholds of phytoplankton growth in polar waters and their consequences for a warming polar ocean. *Frontiers in Marine Science* **4**: 168.

Coello-Camba A, Agustí S, Vaqué D, Holding J, Arrieta JM, Wassmann P, Duarte CM. **2015**. Experimental assessment of temperature thresholds for Arctic phytoplankton communities. *Estuaries and Coasts* **38**: 873–885.

Comiso JC, Hall DK. **2014**. Climate trends in the Arctic as observed from space. *WIREs Climate Change* **5**: 389–409.

Comiso JC, Parkinson CL, Gersten R, Stock L. **2008**. Accelerated decline in the Arctic sea ice cover. *Geophysical Research Letters* **35**.

Cook AJ, Holland PR, Meredith MP, Murray T, Luckman A, Vaughan DG. **2016**. Ocean forcing of glacier retreat in the western Antarctic Peninsula. *Science* **353**: 283–286.

Couteau P. **1996**. Micro-algae. In: Lavens P, Sorgeloos P, eds. Manual on the production and use of live food for aquaculture. Rome: Food and Agriculture Organization (FAO)., 7–49.

Cowey CB. **1956**. A preliminary investigation of the variation of vitamin B_{12} in oceanic and coastal waters. *Journal of the Marine Biological Association of the United Kingdom* **35**: 609–620.

Cox F, Newsham KK, Bol R, Dungait JAJ, Robinson CH. **2016**. Not poles apart: Antarctic soil fungal communities show similarities to those of the distant Arctic (B Casper, Ed.). *Ecology Letters* **19**: 528–536.

Crame JA. **1993**. Bipolar Molluscs and Their Evolutionary Implications. *Journal of Biogeography* **20**: 145.

Crockett EL. **2008**. The cold but not hard fats in ectotherms: consequences of lipid restructuring on susceptibility of biological membranes to peroxidation, a review. *Journal of Comparative Physiology B* **178**: 795–809.

Croft MT, Lawrence AD, Raux-Deery E, Warren MJ, Smith AG. **2005**. Algae acquire vitamin B_{12} through a symbiotic relationship with bacteria. *Nature* **438**: 90–93.

Cui L, Butler HJ, Martin-Hirsch PL, Martin FL. **2016**. Aluminium foil as a potential substrate for ATR-FTIR, transflection FTIR or Raman spectrochemical analysis of biological specimens. *Analytical Methods* **8**: 481–487.

D'Alelio D, Amato A, Kooistra WHCF, Procaccini G, Casotti R, Montresor M. **2009**. Internal transcribed spacer polymorphism in *Pseudo-nitzschia multistriata* (Bacillariophyceae) in the gulf of naples: recent divergence or intraspecific hybridization? *Protist* **160**: 9–20.

Darling KF, Wade CM, Stewart IA, Kroon D, Dingle R, Brown AJL. **2000**. Molecular evidence for genetic mixing of Arctic and Antarctic subpolar populations of planktonic foraminifers. *Nature* **405**: 43–47.

von Dassow P, Petersen TW, Chepurnov VA, Virginia Armbrust E. **2008**. Inter- and intraspecific relationships between nucleur DNA content and cell size in selected members of the centric diatom genus *Thalassiosira* (Bacillariophyceae). *Journal of Phycology* **44**: 335–349.

Davey MP, Horst I, Duong G-H, Tomsett EV, Litvinenko ACP, Howe CJ, Smith AG. **2014**. Triacylglyceride production and autophagous responses in *Chlamydomonas reinhardtii* depend on resource allocation and carbon source. *Eukaryotic Cell* **13**: 392–400.

Davey MP, Norman L, Sterk P, Huete-Ortega M, Bunbury F, Loh BKW, Stockton S, Peck LS, Convey P, Newsham KK, *et al.* 2019. Snow algae communities in Antarctica: metabolic and taxonomic composition. *New Phytologist* **222**: 1242–1255.

Dawson HM, Heal KR, Boysen AK, Carlson LT, Ingalls AE, Young JN. **2020**. Potential of temperature- and salinity-driven shifts in diatom compatible solute concentrations to impact biogeochemical cycling within sea ice (D Helmig and K Arrigo, Eds.). *Elementa: Science of the Anthropocene* **8**.

Deschamps P, Moreira D. **2009**. Signal conflicts in the phylogeny of the primary photosynthetic eukaryotes. *Molecular Biology and Evolution* **26**: 2745–2753.

DeVries AL, Steffensen JF. **2005**. The Arctic and Antarctic polar marine environments. In: Fish Physiology. Elsevier, 1–24.

Di Giuseppe G, Dini F, Vallesi A, Luporini P. **2015**. Genetic relationships in bipolar species of the protist ciliate, Euplotes. *Hydrobiologia* **761**: 71–83.

Dorrell RG, Gile G, McCallum G, Méheust R, Bapteste EP, Klinger CM, Brillet-Guéguen L, Freeman KD, Richter DJ, Bowler C. **2017**. Chimeric origins of ochrophytes and haptophytes revealed through an ancient plastid proteome. *eLife* **6**: e23717.

Dorrell RG, Smith AG. **2011**. Do red and green make brown?: perspectives on plastid acquisitions within Chromalveolates. *Eukaryotic Cell* **10**: 856–868.

Douzery EJP, Snell EA, Bapteste E, Delsuc F, Philippe H. **2004**. The timing of eukaryotic evolution: Does a relaxed molecular clock reconcile proteins and fossils? *Proceedings of the National Academy of Sciences* **101**: 15386–15391.

Doxey AC, Kurtz DA, Lynch MD, Sauder LA, Neufeld JD. **2015**. Aquatic metagenomes implicate Thaumarchaeota in global cobalamin production. *The ISME Journal* **9**: 461–471.

Ducklow HW. **2000**. Bacterial production and biomass in the oceans. In: Kirchman D, ed. Microbial Ecology of the Oceans. New York: Wiley, 85–120.

Ducklow H, Carlson C, Church M, Kirchman D, Smith D, Steward G. **2001**. The seasonal development of the bacterioplankton bloom in the Ross Sea, Antarctica, 1994–1997. *Deep Sea Research Part II: Topical Studies in Oceanography* **48**: 4199–4221.

Dunn R, Manoylov K. **2016**. The effects of initial cell density on the growth and proliferation of the potentially toxic cyanobacterium *Microcystis aeruginosa*. *Journal of Environmental Protection* **7**: 1210–1220.

Dunstan GA, Volkman JK, Barrett SM, Leroi J-M, Jeffrey SW. **1993**. Essential polyunsaturated fatty acids from 14 species of diatom (Bacillariophyceae). *Phytochemistry* **35**: 155–161.

Dunton K. **1992**. Arctic biogeography: The paradox of the marine benthic fauna and flora. *Trends in Ecology & Evolution* **7**: 183–189.

Edelmann M, Aalto S, Chamlagain B, Kariluoto S, Piironen V. **2019**. Riboflavin, niacin, folate and vitamin B_{12} in commercial microalgae powders. *Journal of Food Composition and Analysis* **82**: 103226.

Edgar RC. **2004**. MUSCLE: multiple sequence alignment with high accuracy and high throughput. *Nucleic Acids Research* **32**: 1792–1797.

Ellis KA, Cohen NR, Moreno C, Marchetti A. **2017**. Cobalamin-independent methionine synthase distribution and influence on vitamin B_{12} growth requirements in marine diatoms. *Protist* **168**: 32–47.

Eppley RW. **1972**. Temperature and phytoplankton growth in the sea. *Fish. bull* **70**: 1063–1085.

Falkowski PG. **1998**. Biogeochemical Controls and Feedbacks on Ocean Primary Production. *Science* **281**: 200–206.

Fan T, Deser C, Schneider DP. **2014**. Recent Antarctic sea ice trends in the context of Southern Ocean surface climate variations since 1950. *Geophysical Research Letters* **41**: 2419–2426.

Fiala M, Oriol L. **1990**. Light-temperature interactions on the growth of Antarctic diatoms. *Polar Biology* **10**: 629–636.

Field CB, Behrenfeld MJ, Randerson JT, Falkowski P. **1998**. Primary production of the biosphere: Integrating terrestrial and oceanic components. *Science* **281**: 237–240.

Fry B, Wainright S. **1991**. Diatom sources of 13C-rich carbon in marine food webs. *Marine Ecology Progress Series* **76**: 149–157.

Fryxell GA, Doucette GJ, Hubbard GF. **1981**. The genus Thalassiosira: The bipolar diatom <i>T. antarctica<i> comber: **24**: 321–336.

Fu W, Wichuk K, Brynjólfsson S. **2015**. Developing diatoms for value-added products: challenges and opportunities. *European Congress of Biotechnology - ECB 16* **32**: 547–551.

Gachon CMM, Day JG, Campbell CN, Pröschold T, Saxon RJ, Küpper FC. **2007**. The Culture Collection of Algae and Protozoa (CCAP): A biological resource for protistan genomics. *Gene* **406**: 51–57.

Garrison DL. **1991**. Antarctic sea ice biota. *American Zoologist* **31**: 17–34.

Gérikas Ribeiro C, dos Santos AL, Gourvil P, Le Gall F, Marie D, Tragin M, Probert I, Vaulot D. **2020**. Culturable diversity of Arctic phytoplankton during pack ice melting (JW Deming and C Michel, Eds.). *Elementa: Science of the Anthropocene* **8**.

Ghiglione J-F, Galand PE, Pommier T, Pedros-Alio C, Maas EW, Bakker K, Bertilson S, Kirchman DL, Lovejoy C, Yager PL, *et al.* 2012. Pole-to-pole biogeography of surface and deep marine bacterial communities. *Proceedings of the National Academy of Sciences* **109**: 17633–17638.

Girotti AW. **1990**. Photodynamic lipid peroxidation in biological systems. *Photochemistry and Photobiology* **51**: 497–509.

Godhe A, Rynearson T. **2017**. The role of intraspecific variation in the ecological and evolutionary success of diatoms in changing environments. *Philosophical Transactions of the Royal Society B: Biological Sciences* **372**: 20160399.

Gonzalez JC, Banerjee RV, Huang S, Sumner JS, Matthews RG. **1992**. Comparison of cobalamin-independent and cobalamin-dependent methionine synthases from *Escherichia coli*: two solutions to the same chemical problem. *Biochemistry* **31**: 6045–6056.

Gosselin M, Levasseur M, Wheeler PA, Horner RA, Booth BC. **1997**. New measurements of phytoplankton and ice algal production in the Arctic Ocean. *Deep-Sea Research* **44**: 1623–1644.

Gould SB, Waller RF, McFadden GI. **2008**. Plastid evolution. *Annual Review of Plant Biology* **59**: 491–517.

Griffiths MJ, Harrison STL. **2009**. Lipid productivity as a key characteristic for choosing algal species for biodiesel production. *Journal of Applied Phycology* **21**: 493–507.

Grobbelaar JU. **2010**. Microalgal biomass production: challenges and realities. *Photosynthesis Research* **106**: 135–144.

Guillard RR, Ryther JH. **1962**. Studies of marine planktonic diatoms. I. *Cyclotella nana* Hustedt, and *Detonula confervacea* (cleve) Gran. *Canadian Journal of Microbiology* **8**: 229–239.

Guiry MD. **2012**. How many species of algae are there? *Journal of Phycology* **48**: 1057–1063.

Gupta PL, Lee SM, Choi HJ. **2015**. A mini review: photobioreactors for large scale algal cultivation. *World Journal of Microbiology & Biotechnology* **31**: 1409–1417.

Gwak IG, sic Jung W, Kim HJ, Kang S-H, Jin E. **2010**. Antifreeze protein in Antarctic marine diatom, *Chaetoceros neogracile*. *Marine Biotechnology* **12**: 630–639.

Hamilton ML, Warwick J, Terry A, Allen MJ, Napier JA, Sayanova O. **2015**. Towards the industrial production of omega-3 long chain polyunsaturated fatty acids from a genetically modified diatom *Phaeodactylum tricornutum*. *PloS one* **10**: e0144054.

Hamsher SE, Evans KM, Mann DG, Poulíčková A, Saunders GW. **2011**. Barcoding diatoms: exploring alternatives to COI-5P. *Protist* **162**: 405–422.

Hasle G. **1976**. The biogeography of some marine planktonic diatoms. *Deep Sea Research and Oceanographic Abstracts* **23**: 319-IN6.

Hasle GR, Medlin LK, Syvertsen EE. **1994**. *Synedropsis* gen. nov., a genus of araphid diatoms associated with sea ice. *Phycologia* **33**: 248–270.

Hasle GR, Syvertsen EE. **1996**. Chapter 2 - Marine diatoms. In: Tomas CR, ed. Identifying marine diatoms and dinoflagellates. San Diego: Academic Press, 5–385.

Havermans C, Sonet G, d'Udekem d'Acoz C, Nagy ZT, Martin P, Brix S, Riehl T, Agrawal S, Held C. **2013**. Genetic and morphological divergences in the cosmopolitan deep-sea amphipod *Eurythenes gryllus* reveal a diverse abyss and a bipolar species (D Fontaneto, Ed.). *PLoS ONE* **8**: e74218.

He L, Mazza Rodrigues JL, Soudzilovskaia NA, Barceló M, Olsson PA, Song C, Tedersoo L, Yuan F, Yuan F, Lipson DA, *et al.* 2020. Global biogeography of fungal and bacterial biomass carbon in topsoil. *Soil Biology and Biochemistry* **151**: 108024.

Heal KR, Kellogg NA, Carlson LT, Lionheart RM, Ingalls AE. **2019**. Metabolic consequences of cobalamin scarcity in the diatom *Thalassiosira pseudonana* as revealed through metabolomics. *Protist* **170**: 328–348.

Heal KR, Qin W, Ribalet F, Bertagnolli AD, Coyote-Maestas W, Hmelo LR, Moffett JW, Devol AH, Armbrust EV, Stahl DA, *et al.* 2017. Two distinct pools of B_{12} analogs reveal community interdependencies in the ocean. *Proceedings of the National Academy of Sciences* **114**: 364–369.

Hegseth EN. **1989**. Photoadaptation in marine Arctic diatoms. *Polar Biology* **9**: 479–486.

Helliwell KE. **2011**. Insights into the evolution of vitamin B_{12} auxotrophy from sequenced algal genomes.

Helliwell KE, Collins S, Kazamia E, Purton S, Wheeler GL, Smith AG. **2015**. Fundamental shift in vitamin B_{12} eco-physiology of a model alga demonstrated by experimental evolution. *The ISME Journal* **9**: 1446–1455.

Helliwell KE, Wheeler GL, Leptos KC, Goldstein RE, Smith AG. **2011**. Insights into the evolution of vitamin B_{12} auxotrophy from sequenced algal genomes. *Molecular Biology and Evolution* **28**: 2921–2933.

Hemaiswarya S, Raja R, Ravi Kumar R, Ganesan V, Anbazhagan C. **2011**. Microalgae: a sustainable feed source for aquaculture. *World Journal of Microbiology and Biotechnology* **27**: 1737–1746.

Hernando M, Schloss IR, Almandoz GO, Malanga G, Varela DE, De Troch M. **2018**. Combined effects of temperature and salinity on fatty acid content and lipid damage in Antarctic phytoplankton. *Journal of Experimental Marine Biology and Ecology* **503**: 120–128.

Hildebrand M, Davis AK, Smith SR, Traller JC, Abbriano R. **2012**. The place of diatoms in the biofuels industry. *Biofuels* **3**: 221–240.

Hixson SM, Arts MT. **2016**. Climate warming is predicted to reduce omega-3, long-chain, polyunsaturated fatty acid production in phytoplankton. *Global Change Biology* **22**: 2744–2755.

Hoegh-Guldberg O, Bruno JF. **2010**. The impact of climate change on the World's marine ecosystems. *Science* **328**: 1523–1528.

Hopes A. **2017**. Expanding the molecular toolbox in diatoms: developing a transformation system, CRISPR-Cas and Inverse Yeast-1-hybrid.

Horst I, Parker BM, Dennis JS, Howe CJ, Scott SA, Smith AG. **2012**. Treatment of *Phaeodactylum tricornutum* cells with papain facilitates lipid extraction. *Journal of Biotechnology* **162**: 40–49.

Hulatt CJ, Berecz O, Egeland ES, Wijffels RH, Kiron V. **2017**. Polar snow algae as a valuable source of lipids? *Bioresource Technology* **241**: 1208–1208.

Hunt B, Strugnell J, Bednarsek N, Linse K, Nelson RJ, Pakhomov E, Seibel B, Steinke D, Würzberg L. **2010**. Poles apart: the "bipolar" Pteropod species *Limacina helicina* is genetically distinct between the Arctic and Antarctic Oceans (Z Finkel, Ed.). *PLoS ONE* **5**: e9835.

Huseby S, Degerlund M, Eriksen G, Ingebrigtsen R, Eilertsen H, Hansen E. **2013**. Chemical diversity as a function of temperature in six northern diatom species. *Marine Drugs* **11**: 4232–4245.

Huseby S, Degerlund M, Zingone A, Hansen E. **2012**. Metabolic fingerprinting reveals differences between northern and southern strains of the cryptic diatom *Chaetoceros socialis*. *European Journal of Phycology* **47**: 480–489.

Ingebrigtsen RA, Hansen E, Andersen JH, Eilertsen HC. **2016**. Light and temperature effects on bioactivity in diatoms. *Journal of Applied Phycology* **28**: 939–950.

Ingebrigtsen RA, Hansen E, Andersen JH, Eilertsen HC. **2017**. Field sampling marine plankton for biodiscovery. *Scientific Reports* **7**: 15863.

IPCC. **2021**. Summary for Policymakers. In: Masson-Delmotte V, Zhai P, Pirani A, Connors S, Péan C, Berger S, Caud N, Chen Y, Goldfarb L, Gomis M, et al., eds. Cambridge University Press.

d'Ippolito G, Sardo A, Paris D, Vella FM, Adelfi MG, Botte P, Gallo C, Fontana A. **2015**. Potential of lipid metabolism in marine diatoms for biofuel production. *Biotechnology for Biofuels* **8**: 28.

Iturbide M, Fernández, Jesús, Gutiérrez, José Manuel, Bedia, Joaquín, Cimadevilla, Ezequiel, Díez-Sierra, Javier, Manzanas, Rodrigo, Casanueva, Ana, Baño-Medina, Jorge, Milovac, Josipa, *et al.* 2021. *Repository supporting the implementation of FAIR principles in the IPCC-WGI Atlas*. Zenodo.

Jabre L, Bertrand EM. **2020**. Interactive effects of iron and temperature on the growth of <i>Fragilariopsis cylindrus<i>. *Limnology and Oceanography Letters* **5**: 363–370.

Janech MG, Krell A, Mock T, Kang J-S, Raymond JA. **2006**. Ice-binding proteins from sea ice diatoms (Bacillariophyceae). *Journal of Phycology* **42**: 410–416.

Jeffrey SW, Humphrey GF. **1975**. New spectrophotometric equations for determining chlorophylls a, b, c1 and c2 in higher plants, algae and natural phytoplankton. *Biochemie und Physiologie der Pflanzen* **167**: 191–194.

Jin P, Agustí S. **2018**. Fast adaptation of tropical diatoms to increased warming with trade-offs. *Scientific Reports* **8**: 17771.

Jin X, Gruber N, Dunne JP, Sarmiento JL, Armstrong RA. **2006**. Diagnosing the contribution of phytoplankton functional groups to the production and export of particulate organic carbon, $CaCO_3$, and opal from global nutrient and alkalinity distributions: diagnosing phytoplankton functional groups. *Global Biogeochemical Cycles* **20**: n/a-n/a.

Jones EP, Anderson LG, Swift JH. **1998**. Distribution of Atlantic and Pacific waters in the upper Arctic Ocean: Implications for circulation. *Geophysical Research Letters* **25**: 765–768.

Jordan RW, Ligowski L, Nöthig E-M, Priddle J. **1991**. The diatom genus *Proboscia* in Antarctic waters. *Diatom Research* **6**: 63–78.

Kahru M, Brotas V, Manzano-Sarabia M, Mitchell BG. **2011**. Are phytoplankton blooms occurring earlier in the Arctic? *Global Change Biology* **17**: 1733–1739.

Kahru M, Lee Z, Mitchell BG, Nevison CD. **2016**. Effects of sea ice cover on satellite-detected primary production in the Arctic Ocean. *Biology Letters* **12**: 20160223.

Karsenti E, Acinas SG, Bork P, Bowler C, De Vargas C, Raes J, Sullivan M, Arendt D, Benzoni F, Claverie J-M, *et al.* 2011. A holistic approach to marine eco-systems biology. *PLoS Biology* **9**: e1001177.

Karsten U, Schumann R, Rothe S, Jung I, Medlin L. **2006**. Temperature and light requirements for growth of two diatom species (Bacillariophyceae) isolated from an Arctic macroalga. *Polar Biology* **29**: 476–486.

Katoh K, Rozewicki J, Yamada KD. **2019**. MAFFT online service: multiple sequence alignment, interactive sequence choice and visualization. *Briefings in Bioinformatics* **20**: 1160–1166.

Kazamia E, Czesnick H, Nguyen TTV, Croft MT, Sherwood E, Sasso S, Hodson SJ, Warren MJ, Smith AG. **2012**. Mutualistic interactions between vitamin B_{12}-dependent algae and heterotrophic bacteria exhibit regulation. *Environmental Microbiology* **14**: 1466–1476.

Keeling PJ, Burki F, Wilcox HM, Allam B, Allen EE, Amaral-Zettler LA, Armbrust EV, Archibald JM, Bharti AK, Bell CJ, *et al.* 2014. The Marine Microbial Eukaryote Transcriptome Sequencing Project (MMETSP): illuminating the functional diversity of eukaryotic life in the oceans through transcriptome sequencing (RG Roberts, Ed.). *PLoS Biology* **12**: e1001889.

Kemp AES, Villareal TA. **2018**. The case of the diatoms and the muddled mandalas: Time to recognize diatom adaptations to stratified waters. *Progress in Oceanography* **167**: 138–149.

Kim SM, Jung Y-J, Kwon O-N, Cha KH, Um B-H, Chung D, Pan C-H. **2012**. A potential commercial source of fucoxanthin extracted from the microalga *Phaeodactylum tricornutum*. *Applied Biochemistry and Biotechnology* **166**: 1843–1855.

Kirchman DL, Morán XAG, Ducklow H. **2009**. Microbial growth in the polar oceans — role of temperature and potential impact of climate change. *Nature Reviews Microbiology* **7**: 451–459.

Kling JD, Kelly KJ, Pei S, Rynearson TA, Hutchins DA. **2021**. Irradiance modulates thermal niche in a previously undescribed low-light and cold-adapted nano-diatom. *Limnology and Oceanography* **66**: 2266–2277.

Koch F, Marcoval MA, Panzeca C, Bruland KW, Sañudo-Wilhelmy SA, Gobler CJ. **2011**. The effect of vitamin B_{12} on phytoplankton growth and community structure in the Gulf of Alaska. *Limnology and Oceanography* **56**: 1023–1034.

Kohlbach D, Schaafsma FL, Graeve M, Lebreton B, Lange BA, David C, Vortkamp M, Flores H. **2017**. Strong linkage of polar cod (*Boreogadus saida*) to sea ice algae-produced carbon: Evidence from stomach content, fatty acid and stable isotope analyses. *Progress in Oceanography* **152**: 62–74.

Krisch S, Browning TJ, Graeve M, Ludwichowski K-U, Lodeiro P, Hopwood MJ, Roig S, Yong J-C, Kanzow T, Achterberg EP. **2020**. The influence of Arctic Fe and Atlantic fixed N on summertime primary production in Fram Strait, North Greenland Sea. *Scientific Reports* **10**: 15230.

Kropuenske LR, Mills MM, van Dijken GL, Bailey S, Robinson DH, Welschmeyer NA, Arrigoa KR. **2009**. Photophysiology in two major Southern Ocean phytoplankton taxa: Photoprotection in *Phaeocystis antarctica* and *Fragilariopsis cylindrus*. *Limnology and Oceanography* **54**: 1176–1196.

Kuczynska P, Jemiola-Rzeminska M, Strzalka K. **2015**. Photosynthetic pigments in diatoms. *Marine Drugs* **13**: 5847–5881.

Kuklinski P, Barnes D. **2010**. First bipolar benthic brooder. *Marine Ecology Progress Series* **401**: 15–20.

Kumar S, Stecher G, Li M, Knyaz C, Tamura K. **2018**. MEGA X: Molecular Evolutionary Genetics Analysis across Computing Platforms (FU Battistuzzi, Ed.). *Molecular Biology and Evolution* **35**: 1547–1549.

Kvíderová J, Shukla SP, Pushparaj B, Elster J. **2017**. Perspectives of low-temperature biomass production of polar microalgae and biotechnology expansion into high latitudes. In: Margesin R, ed. Psychrophiles: From Biodiversity to Biotechnology. Cham: Springer International Publishing, 585–600.

Lang I, Hodac L, Friedl T, Feussner I. **2011**. Fatty acid profiles and their distribution patterns in microalgae: a comprehensive analysis of more than 2000 strains from the SAG culture collection. *BMC Plant Biology* **11**: 124.

Lavaud J, Materna AC, Sturm S, Vugrinec S, Kroth PG. **2012**. Silencing of the violaxanthin de-epoxidase gene in the diatom *Phaeodactylum tricornutum* reduces diatoxanthin synthesis and non-photochemical quenching. *PLOS ONE* **7**: e36806.

Lawver LA, Gahagan LM. **2003**. Evolution of Cenozoic seaways in the circum-Antarctic region. *Palaeogeography, Palaeoclimatology, Palaeoecology* **198**: 11–37.

Lawver LA, Müller RD, Srivastava SP, Roest W. **1990**. The Opening of the Arctic Ocean. In: Bleil U, Thiede J, eds. Geological History of the Polar Oceans: Arctic versus Antarctic. Dordrecht: Springer Netherlands, 29–62.

Lebeau T, Robert J-M. **2003**. Diatom cultivation and biotechnologically relevant products. Part II: Current and putative products. *Applied Microbiology and Biotechnology* **60**: 624–632.

Lewin JC, Lewin RA. **1960**. Auxotrophy and heterotrophy in marine littoral diatoms. *Canadian Journal of Microbiology* **6**: 127–134.

Lin Y, Moreno C, Marchetti A, Ducklow H, Schofield O, Delage E, Meredith M, Li Z, Eveillard D, Chaffron S, *et al.* 2021. Decline in plankton diversity and carbon flux with reduced sea ice extent along the Western Antarctic Peninsula. *Nature Communications* **12**: 4948.

Lindstrom SC. **2001**. The Bering Strait connection: dispersal and speciation in boreal macroalgae: Speciation in boreal macroalgae. *Journal of Biogeography* **28**: 243–251.

Littlepage JL. **1965**. Oceanographic investigations in Mcmurdo Sound, Antarctica. In: Biology of the Antarctic Seas II. American Geophysical Union (AGU), 1–37.

Lizotte MP. **2001**. The contributions of sea ice algae to Antarctic marine primary production. *American Zoologist* **41**: 57–73.

Lochhead AG, Thexton RH. **1951**. Vitamin B_{12} as a growth factor for soil bacteria. *Nature* **167**: 1034–1034.

Longhi ML, Schloss IR, Wiencke C. **2003**. Effect of irradiance and temperature on photosynthesis and growth of two antarctic benthic diatoms, *Gyrosigma subsalinum* and *Odontella litigiosa*. *Botanica Marina* **46**.

Lundholm N, Hasle GR. **2008**. Are *Fragilariopsis cylindrus* and *Fragilariopsis nana* bipolar diatoms? – Morphological and molecular analyses of two sympatric species. *Nova Hedwigia* **133**: 231–250.

Lyon B, Mock T. **2014**. Polar microalgae: new approaches towards understanding adaptations to an extreme and changing environment. *Biology* **3**: 56–80.

MacGillivary ML, Kaczmarska I. **2011**. Survey of the efficacy of a short fragment of the *rbc*L gene as a supplemental DNA barcode for diatoms. *Journal of Eukaryotic Microbiology* **58**: 529–536.

Malviya S, Scalco E, Audic S, Vincent F, Veluchamy A, Poulain J, Wincker P, Iudicone D, de Vargas C, Bittner L, *et al.* 2016. Insights into global diatom distribution and diversity in the world's ocean. *Proceedings of the National Academy of Sciences* **113**: E1516–E1525.

Margesin R, Schinner F. **1994**. Properties of cold-adapted microorganisms and their potential role in biotechnology. *Journal of Biotechnology* **33**: 1–14.

Marincovich L, Gladenkov AY. **2001**. New evidence for the age of Bering Strait. *Quaternary Science Reviews* **20**: 329–335.

Marinov I, Doney SC, Lima ID. **2010**. Response of ocean phytoplankton community structure to climate change over the 21st century: partitioning the effects of nutrients, temperature and light. *Biogeosciences* **7**: 3941–3959.

Martin JH. **1990**. Glacial-interglacial CO2 change: the iron hypothesis. *Paleoceanography* **5**: 1–13.

Massana R, del Campo J, Sieracki ME, Audic S, Logares R. **2014**. Exploring the uncultured microeukaryote majority in the oceans: reevaluation of ribogroups within stramenopiles. *The ISME Journal* **8**: 854–866.

McFadden GI. **2001**. Primary and secondary endosymbiosis and the origin of plastids. *Journal of Phycology* **37**: 951–959.

McRose D, Guo J, Monier A, Sudek S, Wilken S, Yan S, Mock T, Archibald JM, Begley TP, Reyes-Prieto A, *et al.* 2014. Alternatives to vitamin B_1 uptake revealed with discovery of riboswitches in multiple marine eukaryotic lineages. *The ISME Journal* **8**: 2517–2529.

Medlin LK, Priddle J. **1990**. *Polar marine diatoms*. British Antarctic Survey.

Meehl GA, Arblaster JM, Chung CTY, Holland MM, DuVivier A, Thompson L, Yang D, Bitz CM. **2019**. Sustained ocean changes contributed to sudden Antarctic sea ice retreat in late 2016. *Nature Communications* **10**: 14.

Meredith MP, King JC. **2005**. Rapid climate change in the ocean west of the Antarctic Peninsula during the second half of the 20th century. *Geophysical Research Letters* **32**.

Mills MM, Brown ZW, Laney SR, Ortega-Retuerta E, Lowry KE, van Dijken GL, Arrigo KR. **2018**. Nitrogen limitation of the summer phytoplankton and heterotrophic prokaryote communities in the chukchi sea. *Frontiers in Marine Science* **5**: 362.

Mock T, Hoch N. **2005**. Long-term temperature acclimation of photosynthesis in steady-state cultures of the polar diatom *Fragilariopsis cylindrus*. *Photosynthesis Research* **85**: 307–317.

Mock T, Otillar RP, Strauss J, McMullan M, Paajanen P, Schmutz J, Salamov A, Sanges R, Toseland A, Ward BJ, *et al.* 2017. Evolutionary genomics of the cold-adapted diatom *Fragilariopsis cylindrus*. *Nature* **541**: 536–540.

Moline MA, Claustre H, Frazer TK, Schofield O, Vernet M. **2004**. Alteration of the food web along the Antarctic Peninsula in response to a regional warming trend: alteration of the Antarctic food web. *Global Change Biology* **10**: 1973–1980.

Montes-Hugo M, Doney SC, Ducklow HW, Fraser W, Martinson D, Stammerjohn SE, Schofield O. **2009**. Recent changes in phytoplankton communities associated with rapid regional climate change along the western Antarctic peninsula. *Science* **323**: 1470–1473.

Montresor M, Lovejoy C, Orsini L, Procaccini G, Roy S. **2003**. Bipolar distribution of the cyst-forming dinoflagellate *Polarella glacialis*. *Polar Biology* **26**: 186–194.

Moody JW, McGinty CM, Quinn JC. **2014**. Global evaluation of biofuel potential from microalgae. *Proceedings of the National Academy of Sciences of the United States of America* **111**: 8691–8696.

Morita RY. **1975**. Psychrophilic bacteria. *Bacteriological reviews* **39**: 144–167.

Moustafa A, Beszteri B, Maier UG, Bowler C, Valentin K, Bhattacharya D. **2009**. Genomic footprints of a cryptic plastid endosymbiosis in diatoms. *Science* **324**: 1724–1726.

Murdock JN, Wetzel DL. **2009**. FT-IR microspectroscopy enhances biological and ecological analysis of algae. *Applied Spectroscopy Reviews* **44**: 335–361.

Nakov T, Beaulieu JM, Alverson AJ. **2018**. Accelerated diversification is related to life history and locomotion in a hyperdiverse lineage of microbial eukaryotes (Diatoms, Bacillariophyta). *New Phytologist* **219**: 462–473.

Natarajan KV. **1970**. Distribution and significance of vitamin B_{12} and thiamine in the subarctic Pacific Ocean. *Limnology and Oceanography* **15**: 655–659.

Nef C, Henry C, Nicolau É, Bérard J-B, Hervé F, Caruana AMN, Kaas R, Mairet F, Garnier M. **2020**. Cobalamin scarcity modifies carbon allocation and impairs DMSP production through methionine metabolism in the haptophyte microalgae *Tisochrysis lutea*. *Frontiers in Marine Science* **7**: 569560.

Nef C, Jung S, Mairet F, Kaas R, Grizeau D, Garnier M. **2019**. How haptophytes microalgae mitigate vitamin B_{12} limitation. *Scientific Reports* **9**: 8417.

Nelson DMD, Trrguer P, Brzezinski MA, Leynaert A, Queguiner B. **1995**. Production and dissolution of biogenic silica in the ocean: Revised global estimates, comparison with regional data and relationship to biogenic sedimentation. *Global Biogeochemical Cycles* **9**: 359–372.

Nichols DS, Nichols PD, Sullivan CW. **1993**. Fatty acid, sterol and hydrocarbon composition of Antarctic sea ice diatom communities during the spring bloom in McMurdo Sound. *Antarctic Science* **5**: 271–278.

Nur MMA, Muizelaar W, Boelen P, Buma AGJ. **2019**. Environmental and nutrient conditions influence fucoxanthin productivity of the marine diatom *Phaeodactylum tricornutum* grown on palm oil mill effluent. *Journal of Applied Phycology* **31**: 111–122.

O'Donnell DR, Hamman CR, Johnson EC, Kremer CT, Klausmeier CA, Litchman E. **2018**. Rapid thermal adaptation in a marine diatom reveals constraints and trade-offs. *Global Change Biology* **24**: 4554–4565.

Okbamichael M, Sañudo-Wilhelmy SA. **2004**. A new method for the determination of Vitamin B_{12} in seawater. *Analytica Chimica Acta* **517**: 33–38.

Orłowska M, Steczkiewicz K, Muszewska A. **2021**. Utilization of cobalamin Is ubiquitous in early-branching fungal phyla. *Genome Biology and Evolution* **13**.

Overland JE, Wang M. **2013**. When will the summer Arctic be nearly sea ice free? *Geophysical Research Letters* **40**: 2097–2101.

Pabi S, van Dijken GL, Arrigo KR. **2008**. Primary production in the Arctic Ocean, 1998–2006. *Journal of Geophysical Research: Oceans* **113**.

Padfield D, O'Sullivan H, Pawar S. **2021**. rTPC and nls.multstart: A new pipeline to fit thermal performance curves in R. *Methods in Ecology and Evolution* **12**: 1138–1143.

Padfield D, Yvon-Durocher G, Buckling A, Jennings S, Yvon-Durocher G. **2016**. Rapid evolution of metabolic traits explains thermal adaptation in phytoplankton. *Ecology Letters* **19**: 133–142.

Pančić M, Hansen PJ, Tammilehto A, Lundholm N. **2015**. Resilience to temperature and pH changes in a future climate change scenario in six strains of the polar diatom *Fragilariopsis cylindrus*. *Biogeosciences* **12**: 4235–4244.

Pang Z, Chong J, Zhou G, de Lima Morais DA, Chang L, Barrette M, Gauthier C, Jacques P-É, Li S, Xia J. **2021**. MetaboAnalyst 5.0: narrowing the gap between raw spectra and functional insights. *Nucleic Acids Research* **49**: W388–W396.

Pankratz S, Oyedun AO, Zhang XL, Kumar A. **2017**. Algae production platforms for Canada's northern climate. *Renewable & Sustainable Energy Reviews* **80**: 109–120.

Panzeca C, Beck AJ, Leblanc K, Taylor GT, Hutchins DA, Sañudo-Wilhelmy SA. **2008**. Potential cobalt limitation of vitamin B_{12} synthesis in the North Atlantic Ocean. *Global Biogeochemical Cycles* **22**: n/a-n/a.

Panzeca C, Beck AJ, Tovar-Sanchez A, Segovia-Zavala J, Taylor GT, Gobler CJ, Sañudo-Wilhelmy SA. **2009**. Distributions of dissolved vitamin B_{12} and Co in coastal and open-ocean environments. *Estuarine, Coastal and Shelf Science* **85**: 223–230.

Panzeca C, Tovar-Sanchez A, Agustí S, Reche I, Duarte CM, Taylor GT, Sañudo-Wilhelmy SA. **2006**. B vitamins as regulators of phytoplankton dynamics. *Eos, Transactions American Geophysical Union* **87**: 593.

Patil V, Reitan KI, Knutsen G, Mortensen LM, Källqvist T, Olsen E, Vogt G, Gislerød HR. **2005**. Microalgae as source of polyunsaturated fatty acids for aquaculture. *Plant Biol* **6**: 57–65.

Pawlowski J, Fahrni J, Lecroq B, LONGET D, Cornelius N, Excoffier L, Cedhagen T, Gooday AJ. **2007**. Bipolar gene flow in deep-sea benthic foraminifera. *Molecular Ecology* **16**: 4089–4096.

Peck LS. **2011**. Organisms and responses to environmental change. *Marine Genomics* **4**: 237–243.

Peck LS, Barnes DKA, Cook AJ, Felming AH, Clarke A. **2010a**. Negative feedback in the cold: ice retreat produces new carbon sinks in Antarctica. *Global Change Biology* **16**: 2614–2623.

Peck LS, Morley SA, Clark MS. **2010b**. Poor acclimation capacities in Antarctic marine ectotherms. *Marine Biology* **157**: 2051–2059.

Peck LS, Morley SA, Richard J, Clark MS. **2014**. Acclimation and thermal tolerance in Antarctic marine ectotherms (SA Davies, JAT Dow, and K Lukowiak, Eds.). *Journal of Experimental Biology* **217**: 16–22.

Person R, Aumont O, Levy M. **2018**. The biological pump and seasonal variability of pCO2 in the Southern Ocean: exploring the role of diatom adaptation to low iron. *Journal of Geophysical Research: Oceans* **123**: 3204–3226.

Pike J, Crosta X, Maddison EJ, Stickley CE, Denis D, Barbara L, Renssen H. **2009**. Observations on the relationship between the Antarctic coastal diatoms *Thalassiosira antarctica* Comber and *Porosira glacialis* (Grunow) Jørgensen and sea ice concentrations during the late Quaternary. *Marine Micropaleontology* **73**: 14–25.

Pizzolato L, Howell SEL, Dawson J, Laliberté F, Copland L. **2016**. The influence of declining sea ice on shipping activity in the Canadian Arctic. *Geophysical Research Letters* **43**: 12,146-12,154.

Pohnert G. **2005**. Diatom/Copepod Interactions in Plankton: The Indirect Chemical Defense of Unicellular Algae. *ChemBioChem* **6**: 946–959.

Postel U, Glemser B, Salazar Alekseyeva K, Eggers SL, Groth M, Glöckner G, John U, Mock T, Klemm K, Valentin K, *et al.* 2020. Adaptive divergence across Southern Ocean gradients in the pelagic diatom *Fragilariopsis kerguelensis*. *Molecular Ecology*. mec.15554.

Priddle J, Fryxell GA, Survey BA. **1985**. *Handbook of the Common Plankton Diatoms of the Southern Ocean: Centrales Except the Genus Thalassiosira*. British Antarctic Survey, Natural Environment Research Council.

Priscu JC, Priscu' LR, Palmisano AC, Sullivan C. **1990**. Estimation of neutral lipid levels in Antarctic sea ice microalgae by nile red fluorescence. *Antarctic Science* **2**: 149–155.

Provasoli L, Carlucci A. **1974**. Vitamins and growth regulators. In: Stewart W, ed. Algal physiology and biochemistry. Blackwell Scientific Publications, 741–787.

Quinn JC, Catton K, Wagner N, Bradley TH. **2012**. Current large-scale US biofuel potential from microalgae cultivated in photobioreactors. *Bioenergy Research* **5**: 49–60.

R Core Team. **2021**. R: A language and environment for statistical computing.

R Studio Team. **2021**. RStudio: integrated development for R.

Remias D, Lutz-Meindl U, Lutz C. **2005**. Photosynthesis, pigments and ultrastructure of the alpine snow alga *Chlamydomonas nivalis*. *European Journal of Phycology* **40**: 259–268.

Renaut S, Devred E, Babin M. **2018**. Northward Expansion and Intensification of Phytoplankton Growth During the Early Ice-Free Season in Arctic. *Geophysical Research Letters* **45**: 10,590-10,598.

Richard J, Morley SA, Deloffre J, Peck LS. **2012**. Thermal acclimation capacity for four Arctic marine benthic species. *Journal of Experimental Marine Biology and Ecology* **424–425**: 38–43.

Rintoul SR, Hughes CW, Olbers D. **2001**. Chapter 4.6 The Antarctic circumpolar current system. In: Siedler G, Church J, Gould J, eds. International Geophysics. Ocean Circulation and Climate. Academic Press, 271.

Ritz C, Baty F, Streibig JC, Gerhard D. **2015**. Dose-response analysis using R (Y Xia, Ed.). *PLOS ONE* **10**: e0146021.

Robinson SA, Klekociuk AR, King DH, Pizarro Rojas M, Zúñiga GE, Bergstrom DM. **2020**. The 2019/2020 summer of Antarctic heatwaves. *Global Change Biology* **26**: 3178–3180.

Rodríguez-Ezpeleta N, Brinkmann H, Burey SC, Roure B, Burger G, Löffelhardt W, Bohnert HJ, Philippe H, Lang BF. **2005**. Monophyly of primary photosynthetic eukaryotes: green plants, red algae, and glaucophytes. *Current Biology* **15**: 1325–1330.

Rousseaux C, Gregg W. **2014**. Interannual variation in phytoplankton primary production at a global scale. *Remote Sensing* **6**: 1–19.

Rozema PD, Venables HJ, van de Poll WH, Clarke A, Meredith MP, Buma AGJ. **2017**. Interannual variability in phytoplankton biomass and species composition in northern Marguerite Bay (West Antarctic Peninsula) is governed by both winter sea ice cover and summer stratification: Changing phytoplankton at the coastal WAP. *Limnology and Oceanography* **62**: 235–252.

Rüger J, Unger N, Schie IW, Brunner E, Popp J, Krafft C. **2016**. Assessment of growth phases of the diatom *Ditylum brightwellii* by FT-IR and Raman spectroscopy. *Algal Research* **19**: 246–252.

Russell NJ, Nichols DS. **1999**. Polyunsaturated fatty acids in marine bacteria - a dogma rewritten. *Microbiology-Uk* **145**: 767–779.

Sackett O, Petrou K, Reedy B, De Grazia A, Hill R, Doblin M, Beardall J, Ralph P, Heraud P. **2013**. Phenotypic plasticity of Southern Ocean diatoms: key to success in the sea ice habitat? (S Lin, Ed.). *PLoS ONE* **8**: e81185.

Saito MA, Goepfert TJ, Noble AE, Bertrand EM, Sedwick PN, DiTullio GR. **2010**. A seasonal study of dissolved cobalt in the Ross Sea, Antarctica: micronutrient behavior, absence of scavenging, and relationships with Zn, Cd, and P. *Biogeosciences* **7**: 4059–4082.

Samuels T, Rynearson TA, Collins S. **2021**. Surviving heatwaves: thermal experience predicts life and death in a Southern Ocean diatom. *Frontiers in Marine Science* **8**: 9.

Sañudo-Wilhelmy SA, Gobler CJ, Okbamichael M, Taylor GT. **2006**. Regulation of phytoplankton dynamics by vitamin B_{12}. *Geophysical Research Letters* **33**: L04604.

Sañudo-Wilhelmy SA, Gómez-Consarnau L, Suffridge C, Webb EA. **2014**. The role of B vitamins in marine biogeochemistry. *Annual Review of Marine Science* **6**: 339–367.

Sazanova KV, Senik SV, Kirtsideli IYu, Shavarda AL. **2019**. Metabolomic profiling and lipid composition of Arctic and Antarctic strains of Micromycetes *Geomyces pannorum* and *Thelebolus microsporus* grown at different temperatures. *Microbiology* **88**: 282–291.

Schaub I, Wagner H, Graeve M, Karsten U. **2017**. Effects of prolonged darkness and temperature on the lipid metabolism in the benthic diatom *Navicula perminuta* from the Arctic Adventfjorden, Svalbard. *Polar Biology* **40**: 1425–1439.

Schaum C-E, Barton S, Bestion E, Buckling A, Garcia-Carreras B, Lopez P, Lowe C, Pawar S, Smirnoff N, Trimmer M, *et al.* 2017. Adaptation of phytoplankton to a decade of experimental warming linked to increased photosynthesis. *Nature Ecology & Evolution* **1**: 0094.

Schaum C-E, Buckling A, Smirnoff N, Studholme DJ, Yvon-Durocher G. **2018**. Environmental fluctuations accelerate molecular evolution of thermal tolerance in a marine diatom. *Nature Communications* **9**: 1719.

Schlie C, Karsten U. **2017**. Microphytobenthic diatoms isolated from sediments of the Adventfjorden (Svalbard): growth as function of temperature. *Polar Biology* **40**: 1043–1051.

Schlüter L, Lohbeck KT, Gutowska MA, Gröger JP, Riebesell U, Reusch TBH. **2014**. Adaptation of a globally important coccolithophore to ocean warming and acidification. *Nature Climate Change* **4**: 1024–1030.

Schoolfield RM, Sharpe PJH, Magnuson CE. **1981**. Non-linear regression of biological temperature-dependent rate models based on absolute reaction-rate theory. *Journal of Theoretical Biology* **88**: 719–731.

Schulte PM, Healy TM, Fangue NA. **2011**. Thermal performance curves, phenotypic plasticity, and the time scales of temperature exposure. *Integrative and Comparative Biology* **51**: 691–702.

Scott FJ, Marchant HJ, Study ABR, Division AA. **2005**. *Antarctic Marine Protists*. Australian Biological Resources Study.

Sedwick PN, DiTullio GR, Mackey DJ. **2000**. Iron and manganese in the Ross Sea, Antarctica: Seasonal iron limitation in Antarctic shelf waters. *Journal of Geophysical Research: Oceans* **105**: 11321–11336.

Shibl AA, Isaac A, Ochsenkühn MA, Cárdenas A, Fei C, Behringer G, Arnoux M, Drou N, Santos MP, Gunsalus KC, *et al.* 2020. Diatom modulation of select bacteria through use of two unique secondary metabolites. *Proceedings of the National Academy of Sciences* **117**: 27445–27455.

Slade R, Bauen A. **2013**. Micro-algae cultivation for biofuels: Cost, energy balance, environmental impacts and future prospects. *Biomass & Bioenergy* **53**: 29–38.

Smedsrud LH, Halvorsen MH, Stroeve JC, Zhang R, Kloster K. **2017**. Fram Strait sea ice export variability and September Arctic sea ice extent over the last 80 years. *The Cryosphere* **11**: 65–79.

Smith R, Baker K, Fraser W, Hofmann E, Karl D, Klink J, Quentin L, Prezelin B, Ross R, Trivelpiece W, *et al.* 1995. The Palmer LTER: A Long-Term Ecological Research Program at Palmer Station, Antarctica. *Oceanography* **8**: 77–86.

Smith AG, Croft MT, Moulin M, Webb ME. **2007**. Plants need their vitamins too. *Current Opinion in Plant Biology* **10**: 266–275.

Smith LC, Stephenson SR. **2013**. New Trans-Arctic shipping routes navigable by midcentury. *Proceedings of the National Academy of Sciences* **110**: E1191–E1195.

Somero GN. **2010**. The physiology of climate change: how potentials for acclimatization and genetic adaptation will determine 'winners' and 'losers'. *Journal of Experimental Biology* **213**: 912–920.

Sommer U, Stibor H, Katechakis A, Sommer F, Hansen T. **2002**. Pelagic food web configurations at different levels of nutrient richness and their implications for the ratio fish production:primary production. In: Vadstein O, Olsen Y, eds. Sustainable Increase of Marine Harvesting: Fundamental Mechanisms and New Concepts: Proceedings of the 1st Maricult Conference held in Trondheim, Norway, 25–28 June 2000. Dordrecht: Springer Netherlands, 11–20.

Speziale BJ, Schreiner SP, Giammatteo PA, Schindler JE. **1984**. Comparison of *N*, *N*-dimethylformamide, dimethyl sulfoxide, and acetone for extraction of phytoplankton chlorophyll. *Canadian Journal of Fisheries and Aquatic Sciences* **41**: 1519–1522.

Sromek L, Lasota R, Szymelfenig M, Wolowicz M. **2015**. Genetic evidence for the existence of two species of the "bipolar" pelagic mollusk *Clione limacina*. *American Malacological Bulletin* **33**: 118–120.

Stahl W, Sies H. **2005**. Bioactivity and protective effects of natural carotenoids. *Biochimica Et Biophysica Acta-Molecular Basis of Disease* **1740**: 101–107.

Stampfli GM, Hochard C, Vérard C, Wilhem C, vonRaumer J. **2013**. The formation of Pangea. *Tectonophysics* **593**: 1–19.

Steinrücken P, Mjøs SA, Prestegard SK, Erga SR. **2018a**. Enhancing EPA content in an Arctic diatom: a factorial design study to evaluate interactive effects of growth factors. *Frontiers in Plant Science* **9**: 491.

Steinrücken P, Prestegard SK, de Vree JH, Storesund JE, Pree B, Mjøs SA, Erga SR. **2018b**. Comparing EPA production and fatty acid profiles of three *Phaeodactylum tricornutum* strains under western Norwegian climate conditions. *Algal Research-Biomass Biofuels and Bioproducts* **30**: 11–22.

Stock W, Vanelslander B, Rüdiger F, Sabbe K, Vyverman W, Karsten U. **2019**. Thermal niche differentiation in the benthic diatom *Cylindrotheca closterium* (Bacillariophyceae) complex. *Frontiers in Microbiology* **10**: 1395.

Sul WJ, Oliver TA, Ducklow HW, Amaral-Zettler LA, Sogin ML. **2013**. Marine bacteria exhibit a bipolar distribution. *Proceedings of the National Academy of Sciences* **110**: 2342–2347.

Sun X-M, Ren L-J, Zhao Q-Y, Ji X-J, Huang H. **2018**. Microalgae for the production of lipid and carotenoids: a review with focus on stress regulation and adaptation. *Biotechnology for Biofuels* **11**: 272.

Suzuki Y, Takahashi M. **1995**. Growth responses of several diatom species from various environments to temperature. *Journal of Phycology* **31**: 880–888.

Svenning JB, Dalheim L, Eilertsen HC, Vasskog T. **2019**. Temperature dependent growth rate, lipid content and fatty acid composition of the marine cold-water diatom *Porosira glacialis*. *Algal Research* **37**: 11–16.

Swanson D, Block R, Mousa SA. **2012**. Omega-3 fatty acids EPA and DHA: health benefits throughout life. *Advances in Nutrition* **3**: 1–7.

Takahashi F, Okabe Y, Nakada T, Sekimoto H, Ito M, Kataoka H, Nozaki H. **2007**. Origins of the secondary plastids of Euglenophyta and Chlorarachniophyta as revealed by an analysis of the plastid-targeting, nuclear-encoded gene *psbO* [1]. *Journal of Phycology* **43**: 1302–1309.

Tang YZ, Koch F, Gobler CJ. **2010**. Most harmful algal bloom species are vitamin B_1 and B_{12} auxotrophs. *Proceedings of the National Academy of Sciences* **107**: 20756–20761.

Taraldsvik M, Myklestad SM. **2000**. The effect of pH on growth rate, biochemical composition and extracellular carbohydrate production of the marine diatom *Skeletonema costatum*. *European Journal of Phycology* **35**: 189–194.

Thomas MK, Kremer CT, Klausmeier CA, Litchman E. **2012**. A Global Pattern of Thermal Adaptation in Marine Phytoplankton. *Science* **338**: 1085–1088.

Thyrring J, Tremblay R, Sejr MK. **2017**. Importance of ice algae and pelagic phytoplankton as food sources revealed by fatty acid trophic markers in a keystone species (*Mytilus trossulus*) from the High Arctic. *Marine Ecology Progress Series* **572**: 155–164.

Tréguer P, Bowler C, Moriceau B, Dutkiewicz S, Gehlen M, Aumont O, Bittner L, Dugdale R, Finkel Z, Iudicone D, *et al.* 2018. Influence of diatom diversity on the ocean biological carbon pump. *Nature Geoscience* **11**: 27–37.

Tremblay J-E, Gratton Y, Fauchot J, Price NM. **2002**. Climatic and oceanic forcing of new, net, and diatom production in the North Water. *The International North Water Polynya Study* **49**: 4927–4946.

Trobajo R, Mann DG. **2019**. A rapid cleaning method for diatoms. *Diatom Research* **34**: 115–124.

Trusel LD, Das SB, Osman MB, Evans MJ, Smith BE, Fettweis X, McConnell JR, Noël BPY, van den Broeke MR. **2018**. Nonlinear rise in Greenland runoff in response to post-industrial Arctic warming. *Nature* **564**: 104–108.

Turner J, Colwell SR, Marshall GJ, Lachlan-Cope TA, Carleton AM, Jones PD, Lagun V, Reid PA, Iagovkina S. **2005**. Antarctic climate change during the last 50 years. *International Journal of Climatology* **25**: 279–294.

Turner J, Hosking JS, Bracegirdle TJ, Marshall GJ, Phillips T. **2015**. Recent changes in Antarctic Sea Ice. *Philosophical Transactions of the Royal Society A: Mathematical, Physical and Engineering Sciences* **373**: 20140163.

Turner J, Lu H, White I, King JC, Phillips T, Hosking JS, Bracegirdle TJ, Marshall GJ, Mulvaney R, Deb P. **2016**. Absence of 21st century warming on Antarctic Peninsula consistent with natural variability. *Nature* **535**: 411–415.

Vancaester E, Depuydt T, Osuna-Cruz CM, Vandepoele K. **2020**. Comprehensive and functional analysis of horizontal gene transfer events in diatoms (FU Battistuzzi, Ed.). *Molecular Biology and Evolution* **37**: 3243–3257.

Vaulot D, Gall FL, Marie D, Guillou L, Partensky F. **2004**. The Roscoff Culture Collection (RCC): a collection dedicated to marine picoplankton. *Nova Hedwigia* **79**: 49–70.

Vidoudez C, Pohnert G. **2012**. Comparative metabolomics of the diatom *Skeletonema marinoi* in different growth phases. *Metabolomics* **8**: 654–669.

Vihtakari M. **2021**. *ggOceanMaps: plot data on oceanographic maps using 'ggplot2'*.

Villareal TA, Fryxell GA. **1983**. Temperature effects on the valve structure of the bipolar diatoms *Thalassiosira antarctica* and *Porosira glacialis*. *Polar Biology* **2**: 163–169.

Villaverde T, Escudero M, Martín-Bravo S, Jiménez-Mejías P, Sanmartín I, Vargas P, Luceño M. **2017**. Bipolar distributions in vascular plants: A review. *American Journal of Botany* **104**: 1680–1694.

Walsh JJ, Dieterle DA, Maslowski W, Whitledge TE. **2004**. Decadal shifts in biophysical forcing of Arctic marine food webs: Numerical consequences. *Journal of Geophysical Research: Oceans* **109**.

Warren MJ, Raux E, Schubert HL, Escalante-Semerena JC. **2002**. The biosynthesis of adenosylcobalamin (vitamin B_{12}). *Natural Product Reports* **19**: 390–412.

Wassmann P, Slagstad D, Ellingsen I. **2010**. Primary production and climatic variability in the European sector of the Arctic Ocean prior to 2007: preliminary results. *Polar Biology* **33**: 1641–1650.

Watanabe F, Takeneka S, Kittaka-katsurak H, Ebara S, Miyamoto E. **2002**. Characterization and bioavailability of vitamin B_{12}-compounds from edible algae. *Journal of Nutritional Science and Vitaminology* **48**: 325–331.

Watanabe F, Yabuta Y, Bito T, Teng F. **2014**. Vitamin B_{12}-containing plant food sources for vegetarians. *Nutrients* **6**: 1861–1873.

Wellburn AR. **1994**. The spectral determination of chlorophylls a and b, as well as total carotenoids, using various solvents with spectrophotometers of different resolution. *Journal of Plant Physiology* **144**: 307–313.

Westacott S, Planavsky NJ, Zhao M-Y, Hull PM. **2021**. Revisiting the sedimentary record of the rise of diatoms. *Proceedings of the National Academy of Sciences* **118**: e2103517118.

Whittaker KA, Rynearson TA. **2017**. Evidence for environmental and ecological selection in a microbe with no geographic limits to gene flow. *Proceedings of the National Academy of Sciences* **114**: 2651–2656.

Wickham H. **2016**. *ggplot2: Elegant graphics for data analysis*. New York: Springer-Verlag.

Wilhelm C, Büchel C, Fisahn J, Goss R, Jakob T, LaRoche J, Lavaud J, Lohr M, Riebesell U, Stehfest K, *et al.* 2006. The regulation of carbon and nutrient assimilation in diatoms is significantly different from green algae. *Protist* **157**: 91–124.

William KWL, Morris I. **1982**. Temperature adaptation in *Phaeodactylum tricornutum* Bohlin: Photosynthetic rate compensation and capacity. *Journal of Experimental Marine Biology and Ecology* **58**: 135–150.

de Wit R, Bouvier T. **2006**. 'Everything is everywhere, but, the environment selects'; what did Baas Becking and Beijerinck really say? *Environmental Microbiology* **8**: 755–758.

Wolf KKE, Romanelli E, Rost B, John U, Collins S, Weigand H, Hoppe CJM. **2019**. Company matters: The presence of other genotypes alters traits and intraspecific selection in an Arctic diatom under climate change. *Global Change Biology* **25**: 2869–2884.

Wright S, Jeffrey S, Mantoura R, Llewellyn C, Bjornland T, Repeta D, Welschmeyer N. **1991**. Improved HPLC method for the analysis of chlorophylls and carotenoids from marine phytoplankton. *Marine Ecology Progress Series* **77**: 183–196.

Xiang H, Yang X, Ke L, Hu Y. **2020**. The properties, biotechnologies, and applications of antifreeze proteins. *International Journal of Biological Macromolecules* **153**: 661–675.

Xie B, Bishop S, Stessman D, Wright D, Spalding MH, Halverson LJ. **2013**. *Chlamydomonas reinhardtii* thermal tolerance enhancement mediated by a mutualistic interaction with vitamin B_{12}-producing bacteria. *The ISME Journal* **7**: 1544–1555.

Yi Z, Xu M, Di X, Brynjolfsson S, Fu W. **2017**. Exploring valuable lipids in diatoms. *Frontiers in Marine Science* **4**: 17.

Yongmanitchai W, Ward OP. **1991**. Growth of and omega-3-fatty-acid production by *Phaeodactylum tricornutum* under different culture conditions. *Applied and Environmental Microbiology* **57**: 419–425.

Yool A, Tyrrell T. **2003**. Role of diatoms in regulating the ocean's silicon cycle. *Global Biogeochemical Cycles* **17**: 1103.

Yoon HS, Hackett JD, Ciniglia C, Pinto G, Bhattacharya D. **2004**. A molecular timeline for the origin of photosynthetic eukaryotes. *Molecular Biology and Evolution* **21**: 809–818.

Zhu CJ, Lee YK. **1997**. Determination of biomass dry weight of marine microalgae. *Journal of Applied Phycology* **9**: 189–194.

Zimmermann J, Jahn R, Gemeinholzer B. **2011**. Barcoding diatoms: evaluation of the V4 subregion on the 18S rRNA gene, including new primers and protocols. *Organisms Diversity & Evolution* **11**: 173–192.

Appendix 1 – Artificial sea water + Guillards *f*/2 diatom media recipe

Artificial sea water was made by dissolving 36 g RedSea salts (Red Sea Fish Pharm Ltd, Israel) in 950 ml deionised water and mixed for 40 minutes as per the instructions. The pH was adjusted to 8.0±0.01 and made up to 1 L with deionised water, filter sterilised (0.2 µm) and stored at 4°C.

f/2 media was made by adding the following to artificial seawater.

Stock solution	Chemical name	Volume added to 1 L media
Nitrates	$NaNO_3$	1
Phosphates	$NaH_2PO_4.2H_2O$	1
Silica	$Na_2SiO_3.9H_2O$	1
Vitamins *	-	1
Trace metals **	-	1

* Vitamin stock solution

Chemical name	Concentration (g/L)
Cyanocobalamin (Vitamin B_{12})	0.0005
Thiamine (Vitamin B_1)	0.1
Biotin (Vitamin B_7)	0.0005

** Trace metals stock solution

Chemical name	Concentration (g/L)
NA_2 EDTA	4.16
$FeCL_3.6H_2O$	3.15
$CuSO_4.5H_2O$	0.01
$ZnSO_4.7H_2O$	0.022
$CoCL_2.6H_2O$	0.01
$MnCL_2.4H_2O$	0.18
$Na_2MoO_4.2H_2O$	0.006

Agar media was prepared by first adding the desired agar concentration in deionised water (Half the desired volume) and autoclaved (121°C, 15 minutes). Once sterilised, the agar solution was added to hot, half volume, double strength artificial seawater to reach the final desired volume. Once cooled to around 40°C the *f*/2 nutrients were added.

Appendix 2 – Polymerase chain reaction conditions

The standard protocol from the manufacture was used for all PCRs.

Thermo Scientific Phire direct plant PCR kit.

PCR protocol using dilution extracts.

PCR component	Volume added for 20 µl reaction (µl)
2X Phire plant PCR buffer	10
Forward primer	1
Reverse primer	1
Phire hot start II polymerase	0.4
Water	2.6
Dilution DNA template	5

Thermo Phire hot start II polymerase kit

PCR protocol using extracted DNA

PCR component	Volume added for 20 µl reaction (µl)
5X Phire PCR buffer	4
Dntps	0.4
Forward primer	1
Reverse primer	1
Phire hot start II polymerase	0.4
Water	12.2
Dilution DNA template	1

PCR thermal cycler protocol

98°C – 5 minutes

98°C – 5 seconds

"Primer specific" – 5 seconds

72°C – 1 minute (adjusted based on product size – 20 seconds/kb)

30-40 cycles

72°C – 1 minute

Appendix 3 – Sodium borate buffer

Sodium borate buffer was made following the protocol of Brody & Kern (2004)

A 20X stock solution was first made:

8 g of Sodium hydroxide (NaOH, Sigma, UK) and 48 g boric acid (Sigma, UK) was dissolved in 900 ml deionised water.

pH was adjusted to 8.0 by adding boric acid or NaOH and the solution made up to 1000 ml with deionised water.

100 ml 20X stock solution was added to 1800 ml deionised water to make a 1X working stock solution (1:20 dilution) equating to 10 mM NaOH, used for electrophoresis.

Appendix 4 – Primers

Target region	Name	Direction F = forward R = reverse	Sequence (5'-3')	Size (bp)	Reference
***rbc*L**	CfD	F	CCRTTYATGCGTTGGAGAGA	748	(Hamsher *et al.*, 2011)
	DprbcL7	R	AARCAACCTTGTGTAAGTCT		
18S	D512	F	ATTCCAGCTCCAATAGCG	400	(Zimmermann *et al.*, 2011)
	D978	R	GACTACGATGGTATCTAATC		
METH	SCMH1**	F	CTGACAACCAACGCTCAACC	828 / 5133**	This study
	SCMH99*	R	CAAACTTGGAGTTGCGTGG		
	SCMH2	F	CACGCAACTCCCAAGTTTGG	3080	
	SCMH98	R	TGGTTACCGTCGCGAAAGAA		
	SCMH3*	F	GGTGACAACCAACGCTCAAAC	829*	
	SCMH97**	R	CTACGAGTCGGCTAGGCTTG		
METE	SCME1	F	CACCCATTGCTGGACCTTGT	6122	
	SCME99	R	CGTTCTGCCTGACCTGTCAT		
	SCME2	F	CATGAGAAGATCGGGCGGAT	6103	
	SCME98	R	TCGCTGTTGTCCTCGCTATC		
	SCME3	F	GCTGCAATGATTGGTACCGG	6140	
	SCME97	R	CCGGAAGTTGGTCGCTTACT		
	SCME4	F	CGGTGTTGTTGACGTTGACG	5657	
	SCME96	R	AAATCCACGGTCGCACTTCT		
	SCME5	F	ACGAGGAAAGGTTGACGTGT	2575	
	SCME95	R	GAGCTGGCTCACTTCCATGT		
	SCME6	F	TCGATCCCTGTCGGAGAACA	2464	
	SCME94	R	CGAAGCGCTTCAATCGTCTC		
	SCME7	F	TGCGTGTCAAAGCACGAAAG	4014	
	SCME93	R	CGGCTACGGCCCACTTAATA		
	SCME8	F	GGCACGGGATTGGTGACG	3631	
	SCME92	R	CTTCTCCGGCTACGGCCC		
	SCME9	F	GAGAGAAGTTGAGAATGATTGG	3277	
	SCME91	R	GCCTAGTAGCACGTATAATGC		

* and ** indicate additional primer pairs using these primers.

Appendix 5 – *C. reinhardtii METH* and *METE* complimentary protein sequences for genome querying

METH

MGKTKNVLLSVTAGVVAVTSRLTGLGGVAAIGCGALVATAVGIALAKVKKDGDAGAPKKSGSRGPSLPQSAAFKP
LDKLMRERIIFIDGAMGTQIQKFTLEEEDFRGERYAKHSHELKGNNDLLVITRPDVISKIHTAYLEAGADIIETNTFNG
TWISQSDYELQADEEVALINRTAAQLAKKCVADFLAKNPGSGPRFVAGAIGPTNKTLSVSPSVENPAFRGITYDEVV
DAYYKQAEALVEGGVDMFLVETIFDTLNAKAAMYALEKFFSDKGMRLPVFVSGTIVDNSGRTLSGQTNEAFWNSI
RHAKPMAVGLNCALGAKDMLKYVANLAACADCYVFCYPNAGLPNAMGGYDQKGDEMAEEIRPFCEGNLVNAI
GGCCGTGPEHIAAIKKMASAYKPRKPVTVPPLMRLSGLEPLNYTPDASNMRRTFLNIGERCNVAGSILFKKAIINND
FDTAVAIALKQVQQGADVLDINMDDGLIEGVGAMTRFVNLLVSDPEISRVPFMIDSSKFHIVEAGLKCSQGKCIVN
SISLKEGEAAFKHQAEEVKRHGAAVVVMAFDEQGQAASYEDKVRICSRAYRILVKEVGFDPQDIIFDPNILTIGTGLP
EHNNYAVDFIRATREIKRCCPGAKISGGVSNIAFSFRGNEAVRRAFHSAFLHHACLAGMDMGIVNAAQVKEDEYS
KIDKELLEFVEDVLLNSKIDKELLEFVEDVLLNRRQDSTERMLEYAATLDPKSKPTAVVRLGGASSGPKITPRLNPIPA
GKDQLAPDAKPAPVPKYKAWKDGVKPTAAFVPLDKLMRERIIFIDGAMGTQIQKFTLEEEDFRGERYAKHSHELKG
NNDLLVITRPDVISKIHTAYLEAGADIIETNTFNGTWISQSDYELQADEEVALINRTAAQLAKKCVADFLAKNPGSG
PRFVAGAIGPTNKTLSVSPSVENPAFRGITYDEVVDAYYKQAEALVEGGVDMFLVETIFDTLNAKAAMYALEKFFSD
KGMRLPVFVSGTIVDNSGRTLSGQTNEAFWNSIRHAKPMAVGLNCALGAKDMLKYVANLAACADCYVFCYPNA
GLPNAMGGYDQKGDEMAEEIRPFCEGNLVNAIGGCCGTGPEHIAAIKKMASAYKPRKPVTVPPLMRLSGLEPLNY
TPDASNMRRTFLNIGERCNVAGSILFKKAIINNDFDTAVAIALKQVQQGADVLDINMDDGMDMGIVNAAQVKE
DEYSKIDKELLEFVEDVLLNRCENATERMLEFAATLDPKSKPTAVVKIASAPAGPKITPRLNPIPAGKDQLAPDAKPA
PVPKYKAWKDGVKPTAAFVPLDKLMRERIIFIDGAMGTQIQKFTLEEEDFRGERYAKHSHELKGNNDLLVITRPDVI
GKIHTAYLEAGADIIETNTFNGTWISQSDYELQADEEVALINRTAAQLAKKCVADFLAKNPGSGPRFVAGAIGPTNK
TLSVSPSVENPAFRGITYDEVVDAYYKQAEALVEGGVDMFLVETIFDTLNAKAAMYALEKFFSDKGMRLPVFVSGTI
VDNSGRTLSGQTNEAFWNSIRHAKPMAVGLNCALGAKDMLKYVANLAACADCYVFCYPNAGLPNAMGGYDQ
KGDEMAEEIRPFCEGNLVNAIGGCCGTGPEHIAAIKKMASAYKPRKPVTVPPLMRLSGLEPLNYTPDASNMRRTFL
NIGERCNVAGSILFKKAIVNNDFDTAVAIALKQVQQGADVLDINMDDGLIEGVGAMTRFVNLLVSDPEISRVPFMI
DSSKFHIVEAGLKCSQGKCIVNSISLKEGEAAFRHQAEVVRRHGAAVVVMAFDEQGQAASYEEKIRICSRAYRILVE
EVGFDPQDIIFDPNILTIGTGLPEHNNYAVDFIRATREIKRLCPGSKVSGGVSNIAFSFRGNEAVRRAFHSAFLHHAC
LAGMDMGIVNAAQVKEDEYSKIDKELLEFVEDVLLNRCENATERMLEFKRLSGNVGENSNAGCFLIATVKGDVHD
IGKNIVSVVLGCNNFKVIDMGVMTPWEKILDAAVEHKADIIGLSGLITPSLDEMVTVAKKMEERGMKTPLLIGGATT
SKMHTAVKIAPVYSGPVVHVLDASRSVPVCQAFVDKNDKQRQSYIEEVSEQYADLREEFYASLEDRKYLSLADARK
RALAVDWKDPVNQPVKPKVLGNKVIRAFPIEDVLDYIDWNPFFQVWQLRGRYPNRGFPRIFNDATVGSEAKKLYE

EAQAMLRDFVVNKRVTLNAVMGLYPAAAVGDDIEVYADDSRAKVVARLAGLRQQAEKDGGEPFYCISDFVAPK
GSGVPDYVGMFACSAGHGLEKVIEGYKAAGDDYSYIMAEALADRLAEALAEKLHELVRREYWGYAPDEKLSVDD
MLKVKYQGIRPAPGYPSQPDHTEKRTMWELLDAEAATDIKLTESLAMWPAASVSGLYFGGKCSSYFAVGKITREQ
VEDYAARKKMDIKDAERWLSTMLNYEP*

METE

MAAMLSTTTIGFPRIGNQRQLKFAMESYFKGDSGEAELLAVAHKVQSDAWALQKAAGIAVIGLDGTLYDQVLDTI
TWLGAIPPRFKHLSGLQRYYAMARGGAALDMSKFFDTNYHYLVPELGPDVLGPATAAGAPLQPDFSGPLDKLAR
GQAVVGRERAVPILIGPVTFVSLSRGCELPLDQAVARLLPTYCALLQQLAAAGAPEVQLHEPVLATSEGAGMRAEFE
TAYAQMAQAAGSVPLHLVTYYDDLGAAYPWAVQLPVAAVTLDFLGPPGAAVPSQTLALLQQHGFPADKRLGAG
VVDGRSVWKDDGTAVALLRALLDTGAVSSDRLVVTSSAPLQHLPYDLGLELEAPKTPEAEPHLPPALAARLGFAKQ
KVEEIVS

VARLAASPAAAAAAAGHGAVVQLQRLQQGKGVEDHTADIPAEWFSRPKPYDVRREQQLQLPAFPTTTIGSFPQT
AEVRRLRQQLKSGRLTQAEYEGLIAGHIAHAVGVQEALGIDVLVHGEAERTDMVEYFGMQLGGMLFTRAGWVQS
YGSRCVRPPLVVDDITYRGPMTCWEYKVASAYTRKPVKGMLTGPVTILNWSFPRKDISRAAQAMQLGLALRQEV
AALEAAGCTIIQVDDPALREGLPLKRERWASYLSWAVDAFRLCTGVAAAGTQVVTHLCYSDFQDILPAIDRMDAD
VLTIENSRSDNAMMAALAAAGYGRDIGPGVYDVHSPVVPSVEFIKSRIRSFVDSGILSGRYDRIWVNPDCGLKTRG
WPETIAALRNMVEAAAQARAELQLAGGAAVAPVAGGVEAAGKGAALGAAAGTSRCVDCCH*

Appendix 6 – CTD casts

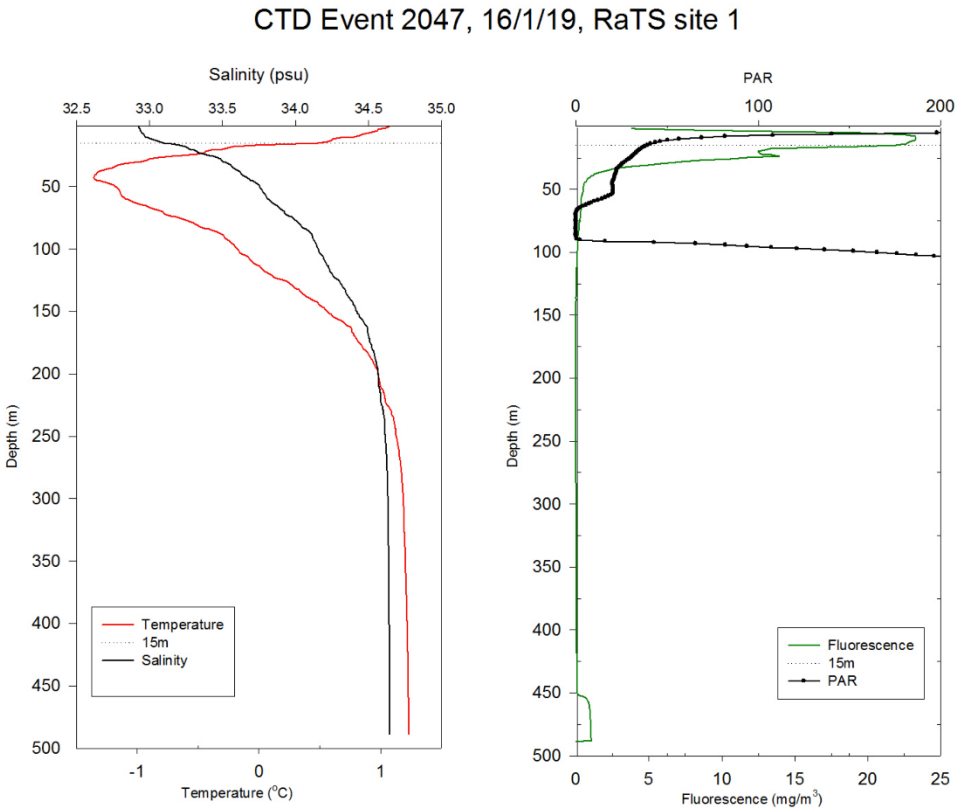

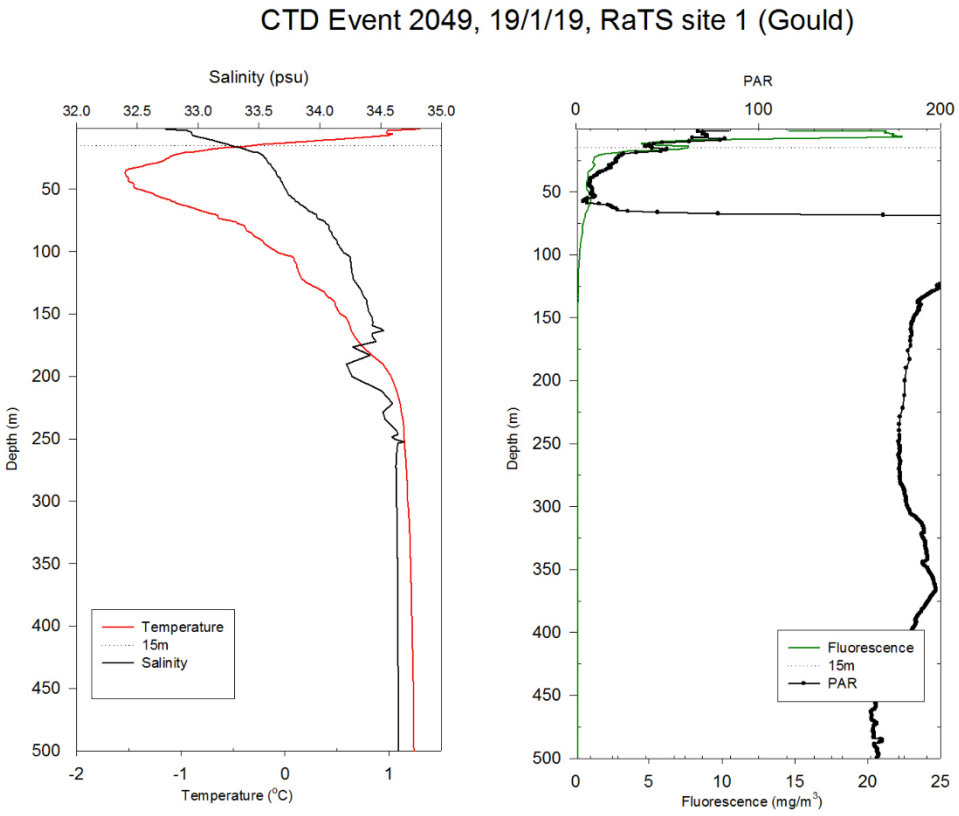

CTD Event 2051, 22/01/19, RaTS site 1

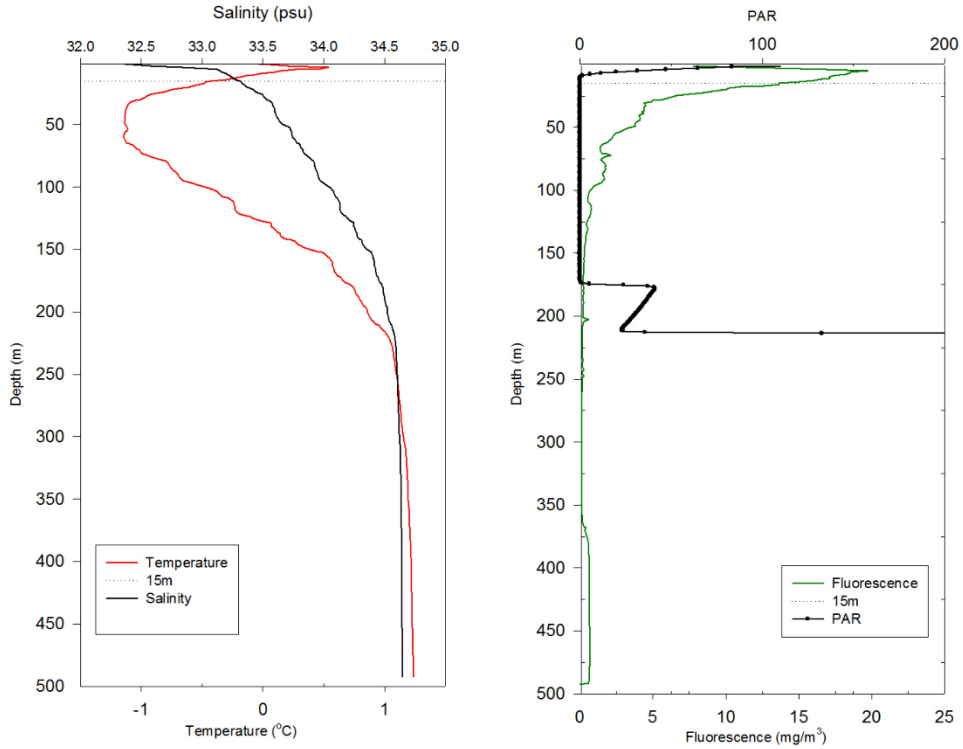

CTD Event 2053, 28/1/2019, RaTS site 1

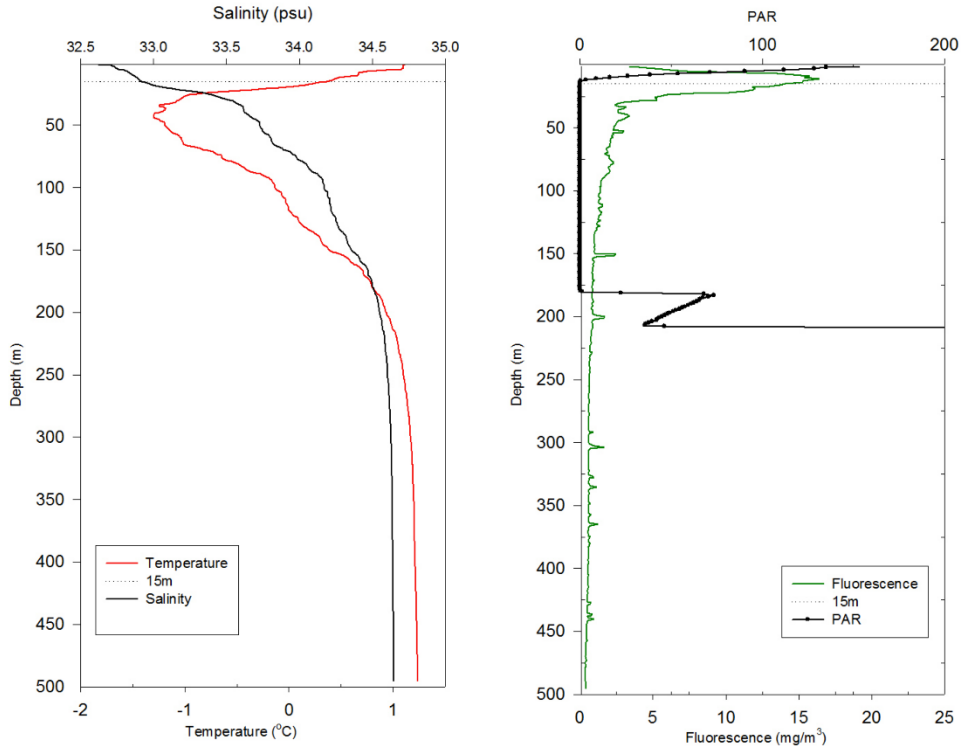

CTD Event 2055, 31/1/2019, RaTS site 1

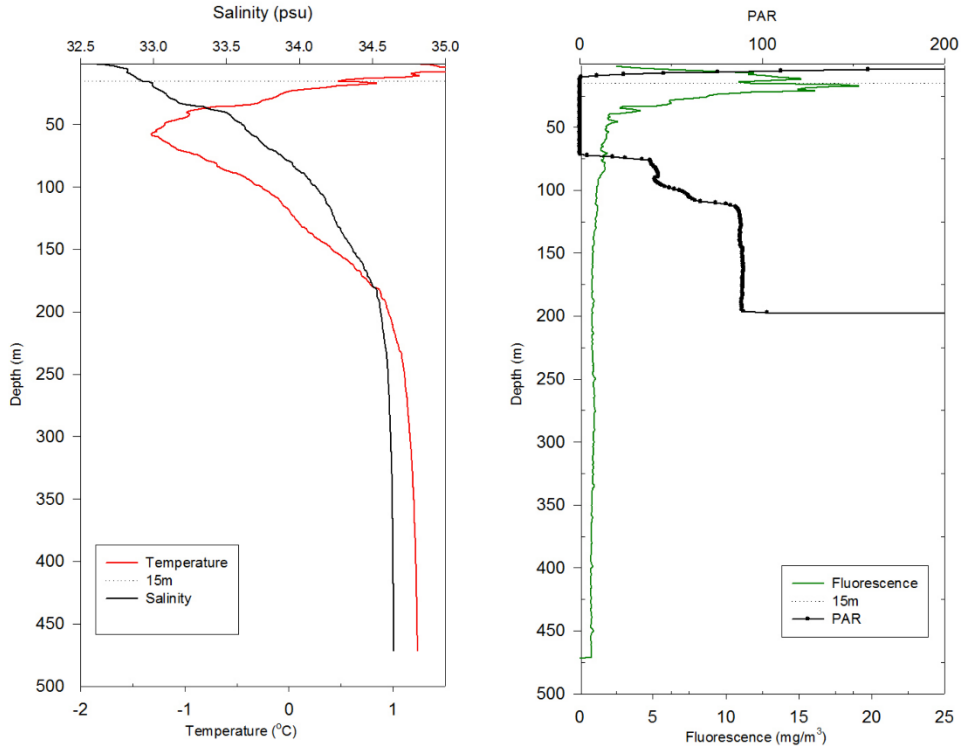

CTD Event 2057, 05/02/2019, RaTS site 1

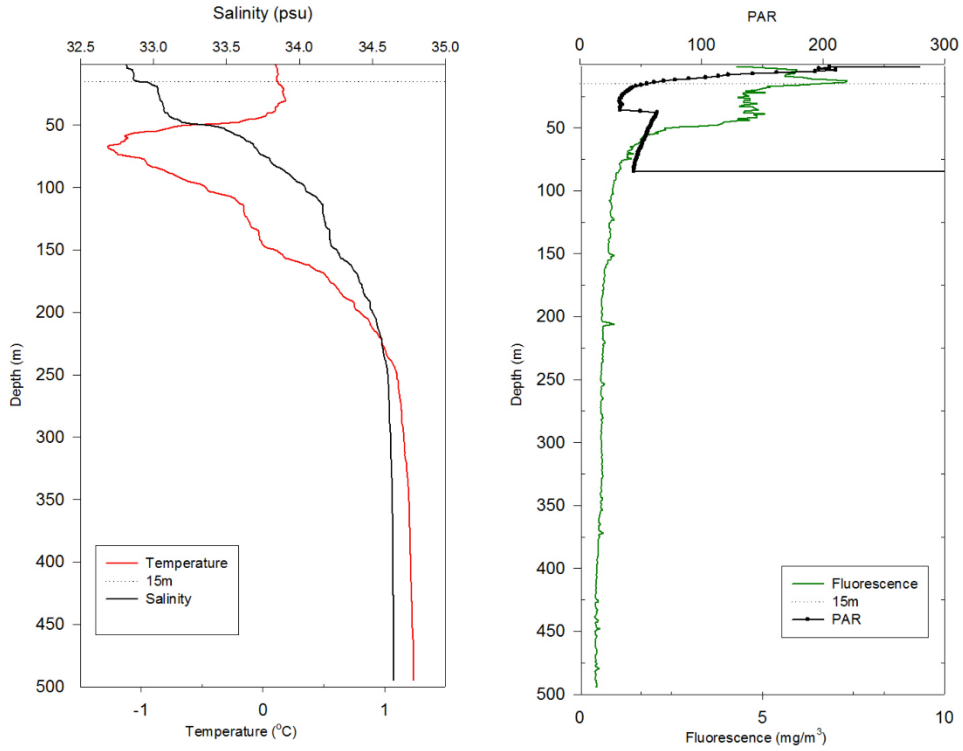

CTD Event 2059, 08/2/19, RaTS site 1

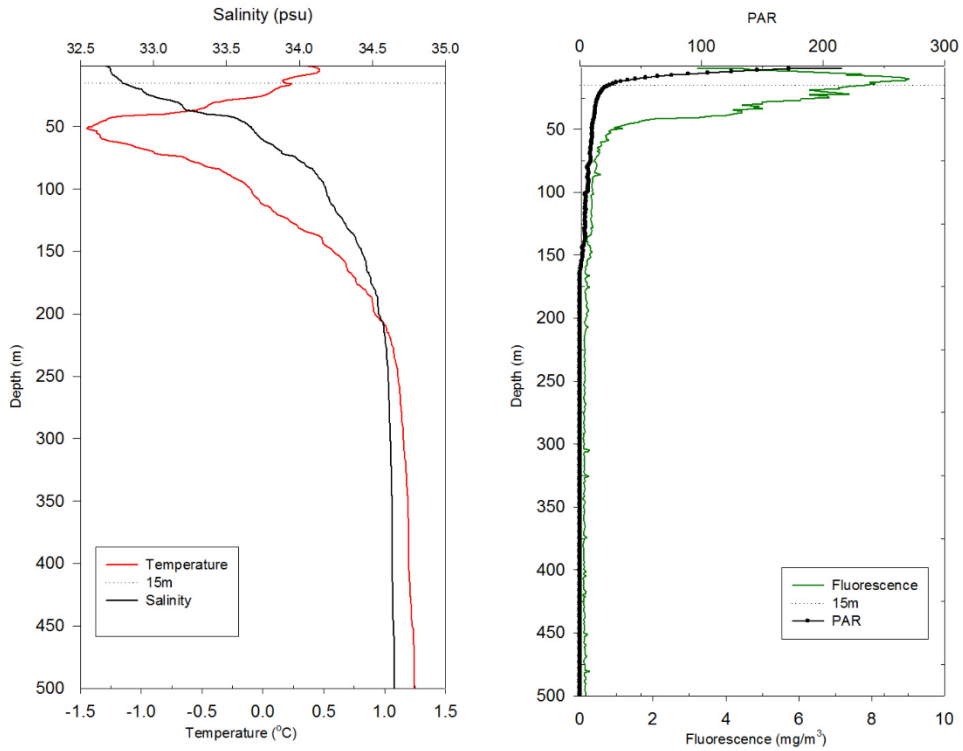

CTD Event 2061, 16/2/19, RaTS site 3

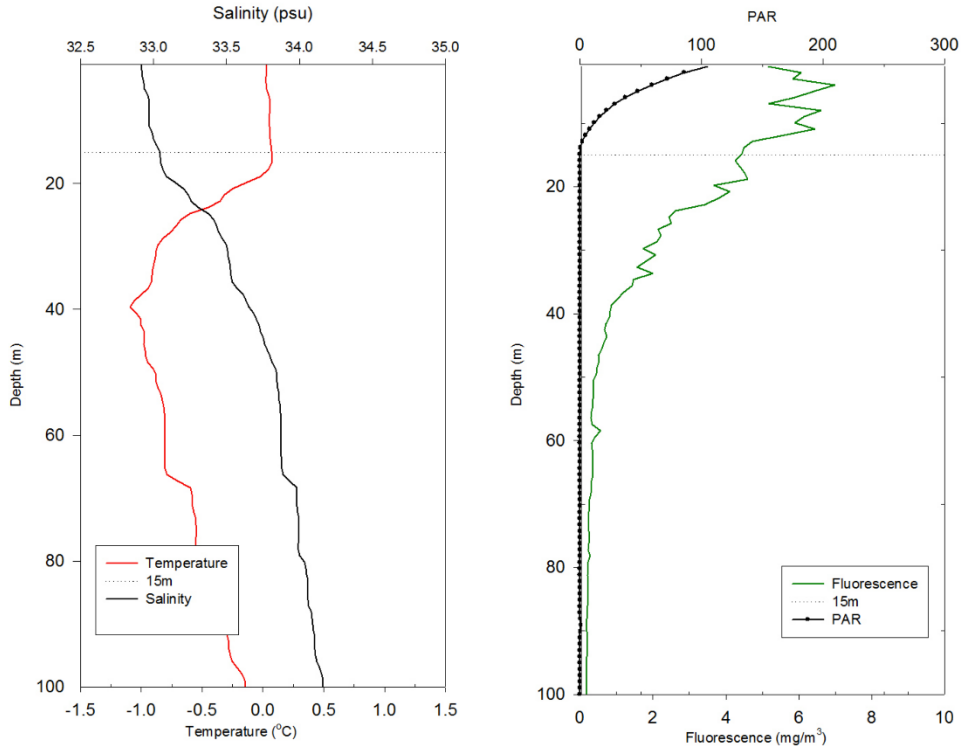

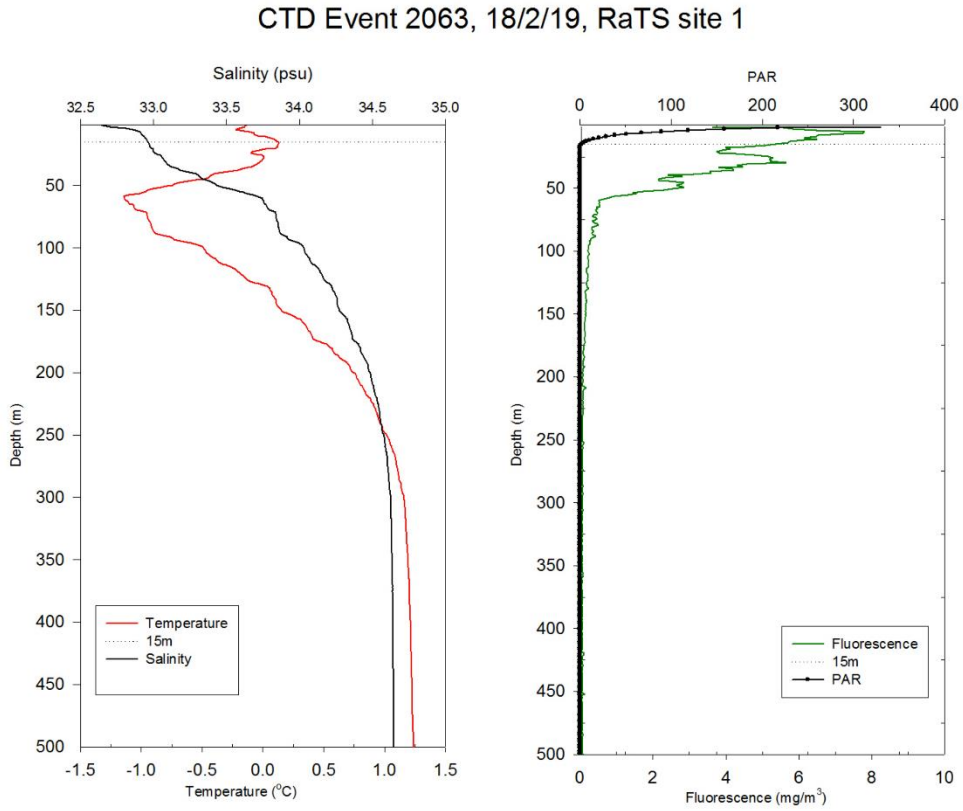
CTD Event 2063, 18/2/19, RaTS site 1
Salinity (psu)
32.5
33.0
33.5
34.0
34.5
35.0
Depth (m)
50
100
150
200
250
300
350
400
450
500
Temperature
15m
Salinity
-1.5
-1.0
-0.5
0.0
0.5
1.0
1.5
Temperature (°C)
PAR
0
100
200
300
400
Depth (m)
Fluorescence
15m
PAR
0
2
4
6
8
10
Fluorescence (mg/m3)

Appendix 7

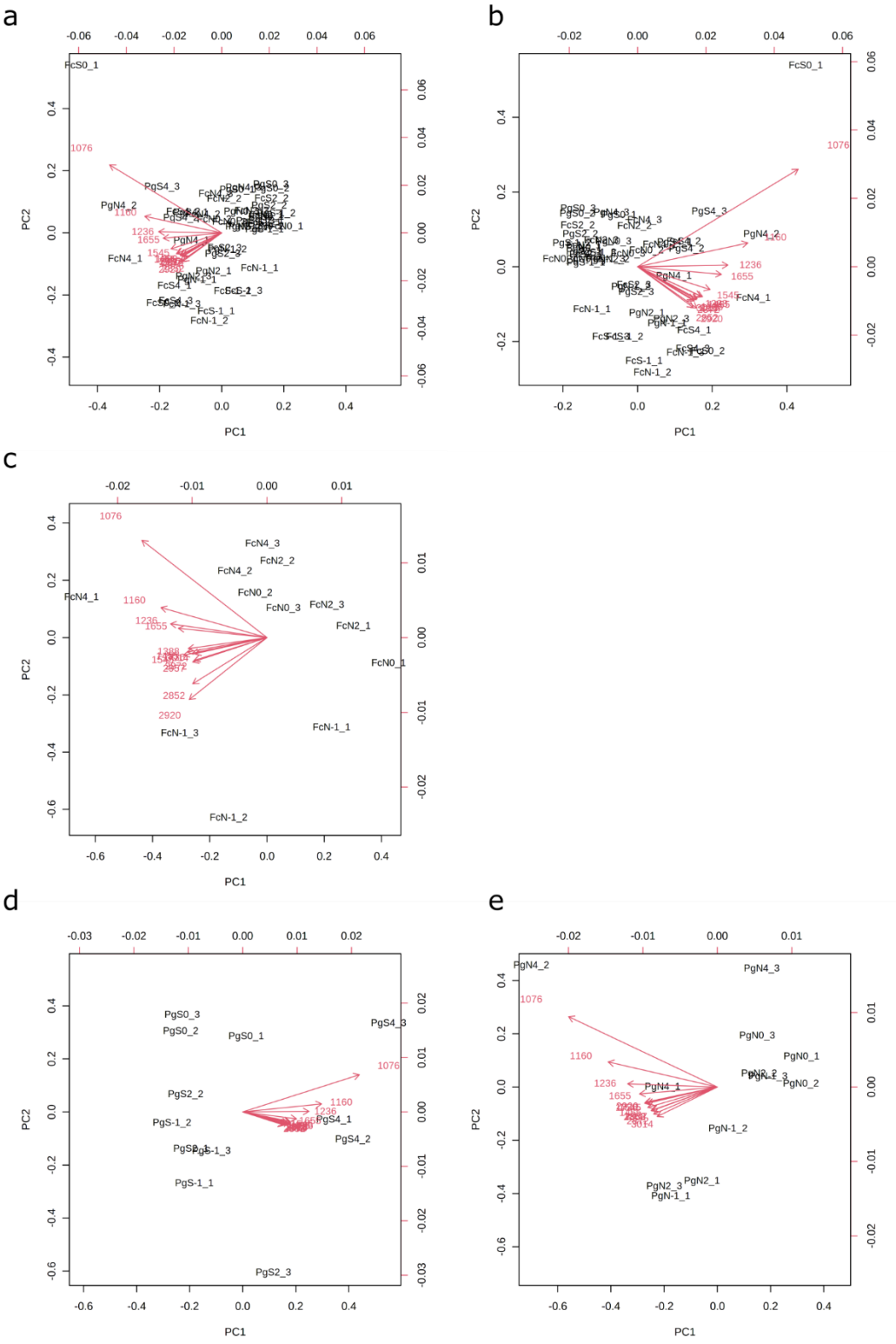

Metabolic fingerprinting PCA biplots. a) Species and strain b) Temperature c) Arctic *F. cylindrus* d) Antarctic *P. glacialis* and e) Arctic *P. glacialis*. Analysis conducted using MetabAnalyst 5.0 (Pang *et al.,* 2021). Antarctic *F. cylindrus* was not analysed due to low sampling number.

Appendix 8

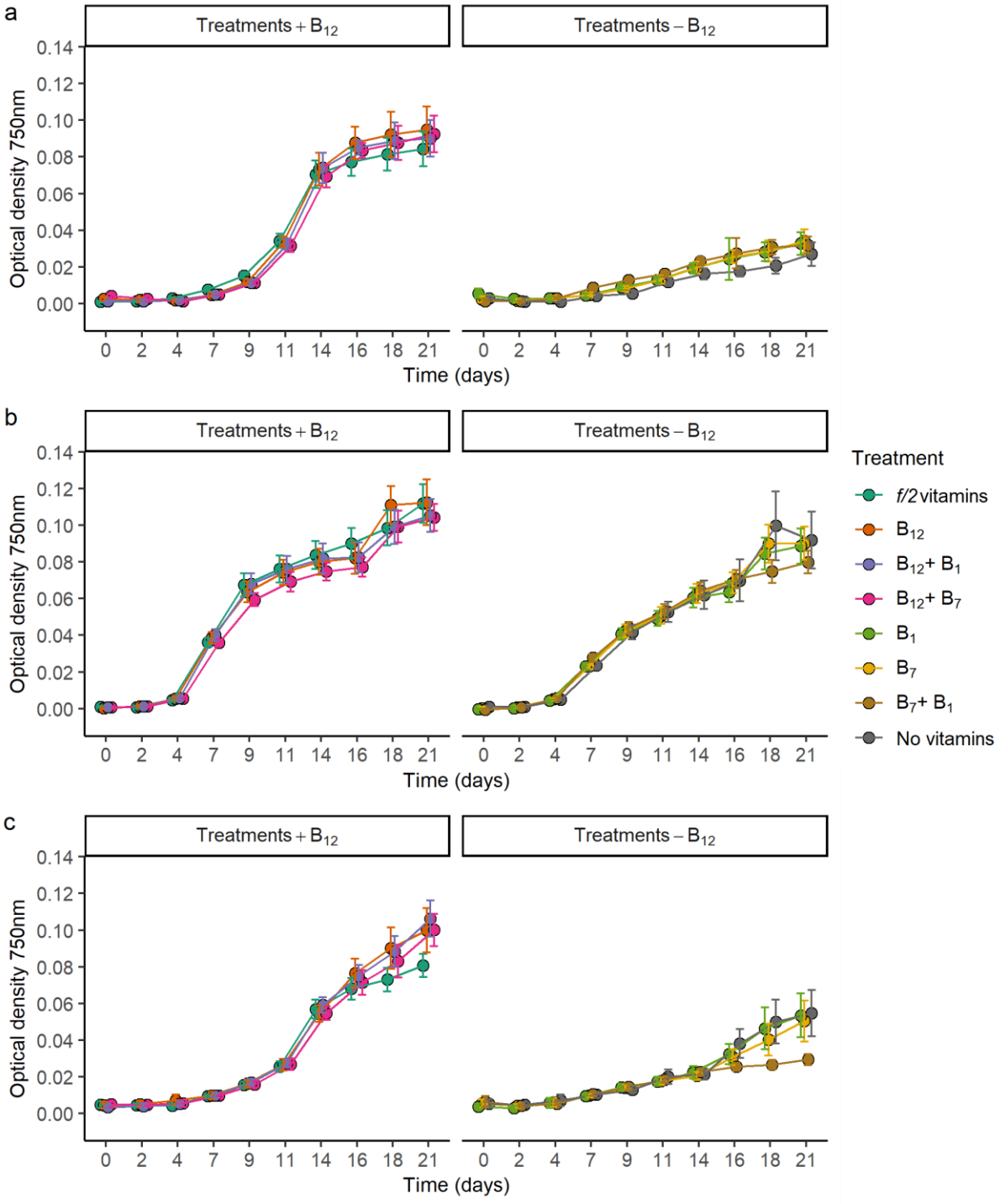

Vitamin growth assay in Arctic *F. cylindrus* strains – 1st subculture. a) RCC 4289 b) RCC 5231 c) RCC 5582. Left panels include treatments + B_{12} and right panels include treatments - B_{12}. Errors bars ±SD.

Appendix 9

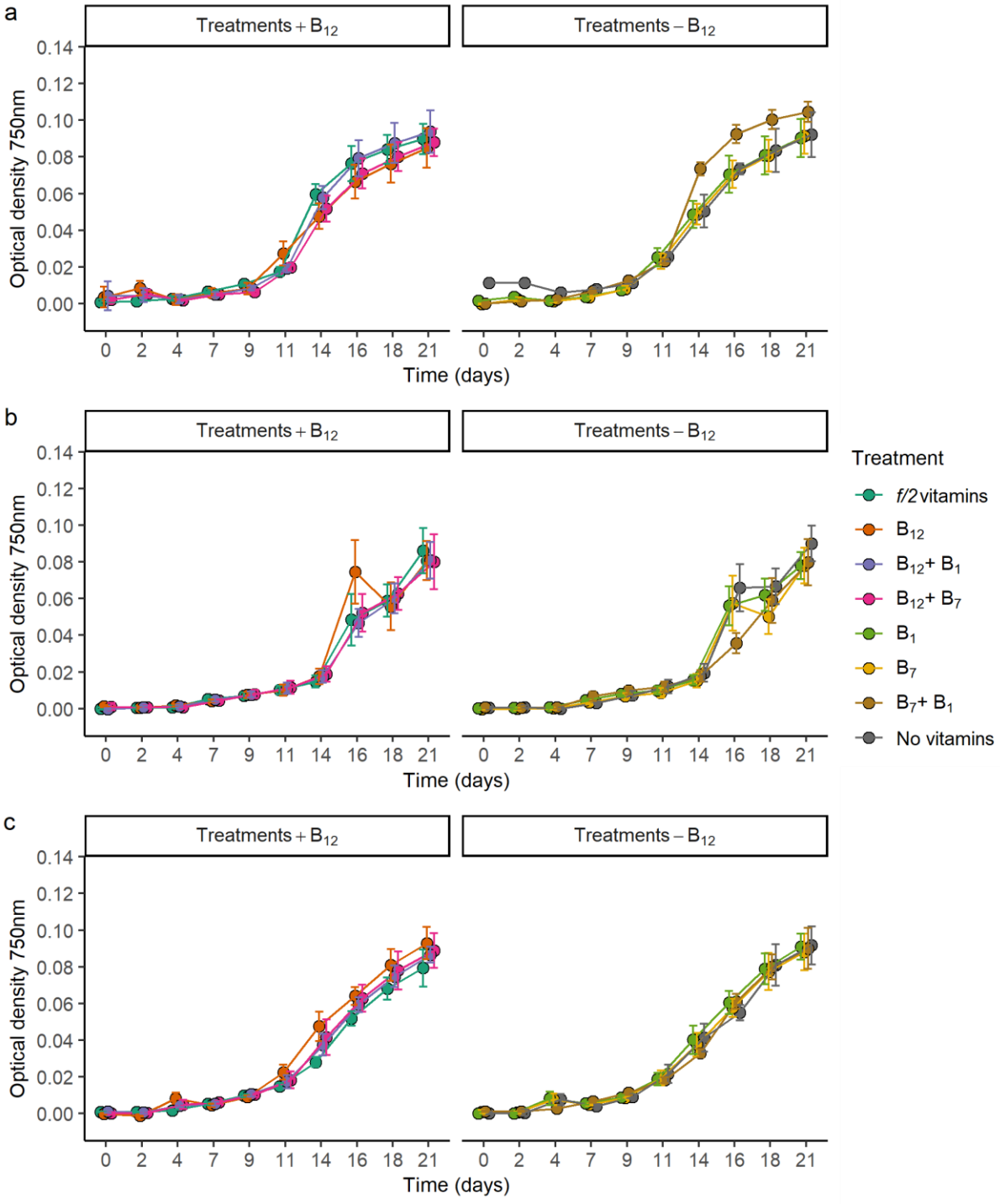

Vitamin growth assay in Antarctic *F. cylindrus* strains – 1st subcultyure. a) CCAP 1023/1 b) CCAP 1023/10 – SC48 c) RCC 6866. Left panels include treatments + B_{12} and right panels include treatments - B_{12}. Errors bars ±SD.

Appendix 10

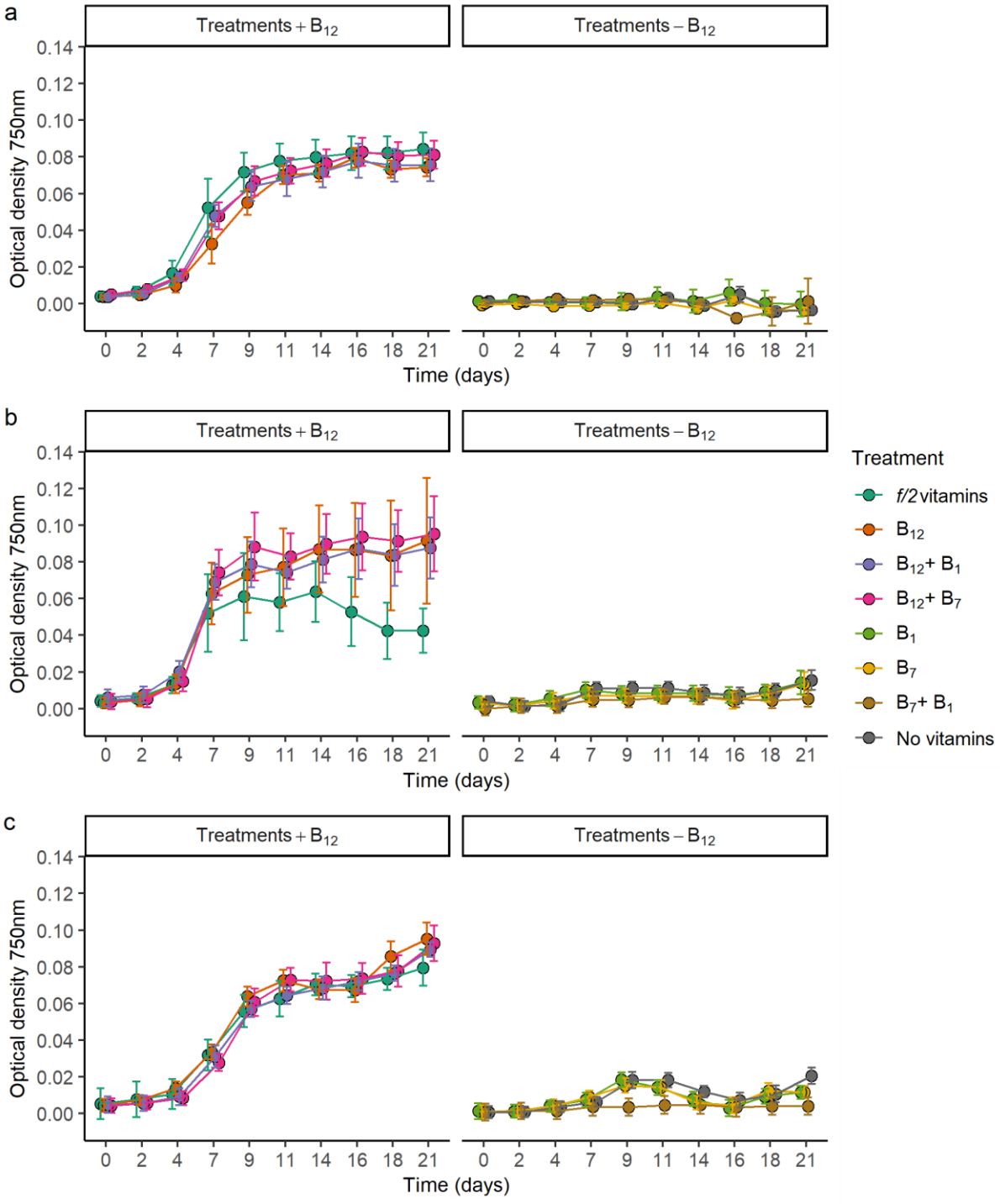

Vitamin growth assay in Arctic *F. cylindrus* strains – 2nd subculture. a) RCC 4289 b) RCC 5231 c) RCC 5582. Left panels include treatments + B_{12} and right panels include treatments - B_{12}. Errors bars ±SD.

Appendix 11

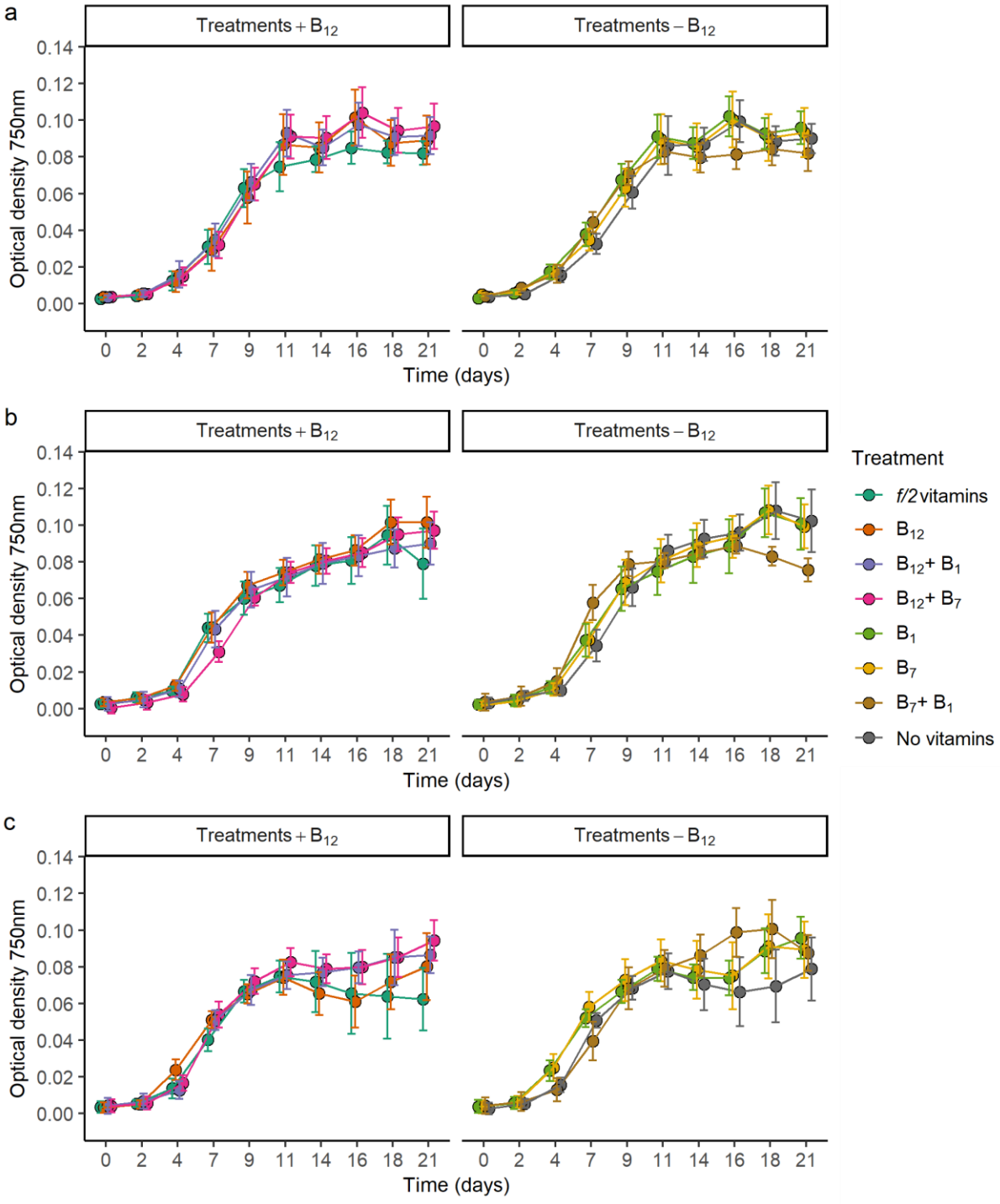

Vitamin growth assay in Antarctic *F. cylindrus* strains – 2nd subculture. a) CCAP 1023/1 b) CCAP 1023/10 – SC48 c) RCC 6866. Left panels include treatments + B_{12} and right panels include treatments - B_{12}. Errors bars ±SD.

Appendix 12 – *METH* nucleotide alignment

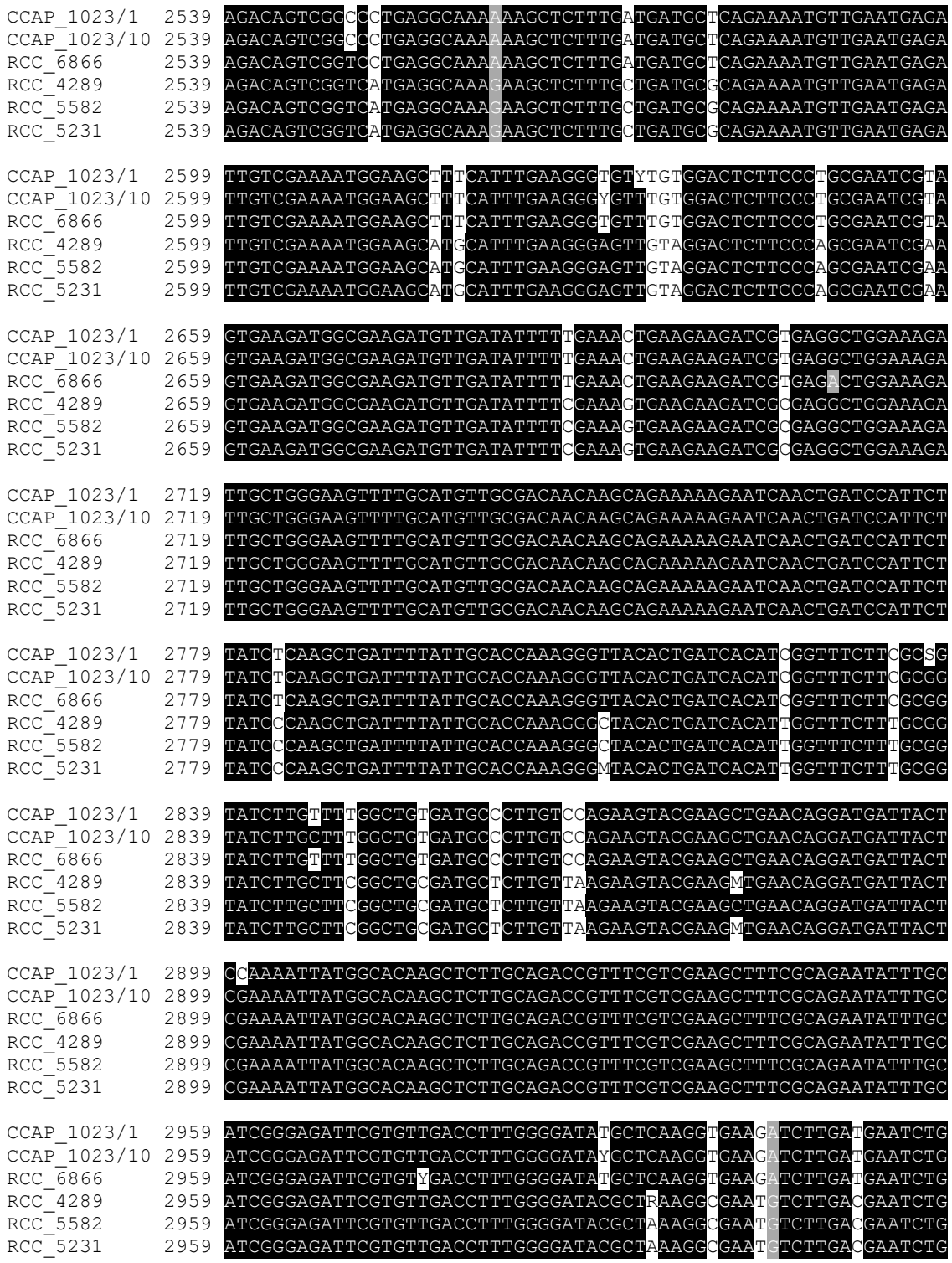

F. cylindrus METH **nucleotide alignment.** Alignment of nucleotide sequences aligned using MAFFT (Katoh et al., 2019). Similarity shading was created using BoxShade (https://embnet.vital-it.ch/software/BOX_form.html).

Appendix 13 – January/February culture growth

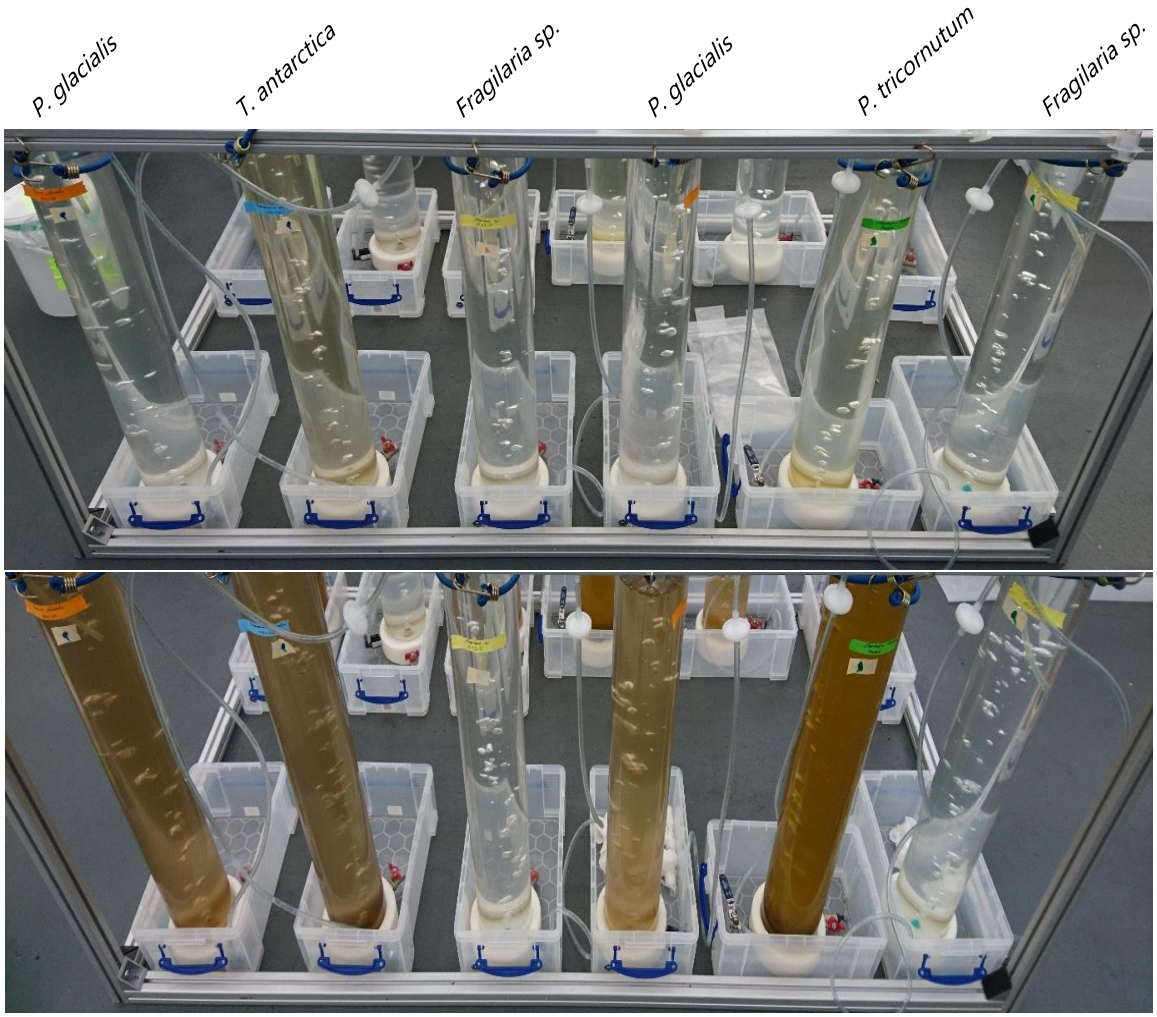

January/February 2018, bubble column cultures at day 13 where first growth was visualised (top) and at the experiment end (day 24, bottom).

Appendix 14 – January/February culture growth

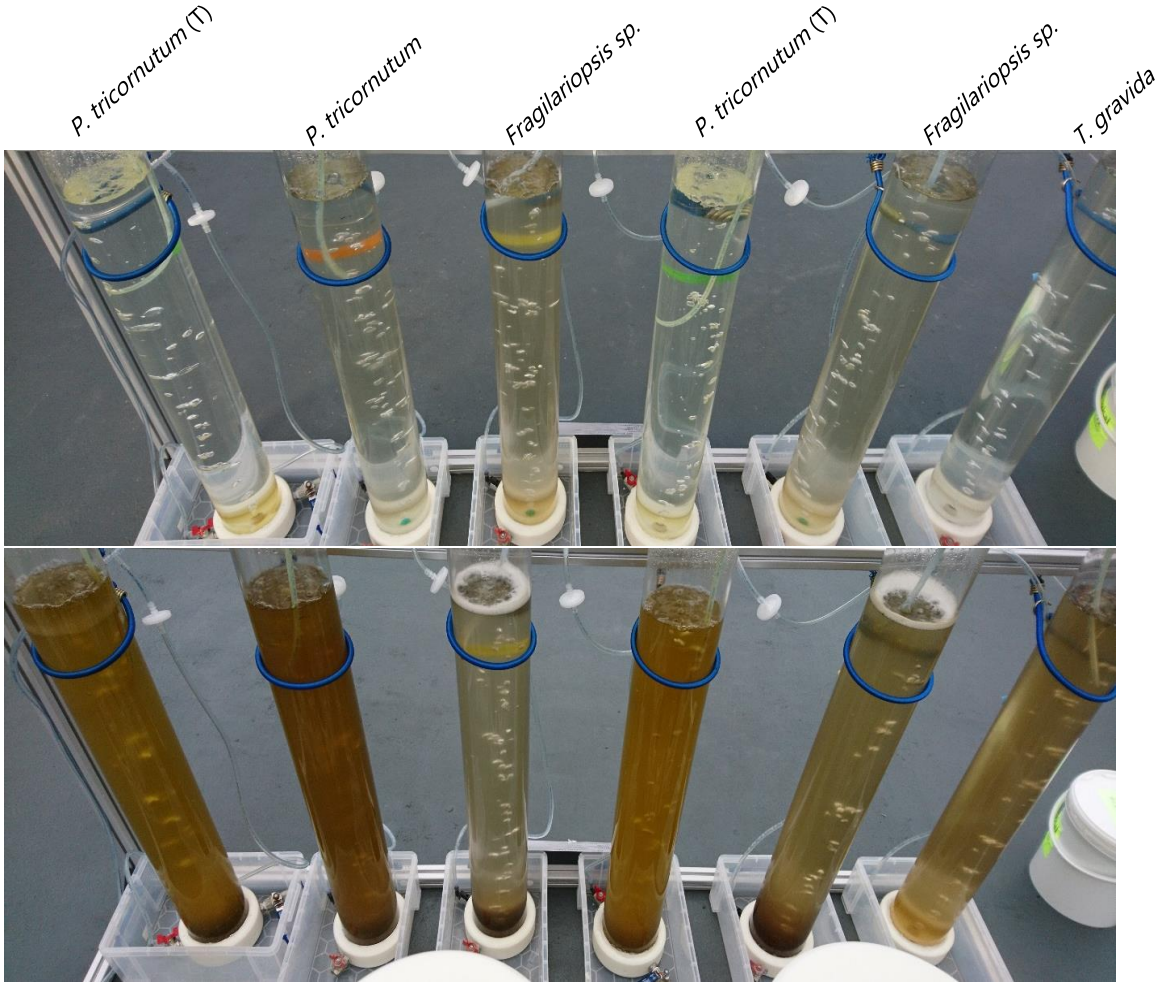

February/March 2018, bubble column cultures at day 10 where first growth was visualised (top) and at the experiment end (day 24, bottom).

Appendix 15 – Pigment analysis of polar strains for biotechnology

Pigment analysis – UV spectrometry

Total chlorophylls and carotenoids showed an increase between week two and the end of the experiments in all strains (Fig. 1 and Fig. 2). Amongst the Antarctic strains, *T. antarctica* had the highest levels of total chlorophylls and carotenoids based on dry weight and showed the smallest difference between week two and experiment end (Fig. 1). *P. glacialis* exhibited an increase in total chlorophylls and carotenoids from week two and the end of the experiment, in which the end values were similar to *P. tricornutum* (T) (Fig.1). There was no significant effect of strain and time point on the total chlorophyll and total carotenoids levels expressed as mg/g CDW (p>0.05). When values are expressed as mg/L, *P. tricornutum* (T) exhibits the highest values of total chlorophylls and carotenoids and all strains showed an increase from week two to the experiment end (Fig. 1). Diatom strain had a significant effect on total chlorophyll (ANOVA, F(2,14) = 6.688, p<0.01) and total carotenoid levels expressed as mg/L (ANOVA, F(2,14), p<0.01). Time point had a significant effect on total chlorophyll (ANOVA, F(2,14) = 116.518, p = 0.001) and total carotenoid levels expressed as mg/L (ANOVA, F(1,14), p = 0.001). Tukey HSD posthoc tests revealed *P. glacialis* had statistically lower pigment levels than *P. triocornutm* (T) and *T. antarctica* (p<0.05), there was no difference between *P. tricornutum* (T) and *T. antarctica.*

Amongst the Arctic strains the Arctic strain of *P. tricornutum* had the highest total chlorophyll and carotenoid levels and had higher levels compared to the temperate strain based on dry weight and culture volume (Fig. 2). *Fragilariopsis* sp. had the highest pigment values at week two, which coincides with the early growth this strain showed (Fig. 6.3a) and had similar end pigment values to the temperate *P. tricornutum*. *T. gravida* showed very low pigment values but exhibited a small increase from week two to the experiment end. There was no significant effect of strain or time on the total chlorophyll and total carotenoid levels when expressed as mg/g CDW (p>0.05). Strain had no significant effect on total chlorophyll and total carotenoids when expressed as mg/L (p>0.05) but, time had a significant effect on total chlorophyll (chi-squared = 13.066, Df = 1, p=0.001) and total carotenoids (chi-squared = 13.051, Df = 1, p=0.001).

Pigment levels showed an expected increase between week two and the experimental end in all strains tested in both experiments. Pigment content corresponded well with the growth of the strains with strains with the highest growth showing the highest pigment levels. Interestingly the Arctic strain of *P. tricornutum* showed higher levels of pigments compared to the temperate strain despite showing comparable growth, suggesting possible intraspecific differences.

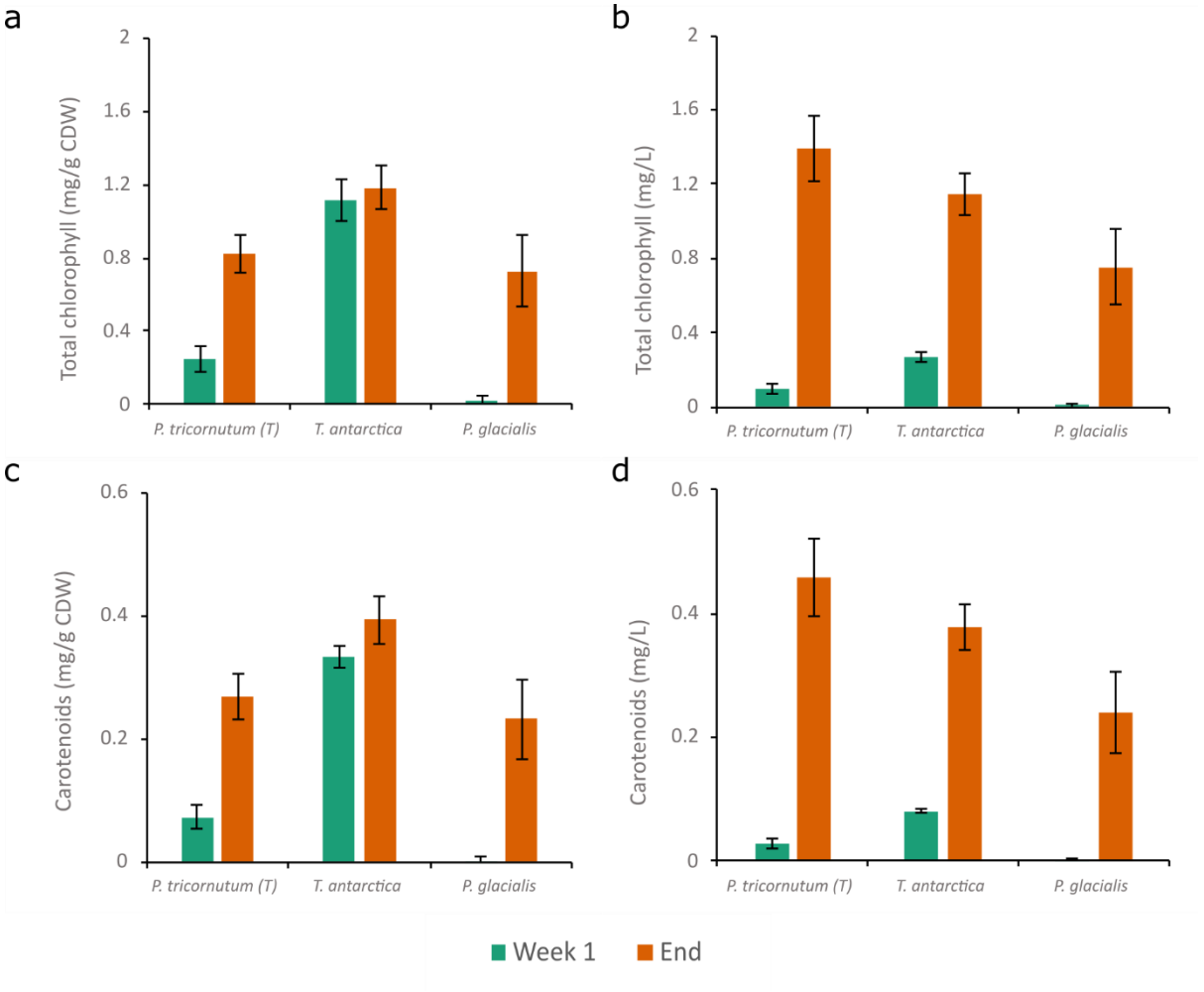

Spectrophotometric analysis of pigment composition of Antarctic strains in January/February 2018. The two time points refer to day 15 (week 2) and day 24 (end). Total chlorophyll (top) and carotenoid (bottom) concentrations given as mg/g CDW (cell dry weight, left) and mg/L (right). n = 3, Mean ± SD.

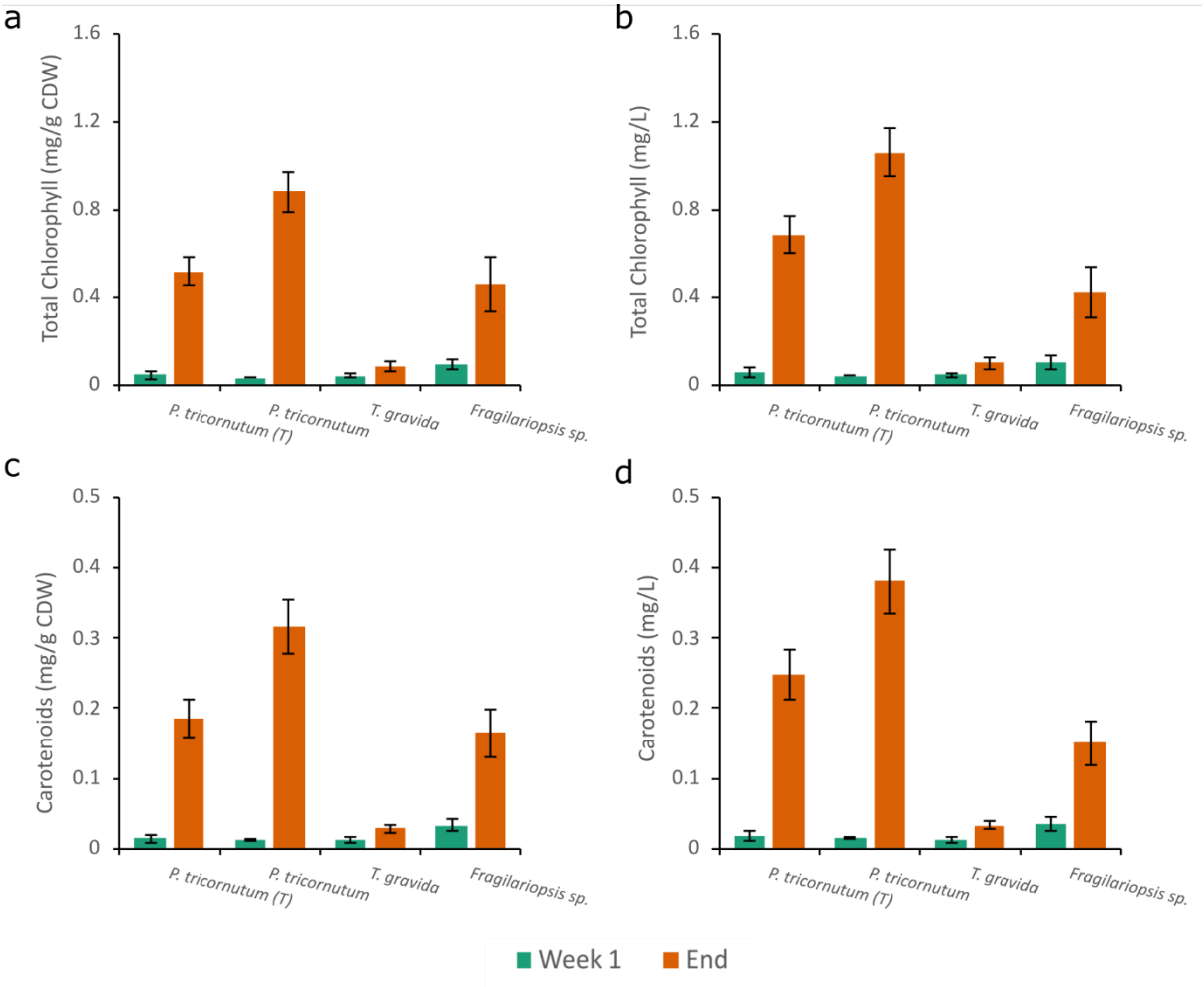

Spectrophotometric analysis of pigment composition of Arctic strains in February/March 2018. The two time points refer to day 14 (week 2) and day 24 (end). Total chlorophyll (top) and carotenoid (bottom) concentrations given as mg/g CDW (left) and mg/L (right). n = 3, Mean ± SD.